Control of biofilms to control caries

Edited by
Jin Xiao, Xiaojing Huang, Mingyun Li, Richard L. Gregory
and Keke Zhang

About Frontiers

Frontiers is more than just an open access publisher of scholarly articles: it is a pioneering approach to the world of academia, radically improving the way scholarly research is managed. The grand vision of Frontiers is a world where all people have an equal opportunity to seek, share and generate knowledge. Frontiers provides immediate and permanent online open access to all its publications, but this alone is not enough to realize our grand goals.

Frontiers journal series

The Frontiers journal series is a multi-tier and interdisciplinary set of open-access, online journals, promising a paradigm shift from the current review, selection and dissemination processes in academic publishing. All Frontiers journals are driven by researchers for researchers; therefore, they constitute a service to the scholarly community. At the same time, the *Frontiers journal series* operates on a revolutionary invention, the tiered publishing system, initially addressing specific communities of scholars, and gradually climbing up to broader public understanding, thus serving the interests of the lay society, too.

Dedication to quality

Each Frontiers article is a landmark of the highest quality, thanks to genuinely collaborative interactions between authors and review editors, who include some of the world's best academicians. Research must be certified by peers before entering a stream of knowledge that may eventually reach the public – and shape society; therefore, Frontiers only applies the most rigorous and unbiased reviews. Frontiers revolutionizes research publishing by freely delivering the most outstanding research, evaluated with no bias from both the academic and social point of view. By applying the most advanced information technologies, Frontiers is catapulting scholarly publishing into a new generation.

What are Frontiers Research Topics?

Frontiers Research Topics are very popular trademarks of the *Frontiers journals series*: they are collections of at least ten articles, all centered on a particular subject. With their unique mix of varied contributions from Original Research to Review Articles, Frontiers Research Topics unify the most influential researchers, the latest key findings and historical advances in a hot research area.

Find out more on how to host your own Frontiers Research Topic or contribute to one as an author by contacting the Frontiers editorial office: frontiersin.org/about/contact

Control of biofilms to control caries

Topic editors

Jin Xiao — University of Rochester Medical Center, United States
Xiaojing Huang — Fujian Medical University, China
Mingyun Li — Sichuan University, China
Richard L. Gregory — Indiana University, Purdue University Indianapolis, United States
Keke Zhang — Wenzhou Medical University, China

Table of
contents

Editorial: Control of biofilms to control caries

Wen Zhou and Xiaojing Huang*

Fujian Key Laboratory of Oral Diseases and Fujian Provincial Engineering Research Center of Oral Biomaterial and Stomatological Key Lab of Fujian College and University, School and Hospital of Stomatology, Fujian Medical University, Fuzhou, China

Editrorial on the Research Topic
Control of biofilms to control caries

Dental caries, a disease caused by bacterial biofilms, is one of the most prevalent chronic diseases in humans globally. A dysbiotic shift at the interface of the biofilm–tooth surface leads to a prolonged low-pH environment at the interface, resulting in net mineral loss from the teeth (Zheng et al., 2023). For the prevention and treatment of caries, biofilm control is of critical importance (Comeau et al., 2022). To develop novel and effective strategies for the control of biofilms and caries, it is necessary to investigate biofilms in greater depth. Accordingly, their pathogenic mechanisms and interactions among microorganisms should be explored along with new biofilm control strategies. Herein, we discuss the issues related to biofilm control in detail.

The cariogenic mechanism of specific bacteria is an important topic in caries research. Protein lysine malonylation (Kmal) is a novel post-translational modification that is crucial for regulating metabolism and virulence expression in *Streptococcus mutans* (*S. mutans*). However, the Kmal of *S. mutans* remains poorly understood. Li et al. revealed that approximately 50% of the total malonyl lysine sites in *S. mutans* were identified as Kmal sites. It provides a multidimensional comprehension of the bacterial virulence and physiological functions of *S. mutans*. In addition, the cross-kingdom interactions of *S. mutans* and *Candida albicans* (*C. albicans*) have been found to promote the cariogenicity of *S. mutans* (Katrak et al., 2023). In this Research Topic, Li et al. reported that inhibiting the activity of glycosyl transferases (Gtfs) or glucans to hinder extracellular polysaccharide production may weaken the co-adhesion between the two species. Lu et al. summarized the coexistence and synergistic or antagonistic interactions of the two species, aiding in understanding the interactions of *S. mutans* and *C. albicans*.

There is an urgent need for developing novel and effective antibacterial agents. As part of the present Research Topic, Liu et al. revealed that areca nut essential oils reduce the cariogenicity of *S. mutans* through the targeted inhibition of Gtfs. Fang et al. explored mesoporous silica nanoparticles, which are a promising drug delivery vehicle for antibacterial agents. Furthermore, Zhao et al. reported a cold atmospheric plasma device that could easily produce plasma through a double-ring discharge structure with quartz tubes. This device was demonstrated to have a stronger bactericidal effect on caries-related biofilms than ultraviolet radiation under the same test conditions.

Achieving antibiofilm activity in a pH-sensitive way is another research hotspot. For example, Wang et al. developed a novel resin infiltrant containing a smart monomer, dodecylmethylaminoethyl methacrylate, which showed stronger antibacterial effectiveness at lower pH. Their findings shed light on the promising future of pH-sensitive anti-caries agents. In addition, Huang et al. summarized the state-of-the-art pH-activated antibiofilm strategies for the control of dental caries, focusing on their effects, mechanisms of action, and biocompatibility. The limitations of previous studies have also been discussed, thus highlighting aspects for future study.

Currently, drug-resistant strains of oral bacteria are often detected. Shen et al. reported that the fluoride-resistant strains of *S. mutans* can significantly increase the diversity of the oral microbial community. To better cope with potential drug resistance challenges in the future, there is a critical need for novel antimicrobial approaches. Based on in silico screening and computational methods, Zhang et al. used computer-aided drug design to identify compounds with optimal interactions with the target. Synthetic antimicrobial peptides obtained through rational design, computational design, or high-throughput screening have demonstrated increased selectivity for both single-species and multispecies biofilms, making the development of new antimicrobial modalities a crucial challenge for researchers in this field.

In future research, the mechanism by which *S. mutans* causes dental caries requires further exploration. For example, *C. albicans* synergistically promotes the pathogenicity of *S. mutans* through the bacterial quorum-sensing system. The use of natural products as drugs and pH-responsive antibacterial agents has great potential and is an important future Research Topic. Furthermore, there is a need to develop prevention and treatment strategies for oral cariogenic bacteria. The emergence of antibiotic resistance has necessitated the search for novel antibacterial agents that target specific oral bacterial pathogens or can be delivered through targeted drug delivery systems. Through rational design, computational design, and high-throughput screening, computer-aided drug design has led to the identification of potential therapeutic agents that can promote the targeted control of oral microbial biofilms in the near future.

Conflict of interest

The authors declare that the research was conducted in the absence of any commercial or financial relationships that could be construed as a potential conflict of interest.

Publisher's note

All claims expressed in this article are solely those of the authors and do not necessarily represent those of their affiliated organizations, or those of the publisher, the editors and the reviewers. Any product that may be evaluated in this article, or claim that may be made by its manufacturer, is not guaranteed or endorsed by the publisher.

References

Comeau, P., Panariello, B., Duarte, S., and Manso, A. (2022). Impact of curcumin loading on the physicochemical, mechanical and antimicrobial properties of a methacrylate-based experimental dental resin. *Sci. Rep.* 4, 12(1),18691. doi: 10.1038/s41598-022-21363-5

Katrak, C., Garcia, B. A., Dornelas-Figueira, L. M., Nguyen, M., Williams, R. B., Lorenz, M. C., et al. (2023). Catalase produced by *Candida albicans* protects *Streptococcus mutans* from H_2O_2 stress-one more piece in the cross-kingdom synergism puzzle. *mSphere* 8 (5), e0029523. doi: 10.1128/msphere.00295-23

Zheng, T., Jing, M., Gong, T., Yan, J., Wang, X., Xu, M., et al. (2023). Regulatory mechanisms of exopolysaccharide synthesis and biofilm formation in *Streptococcus mutans*. *J. Oral. Microbiol.* 15 (1), 2225257. doi: 10.1080/20002297.2023.2225257

Novel dental resin infiltrant containing smart monomer dodecylmethylaminoethyl methacrylate

Xiaoyu Huang[1,2,3,4†], Jingou Liang[1,3,5†], Wen Zhou[1,2,3,6], Tao Ma[7], Michael D. Weir[3], Gary D. Hack[3], Guadalupe Garcia Fay[3], Thomas W. Oates[3], Lei Cheng[1,2]* and Hockin H. K. Xu[3,8,9]*

[1]State Key Laboratory of Oral Diseases, National Clinical Research Center for Oral Diseases, West China School of Stomatology, Sichuan University, Chengdu, China, [2]Department of Operative Dentistry and Endodontics, West China Hospital of Stomatology, Sichuan University, Chengdu, China, [3]Department of Advanced Oral Sciences and Therapeutics, University of Maryland Dental School, Baltimore, MD, United States, [4]Stomatology Hospital, School of Stomatology, Zhejiang University School of Medicine, Zhejiang Provincial Clinical Research Center for Oral Diseases, Key Laboratory of Oral Biomedical Research of Zhejiang Province, Cancer Center of Zhejiang University, Hangzhou, China, [5]Department of Pediatric Dentistry, West China School of Stomatology, Sichuan University, Chengdu, China, [6]Fujian Key Laboratory of Oral Diseases & Fujian Provincial Engineering Research Center of Oral Biomaterial & Stomatological Key lab of Fujian College and University, School and Hospital of Stomatology, Fujian Medical University, Fuzhou, China, [7]Department of Oncology and Diagnostic Sciences, University of Maryland School of Dentistry, Baltimore, MD, United States, [8]Center for Stem Cell Biology & Regenerative Medicine, University of Maryland School of Medicine, Baltimore, MD, United States, [9]Marlene and Stewart Greenebaum Cancer Center, University of Maryland School of Medicine, Baltimore, MD, United States

Objectives: White spot lesions (WSLs) are prevalent and often lead to aesthetic problems and progressive caries. The objectives of this study were to: (1) develop a novel resin infiltrant containing smart monomer dodecylmethylaminoethyl methacrylate (DMAEM) to inhibit WSLs, and (2) investigate the effects of DMAEM incorporation on cytotoxicity, mechanical properties, biofilm-inhibition and protection of enamel hardness for the first time.

Methods: DMAEM was synthesized using 1-bromododecane, 2-methylamino ethanol and methylmethacrylate. DMAEM with mass fractions of 0%, 1.25%, 2.5% and 5% were incorporated into a resin infiltant containing BisGMA and TEGDMA. Cytotoxicity, mechanical properties and antibacterial effects were tested. After resin infiltration, bovine enamel was demineralized with saliva biofilm acids, and enamel hardness was measured.

Result: DMAEM infiltration did not increase the cytotoxicity or compromise the physical properties when DMAEM mass fraction was below 5% ($p > 0.05$). Biofilm metabolic activity was reduced by 90%, and biofilm lactic acid production was reduced by 92%, *via* DMAEM ($p < 0.05$). Mutans streptococci biofilm CFU was reduced by 3 logs ($p < 0.05$). When demineralized in acid and then under biofilms, the infiltrant + 5% DMAEM group produced an enamel hardness (mean $\pm$ sd; n = 6) of 2.90 $\pm$ 0.06 GPa, much higher than 0.85 $\pm$ 0.12 GPa of the infiltrant + 0% DMAEM group ($p < 0.05$).

Significance: A novel resin infiltrant with excellent mechanical properties, biocompability, strong antibacterial activity and anti-demineralization effect was developed using DMAEM for the first time. The DMAEM resin infiltrant is promising for inhibiting WSLs, arresting early caries, and protecting enamel hardness.

1 Introduction

Dental caries is one of the most prevalent oral diseases globally (Peres et al., 2019). White spot lesions (WSLs) are early-stage caries, which have been reported to affect between 50% and 96% of patients receiving fixed orthodontic treatments (Sardana et al., 2019; Sonesson et al., 2020). Treatments for patients suffering from WSLs include fluoride, phosphopeptide compounds, and resin infiltration (Wegehaupt and Attin, 2010; Leila et al., 2017). Resin infiltant can penetrate into the pores of enamel and seal the passage of acid. It is minimally invasive and has been an emerging therapeutic modality in the treatment of WSLs. However, resin infiltant can only seal off about 30-60% of the enamel pore volume (Kielbassa et al., 2009; Yim et al., 2014). Furthermore, after the attack of acid produced by cariogenic microorganisms, the hardness of enamel decreased significantly (Dai et al., 2022).

In the oral cavity, dental caries starts with the breakdown of the dynamic balance of oral microecology (Pitts et al., 2017). During the development of caries, oral microbial diversity is decreased, and the acidogenic bacteria can multiply and produce acids, causing the pH to decrease and leading to hard tissue demineralization (Selwitz et al., 2007). Antibacterial agents such as silver nanoparticles (AgNP) (Kielbassa et al., 2020; Li et al., 2020), quaternary ammonium methacrylate (Yu et al., 2020), and ionic liquid-loaded microcapsules (Cuppini et al., 2021) were incorporating into dental materials to inhibit the growth of plaque. However, oral commensal microbiome colonizes on dental tissue plays an essential role in oral microecology (Rosier et al., 2018). The oral probiotics were also inhibited by the agents mentioned above, that would break the balance of oral microecology (Pitts et al., 2017; Liang et al., 2020). Therefore, an intelligent resin infiltrant that could show an antibacterial effect only during dysbiosis, rather than killing all the bacteria, is highly preferred to inhibit WSLs.

Recently, microecosystem-regulating effects of intelligent pH-sensitive resin materials have received more attention (Fenton et al., 2018). Dodecylmethylaminoethyl methacrylate (DMAEM) is a novel tertiary amine (TA) smart material that responds to pH change. Its central nitrogen atom is connected to 3 alkyl or aromatic groups. When the local pH is low, such as during biofilm acid attacks, the nitrogen atoms of TA is protonated to form quaternary ammonium salts (QAMs), which are antibacterial. The QAMs-modified dental materials demonstrated excellent antibacterial effect (Han et al., 2017; Wang et al., 2019; Zhou et al., 2019). In previous studies, the MIC and MBC of DMAEM against *Streptococcus mutans* UA159 (*S. mutans*), *Streptococcus gordonii* DL1 (*S. gordonii*), and *Streptococcus sanguinis* SK1 (*S. sanguinis*) under different pH were tested by serial microdilution assays (Liang et al., 2020). When the pH was 5, the MIC of DMAEM against *S. mutans*, *S. sanguinis* and *S. gordonii* were 0.18 µg/mL, 0.37 µg/mL, and 5.95 µg/mL, respectively. The MBC against *S. mutans*, *S. sanguinis* and *S. gordonii* were 1.4 µg/mL, 2.9 µg/mL, and 11.9 µg/mL, respectively. These values indicate a strong antibacterial activity at pH 5.

However, when the pH was 7.4, the MIC and MBC of DMAEM became much higher, at more than 13.5 mg/mL, which meant much lower antibacterial activity (Liang et al., 2020). Therefore, DMAEM was strongly antibacterial only when pH was low and when tooth-protection was most needed. These results indicate that DMAEM was smart and had a pH-sensitive capability (Liang et al., 2020). In addition, the smart DMAEM-modified resin adhesives could successfully combat secondary caries *in vivo* and *in vitro* (Liang et al., 2020). Furthermore, smart DMAEM sealants showed the potential to reduce microleakage, thus preventing dental caries (Li et al., 2021).

To date, there has been no report on pH-sensitive modification of resin infiltrant to inhibit WSLs. Considering the unique pH-responsive feature of DMAEM, which was suitable for the unique acidic environment of WSLs, we designed an intelligent pH-sensitive resin infiltrant containing DMAEM for the first time. The objectives of the present study were to: (1) develop a novel intelligent resin infiltrant containing smart monomer dodecylmethylaminoethyl methacrylate (DMAEM) to inhibit WSLs, and (2) evaluate the cytotoxicity, mechanical properties, biofilm-inhibition and protection of enamel hardness of the novel resin infiltrant. The following

hypotheses were tested: (1) Novel resin infiltrant containing DMAEM could be successfully synthesized; (2) DMAEM resin infiltrant could inhibit biofilm growth and acid production; and (3) DMAEM resin infiltration could protect enamel and retain its hardness after biofilm acid attacks.

2 Methods and materials

2.1 Synthesis of DMAEM and preparation of specimen

According to the work described previously, DMAEM was synthesized and verified (Liang et al., 2020; Li et al., 2021). In brief, 100 mmol of 1-bromododecane was added to 500 mmol of 2-methylamino ethanol in 80 mL isopropanol at room temperature. After stirring for 8-10 h under reflux at 85°C, the mixture was cooled to room temperature and slowly poured into 150 mL of diethyl ether. Then the mixture was washed with deionized water and brine, dried over anhydrous Na_2SO_4 and vacuumized. Then 31.8 mL methylmethacrylate, catalyst CAA (107 mg, 0.4 mol%) and polymerization inhibitor methoxyphenol (100 mg, 2 mol%) were added at room temperature. After stirring at 100-110°C for 12 h, CAA (150 g, 0.6 mol%) was supplementary, and then stirred for another 12 h, cooled to room temperature and evaporated.

According to the study published before, the experimental resin infiltrant contains bisphenol-Adiglycidyl methacrylate (BisGMA, Esstech; Essington, PA, USA), triethylene glycol dimethacrylate (TEGDMA, Esstech; Essington, PA, USA), and a light cure initiator system based on camphorquinone (CQ) and ethyl 4-N, N-dimethylaminobenzoate (4E) (Hashemian et al., 2021; Prodan et al., 2022). DMAEM was mixed with the experimental resin infiltrant in the dark, at a DMAEM mass fraction of 1.25%, 2.5%, 5% and 7.5%, respectively (Table 1). And a magnetic stirrer stirred the mixture constantly for 24 h in a yellow room. The infiltrant + 0% DMAEM group served as the control group.

2.2 Cell viability test

A 96-well plate (Costar; Corning Inc., NY, USA) was used as a mold for the samples (Yu et al., 2020). 5 µL of resin infiltrant were added to each well, and then light-cured for 40 s (Triad 2000; Dentsply, York, PA, USA). To remove the uncured monomers, all the samples were immersed in deionized water for 24 h. The samples were sterilized by ethylene oxide in an ethylene oxide sterilizer (Anprolene AN 74i; Andersen, Haw River, NC, USA). Samples of the same group (n = 6) were immersed in 200 µL of cell medium and soaked at 37 °C for 24 h to obtain the extracts, which were collected and diluted to 10 mL, and the extract was diluted to 36 times, 64 times, 128 times with fresh medium (Zhang et al., 2013; Zhang et al., 2013). The NOKSI immortalized normal oral keratinocyte cell line (provided by Dr. Tao Ma, University of Maryland) were cultured and maintained in keratinocyte serum-free medium with growth factor supplement (Gibco; Thermo, Carlsbad, USA) and 1% antibiotic/antimycotic (AA) (Millipore Sigma; Merck KGaA, Darmstadt, Germany) at a density of 40,000 cells per mL. Cells were cultured at 37°C and 5% CO_2 (Wisniewski et al., 2021). The negative control group was inoculated into the medium without extract. All groups were replaced with fresh medium after 24 h. After 48 h of incubation, 10 µL of CCK-8 solution (Cell Counting Kit-8; Dojindo, Kumamoto, Japan) was added and incubated at a constant temperature incubator for one hour. Optical density (OD) was measured at a wavelength of 450 nm using a microplate reader (SpectraMax M5; Molecular Devices, Sunnyvale, CA, USA). Six replicates were tested for each group.

2.3 Mechanical properties test

Rectangular molds (2 × 2 × 25 mm) were used for mechanical testing (Cheng et al., 2012). After composite bars were immersed in distilled water at 37 °C for 1 d, a computer-controlled Universal Testing Machine (5500R; MTS, Cary, NC, USA) was used to test the mechanical properties. In brief, the specimens were fractured in three-point flexure with a 10-mm span at a crosshead-speed of 1 mm/min. Flexural strength (S) was calculated as: S = 3PmaxL/(2bh2), where Pmax is the fracture load, L is span, b is specimen width, and h means specimen thickness. And, elastic modulus (E) was calculated as: E = (P/d) (L3/[4bh3]), where load P divided by displacement d is the slope of the load-displacement curve in the linear elastic region. Six specimens were tested for each material (n = 6).

TABLE 1   Component of experimental resin infiltrant (%).

Materials	BisGMA	TEGDMA	CQ	4E	DMAEM
Infiltrant + 0% DMAEM (Control)	24	75	0.5	0.5	0
Infiltrant + 1.25% DMAEM	23.7	74.06	0.49	0.49	1.25
Infiltrant + 2.5% DMAEM	23.4	73.13	0.49	0.49	2.5
Infiltrant + 5.0% DMAEM	22.8	71.25	0.48	0.48	5
Infiltrant + 7.5% DMAEM	22.2	69.375	0.4625	0.4625	7.5

2.4 Bacterial inoculation

Saliva derived biofilm was used in the study. Ten healthy individuals without active caries with natural dentition served as donors. Donors did not take any antibiotics in the three months previous to donation and fasted for two hours. The saliva was diluted two-fold with sterile 50% glycerol. Then the saliva was stored at -80 °C (Li et al., 2017).

Each well of 96-well plate with resin infiltrant was added with 300µL Mcbain medium (Yu et al., 2020). The saliva-glycerol stock was seeded (1:50 final dilution) into plates and incubated under aerobic environment at 5% CO_2 with 37 °C. The medium was refreshed every 12 h. After 24 h, phosphate-buffered saline (PBS) was used to rinse the biofilms to remove loose bacteria.

2.5 Anti-bacterial test

2.5.1 Biofilm accumulation

A crystal violet assay was performed to analyze biomass accumulation (Huang et al., 2019). Briefly, each group included six duplicate samples. After the biofilm was rinsed with PBS, 200 µL 95% methyl alcohol was added to each well and incubated for 15 min to fix the biofilm. After the biofilm was rinsed with PBS, submerging in 300 µL 0.1% crystal violet solution for 30 min. Then, washing with PBS. Finally, 300 µL 95% ethanol solution was added to each well and the plate was shaken at 80 rpm for 45 min at room temperature. Subsequently, 100 µL ethanol of the solution from each well was transferred to a 96-well plate, and a microplate reader was used to measure the absorbance of the solution at a wavelength of 595 nm.

2.5.2 MTT test

The biomass accumulation reflects the whole biofilm which contains live cells and dead cells. It is important to evaluate the metabolic activity that was produced by live cells only. In the present study, the MTT (3-(4,5-Dimethyl-thiazol-2-yl)-2,5-diphenyltetrazolium bromide) assay was used to measure metabolic activity (Zhou et al., 2020). Each group involved six duplicate samples. After proliferation for 24 h, the biofilms were rinsed with PBS and 200 µL MTT dye was added to each well (0.5 mg/mL MTT in PBS). Then, the biofilm plates were cultured for 1 h at 37 °C. After removing the MTT solution, 300 µL dimethyl sulfoxide (DMSO) was added and shaken at 80 rpm for 20 min in the dark to dissolve the formazan crystals. Finally, 100 µL of DMSO was placed into a 96-well plate, and the absorbance was read at a wavelength of 540 nm using a microplate reader.

2.5.3 Lactic acid test

First, biofilms were rinsed by cysteine peptone water (CPW) to remove loose bacteria (Cheng et al., 2012). And 300 µL of buffered peptone water (BPW) supplemented with 0.2% sucrose was added, and incubated at 5% CO_2 with 37°C for 3 h to produce acid. After 3 h, the BPW solution was used for lactate analysis. An enzymatic (lactate dehydrogenase) method was used to evaluate the lactate concentrations. Microplate reader was used to measure the absorbance at 340 nm for the collected BPW solutions. Standard curves were prepared using a lactic acid standard (Supelco Analytical; Bellefonte, PA, USA).

2.5.4 Live/dead staining

BacLight Live/Dead Bacterial Viability Kit (Molecular Probes; Eugene, OR, USA) was used in the study (Huang et al., 2021). Live bacteria cells were stained with SYTO 9 to produce green fluorescence, and cells with compromised membranes were stained red by propidium iodide. The disks were examined using inverted epifluorescence microscope (TE2000-S; Nikon, Melville, NY, USA), and percent of live bacteria (%) was calculated by ImageJ software (ImageJ_v1.8.0; National Institutes of Health, USA). Percent of live bacteria (%) = live bacteria/(live bacteria + dead bacteria). Six replicates were tested for each group.

2.5.5 CFU

After 24 h incubation, biofilms were harvested for colony-forming unit (CFU) analysis (Cheng et al., 2016). Three types of agar plates were prepared. First, tryptic soy blood agar culture plates were used to determine the total number of microorganisms. Second, mitis salivarius agar (MSA) culture plates, containing 15% sucrose, were used to determine the total number of *streptococci*. Third, MSA agar culture plates plus 0.2 units of bacitracin per mL were used to determine the number of *mutant streptococci* (Zhang et al., 2012).

2.6 Enamel hardness test

For anti-demineralization test, bovine teeth were used as previously described (Yu et al., 2020). In brief, bovine permanent incisors free of lesions and cracks were selected. Crowns were cut into sections measuring $4 \times 4 \times 2$ mm by using a diamond-coated band saw with continuous water cooling (Isomet; Buehler, Lake Bluff, IL, USA). These surfaces were then ground flat with water-cooled carborundum discs made of waterproof silicon carbide paper (Extec; Enfield, CT, USA) with various grits (1000, 1200, 2400, 3000, and 4000) (Cheng et al., 2008; Iizuka et al., 2014; He et al., 2015). To remove the residual abrasives, all of the polished samples were individually sonicated in distilled water for five minutes.

Initial enamel caries was produced in enamel blocks, as described earlier (Rocha Gomes Torres et al., 2011). The demineralization solution contained 75mM acetic acid (pH 4), 8.7 mM Ca(Cl)$_2$, 8.7 mM KH_2PO_4, and 0.05 ppm NaF (acetic

acid, Ca(Cl)$_2$, KH$_2$PO$_4$, NaF; Biofroxx, Hessen, Germany) (Gao et al., 2020). The blocks were immersed in the demineralization solution (8 mL per block) at 37°C for 16 h with stirring. After dried, 37% phosphoric acid was coated on the demineralization site of the samples for two minutes. Then, rinsed with water for 30 s, and the samples were dried with an air syringe without oil or water. In the demineralization area, 1 μL 99% ethanol was used to dehydrate the area thoroughly. After 30 s, the areas were dried with a water-free and oil-free air syringe. Resin-infiltrant (1 μL) was applied to the demineralized zone for three minutes. After removing the excess material, the area was light-cured for 40 s. Afterward, infiltrant was applied again. After one minute, the excess material was removed again and light-cured for 60 s (Figure 1). All samples were sterilized in an ethylene oxide sterilizer.

Enamel hardness was measured before the demineralized treatment, after demineralization in acid solution, after resin infiltration and after demineralization under biofilms. A hardness tester (Shimadzu HMV-2000, Kyoto, Japan) was employed using a Vickers diamond indenter with a load of 25 g for 5 s dwell time (Liang et al., 2019; Gao et al., 2020). Six indentations were made in each enamel specimens, and each group had six specimens.

2.7 Statistical analysis

Statistical analyses were performed with SPSS, version 22.0 (SPSS; Chicago, IL, USA). One-way analysis of variance (ANOVA) was performed to detect the significant effects of the variables. Tukey's multiple comparison test was used to compare the means of each group at a p-value of 0.05.

3 Results

Cell viability results of resin infiltrant are plotted in Figure 2. Results showed that all the groups except for infiltrant + 7.5% DMAEM group ($p < 0.05$) had acceptable cell viability ($p > 0.05$).

Mechanical properties of resin infiltrant are shown in Figure 3. All DMAEM resin infiltant had flexural strength and elastic modulus comparable to the infiltrant + 0% DMAEM group (control), which are around 130 MPa and 4 GPa respectively ($p > 0.05$). The DMAEM modification did not affect the mechanical properties of resin infiltrant.

Figure 4 showed the quantification of biofilm viability. MTT assay showed that the metabolism of biofilm decreased with the increase of DMAEM concentration ($p < 0.05$), while the infiltrant + 1.25% DMAEM group didn't show significant difference ($p > 0.05$). Crystal violet assay and lactic acid production assay plotted similar results, with the increase of DMAEM concentration, the biofilm accumulation and the lactic acid production decreased ($p < 0.05$).

CFU is plotted in Figure 5. For total microorganisms, compared to the infiltrant + 0% DMAEM group (control), the infiltrant + 1.25% DMAEM group reduced around 1 log, the infiltrant + 2.5% DMAEM group reduced more than 2 logs, and the infiltrant + 5% DMAEM group reduced more than 3 logs ($p < 0.05$). CFU has reduced the total *streptococci* counts by around 1 log from the infiltrant + 0% DMAEM group (control) to the infiltrant + 1.25% DMAEM group, by more than 2 logs to the infiltrant + 2.5% DMAEM group, and by more than 4 logs to the infiltrant + 5% DMAEM group ($p < 0.05$). For *mutans streptococci* counts, the infiltrant + 1.25% DMAEM group reduced around 1 log, the infiltrant + 2.5% DMAEM group reduced around 2 logs, and the infiltrant + 5% DMAEM group reduced more than 3 logs compared to the control group ($p < 0.05$).

Live/dead staining images (Figure 6) showed that the infiltrant + DMAEM groups had much more red staining, indicating a strong anti-bacterial effect, while the infiltrant + 0% DMAEM group (control) had more green staining and little red staining, which represented little anti-biofilm activity. Figure 6E showed live/dead ratio, the infiltrant + DMAEM groups had lower percent of live bacteria ($p < 0.05$), and the percent of live bacteria decreased with increasing DMAEM concentration ($p < 0.05$).

Enamel hardness test is plotted in Figure 7. Results showed that the hardness of enamel decreased after being demineralized in acid solution ($p < 0.05$), while the resin infiltration recovered the hardness ($p > 0.05$) (Figure 7A). After 48 h biofilm demineralization, the hardness of all the groups except for the infiltrant + 5% DMAEM group decreased ($p < 0.05$). After two stages of demineralization: first in acid solution, second in biofilm culture, the enamel showed the lowest hardness in all the group ($p < 0.05$). While the hardness value increased as the increasing of the DMAEM concentration ($p < 0.05$) (Figure 7B).

4 Discussion

In the present study, a novel pH-sensitive DMAEM infiltrant with antibacterial and anti-demineralizing properties was developed. The hypotheses were proven that the new resin infiltrant had the acceptable mechanical properties without jeopardizing the biocompability, which had normal oral keratinocyte viability similar to that of the infiltrant + 0% DMAEM group (control). Additionally, the antibacterial effect enhanced the anti-demineralizing properties under the attack of biofilm for 7 days.

New materials used for dental treatment are required to be non-cytotoxic and biocompatible. In the present study, cytotoxicity test was carried out according to ISO 10993-5-2016 standard (Li et al., 2015). According to the ISO standard, *in vitro* cytotoxicity tests, the MTT value is not less than 80% prove to be slightly cytotoxic (Li et al., 2015). NOKSI were used in the present study because they are clinically relevant and in close proximity to
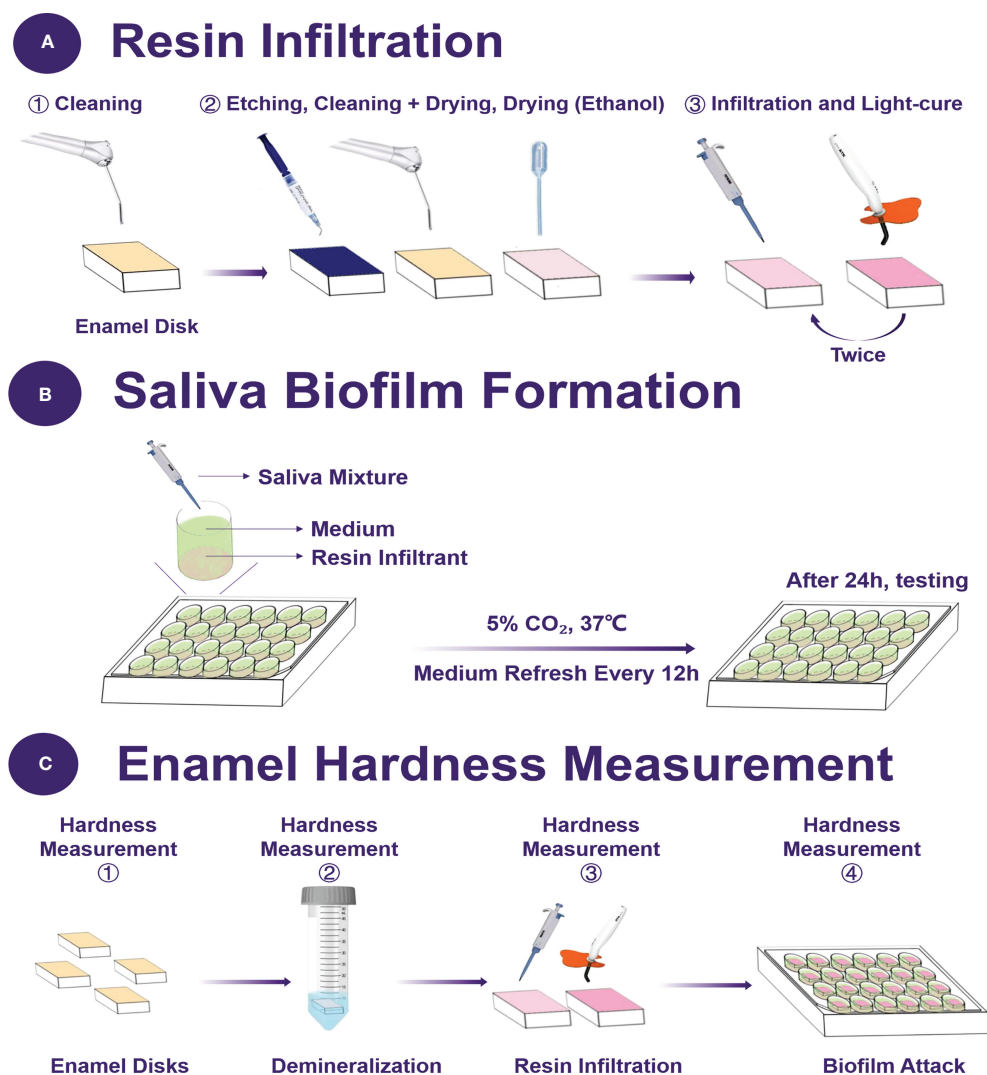
FIGURE 1

Schematic of the experimental design. **(A)** The protocol of resin infiltration, **(B)** the saliva biofilm formation on the resin disks, **(C)** the time point of enamel hardness measurement.

dental restorations. Our findings suggest that the new resin infiltrant did not induce any significant toxicity when the mass fraction of DMAEM was below 5%, which was similar to the previous study (Liang et al., 2020). Therefore, the concentration of subsequent experiments was selected. These findings indicate that DMAEM resin infiltrant is suitable for clinical applications. Future *in vivo* experiments are needed to investigate the biocompatibility of the infiltrant containing DMAEM.

Mechanical properties of resin infiltrant may influence the hardness of the enamel, as well as the longevity of treatment (Paris et al., 2013). To evaluate whether DMAEM would jeopardize the mechanical properties, we made the resin infiltrant into a cuboid with the size of $2 \times 2 \times 25$ mm. The result demonstrated that the modification did not affect the mechanical properties of resin infiltrant ($p > 0.05$). In detail, flexural strength of the resin infiltrant was around 120-130 MPa, while the elastic modulus was about 4 GPa, which were similar to other results (Prodan et al., 2022). The DMAEM could covalently grafted to resin infiltrant by reaction of acrylate groups with methacrylate groups, yielding the non-release antibacterial dental material. The covalent binding explained the similar mechanical properties of infiltant + DMAEM groups to the control group. The mechanism was similar to that of the DMADDM-modified and DMAHDM-modified dental resins, which had been reported before (Han et al., 2017; Cheng et al., 2017).
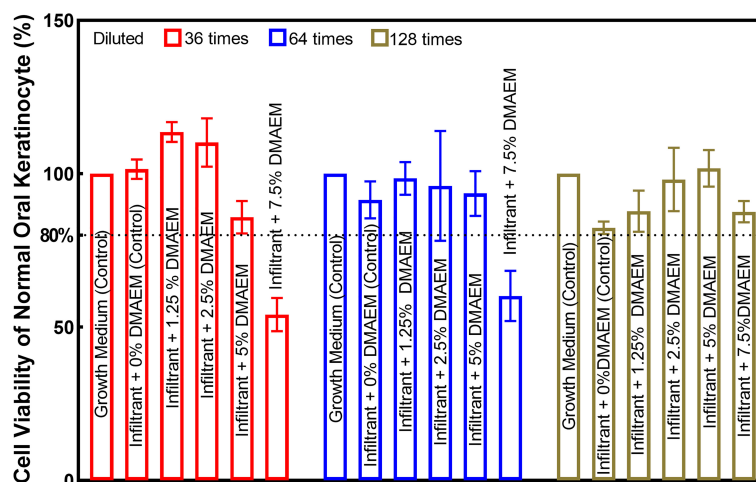
FIGURE 2
Cell viability of normal oral keratinocyte was used to test the biocompability of DMAEM resin infiltrant. The viability was acceptable when that was not less than 80% of the control group according to ISO 10993-5-2016 standard.

WSLs are early-stage of dental caries, which are common side effects of orthodontic treatments (Paula et al., 2017). WSLs are caused by cariogenic biofilm, leading to demineralization of the enamel (Zou et al., 2018). In detail, during the dental caries, the oral microbial diversity is decreased, cariogenic microorganisms proliferate, whereas pH value decreases in a certain period of time (Zou et al., 2018). The balance of demineralization and re-mineralization is shifted to mineral loss, finally the caries is formed (Zou et al., 2018). Therefore, biofilm inhibition is the first step to solve WSLs (Abdullah and John, 2016; Horst, 2018).

The resin infiltration concept was first developed in the 1970's (Cheng et al., 2017), low viscosity resin materials had been used to restore decalcified enamel at that time (Paula et al., 2017; Zou et al., 2018), such as sealant and adhesive. At the end of the 2000's, with the development of dental materials, resin infiltrant was applied for caries arrestment, which meet the principle of microinvasive therapies nowadays (Borges et al., 2017). With resin infiltration, demineralization of enamel is hampered, for the reason a diffusion barrier of acids produced by biofilm is created (Paris et al., 2020). A three-year follow-up clinical study revealed that resin infiltration reduced 65-90% of the risk of caries compared with varying self-applied non-invasive interventions alone (Paris et al., 2020). However, it was difficult for infiltration treatment when lesions extending into deeper enamel or even dentine: complete penetration is less reliable (Yim et al., 2014; Min et al., 2015). Furthermore, it has been reported that the application of resin infiltrant can only seal off around 30-60% of lesion depth (Yim et al., 2014; Min et al., 2015). In addition, enamel surfaces are constantly exposed to the oral microflora, many *in vitro* studies reported that there even was a hardness loss for the resin-infiltrated area after acid attack (Tawakoli et al., 2016). Common methacrylates in restorative materials, such as TEGDMA and BisGMA, do not possess strong antimicrobial activities (Flor-Ribeiro et al., 2019). To give the material antibacterial properties, researchers added antibacterial agents into resin infiltrant. Several studies modified the materials with AgNP (Kielbassa et al., 2020), quaternary ammonium methacrylate (Yu et al., 2020), ionic liquid (Cuppini et al., 2021), etc., which has potential results. But they had the same limitation, that is killing all the bacteria instead of showing an antibacterial effect only during microdysbiosis. They not only killed cariogenic bacteria, but also inhibited probiotics, the balance of oral eubiosis was affected once again (Liang et al., 2020; Li et al., 2021). Thus, a novel intelligent antibacterial resin infiltrant was needed.

We modified the resin infiltrant with DMAEM at the first time, which showed an antibacterial effect only during microdysbiosis. The total microorganisms were reduced by 1-4 logs. And the CFUs of *Mutans Streptococci* were reduced by 1-3 logs. Moreover, lactic acid production of the infiltrant + 5% DMAEM group was greatly reduced, which reduced by 92% compared to the infiltrant + 0% DMAEM group (control). Metabolic ability and biofilm accumulation were all reduced significantly with the increase of DMAEM concentration ($p < 0.05$). Therefore, the new intelligent resin infiltrant containing DMAEM are promising to inhibit biofilm growth. The pH-sensitive ability of DMAEM confers intelligent antibacterial properties to the novel resin infiltrant. DMAEM is a kind of intelligent materials, that could respond to the decrease of pH. In our previous work, DMAEM showed strong antibacterial
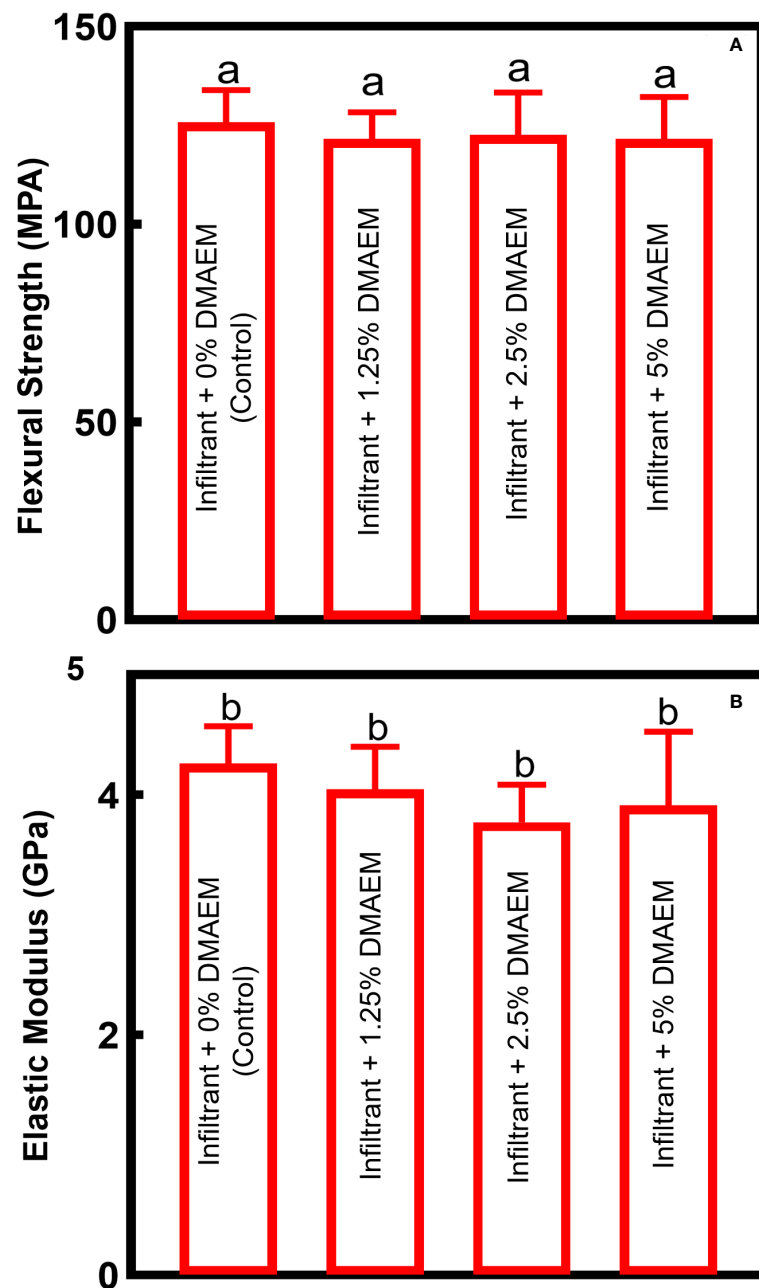
FIGURE 3
Mechanical properties of DMAEM resin infiltran. **(A)** The flexural strength, **(B)** the elastic modulus (mean $\pm$ SD; n = 6). The different letters indicate the significant difference between the bars (a, b, c), there were no significant difference among the four groups (p > 0.05).

effects when pH was 5. While when pH was 7.4, the MIC and MBC of DMAEM were more than 13.5, which showed lower antibacterial activity (Liang et al., 2020). Both *in vivo* and *in vitro* experiments indicated that in resin adhesives, DMAEM provided long-term antibacterial effect *via* its reversible pH-responsive activity (Liang et al., 2020). And DMAEM sealant demonstrated possibility to prevent microleakage in sealant application (Li et al., 2021). Also, it has been proved that DMAEM could maintain the diversity of oral microbiome, and was friendly to commensal microbiota due to its pH-sensitive activity (Liang et al., 2020). The reason why DMAEM showed antibacterial effect when pH was 5 is for the nitrogen atoms of DMAEM. In lower pH, the nitrogen atoms could be protonated
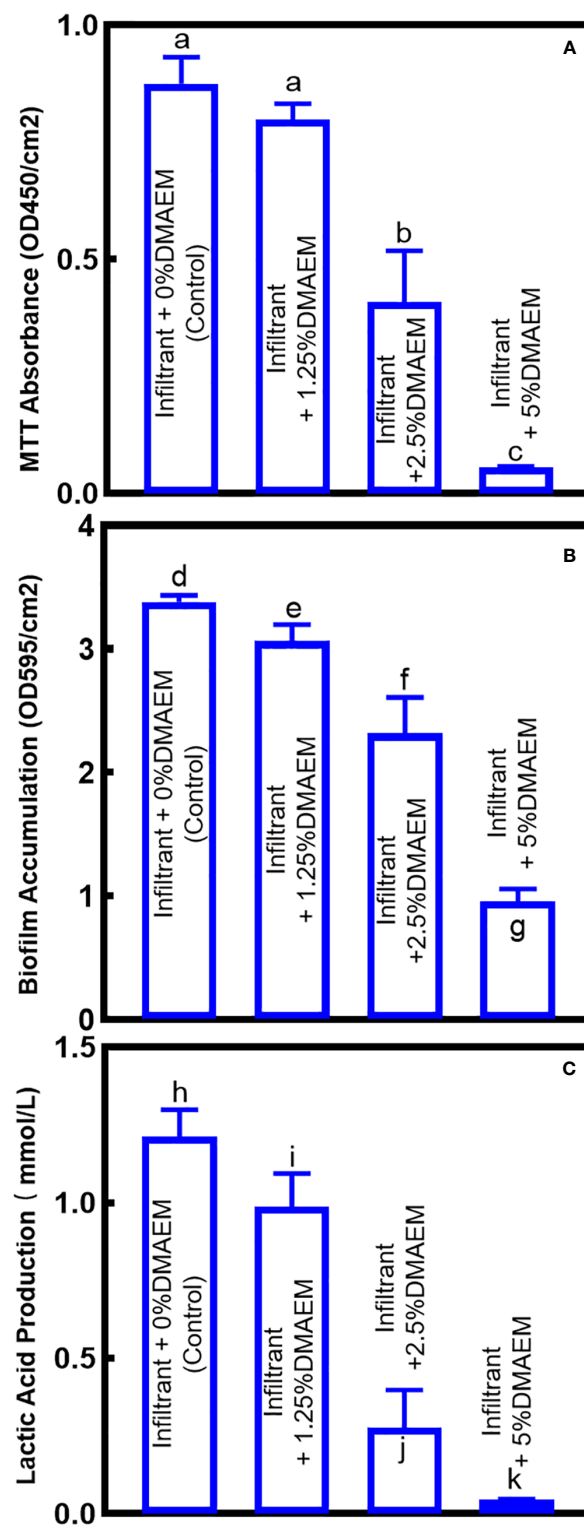
FIGURE 4
Antibacterial effects of composites on saliva-derived biofilm. **(A)** The biofilm metabolism evaluation, **(B)** biofilm accumulation, **(C)** production of lactic acid of the biofilm sites (mean $\pm$ SD; n = 6). The different letters indicate the significant difference between the bars (a, b, c).
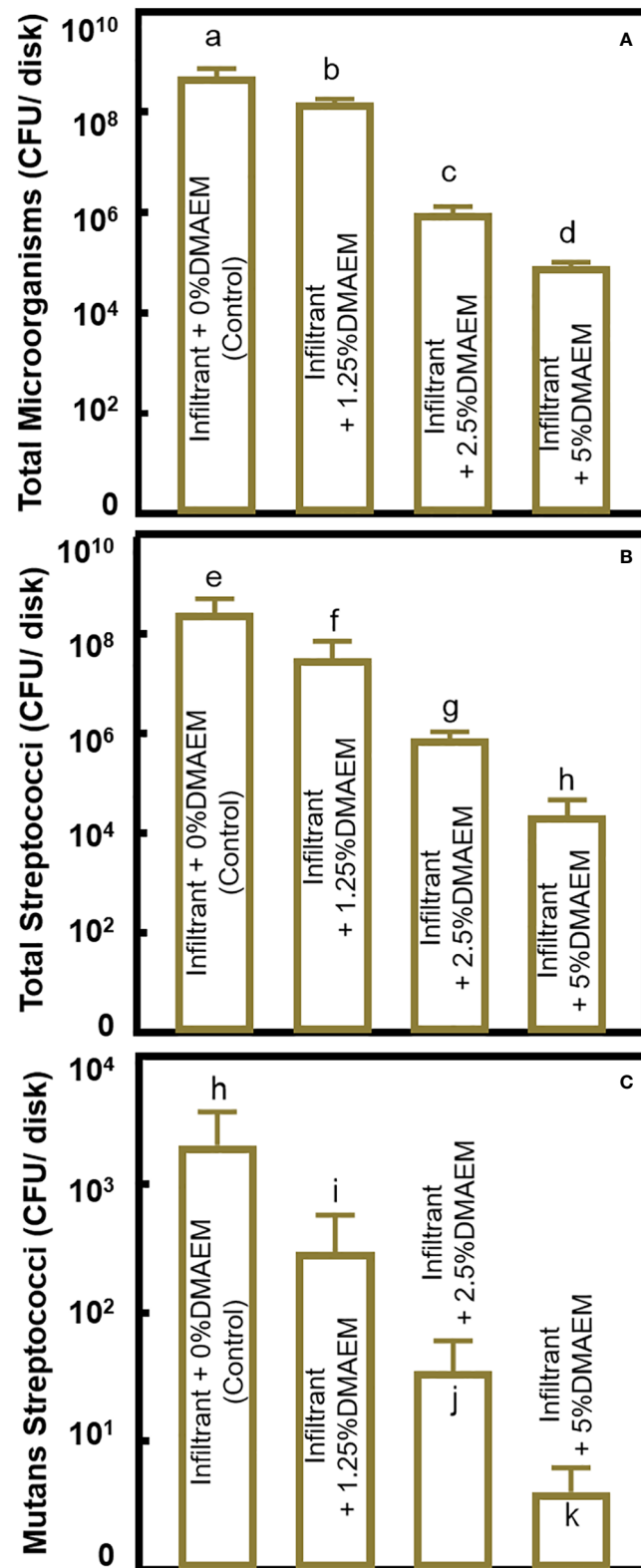
FIGURE 5

CFUs of the biofilm. **(A)** CFU of total microorganisms, **(B)** CFU of total *streptococci*, **(C)** CFU of *mutans streptococci* (mean ± SD; n = 6). The different letters indicate the significant difference between the bars (a, b, c).
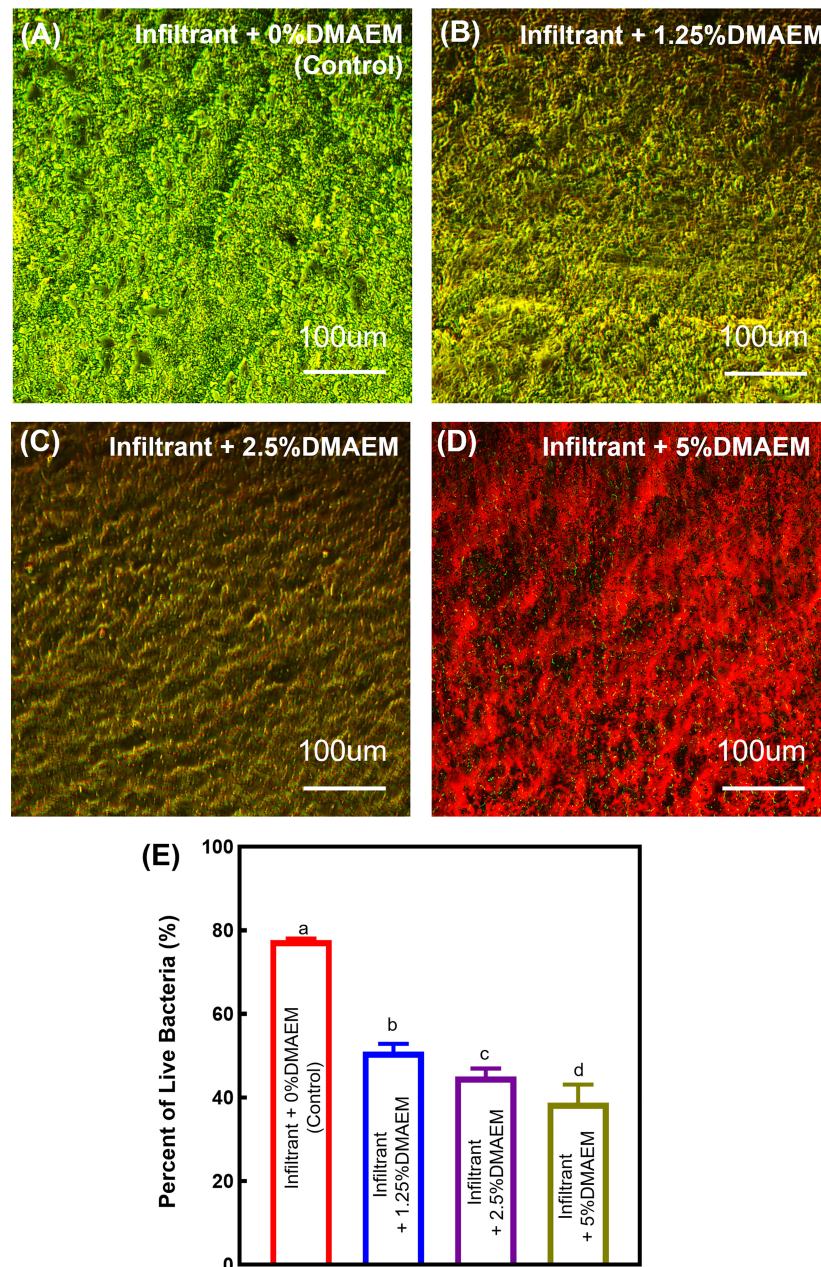
FIGURE 6
Representative images of live/dead stained biofilms grown for 24 h on composites. (A) Infiltrant + 0% DMAEM group, (B) infiltrant + 1.25% DMAEM group, (C) infiltrant + 2.5% DMAEM group, (D) infiltrant + 5% DMAEM group, (E) percent of live bacteria(%). Live bacteria were stained green and dead bacteria were stained red. Infiltrant + 0% DMAEM group had primarily live bacteria, while infiltrant + 5% DMAEM group produced mostly red staining.

to form QAMs, which showed strong antibacterial effect, while as pH increases, they are deprotonated and returned to DMAEM structure (Liang et al., 2020; Li et al., 2021). QAMs were proved strong antibacterial effect: the electrostatic interaction between the negatively-charged bacterial cell membrane and the positively-charged (N+) sites of a QAM resin causes the bacterium bursts; in addition, QAMs with long alkyl chains can physically pierce the

bacterial cell wall, puncturing the cell membrane and releasing its cellular contents (Cheng et al., 2017). Therefore, DMAEM resin infiltrant could overcome the limitations of the present materials. Although DMAEM yielded covalently grafting to the resin infiltrant, which should have a long-term effect theoretically, future experiments are still needed to investigate the longevity of antibacterial effect.
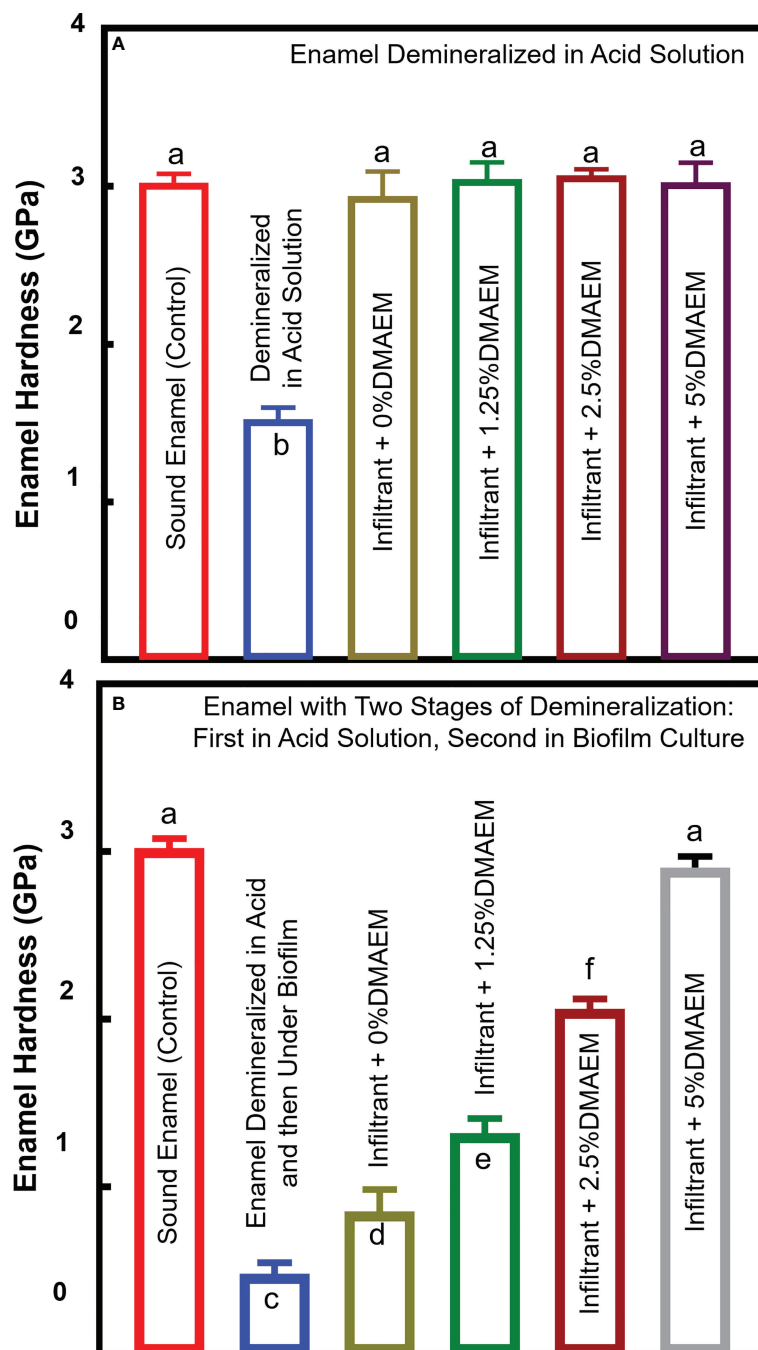
FIGURE 7

Enamel hardness. **(A)** Enamel samples were demineralized in acid solution, after then, infiltrant was applied as Figure 1. **(B)** Enamel samples were first demineralized like **(A)** and after infiltration, all the samples were second demineralized under biofilm (mean $\pm$ SD; n = 6). The different letters indicate the significant difference between the bars (a, b, c). The resin infiltration showed similar hardness value of sound enamel ($p > 0.05$), and after biofilm attack, only the hardness of the infiltrant + 5% DMAEM group did not decrease ($p > 0.05$).

Enamel surfaces are constantly exposed to the oral microflora (Arslan et al., 2015). Therefore, we used a saliva-derived biofilm to evaluate antibacterial effect and anti-demineralization effect of resin infiltrant. To simulate the

conditions of caries, sucrose was added to the culture medium. Thus, cariogenic bacteria such as *S. mutans* and *Lactobacilli* metabolize carbohydrates to acids, causing demineralization of the tooth structure and the tooth-restoration margins beneath

the biofilm (Cheng et al., 2012). Furthermore, to imitating an extreme clinical situation, and allowing demineralization to occur in a short time, the biofilms were cultured for 7 days continuously. The biofilm model successfully resulted in significant demineralization within 7 days, comparable to that with the use of a chemically-prepared acidic gel system for 21 days (Zhang et al., 2019). The biofilm model used in this study had main advantages over the traditional chemically-induced demineralization. It is more clinically relevant as it mimics a cariogenic situation, and it takes less time to construct a caries demineralization model.

Demineralization, which could reduce the enamel hardness, is an important process as well as outcome in the occurrence of WSLs. The microorganisms along the demineralized area could re-penetrate deeper, leading to further demineralization, and finally the cavities formed (Paris et al., 2013; Neres et al., 2017). Therefore, it is important to evaluate whether the resin infiltrant can inhibit demineralization. It has been proved that resin infiltrant could significantly increase both micro-hardness and demineralization resistance of enamel, which prevent or reduce the progression of caries (Brignardello-Petersen, 2020). Reported surface micro-hardness (352 HVN ≈ 3.45 GPa) for sound human enamel was consistent with sound bovine enamel hardness in our study; moreover, the hardness of natural carious enamel (0.29-3.29 GPa) was similar to hardness of artificial caries found in this study, either (Maupomé et al., 1998; Huang et al., 2010; Paris et al., 2013). After resin infiltration, the hardness of demineralized enamel recovered as sound enamel. It is doubtful whether the hardness could recover after resin infiltration. Some studies showed that the hardness of infiltrated enamel was less than sound enamel, while others showed increased hardness value (Maupomé et al., 1998; Huang et al., 2010; Paris et al., 2013; Dai et al., 2022). For instance, in Dai's *in vitro* study, the enamel treated with ICON showed lower hardness (1.7 GPa) compared to sound enamel and experimental resin infiltrant containing TEGDMA and BisGMA (Dai et al., 2022). The reason may be that the ICON infiltrant possessed a polymer network mainly consisting of TEGDMA, which composition is likely to lead to lower hardness properties for the ICON infiltrant (Chen et al., 2019; Dai et al., 2022). Furthermore, BisGMA and TEGDMA based infiltrants may reduce polymerization shrinkage due to higher molecular weight (Paris et al., 2013). And except for the different materials, the operation could be another reason. For example, removing the excess infiltrant, polishing the surface, and the way to etch the surface could be different, that may influence the outcome (Zakizade et al., 2020). Then, after one-week biofilm attack, the hardness decreased again except for

the infiltrant + 5% DMAEM group. In addition, the hardness value increases with the increase of DMAEM concentration. Our results indicated that under the cariogenic microbial environment, the resin infiltant may not be enough to resist demineralization. The possible reason for the continued decrease in the other groups is the continuous biofilm attack under an extremely severe cariogenic condition, for three reasons. First, unlike the oral environment, brushing teeth or chewing will partially eliminate the biofilm. Second, there wasn't any buffer in the medium, and more sugar was added to mimic an environment prone to caries, and that was much more aggressive than what happened intraorally, where the saliva served as a buffer. Third, no source of minerals for remineralization was added in the medium, but there were minerals in the saliva intraorally. Considering resin infiltrant only seals the demineralized area, and the DMAEM resin infiltrant was a contact antibacterial material, future studies could combine release type of antimicrobial agent to further prevent the caries progression. Furthermore, although the experimental resin infiltrant was used in several studies, it did not outperform the commercial infiltrant (Paris et al., 2013), so more work needs to be done before it can be applied clinically.

Under these conditions, with the modification by DMAEM, the novel resin infiltrant showed comparable biocompability, mechanical properties, and strong antibacterial effect in an acidic environment. Moreover, these results demonstrated the anti-demineralization properties in the carious oral environment, which could prevent the progression of WSLs.

5 Conclusion

Development of novel dental materials that show an antibacterial effect only during microdysbiosis is an ideal way to inhibiting WSLs while maintaining a healthy oral eubiosis. In the present study, a novel pH-sensitive resin infiltrant containing DMAEM was synthesized for the first time. The new resin infiltrant presented good biocompability when the mass fraction of DMAEM was below 5% ($p > 0.05$). Biofilm metabolic activities, biofilm biomass, lactic acid production were substantially reduced, and biofilm CFU was reduced by up to 3 log. After acid attack by acid solution and then under by biofilms, the infiltrant + 5% DMAEM group produced an enamel hardness of 2.90 GPa, much higher than 0.85 GPa of the control infiltrant + 0% DMAEM group. Therefore, the novel intelligent resin infiltrant is highly promising for enamel infiltration to protect tooth structures and inhibit dental caries.

Data availability statement

The original contributions presented in the study are included in the article/supplementary material. Further inquiries can be directed to the corresponding authors.

Author contributions

XH and JL: Conceptualization, Methodology, Investigation, Writing - original draft. WZ, TM, and MW: Investigation. GH, GF, and TO: review & editing. HX and LC: Conceptualization, review & editing, project administration. XH, JL and LC: Funding acquisition. All authors contributed to the article and approved the submitted version.

Funding

Conflict of interest

The authors declare that the research was conducted in the absence of any commercial or financial relationships that could be construed as a potential conflict of interest.

Publisher's note

All claims expressed in this article are solely those of the authors and do not necessarily represent those of their affiliated organizations, or those of the publisher, the editors and the reviewers. Any product that may be evaluated in this article, or claim that may be made by its manufacturer, is not guaranteed or endorsed by the publisher.

References

Abdullah, Z., and John, J. (2016). Minimally invasive treatment of white spot lesions–a systematic review. *Oral. Health Prev. Dent.* 14 (3), 197–205. doi: 10.3290/j.ohpd.a35745

Arslan, S., Zorba, Y. O., Atalay, M. A., Ozcan, S., Demirbuga, S., Pala, K., et al. (2015). Effect of resin infiltration on enamel surface properties and streptococcus mutans adhesion to artificial enamel lesions. *Dent. Mater J.* 34 (1), 25–30. doi: 10.4012/dmj.2014-078

Borges, A. B., Caneppele, T. M., Masterson, D., and Maia, L. C. (2017). Is resin infiltration an effective esthetic treatment for enamel development defects and white spot lesions? a systematic review. *J. Dent.* 56, 11–18. doi: 10.1016/j.jdent.2016.10.010

Brignardello-Petersen, R. (2020). Resin infiltration reduces the risk of experiencing proximal caries progression after 7 years. *J. Am. Dent. Assoc.* 151 (8), e67. doi: 10.1016/j.adaj.2020.02.005

Cheng, L., Li, J., Hao, Y., and Zhou, X. (2008). Effect of compounds of galla chinensis and their combined effects with fluoride on remineralization of initial enamel lesion *in vitro*. *J. Dent.* 36 (5), 369–373. doi: 10.1016/j.jdent.2008.01.011

Cheng, L., Weir, M. D., Xu, H. H., Antonucci, J. M., Kraigsley, A. M., Lin, N. J., et al. (2012). Antibacterial amorphous calcium phosphate nanocomposites with a quaternary ammonium dimethacrylate and silver nanoparticles. *Dent. Mater* 28 (5), 561–572. doi: 10.1016/j.dental.2012.01.005

Cheng, L., Zhang, K., Melo, M. A., Weir, M. D., Zhou, X., and Xu, H. H. (2012). Anti-biofilm dentin primer with quaternary ammonium and silver nanoparticles. *J. Dent. Res.* 91 (6), 598–604. doi: 10.1177/0022034512444128

Cheng, L., Zhang, K., Zhang, N., Melo, M. A. S., Weir, M. D., Zhou, X. D., et al. (2017). Developing a new generation of antimicrobial and bioactive dental resins. *J. Dent. Res.* 96 (8), 855–863. doi: 10.1177/0022034517709739

Cheng, L., Zhang, K., Zhou, C. C., Weir, M. D., Zhou, X. D., and Xu, H. H. (2016). One-year water-ageing of calcium phosphate composite containing nano-silver and quaternary ammonium to inhibit biofilms. *Int. J. Oral. Sci.* 8 (3), 172–181. doi: 10.1038/ijos.2016.13

Chen, M., Li, J. Z., Zuo, Q. L., Liu, C., Jiang, H., and Du, M. Q. (2019). Accelerated aging effects on color, microhardness and microstructure of ICON

resin infiltration. *Eur. Rev. Med. Pharmacol. Sci.* 23 (18), 7722–7731. doi: 10.26355/eurrev_201909_18981

Cuppini, M., Garcia, I. M., de Souza, V. S., Zatta, K. C., Visioli, F., Leitune, V. C. B., et al. (2021). Ionic liquid-loaded microcapsules doped into dental resin infiltrants. *Bioact. Mater* 6 (9), 2667–2675. doi: 10.1016/j.bioactmat.2021.02.002

Dai, Z., Xie, X., Zhang, N., Li, S., Yang, K., Zhu, M., et al. (2022). Novel nanostructured resin infiltrant containing calcium phosphate nanoparticles to prevent enamel white spot lesions. *J. Mech. Behav. BioMed. Mater.* 126, 104990. doi: 10.1016/j.jmbbm.2021.104990

Fenton, O. S., Olafson, K. N., Pillai, P. S., Mitchell, M. J., and Langer, R. (2018). Advances in biomaterials for drug delivery. *Advanced materials (Deerfield Beach Fla.)* 30 ,e1705328. doi: 10.1002/adma.201705328

Flor-Ribeiro, M. D., Graziano, T. S., Aguiar, F. H. B., Stipp, R. N., and Marchi, G. M. (2019). Effect of iodonium salt and chitosan on the physical and antibacterial properties of experimental infiltrants. *Braz. Oral. Res.* 33, e075. doi: 10.1590/1807-3107bor-2019.vol33.0075

Gao, Y., Liang, K., Weir, M. D., Gao, J., Imazato, S., Tay, F. R., et al. (2020). Enamel remineralization *via* poly(amido amine) and adhesive resin containing calcium phosphate nanoparticles. *J. Dent.* 92, 103262. doi: 10.1016/j.jdent.2019.103262

Han, Q., Li, B., Zhou, X., Ge, Y., Wang, S., Li, M., et al. (2017). Anti-caries effects of dental adhesives containing quaternary ammonium methacrylates with different chain lengths. *Materials (Basel)* 10 (6), 643. doi: 10.3390/ma10060643

Hashemian, A., Shahabi, S., Behroozibakhsh, M., Najafi, F., Abdulrazzaq Jerri Al-Bakhakh, B., and Hajizamani, H. (2021). A modified TEGDMA-based resin infiltrant using polyurethane acrylate oligomer and remineralising nano-fillers with improved physical properties and remineralisation potential. *J. Dent.* 113, 103810. doi: 10.1016/j.jdent.2021.103810

He, L., Deng, D., Zhou, X., Cheng, L., ten Cate, J. M., Li, J., et al. (2015). Novel tea polyphenol-modified calcium phosphate nanoparticle and its remineralization potential. *J. BioMed. Mater Res. B Appl. Biomater* 103 (8), 1525–1531. doi: 10.1002/jbm.b.33333

Horst, J. A. (2018). Silver fluoride as a treatment for dental caries. *Adv. Dent. Res.* 29 (1), 135–140. doi: 10.1177/0022034517743750

Huang, X., Ge, Y., Yang, B., Han, Q., Zhou, W., Liang, J., et al. (2021). Novel dental implant modifications with two-staged double benefits for preventing infection and promoting osseointegration *in vivo* and *in vitro*. *Bioact. Mater* 6 (12), 4568–4579. doi: 10.1016/j.bioactmat.2021.04.041

Huang, T. T., He, L. H., Darendeliler, M. A., and Swain, M. V. (2010). Nano-indentation characterisation of natural carious white spot lesions. *Caries Res.* 44 (2), 101–107. doi: 10.1159/000286214

Huang, X., Zhou, W., Zhou, X. D., Hu, Y., Xiang, P., Li, B., et al. (2019). Effect of novel micro-arc oxidation implant material on preventing peri-implantitis. *Coatings* 9 (11), 691. doi: 10.3390/coatings9110691

Iizuka, J., Mukai, Y., Taniguchi, M., Mikuni-Takagaki, Y., Ten Cate, J. M., and Teranaka, T. (2014). Chemical alteration by tooth bleaching of human salivary proteins that infiltrated subsurface enamel lesions–experimental study with bovine lesion model systems. *Dent. Mater J.* 33 (5), 663–668. doi: 10.4012/dmj.2014-046

Kielbassa, A. M., Leimer, M. R., Hartmann, J., Harm, S., Pasztorek, M., and Ulrich, I. B. (2020). Ex vivo investigation on internal tunnel approach/internal resin infiltration and external nanosilver-modified resin infiltration of proximal caries exceeding into dentin. *PloS One* 15 (1), e0228249. doi: 10.1371/journal.pone.0228249

Kielbassa, A. M., Muller, J., and Gernhardt, C. R. (2009). Closing the gap between oral hygiene and minimally invasive dentistry: A review on the resin infiltration technique of incipient (Proximal) enamel lesions. *Quintessence Int.* 40 (8), 663–681.

Leila, B., Nemati, S., Neda, H., and Khanehmasjedi, M. (2017). The effect of MIpaste plus and reminpro on incipient caries using DIAGNOdent and SEM: An invitro study. *J. Natl. Med. Assoc.* 109 (3), 192–197. doi: 10.1016/j.jnma.2017.02.009

Liang, J., Liu, F., Zou, J., Xu, H. H. K., Han, Q., Wang, Z., et al. (2020). pH-responsive antibacterial resin adhesives for secondary caries inhibition. *J. Dent. Res.* 99 (12), 1368–1376. doi: 10.1177/0022034520936639

Liang, K., Wang, S., Tao, S., Xiao, S., Zhou, H., Wang, P., et al. (2019). Dental remineralization *via* poly(amido amine) and restorative materials containing calcium phosphate nanoparticles. *Int. J. Oral. Sci.* 11 (2), 15. doi: 10.1038/s41368-019-0048-z

Li, B., Ge, Y., Wu, Y., Chen, J., Xu, H. H. K., Yang, M., et al. (2017). Anti-bacteria and microecosystem-regulating effects of dental implant coated with dimethylaminododecyl methacrylate. *Molecules* 22 (11), 2013. doi: 10.3390/molecules22112013

Li, H., Huang, Y., Zhou, X., Zhu, C., Han, Q., Wang, H., et al. (2021). Intelligent pH-responsive dental sealants to prevent long-term microleakage. *Dent. Mater* 37, 1529–1541. doi: 10.1016/j.dental.2021.08.002

Li, W., Qi, M., Sun, X., Chi, M., Wan, Y., Zheng, X., et al. (2020). Novel dental adhesive containing silver exchanged EMT zeolites against cariogenic biofilms to combat dental caries. *Microporous Mesoporous Materials* 299, 110113. doi: 10.1016/j.micromeso.2020.110113

Li, W., Zhou, J., and Xu, Y. (2015). Study of the *in vitro* cytotoxicity testing of medical devices. *BioMed. Rep.* 3 (5), 617–620. doi: 10.3892/br.2015.481

Maupomé, G., Díez-de-Bonilla, J., Torres-Villaseñor, G., Andrade-Delgado, L. C., and Castaño, V. M. (1998). *In vitro* quantitative assessment of enamel microhardness after exposure to eroding immersion in a cola drink. *Caries Res.* 32 (2), 148–153. doi: 10.1159/000016445

Min, J. H., Inaba, D., Kwon, H. K., Chung, J. H., and Kim, B. I. (2015). Evaluation of penetration effect of resin infiltrant using optical coherence tomography. *J. Dent.* 43 (6), 720–725. doi: 10.1016/j.jdent.2015.03.006

Neres, E. Y., Moda, M. D., Chiba, E. K., Briso, A., Pessan, J. P., and Fagundes, T. C. (2017). Microhardness and roughness of infiltrated white spot lesions submitted to different challenges. *Oper Dent.* 42 (4), 428–435. doi: 10.2341/16-144-L

Paris, S., Bitter, K., Krois, J., and Meyer-Lueckel, H. (2020). Seven-year-efficacy of proximal caries infiltration - randomized clinical trial. *J. Dent.* 93, 103277. doi: 10.1016/j.jdent.2020.103277

Paris, S., Schwendicke, F., Seddig, S., Müller, W. D., Dörfer, C., and Meyer-Lueckel, H. (2013). Micro-hardness and mineral loss of enamel lesions after infiltration with various resins: influence of infiltrant composition and application frequency *in vitro*. *J. Dent.* 41 (6), 543–548. doi: 10.1016/j.jdent.2013.03.006

Paula, A. B., Fernandes, A. R., Coelho, A. S., Marto, C. M., Ferreira, M. M., Caramelo, F., et al. (2017). Therapies for white spot lesions-a systematic review. *J. Evid Based Dent. Pract.* 17 (1), 23–38. doi: 10.1016/j.jebdp.2016.10.003

Peres, M. A., Macpherson, L. M. D., Weyant, R. J., Daly, B., Venturelli, R., Mathur, M. R., et al. (2019). Oral diseases: a global public health challenge. *Lancet* 394 (10194), 249–260. doi: 10.1016/s0140-6736(19)31146-8

Pitts, N. B., Zero, D. T., Marsh, P. D., Ekstrand, K., Weintraub, J. A., Ramos-Gomez, F., et al. (2017). Dental caries. *Nat. Rev. Dis. Primers* 3, 17030. doi: 10.1038/nrdp.2017.30

Prodan, D., Moldovan, M., Chisnoiu, A. M., Saroşi, C., Cuc, S., Filip, M., et al. (2022). Development of new experimental dental enamel resin infiltrants-synthesis and characterization. *Materials (Basel)* 15 (3), 803. doi: 10.3390/ma15030803

Rocha Gomes Torres, C., Borges, A. B., Torres, L. M., Gomes, I. S., and de Oliveira, R. S. (2011). Effect of caries infiltration technique and fluoride therapy on the colour masking of white spot lesions. *J. Dent.* 39 (3), 202–207. doi: 10.1016/j.jdent.2010.12.004

Rosier, B. T., Marsh, P. D., and Mira, A. (2018). Resilience of the oral microbiota in health: Mechanisms that prevent dysbiosis. *J. Dent. Res.* 97 (4), 371–380. doi: 10.1177/0022034517742139

Sardana, D., Zhang, J., Ekambaram, M., Yang, Y., McGrath, C. P., and Yiu, C. K. Y. (2019). Effectiveness of professional fluorides against enamel white spot lesions during fixed orthodontic treatment: A systematic review and meta-analysis. *J. Dent.* 82, 1–10. doi: 10.1016/j.jdent.2018.12.006

Selwitz, R. H., Ismail, A. I., and Pitts, N. B. (2007). Dental caries. *Lancet* 369 (9555), 51–59. doi: 10.1016/s0140-6736(07)60031-2

Sonesson, M., Brechter, A., Abdulraheem, S., Lindman, R., and Twetman, S. (2020). Fluoride varnish for the prevention of white spot lesions during orthodontic treatment with fixed appliances: a randomized controlled trial. *Eur. J. Orthod* 42 (3), 326–330. doi: 10.1093/ejo/cjz045

Tawakoli, P. N., Attin, T., and Mohn, D. (2016). Oral biofilm and caries-infiltrant interactions on enamel. *J. Dent.* 48, 40–45. doi: 10.1016/j.jdent.2016.03.006

Wang, L., Xie, X., Qi, M., Weir, M. D., Reynolds, M. A., Li, C., et al. (2019). Effects of single species versus multispecies periodontal biofilms on the antibacterial efficacy of a novel bioactive class-V nanocomposite. *Dent. Mater* 35 (6), 847–861. doi: 10.1016/j.dental.2019.02.030

Wegehaupt, F. J., and Attin, T. (2010). The role of fluoride and casein phosphopeptide/amorphous calcium phosphate in the prevention of erosive/abrasive wear in an *in vitro* model using hydrochloric acid. *Caries Res.* 44 (4), 358–363. doi: 10.1159/000316542

Wisniewski, D. J., Ma, T., and Schneider, A. (2021). Fatty acid synthase mediates high glucose-induced EGFR activation in oral dysplastic keratinocytes. *J. Oral. Pathol. Med. Off. Publ. Int. Assoc. Oral. Pathologists Am. Acad. Oral. Pathol.* 50 (9), 919–926. doi: 10.1111/jop.13235

Yim, H. K., Min, J. H., Kwon, H. K., and Kim, B. I. (2014). Modification of surface pretreatment of white spot lesions to improve the safety and efficacy of resin infiltration. *Korean J. Orthod* 44 (4), 195–202. doi: 10.4041/kjod.2014.44.4.195

Yu, J., Huang, X., Zhou, X., Han, Q., Zhou, W., Liang, J., et al. (2020). Anti-caries effect of resin infiltrant modified by quaternary ammonium monomers. *J. Dent.* 97, 103355. doi: 10.1016/j.jdent.2020.103355

Zakizade, M., Davoudi, A., Akhavan, A., and Shirban, F. (2020). Effect of resin infiltration technique on improving surface hardness of enamel lesions: A systematic review and meta-analysis. *J. Evid Based Dent. Pract.* 20 (2), 101405. doi: 10.1016/j.jebdp.2020.101405

Zhang, K., Cheng, L., Imazato, S., Antonucci, J. M., Lin, N. J., Lin-Gibson, S., et al. (2013). Effects of dual antibacterial agents MDPB and nano-silver in primer on microcosm biofilm, cytotoxicity and dentine bond properties. *J. Dent.* 41 (5), 464–474. doi: 10.1016/j.jdent.2013.02.001

Zhang, K., Cheng, L., Wu, E. J., Weir, M. D., Bai, Y., and Xu, H. H. (2013). Effect of water-ageing on dentine bond strength and anti-biofilm activity of bonding agent containing new monomer dimethylaminododecyl methacrylate. *J. Dent.* 41 (6), 504–513. doi: 10.1016/j.jdent.2013.03.011

Zhang, J., Lynch, R. J. M., Watson, T. F., and Banerjee, A. (2019). Chitosan-bioglass complexes promote subsurface remineralisation of incipient human carious enamel lesions. *J. Dent.* 84, 67–75. doi: 10.1016/j.jdent.2019.03.006

Zhang, K., Melo, M. A., Cheng, L., Weir, M. D., Bai, Y., and Xu, H. H. (2012). Effect of quaternary ammonium and silver nanoparticle-containing adhesives on dentin bond strength and dental plaque microcosm biofilms. *Dent. Mater* 28 (8), 842–852. doi: 10.1016/j.dental.2012.04.027

Zhou, W., Peng, X., Ma, Y., Hu, Y., Wu, Y., Lan, F., et al. (2019). Two-staged time-dependent materials for the prevention of implant-related infections. *Acta Biomater* 101, 128–140. doi: 10.1016/j.actbio.2019.10.023

Zhou, W., Zhou, X., Huang, X., Zhu, C., Weir, M. D., Melo, M. A. S., et al. (2020). Antibacterial and remineralizing nanocomposite inhibit root caries biofilms and protect root dentin hardness at the margins. *J. Dent.* 97, 103344. doi: 10.1016/j.jdent.2020.103344

Zou, J., Meng, M., Law, C. S., Rao, Y., and Zhou, X. (2018). Common dental diseases in children and malocclusion. *Int. J. Oral. Sci.* 10 (1), 7. doi: 10.1038/s41368-018-0012-3

Systematic analysis of lysine malonylation in *Streptococcus mutans*

Zhengyi Li[1], Qinrui Wu[1,2], Yixin Zhang[1,2], Xuedong Zhou[1,2]* and Xian Peng[1]*

[1]State Key Laboratory of Oral Diseases, National Clinical Research Center for Oral Diseases, West China Hospital of Stomatology, Sichuan University, Chengdu, China, [2]Department of Cariology and Endodontics, West China Hospital of Stomatology, Sichuan University, Chengdu, China

Protein lysine malonylation (Kmal) is a novel post-translational modification (PTM) that regulates various biological pathways such as energy metabolism and translation. Malonylation in prokaryotes, however, is still poorly understood. In this study, we performed a global Kmal analysis of the cariogenic organism *Streptococcus mutans* by combining antibody-based affinity enrichment and high-performance liquid chromatography-tandem mass spectrometry (HPLC-MS/MS) analysis. Altogether, 392 malonyllysine sites in 159 proteins were identified. Subsequent bioinformatic analysis revealed that Kmal occurs in proteins involved in various metabolic pathways including translation machinery, energy metabolism, RNA degradation, and biosynthesis of various secondary metabolites. Quantitative analysis demonstrated that Kmal substrates were globally altered in the biofilm growth state compared to the planktonic growth state. Furthermore, a comparative analysis of the lysine malonylome of our study with previously determined lysine acetylome in *S. mutans* revealed that a small proportion of Kmal sites overlapped with acetylated sites, whereby suggesting that these two acylations have distinct functional implications. These results expand our knowledge of Kmal in prokaryotes, providing a resource for researching metabolic regulation of bacterial virulence and physiological functions by PTM.

Introduction

During the past decade, various PTMs have been detected and characterized in prokaryotes as there have been advancements in high-quality antibodies and high sensitivity mass spectrometry. However, their functional and structural determination are particularly challenging, as most PTMs occur in relatively low number of prokaryotic

proteins compared to eukaryotic proteins, and most of modified proteins have low levels of sub-stoichiometric modification (Macek et al., 2019). Protein phosphorylation, acetylation, succinylation, glycosylation, lipidation and pupylation are common PTM types in bacteria. These PTMs play vital roles in various cellular processes, including protein synthesis, carbon and nitrogen metabolism, cell cycle, persistence, and virulence. There are various PTMs on lysine residues, such as acetylation, crotonylation, and 2-hydroxyisobutyrylation, suggesting complicated regulatory mechanisms of protein functions (Hirschey and Zhao, 2015; Huang et al., 2020). Among these modifications, acetylation and succinylation are the most ubiquitous PTMs in bacteria, with global proteomic studies have reported that the numbers of acetylated and succinylated proteins typically surpass the numbers of proteins modified by other PTMs (Macek et al., 2019). However, the functional roles of these PTMs and the enzymes responsible for their attachment (writer) and removal (eraser) remain to be extensively studied.Lysine malonylation is an evolutionarily conserved PTM from bacteria to mammals and involves malonyl-coenzyme (CoA) as a cofactor. Since the malonyl group has an acidic carboxylic group under physiological pH, malonylated lysine is negatively charged, which might impact on protein function and enzymatic activities (Peng et al., 2011). Like other short-chain acyl-CoAs, malonyl-CoA can be synthesized from its corresponding short-chain acyl salt, malonate, catalyzed by malonyl-CoA synthetase (Witkowski et al., 2011). In addition, malonyl-CoA can be produced during the carboxylation of acetyl-CoA by acetyl-CoA carboxylase (ACC), the carboxylation of acetyl-CoA by propionyl-CoA carboxylase, and the β-oxidation of old-chain-length dicarboxylic acids (Peng et al., 2011). Most studies on Kmal have been performed in mammalian systems and identified thousands of malonylated sites, revealing its role in the progress of diseases like type 2 diabetes, schizophrenia, and cardiac hypertrophy (Du et al., 2015; Smith et al., 2022; Wu et al., 2022). There has been increasing interest in dissecting the regulatory roles of Kmal in several bacterial species, such as *Escherichia coli* (Qian et al., 2016), *Bacillus amyloliquefaciens* (Fan et al., 2017), *Mycobacterium tuberculosis* (Bi et al., 2022), and *Staphylococcus aureus* (Shi et al., 2021), which demonstrates that Kmal exists in diverse prokaryotic organisms and participates in the regulation of various physiological processes. Even so, whether Kmal exists and affects protein functions in streptococci remains unknown.

S. mutans is considered to be the most prevalent and cariogenic species in active carious lesions of humans, residing primarily in dental plaque, which is a biofilm that forms on the tooth surfaces. During the past decades, studies of *S. mutans* have focused on revealing the molecular mechanisms underlying the robust biofilm formation on tooth surfaces, the metabolism of a wide variety of carbohydrates obtained from the host diet, and the adaption of numerous environmental challenges (Lemos

et al., 2019). Several studies have been performed to reveal the roles of PTMs in biofilm and cariogenic virulence. Wang et al. found that the phosphorylation of the response regulator of the two-component system VicRK could inhibit the expression of the glucosyltransferases GtfB and GtfC, thereby reducing the synthesis of extracellular polysaccharides (EPS), the major component of cariogenic biofilm (Wang et al., 2021). Acetylome study on the *S. mutans* depicted that acetylated substrates were globally altered in the biofilm state compared to the planktonic state, and the acetylated GtfB and C showed decreased activities (Lei et al., 2021; Ma et al., 2021). Our previous study revealed that the S-glutathionylation of a thioredoxin-like protein is important for interspecies competition and cariogenicity of *S. mutans* (Li et al., 2020). These results suggest that various PTM types exist in *S. mutans* and participate in diverse physiological processes. The genome of *S. mutans* UA159 encodes an acetyl coenzyme A carboxylase (ACC), which could synthesize malonyl-CoA through the carboxylation of acetyl-CoA (Ajdić et al., 2002), implying the existence of malonylation in this bacterium.

Therefore, this study aimed to confirm the existence of Kmal in *S. mutans* and identify the malonylated sites globally. The present findings provide a systematic view of the functional roles of Kmal in various metabolic pathways of *S. mutans*.

Materials and methods

Bacterial strain and growth conditions

Streptococcus mutans serotype c (strain ATCC 700610/ UA159) was obtained from the Oral Microbiome Bank of China (Peng et al., 2020), and grown at 37 °C under an aerobic (5% CO2, 95% air) condition in brain heart infusion (BHI) broth (Difco, Sparks, MD, USA). For biofilm formation, the bacteria in the mid-exponential phase were inoculated into fresh BHI supplemented with 1% sucrose with a 1:100 dilution.

Protein extraction

After 24h growing in the media with or without sucrose, the cells were collected by centrifugation and washed twice with PBS. Cell pellets were placed in ground liquid nitrogen to break the cell wall. Four times the volume of lysis buffer (8M urea, 1% proteinase inhibitor cocktail, 3 μM trichostatin A, 50 mM nicotinamide) was added to resuspend them. The samples were then sonicated and centrifuged (12000 × g at 4 °C for 10 min) for removing cellular debris. The supernatants were transferred to a new centrifuge tube, and the protein concentration was determined a with bicinchoninia acid (BCA) kit (Beyotime Biotechnology, JiangSu, China) according to the manufacturer's instructions.

Western blotting

Extracted proteins were standardized to the same concentration and boiled in SDS loading buffer for 5 min. Samples were then subjected to 11% SDS-PAGE and transferred to a nitrocellulose (NC) membrane. The membrane was blocked for 1 h in TBST buffer (25mM Tris-HCl, pH8.0, 150 mM NaCl, 0.1% Tween-20) supplemented with 5% defatted milk powder with further incubation overnight at 4°C with the pan anti-Kmal monoclonal antibody (cat. #PTM-902, PTM Bio Inc., Hangzhou) (1:1000, in TBST buffer with 5% defatted milk powder). After three consecutive washes with TBST buffer, the membrane was incubated with goat anti-mouse IgG antibody horseradish peroxidase conjugate (1:5000 in TBST buffer; Thermo Fisher Scientific, Waltham, MA, USA). After six times washing, an ECL substrate kit (Millipore) was used for protein visualization.

Trypsin digestion

The same amount of protein from each sample was separated for digestion. One volume of precooled acetone was initially added to the samples. Four times the volume of acetone was then added after mixing thoroughly with a vortex and allowing them to precipitate at -20°C for 2 h. Then, centrifugation was performed for 5 min, and the supernatants were discarded. The precipitation was washed twice with precooled acetone. Next, 200 mM tetraethylammonium bromide (TEAB) was added to dry precipitation and sonicate for dispersion. Trypsin was added at a 1:50 (trypsin: protein) mass ratio and digested overnight at 37°C. The peptides were then reduced with 5mM dithiothreitol for 30 min at 56°C and alkylated with 11 mM iodoacetamide in darkness for 15min at room temperature.

Enrichment of malonyated peptides

Tryptic peptides were dissolved in an immunoprecipitating (IP) buffer (100 mM NaCl, 1 mM EDTA, 50 mM Tris-HCl, 0.5% NP-40, pH 8.0) and incubated with pre-washed pan anti-Kmal antibody resins (cat. #PTM-904, PTM Bio Inc., Hangzhou) at 4°C, overnight, with gentle shaking in the dark. The resins were washed four times with an IP buffer and twice with deionized water. The bound peptides were eluted from the resins three times with 0.1% trifluoroacetic acid. Finally, the enriched peptides were desalted using C18 ZipTips (Millipore) and dried by vacuum.

Peptides analysis by high-performance liquid chromatography-tandem mass spectrometry

The peptides were dissolved in solvent A (0.1% formic acid and 2% acetonitrile in water) and a NanoElute UPLC system

(ThermoFisher Scientific) was used for separation. The gradient comprised 6%–22% solvent B (0.1% formic acid in 100% acetonitrile) in 0–40 min, 22%–30% in 40–52 min, 30%–80% in 52–56 min, climbing to 80% in 56–60 min, all at a constant flow rate of 450 nL/min. The eluted peptides were subjected to a capillary nanospray ionization (NSI) source followed by tandem mass spectrometry (MS/MS) in timesTOF Pro (Bruker Daltonics). The electrospray voltage applied was 1.65 kV. Precursors and fragments were analyzed using the TOF detector, with a MS/MS scan range of 100 to 1700 m/z. The timsTOF Pro tool was operated in parallel accumulation serial fragmentation (PASEF) mode. Precursors with charge states of 0 to 5 were selected for fragmentation, and 10 times of PASEF-MS/MS scans were acquired per cycle. The dynamic exclusion was set to 24 s.

Database search

Fragmentation data were then processed using the Maxquant search engine (v.1.6.15.0) against the Blast *Streptococcus mutans* serotype C (UA159/ATCC700610) containing 1,953 sequences and concatenated with the reverse decoy database. Trypsin/P was specified as a cleavage enzyme, allowing up to four missing cleavages and 5 modifications per peptide. The mass error for precursor ions was set to 20 ppm for the first search and 20 ppm for the main search. The mass error for fragment ions was set to 20ppm. Peptides with a length of at least seven amino acid residues were used for further analysis. Carbamidomethyl Cys was specified as fixed modification, while acetylation of protein N-terminal, lysine malnoylation and methionine oxidation were specified as variable modifications. The maximum false discovery rate (FDR) threshold for proteins, peptides, and the spectrum was adjusted to < 1%.

Motif analysis

All identified Kmal substrates in *S. mutans* were used to analyze the flanking sequences at sites of Kmal with Motif-X algorithms-based MoMo software. Ten neighboring amino acid residues on each side of the modification site were selected as the positive set. All genes of *Streptococcus mutans* serotype C (UA159/ATCC700610) amounted to the negative set.

Protein annotation and functional enrichment

Protein annotation and functional enrichment were performed as previously described (Li et al., 2020). The Gene Ontology (GO) annotation proteome was derived from the UniProt-GOA database (http://www.ebi.ac.uk/GOA/). The domain functional descriptions were annotated by Pfamscan

based on the protein sequence alignment method and the Pfam domain database (https://pfam.xfam.org/). The Kyoto Encyclopedia of Genes and Genomes (KEGG) database (https://www.kegg.jp/kegg/) was used to annotate the protein pathways. The prokaryotic organism subcellular localization prediction software CELLO was used to predict subcellular localization. The clusters of Orthologous Groups (COG) database (http://www.ncbi.nlm.nih.gov/COG) were used to align and classify the orthologs of proteins.

For each GO category, a two-tailed Fisher's exact test was employed to test the enrichment of differentially expressed proteins against all the identified proteins. The GO terms with a corrected $P < 0.05$ were considered significant. The KEGG database was used to identify the enriched pathways by a two-tailed Fisher's exact test and assess the enrichment of differentially expressed proteins against all the identified proteins. The pathways with a corrected $P < 0.05$ were considered significant. These pathways were classified into hierarchical categories according to the KEGG website. For each category of proteins, the Pfam database was researched, and a two-tailed Fisher's exact test was employed to test the enrichment of differentially modified proteins against all the identified proteins. Protein domains with a corrected $P < 0.05$ were considered significant.

Functional enrichment-based clustering

After functional enrichment, we collated all the categories and their P values. This was followed by filtering for categories that were at least significantly enriched ($P < 0.05$) in at least one of the clusters and transforming these P-value matrixes by the function X = –log10 (P-value). These X values were then Z-transformed for each functional category. These Z scores were finally clustered by one-way hierarchical clustering (Euclidean distance, average linkage clustering) in Genesis. The heatmap.2 function from the gplots R-package was applied to visualize the cluster membership.

Protein-protein interaction network analysis

The STRING database (version 10.5) was used for the enrichment analysis of S. mutans Kla protein-protein interaction networks. Only high-confidence interactions (with a score > 0.7) in the STRING database were fetched for the analysis. The MCODE plug-in toolkit was used to identify highly connected clusters, and the interaction network was visualized by Cytoscape software version 3.7.2.

Statistical analysis

For proteomic studies, the relative quantitative values of every site/protein in each group were performed with a t-test to assess for a significant difference. For all above enrichment methods, a Fisher's exact test was employed to assess the enrichment of differentially expressed proteins against all the identified proteins. A difference was considered significant if $P < 0.05$.

Results

Lysine malonylome profiling in *Streptococcus mutans*

To demonstrate the existence of Kmal in *S. mutans* and evaluate the alterations of Kmal in different growth states, we first compared the Kmal levels of *S. mutans* cells in biofilm growth (BG) with those in planktonic growth (PG) using a pan anti-Kmal antibody (Figure 1A). Multiple protein bands spanning a wide mass range were detected, and the Kmal levels of some proteins were significantly changed between these growth conditions. To elucidate Kmal in *S. mutans* systematically, we performed a quantitative proteomic analysis of Kmal substrates using by combining antibody-based affinity enrichment and high-resolution LC-MS/MS analysis. A total of 392 malonylated residues of 392 peptides were identified in 159 proteins using a highly conservative threshold (FDR < 1%) (Supplementary Table 1, Supplementary Figure 1). Among these modified proteins, 45.9% were modified in only one site, while only 8.2% were modified in six or more sites (Figure 1B). The most heavily malonylated proteins included putative bacitracin synthetase 1 (14 sites), pyruvate kinase (12 sites), and chaperone protein DnaK (10 sites). Moreover, the proportion of malonylated proteins among the total proteins of *S. mutans* UA159 was about 8.1% (159/1953); these proportions for in *E. coli* (Qian et al., 2016) was 13.8% (594/4306), 10.2% (382/3728) in *B. amyloliquefaciens* (Fan et al., 2017), 25.7% (1026/3993) in *M. tuberculosis* (Bi et al., 2022), and 9.7% (281/2889) in *S. aureus* (Shi et al., 2021).

PSORTb software was used to predict and annotate the subcellular localization of the manoylated proteins (Yu et al., 2010). The results showed that most of the modified proteins (119) were cytoplasmic, accounting for 74.8% of the total modified proteins (Figure 1C). Eighteen malonylated proteins were predicted to reside in the cytoplasmic membrane, these proteins might be related to transmembrane transportation, bacterial adhesion, and resistance to fluctuating environments, for example, the PTS system sucrose-specific EIIBCA component, which is responsible for the internalization of sucrose. In addition, several proteins were located outside of the cell or on the cell wall, involving the glucosyltransferase GtfC and the levansucrase Ftf, suggesting that Kmal is related to EPSs synthesis and biofilm formation (Table 1).

To assess the conserved substrate motifs of malonylated residues, we analyzed the adjacent amino acids of the
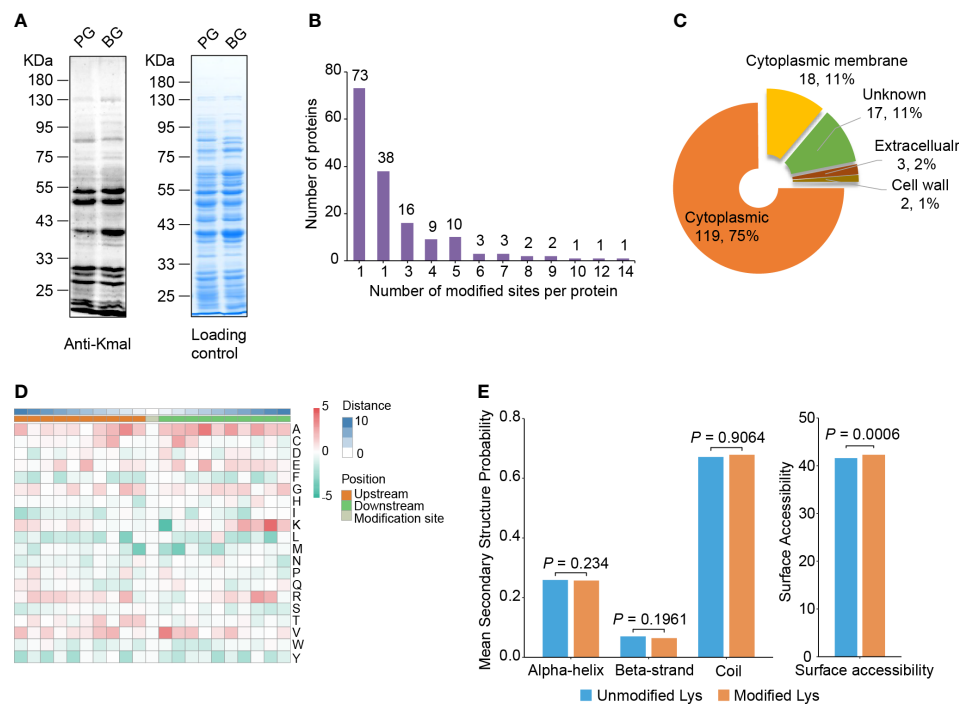
FIGURE 1

Lysine malonylome profiling in *S. mutans*. **(A)** Immunoblot analysis of malonylated proteins with pan anti-Kmal antibody in *S. mutans* from planktonic growth (PG) and biofilm growth (BG). Coomassie brilliant blue R-250 staining of SDS-PAGE gel as the loading control. **(B)** The number of malonylated sites identified per protein in *S. mutans*. **(C)** Subcellular localization prediction of modified proteins. **(D)** Motif analysis of all identified Kmal proteins. Red indicates high frequency and green means low frequency. **(E)** Distribution of Kmal sites in different secondary structures (left panel) and their surface accessibility (right panel). The *P* values were calculated with the Wilcoxon test.

malonylated lysine from -10 to +10 using Motif-X algorithms (Figure 1D) (Schwartz and Gygi, 2005). The results revealed that the aliphatic amino acids alanine and valine were overrepresented in the region flanking Kmal sites. Meanwhile, the sulfur-containing amino acid methionine and the aromatic phenylalanine, tryptophan and tyrosine were underrepresented. These results differed from the study on Kac in *S. mutans* (Lei et al., 2021), indicating that these two lysine modifications have distinct sequence alignments.

Furthermore, secondary structure distributions and surface accessibility of malonylated residues were analyzed using the NetSurP algorithm (Høie et al., 2022). The distribution pattern of Kmal exhibited no significant difference from that of non-modified lysine residues, which suggests that there was no structural preference for Kmal in *S. mutans* (Figure 1E). The average surface accessibility of malonylated lysine residues was significantly higher (*P* = 0.0006) than that of unmodified lysine, indicating that Kmal is preferably located on the surface of the protein structure. These results were similar to those of a previous study on Kmal in *Staphylococcus aureus* (Shi et al., 2021).

Functional analysis of the malonylome in *Streptococcus mutans*

To investigate the function of Kmal in regulating the cellular physiological processes of *S. mutans*, we conducted functional enrichment analyses of the Kmal substrates that we identified. GO-based enrichment (Figure 2A) showed that malonylated proteins were mostly enriched in protein expression-related processes, with specific enrichment in the peptide biosynthetic process ($P = 9.6 \times 10^{-17}$), the peptide metabolic process ($P = 3.7 \times 10^{-16}$), and the amide biosynthetic process ($P = 4.7 \times 10^{-14}$). The molecular functions of Kmal substrates were mainly enriched in the structural molecule activity ($P = 1.3 \times 10^{-18}$) and the structural constituent of ribosome ($P = 1.3 \times 10^{-18}$). Correspondingly, many modified proteins were primarily located in the ribosome ($P = 2.8 \times 10^{-16}$). Moreover, domain analysis based on the Pfam database (Figure 2B) revealed that Kmal substrates were significantly enriched in the functional domains of elongation factors, which are vital for the elongation of peptides during the translation process, suggesting a role of Kmal in protein synthesis in *S. mutans*.

TABLE 1 The malonylated proteins that are located in the cytoplasmic membrane, cell wall or extracellular.

Subcellular localization	Proteinaccession	Gene name	Protein description	Modified sites
Cytoplasmic membrane	I6L922	*SMU_765*	NADH oxidase/alkyl hydroperoxidase reductase peroxide-forming	109
	P12655	*scrA*	PTS system sucrose-specific EIIBCA component	46, 601
	Q8CVC6	*prsA*	Foldase protein PrsA	253
	Q8DRU8	*opuCa*	Putative osmoprotectant amino acid ABC transporter, ATP-binding protein	23
	Q8DRV8	*SMU_2104*	APC family permease(predicted)	472
	Q8DS76	*SMU_1957*	Putative PTS system, mannose-specific IID component	162, 211
	Q8DSQ4	*SMU_1719c*	UPF0154 protein	59
	Q8DSX5	*pfs*	5'-methylthioadenosine/S-adenosylhomocysteine nucleosidase	37
	Q8DSZ9	*SMU_1602*	Putative NAD(P)H-flavin oxidoreductase	109
	Q8DT86	*SMU_1479*	DUF3042 family protein(predicted)	31, 40
	Q8DTJ2	*SMU_1345c*	Putative peptide synthetase	28, 123, 121, 355
	Q8DTJ4	*SMU_1343c*	Putative polyketide synthase	321
	Q8DTL0	*ftsE*	Cell division ATP-binding protein FtsE	130
	Q8DV71	*SMU_635*	VIT family protein(predicted)	105, 96
	Q8DVD4	*divIVA*	Putative cell division protein DivIVA	108, 110, 133, 221
	Q8DVD9	*ftsZ*	Cell division protein FtsZ	65, 320
	Q8DVE5	*bipA*	50S ribosomal subunit assembly factor BipA	544
	Q8DW45	*ilvB*	Acetolactate synthase	169
Cell wall	P11000	*wapA*	Wall-associated protein	184
	P23504	*spaP*	Cell surface antigen I/II	102, 184, 1002, 1157
Extracellular	P13470	*gtfC*	Glucosyltransferase-SI	156, 870, 928
	P11701	*ftf*	Levansucrase	105
	Q8DWM3	*gbpB*	Putative secreted antigen GbpB/SagA putative peptidoglycan hydrolase	105, 221

Interestingly, the phosphopantetheine attachment site was the most significantly enriched term in this analysis ($P = 1.0 \times 10^{-3}$), and two acyl carrier proteins (Q8DSN3, Q8DWL8) were involved, indicating that Kmal might play a functional role in regulating fatty acid or polyketide biosynthesis.

According to KEGG-based metabolic pathway enrichment (Figure 2C), the top enriched pathways were ribosome ($P = 4.6 \times 10^{-23}$) and glycolysis/gluconeogenesis ($P = 2.5 \times 10^{-5}$). Glycolysis/gluconeogenesis is the key energy metabolic pathway of the facultative aerobic *S. mutans*. A total of 55 Kmal sites were identified on 12 glycolytic enzyme (Figure 2D), among which pyruvate kinase (PYK) harbored 12 Kmal sites, while fructose-1,6-biphosphate aldolase (FBA) and L-lactate dehydrogenase (LDH) harbored seven and six Kmal sites, respectively. These functional enrichment results suggested that Kmal has profound effects on various vital biological pathways by regulating the functions of many enzymes.

Protein-protein interactions (PPI) are vital for biochemical reactions and vulnerable to PTMs (Yao et al., 2019). The interactions between all identified malonylated proteins in this study were mapped using the STRING database (Szklarczyk et al., 2021). Combining cluster analysis with the MCODE module in Cytoscape software characterized nine highly

interconnected networks (Supplementary Table 2). We visualized the top three enriched interaction clusters from the analysis (Figure 3). Interestingly, almost all proteins in cluster 1 are ribosome- associated proteins (Figure 3A), while most proteins in cluster 2 are glycolytic enzymes (Figure 3B). These results are aligned with the KEGG pathway enrichment conducted. Taken together, Kmal in *S. mutans* might potentially impact the PPIs, thus contributing to the regulation of metabolic pathways.

Lysine malonylome in biofilm is significantly different from that of planktonic growth

Cariogenic biofilms are vital for develop ing dental caries (Lemos et al., 2019). Thus, we investigated the role of Kmal in biofilm formation by comparing the lysine malonylome of *S. mutans* cells from biofilm (BG group) with that of planktonic cells (PG group). Of all the identified Kla sites in these two groups, 118 sites were present in cells from both groups, only seven sites were detected only in the planktonic cells, whereas 267 sites were present only in the cells from biofilm (Figure 4A).
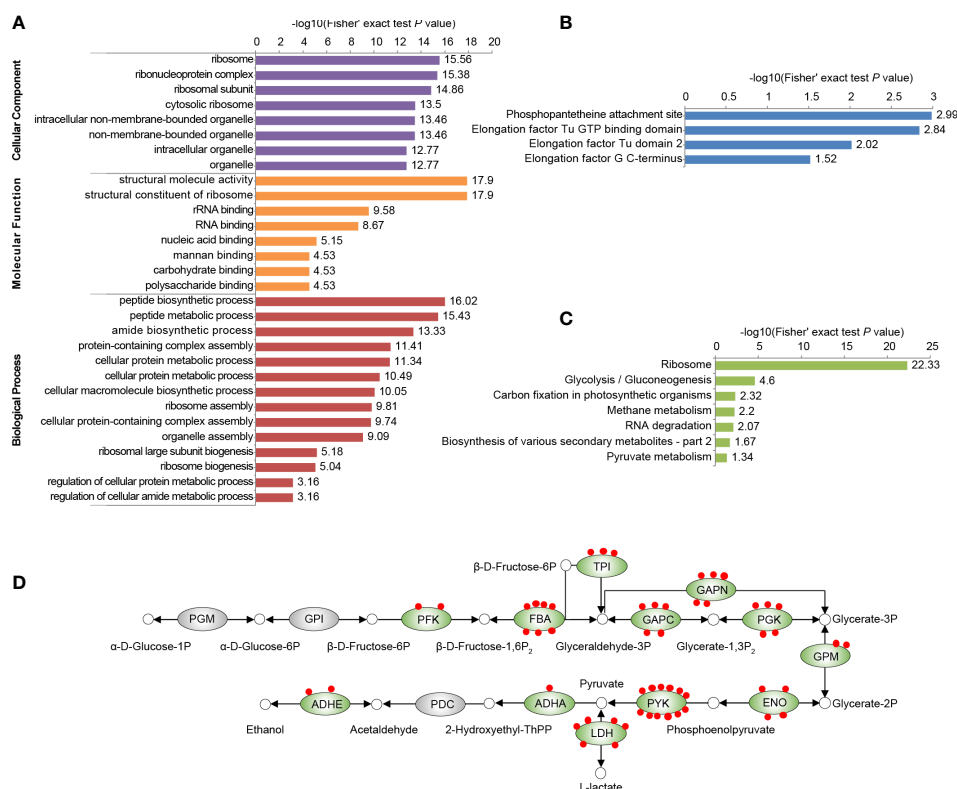
FIGURE 2

Functional enrichment analysis of all identified Kmal substrates in our proteomic study. **(A)** GO-based enrichment analysis of malonylated proteins. **(B)** Pfam-based enrichment analysis of domains related to malonylated proteins. **(C)** KEGG pathway-based enrichment analysis of malonylated proteins. For each category, a two-tailed Fisher's exact test was employed to test the enrichment of the identified modified proteins against all proteins in the species database. Fold enrichment > 1.5 and adjusted *P* values < 0.05 were considered significant. **(D)** Malonylated enzymes involved in glycolysis in *S. mutans*. Green ovals indicate proteins subjected to malonylation, red dots represent Kmal sites. PGM, Phosphoglycerate mutase; GPI, glucose-6-phosphate isomerase; PFK, ATP-dependent 6-phosphofructokinase; FBA, fructose-1,6-biphosphate aldolase; TPI, triosephosphate isomerase; GAPC, glyceraldehyde-3-phosphate dehydrogenase; GAPN, NADP-dependent glyceraldehyde-3-phosphate dehydrogenase; PGK, phosphoglycerate kinase; GPM, glucosephosphate-mutase; ENO, enolase; PYK, pyruvate kinase; LDH, L-lactate dehydrogenase; ADHA, putative acetoin dehydrogenase (TPP-dependent), E1 component alpha subunit; PDC, pyruvate decarboxylase; ADHE, Aldehyde-alcohol dehydrogenase.

Subsequent quantitative analysis depicted that 117 residues from 66 proteins could be quantified in both groups using MaxQuant software (Supplementary Figure 1, Supplementary Table 1). We examined the change in these quantifiable sites in the BG group relative to the PG group. Finally, the modification levels of 66 lysine residues on 44 proteins were upregulated, but only four sites on four proteins were downregulated (Figure 4B) (filtered with a threshold value of modification fold change >1.5 or <1.5) (Supplementary Table 3). Additionally, since 68.1% of the malonylome (267 of 392 sites) is present in only the BG group, the increase in Kmal is more vigorous than the quantitative analysis.

To investigate the functional roles of these differentially modified proteins during biofilm formation, we performed functional analyses of these proteins corresponding to the differentially modified sites. Classification based on prokaryotic orthologous groups (COG) revealed that the differentially

modified proteins broadly participated in translation, ribosomal structure and biogenesis, carbohydrate transportation, and metabolism (Figure 4C). After that, we performed a cluster analysis of these differentially modified sites. The differentially modified sites were divided into four quorums based on the fold change (FC) values, namely Q1, 0< FC <0.5; Q2, 0.5 < FC < 1/1.5; Q3, 1.5 < FC < 2; Q4, FC > 2 (Supplementary Figure 2A). Functional enrichment analysis was conducted for these quorums (Supplementary Figure 2B). GO-based cluster analysis showed that the proteins with upregulated sites were enriched on the cell surface. Meanwhile, the proteins in Q4 were enriched in the response to heat, the symbiotic process, and the interspecies interaction between organisms. Meanwhile, the KEGG-based analysis showed that the proteins with increased modified sites were enriched in purine metabolism. These results suggested that Kmal might be an important tool for regulating the biological processes in biofilm for *S. mutans*.

FIGURE 3

The top three clusters of highly interconnected malonylated PPI networks. Interaction network of lysine-lactylated proteins (listed in gene names) were analyzed using the MCODE plug-in toolkit in the Cytoscape software (version 3.7.2). **(A)** Cluster 1: MCODE score = 42.186, nodes = 44, edges = 907. **(B)** Cluster 2: MCODE score = 11.091, nodes = 12, edges = 61. **(C)** Cluster 3: MCODE score = 6, nodes = 6, edges = 15.

Comparison of acetylome and malonylome in *Streptococcus mutans*

To investigate the similarities and differences among the various lysine acylation modifications, we further compared our malonylome dataset with a previously reported acetylome dataset in *S. mutans* UA159 (Lei et al., 2021). It was found that 31.4% of the malonylation sites could also be acetylated (Figure 5A, Supplementary Table 4). These two kinds of modifications are highly overlapping in several proteins, including pyruvate kinase (Q8DTX7, seven overlapping sites), chaperone protein DnaK (O06942, six overlapping sites), and L-lactate dehydrogenase (P26283, six overlapping sites). Moreover, 87.4% of Kac sites were identified in only the lysine malonylome dataset, and 68.6% of Kmal sites were identified in only the lysine acetylome dataset.

Afterward, performed functional analyses of these common and unique sites of the two acylome datasets. Pfam-based domain enrichment showed that the sites bearing either or both of the modifications broadly resided in the same domains, including the tRNA synthetases class II, the elongation factor Tu GTP-binding domain, and the elongation factor G C-terminus (Figure 5B). These domains are important for protein synthesis. In support of this observation, many proteins with either or both of these modifications were significantly enriched in ribosome based on the KEGG analysis (Figure 5C), whereby indicating that both of these modifications have functions in regulating protein expression in *S. mutans*. In addition, the glycolysis/gluconeogenesis pathway was also the common pathway enriched by both of these modifications. However, enrichment analysis also demonstrated that these

two modifications were enriched in many different metabolic pathways. For example, the proteins with sites that were identified in only the Kac dataset depicted significant enrichment in pathways such as aminoacyl-tRNA biosynthesis, galactose metabolism and pentose phosphate, while the proteins bearing sites that were only modified by malonylation were enriched in methane metabolism and RNA degradation. These results suggested that Kmal could have distinct physiological roles from those of Kac.

For those sites identified in both Kmal and Kac datasets, their functional enrichment results showed significant enrichment in methane metabolism, RNA degradation, fructose and mannose metabolism and pyruvate metabolism, except for the pathways enriched by the unique sites of the two acylome datasets.

Discussion

Our proteomic approach identified 392 lysine-malonylated sites on 159 proteins of *S. mutans*, generating the first malonylome dataset for streptococci. These malonylated proteins are distributed in various cellular components and participate in multiple crucial biological pathways. Compared with the bacteria growing in a planktonic state, the levels of malonylation in bacteria growing in a biofilm state have significantly improved, which suggests a crucial role of Kmal in regulating the physiological activities in cariogenic biofilm. Combining analysis with the acetylome dataset of *S. mutans*, we observed that a small proportion of acetylated sites could also be malonylated, suggesting that these two kinds of modification

FIGURE 4

Lysine malonylome in biofilm is significantly different from that of planktonic growth. **(A)** Venn diagram showing the total number of PG-only (~1.79%), BG-only (~68.11%) and overlapping (~30.1%) modified sites (filtered with a threshold value of modification fold change >1.5 or <1.5). **(B)** Bar graph for the number of differentially modified sites and the corresponding proteins. **(C)** COG-based classification of the differentially modified proteins.

have connection or interaction in regulating the functions of protein. In conclusion, this study provides significant resources for further functional investigations into Kmal in bacteria.

Like other large-scale studies of malonylation in bacteria (Qian et al., 2016; Shi et al., 2021; Bi et al., 2022), our data revealed that many Kmal substrates were enriched in ribosomal and translation-associated proteins, but there is no report revealing the functional role of Kmal in translation. Few studies have investigated the impacts of PTMs on ribosomal proteins. In *E. coli*, Kac has been proven to promote the dissociation or inhibit the association of 30S and 50S ribosomal subunits, thus interfering with translation (Feid et al., 2022). Phosphoproteome profiling across ribosomal

subcomplexes revealed that phosphorylation on the ribosomal protein RPL12/uL11 was strongly depleted in polysomes, with subsequent experiments demonstrating that this modification regulates the translation of mitosis-regulated mRNAs, thus contributing to the regulation of translation during mitosis (Imami et al., 2018). An investigation into UFMylation in human cells revealed that RPL26 UFMylation plays a direct role in cotranslational protein translocation into the endoplasmic reticulum (ER). The inhibition of RPL26 UFMylation leads to impaired ER protein homeostasis, suggesting that UFMylation of RPL26 has an impact on protein biogenesis in the early secretory pathway (Walczak et al., 2019). Moreover, the regulatory mechanisms of the

FIGURE 5
Comparison of acetylome and malonylome in *S. mutans*. **(A)** Venn diagram showing the total number of Kac-only, Kmal-only and overlapping sites. **(B)** Pfam-based domain enrichment for these common and unique sites of the two acylome datasets. **(C)** KEGG-based pathway enrichment for these common and unique sites of the two acylome datasets. For each category, a two-tailed Fisher's exact test was employed to test the enrichment of the identified modified proteins against all proteins in the species database. Fold enrichment > 1.5 and adjusted *P* values < 0.05 were considered significant.

modification status of ribosomal proteins have been dissected in several studies. For example, oligoglutamylation of the *E. coli* ribosomal protein S6 is carried out by the ATP-dependent glutamate ligase RimK (Kang et al., 1989; Kino et al., 2011; Zhao et al., 2013), which is also widespread and conserved in hundreds of prokaryotic and eukaryotic genomes (Little et al., 2016). In our quantitative analysis of Kmal in *S. mutans*, 20 of the 44 proteins with increased modified sites were involved in translational processes (Figure 4C), which implies that Kmal plays a vital role in regulating protein synthesis in cariogenic biofilm.

Reversible PTMs are tightly regulated through the addition and removal of chemical groups by regulatory enzymes. In mammalian cells, the lysine deacetylase SIRT5 was demonstrated to catalyze a lysine demalonylation reaction (Peng et al., 2011). Recently, the lysine acetyltransferase KAT2A

showed lysine malonyltransferase activity in malonylation of the histone H2B_K5 (Zhang et al., 2022). However, no prokaryotic demalonylase or malonyltransferase has been reported as of yet. New reports on the characterization of lysine acetyltransferase (KAT) and deacetylase are appearing continuously, such as the KAT PatZ and the deacetylases CobB and YcgC from *E. coli* (Colak et al., 2013; Tu et al., 2015; Dash and Modak, 2021), the KAT Eis from *M. tuberculosis* (Ghosh et al., 2016), and the ActG from *S. mutans* (Ma et al., 2021). Interestingly, the deacetylase CobB also possesses a desuccinylase activity in *E. coli* (Colak et al., 2013), suggesting that the multifunctional roles of these identified acetyltransferase and deacetylase need to be investigated. Additionally, given that both acetylation and succinylation can also occur nonenzymatically (Wagner and Payne, 2013; Wolfe, 2016), efforts should be made to verify nonenzymatic malonylation in bacteria.

Kac neutralizes the positive charge on the side chain of a lysine residue, while Kmal adds a negative charge. Our comparative analysis showed that the same lysine residue could be either acetylated or malonylated. These two kinds of PTMs could have different effects on protein structure, PPIs, DNA–protein interactions, and enzymatic activities, thus contributing to bacterial rapid adaptation to environmental changes (Macek et al., 2019). As shown in Figure 5, these enrichment results of Kmal were to some extent similar to those of Kac. This similarity might be due to the common shared pathways among these two kinds of PTMs. It is also possibly cause by the intrinsic antibody-based enrichment approach bias toward the capture of modified peptides from abundant proteins. In addition, our enrichment analysis results were biased toward high abundant proteins as we did not take into consideration the information on the number of Kmal sites on each protein or Kmal peptide intensity. Therefore, these bioinformatics analysis results can only be used as a reference, and the detailed functional importance and mechanisms of Kmal in *S. mutans* needs to be further studied.

Data availability statement

The MS proteomics data presented in the study are deposited in the PRIDE repository (https://www.ebi.ac.uk/pride), accession number PXD038045.

Author contributions

XP, ZL and YZ conceived and designed the experiments. ZL, QW and YZ performed the experiments. ZL analyzed the data. YZ and XP further contributed reagents and materials tools. ZL wrote initial draft of the manuscript. All authors contributed to the article and approved the submitted version.

Conflict of interest

The authors declare that the research was conducted in the absence of any commercial or financial relationships that could be construed as a potential conflict of interest.

Publisher's note

All claims expressed in this article are solely those of the authors and do not necessarily represent those of their affiliated organizations, or those of the publisher, the editors and the reviewers. Any product that may be evaluated in this article, or claim that may be made by its manufacturer, is not guaranteed or endorsed by the publisher.

Supplementary material

The Supplementary Material for this article can be found online at: https://www.frontiersin.org/articles/10.3389/fcimb.2022.1078572/full#supplementary-material

References

Ajdić, D., McShan, W. M., McLaughlin, R. E., Savić, G., Chang, J., Carson, M. B., et al. (2002). Genome sequence of streptococcus mutans UA159, a cariogenic dental pathogen. *Proc. Natl. Acad. Sci.* 99 (22), 14434–14439. doi: 10.1073/pnas.172501299

Bi, J., Guo, Q., Zhou, Z., Huang, X., Qin, L., Tao, X., et al. (2022). Malonylome analysis uncovers the association of lysine malonylation with metabolism and acidic stress in pathogenic mycobacterium tuberculosis. *Microbiol. Res.* 265, 127209. doi: 10.1016/j.micres.2022.127209

Colak, G., Xie, Z., Zhu, A. Y., Dai, L., Lu, Z., Zhang, Y., et al. (2013). Identification of lysine succinylation substrates and the succinylation regulatory enzyme CobB in escherichia coli. *Mol. Cell. Proteomics* 12 (12), 3509–3520. doi: 10.1074/mcp.M113.031567

Dash, A., and Modak, R. (2021). Protein acetyltransferases mediate bacterial adaptation to a diverse environment. *J. Bacteriol.* 203 (19), e00231–e00221. doi: 10.1128/JB.00231-21

Du, Y., Cai, T., Li, T., Xue, P., Zhou, B., He, X., et al. (2015). Lysine malonylation is elevated in type 2 diabetic mouse models and enriched in metabolic associated proteins. *Mol. Cell. Proteomics* 14 (1), 227–236. doi: 10.1074/mcp.M114.041947

Fan, B., Li, Y.-L., Li, L., Peng, X.-J., Bu, C., Wu, X.-Q., et al. (2017). Malonylome analysis of rhizobacterium bacillus amyloliquefaciens FZB42 reveals involvement of lysine malonylation in polyketide synthesis and plant-bacteria interactions. *J. Proteomics* 154, 1–12. doi: 10.1016/j.jprot.2016.11.022

Feid, S. C., Walukiewicz, H. E., Wang, X., Nakayasu, E. S., Rao, C. V., and Wolfe, A. J. (2022). Regulation of translation by lysine acetylation in escherichia coli. *mBio* 13 (3), e01224–e01222. doi: 10.1128/mbio.01224-22

Ghosh, S., Padmanabhan, B., Anand, C., and Nagaraja, V. (2016). Lysine acetylation of the mycobacterium tuberculosis HU protein modulates its DNA binding and genome organization. *Mol. Microbiol.* 100 (4), 577–588. doi: 10.1111/mmi.13339

Hirschey, M. D., and Zhao, Y. (2015). Metabolic regulation by lysine malonylation, succinylation, and glutarylation. *Mol. Cell. Proteomics* 14 (9), 2308–2315. doi: 10.1074/mcp.R114.046664

Høie, M. H., Kiehl, E. N., Petersen, B., Nielsen, M., Winther, O., Nielsen, H., et al. (2022). NetSurfP-3.0: Accurate and fast prediction of protein structural features by protein language models and deep learning. *Nucleic Acids Res* 50 (W1), W510-5. doi: 10.1093/nar/gkac439

Huang, S., Tang, D., and Dai, Y. (2020). Metabolic functions of lysine 2-hydroxyisobutyrylation. *Cureus* 12 (8), e9651. doi: 10.7759/cureus.9651

Imami, K., Milek, M., Bogdanow, B., Yasuda, T., Kastelic, N., Zauber, H., et al. (2018). Phosphorylation of the ribosomal protein RPL12/uL11 affects translation during mitosis. *Mol. Cell* 72 (1), 84–98. e89. doi: 10.1016/j.molcel.2018.08.019

Kang, W.-K., Icho, T., Isono, S., Kitakawa, M., and Isono, K. (1989). Characterization of the generimK responsible for the addition of glutamic acid residues to the c-terminus of ribosomal protein S6 inEscherichia coli K12. *Mol. Gen. Genet. MGG* 217 (2), 281–288. doi: 10.1007/BF02464894

Kino, K., Arai, T., and Arimura, Y. (2011). Poly-α-glutamic acid synthesis using a novel catalytic activity of RimK from escherichia coli K-12. *Appl. Environ. Microbiol.* 77 (6), 2019–2025. doi: 10.1128/AEM.02043-10

Lei, L., Zeng, J., Wang, L., Gong, T., Zheng, X., Qiu, W., et al. (2021). Quantitative acetylome analysis reveals involvement of glucosyltransferase acetylation in streptococcus mutans biofilm formation. *Environ. Microbiol. Rep.* 13 (2), 86–97. doi: 10.1111/1758-2229.12907

Lemos, J., Palmer, S., Zeng, L., Wen, Z., Kajfasz, J., Freires, I., et al. (2019). The biology of streptococcus mutans. *Microbiol. Spectr.* 7 (1), 7.1. 03. doi: 10.1128/microbiolspec.GPP3-0051-2018

Little, R. H., Grenga, L., Saalbach, G., Howat, A. M., Pfeilmeier, S., Trampari, E., et al. (2016). Adaptive remodeling of the bacterial proteome by specific ribosomal modification regulates pseudomonas infection and niche colonisation. *PloS Genet.* 12 (2), e1005837. doi: 10.1371/journal.pgen.1005837

Li, Z., Zhang, C., Li, C., Zhou, J., Xu, X., Peng, X., et al. (2020). S-glutathionylation proteome profiling reveals a crucial role of a thioredoxin-like protein in interspecies competition and cariogenecity of streptococcus mutans. *PloS Pathog.* 16 (7), e1008774. doi: 10.1371/journal.ppat.1008774

Macek, B., Forchhammer, K., Hardouin, J., Weber-Ban, E., Grangeasse, C., and Mijakovic, I. (2019). Protein post-translational modifications in bacteria. *Nat. Rev. Microbiol.* 17 (11), 651–664. doi: 10.1038/s41579-019-0243-0

Ma, Q., Pan, Y., Chen, Y., Yu, S., Huang, J., Liu, Y., et al. (2021). Acetylation of glucosyltransferases regulates streptococcus mutans biofilm formation and virulence. *PloS Pathog.* 17 (12), e1010134. doi: 10.1371/journal.ppat.1010134

Peng, C., Lu, Z., Xie, Z., Cheng, Z., Chen, Y., Tan, M., et al. (2011). The first identification of lysine malonylation substrates and its regulatory enzyme. *Mol. Cell. Proteomics* 10 (12), M111.012658. doi: 10.1074/mcp.M111.012658

Peng, X., Zhou, X., Xu, X., Li, Y., Li, Y., Li, J., et al. (2020). "The oral microbiome bank of China," in *Atlas of oral microbiology: From healthy microflora to disease* (Singapore: Springer), 287–300.

Qian, L., Nie, L., Chen, M., Liu, P., Zhu, J., Zhai, L., et al. (2016). Global profiling of protein lysine malonylation in escherichia coli reveals its role in energy metabolism. *J. Proteome Res.* 15 (6), 2060–2071. doi: 10.1021/acs.jproteome.6b00264

Schwartz, D., and Gygi, S. P. (2005). An iterative statistical approach to the identification of protein phosphorylation motifs from large-scale data sets. *Nat. Biotechnol.* 23 (11), 1391–1398. doi: 10.1038/nbt1146

Shi, Y., Zhu, J., Xu, Y., Tang, X., Yang, Z., and Huang, A. (2021). Malonyl-proteome profiles of staphylococcus aureus reveal lysine malonylation modification

in enzymes involved in energy metabolism. *Proteome Sci.* 19 (1), 1–11. doi: 10.1186/s12953-020-00169-1

Smith, B. J., Brandão-Teles, C., Zuccoli, G. S., Reis-de-Oliveira, G., Fioramonte, M., Saia-Cereda, V. M., et al. (2022). Protein succinylation and malonylation as potential biomarkers in schizophrenia. *J. pers. Med.* 12 (9), 1408. doi: 10.3390/jpm12091408

Szklarczyk, D., Gable, A. L., Nastou, K. C., Lyon, D., Kirsch, R., Pyysalo, S., et al. (2021). The STRING database in 2021: Customizable protein–protein networks, and functional characterization of user-uploaded gene/measurement sets. *Nucleic Acids Res.* 49 (D1), D605–D612. doi: 10.1093/nar/gkab835

Tu, S., Guo, S.-J., Chen, C.-S., Liu, C.-X., Jiang, H.-W., Ge, F., et al. (2015). YcgC represents a new protein deacetylase family in prokaryotes. *Elife* 4, e05322. doi: 10.7554/eLife.05322.021

Wagner, G. R., and Payne, R. M. (2013). Widespread and enzyme-independent nϵ-acetylation and nϵ-succinylation of proteins in the chemical conditions of the mitochondrial matrix*◆. *J. Biol. Chem.* 288 (40), 29036–29045. doi: 10.1074/jbc.M113.486753

Walczak, C. P., Leto, D. E., Zhang, L., Riepe, C., Muller, R. Y., DaRosa, P. A., et al. (2019). Ribosomal protein RPL26 is the principal target of UFMylation. *Proc. Natl. Acad. Sci.* 116 (4), 1299–1308. doi: 10.1073/pnas.1816202116

Wang, S., Long, L., Yang, X., Qiu, Y., Tao, T., Peng, X., et al. (2021). Dissecting the role of vick phosphatase in aggregation and biofilm formation of streptococcus mutans. *J. Dental Res.* 100 (6), 631–638. doi: 10.1177/0022034520979798

Witkowski, A., Thweatt, J., and Smith, S. (2011). Mammalian ACSF3 protein is a malonyl-CoA synthetase that supplies the chain extender units for mitochondrial fatty acid synthesis. *J. Biol. Chem.* 286 (39), 33729–33736. doi: 10.1074/jbc.M111.291591

Wolfe, A. J. (2016). Bacterial protein acetylation: New discoveries unanswered questions. *Curr. Genet.* 62 (2), 335–341. doi: 10.1007/s00294-015-0552-4

Wu, L.-F., Wang, D.-P., Shen, J., Gao, L.-J., Zhou, Y., Liu, Q.-H., et al. (2022). Global profiling of protein lysine malonylation in mouse cardiac hypertrophy. *J. Proteomics* 266, 104667. doi: 10.1016/j.jprot.2022.104667

Yao, Z., Guo, Z., Wang, Y., Li, W., Fu, Y., Lin, Y., et al. (2019). Integrated succinylome and metabolome profiling reveals crucial role of s-ribosylhomocysteine lyase in quorum sensing and metabolism of aeromonas hydrophila*[S]. *Mol. Cell. Proteomics* 18 (2), 200–215. doi: 10.1074/mcp.RA118.001035

Yu, N. Y., Wagner, J. R., Laird, M. R., Melli, G., Rey, S., Lo, R., et al. (2010). PSORTb 3.0: improved protein subcellular localization prediction with refined localization subcategories and predictive capabilities for all prokaryotes. *Bioinformatics* 26 (13), 1608–1615. doi: 10.1093/bioinformatics/btq249

Zhang, R., Bons, J., Bielska, O., Carrico, C., Rose, J., Heckenbach, I., et al. (2022). Histone malonylation is regulated by SIRT5 and KAT2A. *bioRxiv*. doi: 10.1101/2022.06.07.495150

Zhao, G., Jin, Z., Wang, Y., Allewell, N. M., Tuchman, M., and Shi, D. (2013). Structure and function of escherichia coli RimK, an ATP-grasp fold, l-glutamyl ligase enzyme. *Proteins: Struct. Funct. Bioinf.* 81 (10), 1847–1854. doi: 10.1002/prot.24311

Novel antimicrobial agents targeting the *Streptococcus mutans* biofilms discovery through computer technology

Bin Zhang[1,2], Min Zhao[1,2], Jiangang Tian[1,2], Lei Lei[3]*
and Ruizhe Huang[1,2]*

[1]Key Laboratory of Shaanxi Province for Craniofacial Precision Medicine Research, College of
Stomatology, Xi'an Jiaotong University, Xi'an, China, [2]Clinical Research Center of Shaanxi Province
for Dental and Maxillofacial Diseases, Center of Oral Public Health, College of Stomatology, Xi'an
Jiaotong University, Xi'an, China, [3]State Key Laboratory of Oral Diseases, Department of Preventive
Dentistry, West China Hospital of Stomatology, Sichuan University, Chengdu, China

Dental caries is one of the most prevalent and costly biofilm-associated
infectious diseases worldwide. *Streptococcus mutans* (*S. mutans*) is well
recognized as the major causative factor of dental caries due to its
acidogenicity, aciduricity and extracellular polymeric substances (EPSs)
synthesis ability. The EPSs have been considered as a virulent factor of
cariogenic biofilm, which enhance biofilms resistance to antimicrobial agents
and virulence compared with planktonic bacterial cells. The traditional anti-
caries therapies, such as chlorhexidine and antibiotics are characterized by
side-effects and drug resistance. With the development of computer
technology, several novel approaches are being used to synthesize or
discover antimicrobial agents. In this mini review, we summarized the novel
antimicrobial agents targeting the *S. mutans* biofilms discovery through
computer technology. Drug repurposing of small molecules expands the
original medical indications and lowers drug development costs and risks.
The computer-aided drug design (CADD) has been used for identifying
compounds with optimal interactions with the target *via* silico screening and
computational methods. The synthetic antimicrobial peptides (AMPs) based on
the rational design, computational design or high-throughput screening have
shown increased selectivity for both single- and multi-species biofilms. These
methods provide potential therapeutic agents to promote targeted control of
the oral microbial biofilms in the near future.

KEYWORDS

extracellular polymeric substances, drug repurposing, computer-aided drug design,
synthetic antimicrobial peptides, computer technology

Introduction

The human oral cavity has over 700 bacterial species, harboring the second most diverse microbiome in the body (Pathak et al., 2021). Dental caries is one of the prominent chronic diseases worldwide. *S. mutans* is considered as the most significant contributor to dental caries due to its cariogenic ability of acid production, acid tolerance and biofilm formation (Pitts et al., 2017; Cui et al., 2019). The biofilm is a structured community that consists of a wide range of microbial species embedded in a self-organized matrix of extracellular polymeric substances (EPSs) (Flemming et al., 2016; Jakubovics et al., 2021). The EPSs not only provide a scaffold for biofilm maturation but also enhance the biofilm tolerance to antimicrobial agents (Jakubovics et al., 2021). The traditional antimicrobial agents, such as the broad-spectrum antimicrobials, pose the challenges for maintaining commensal bacteria (Huang et al., 2021). Though chlorhexidine has a strong bactericidal ability (Coelho et al., 2017), the side effects such as tooth staining, unpleasant taste, mouth irritation, and disturbing the homeostasis of the oral microbiome have limited its usage (Brookes et al., 2020). A larger number of evidence showed that natural products and their derivatives exhibited inhibitory activities against *S. mutans* growth (Sparks et al., 2017). However, the identification and isolation of active compounds from plants are complex and time-consuming. Moreover, the emergence of antibiotic resistance has necessitated the search for novel antibacterial agents target specific oral bacterial pathogens and inhibit EPSs formation (Coelho et al., 2017; Xia et al., 2019).

The ideal anti-biofilm approach is to facilitate the biofilm dispersion, inhibit the reproduction and metabolism of pathogens, as well as avoid the emergence of antibiotic-resistant bacteria and not disturb the homeostasis of the oral microbiome (Kanwar et al., 2017; Simon et al., 2019). Based on FDA-approved drugs database and small molecule database screening, the drug repurposing has advantages of lower toxicity and faster clinical transition (Wishart et al., 2006; Cui et al., 2019). And the rapid advance of computer technology makes it possible to investigate the biomolecular interactions and design/redesign chemical molecules, which enhance a better understanding the mechanism of inhibition and reveal essential structural properties at the molecular level. The antimicrobial peptides (AMPs) have been considered as potential drug candidates (Bin Hafeez et al., 2021), but it is challenging to improve the specificity of AMPs against *S. mutans* (Mai et al., 2011). Computational tools enable exploration of previously unexplored regions of AMP sequence space which may yield synthetic peptides with enhanced biological function (Torres et al., 2021). This review introduced emerging computer approaches including drugs repurposing of small-molecule compounds, computer-aided drug design (CADD), and new synthetic antimicrobial peptides (Figure 1).

FIGURE 1

The computer technologies employed to discover novel antimicrobial agents including: **(A)** drug repurposing of small-molecule compounds; **(B)** computer-aided drug design; **(C)** the synthetic antimicrobial peptides. Then *in vitro* testing targeting the *S.mutans* was conducted to select the lead candidates with optimal features.
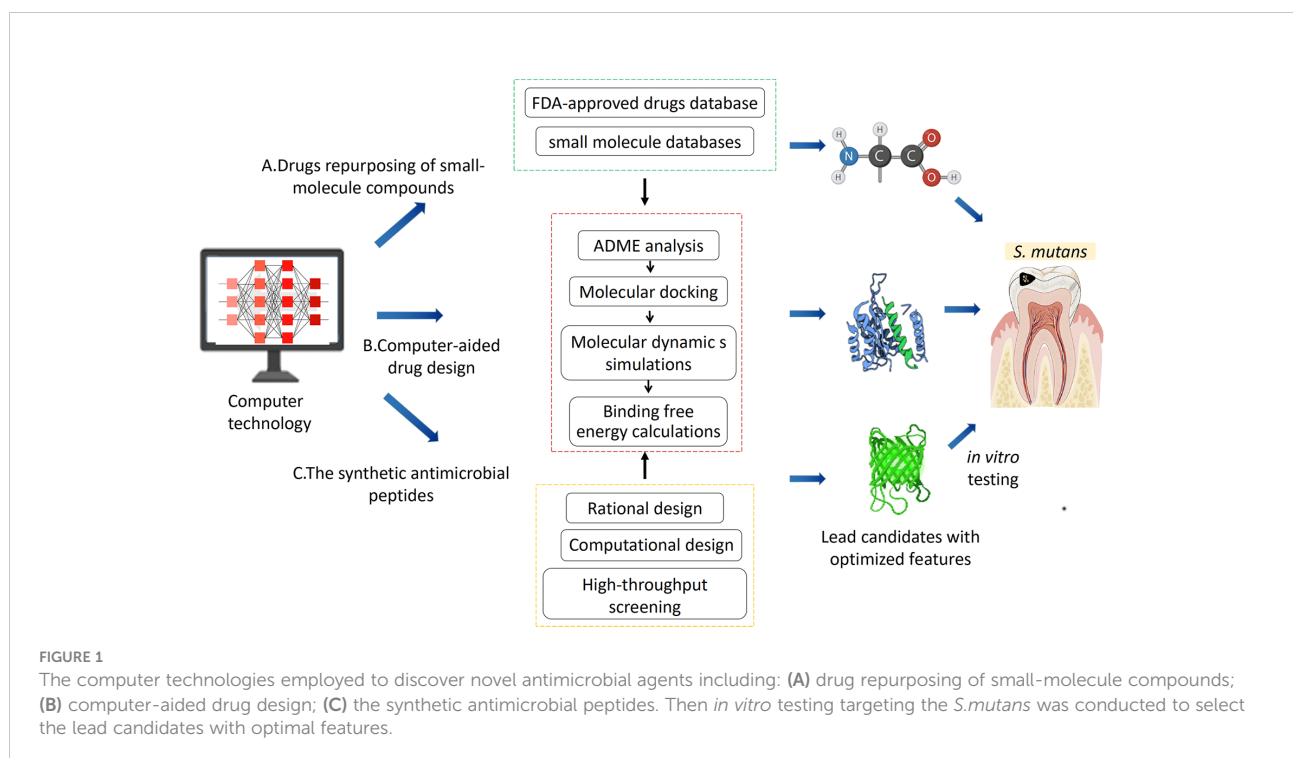
Drugs repurposing of small-molecule compounds

Drug repurposing is a method for discovering new uses of the original drugs beyond the scope of the medical indications. Compared to new drug discovery and development, it offers the advantages of lowering drug development cost and risk as existing drugs have already gone through clinical development stages (Ashburn and Thor, 2004). Small molecule compounds, with a molecular weight <1000 Da, have shown good antimicrobial activity, good stability and low toxicity (Xie et al., 2017; Roman, 2021). Recently, a number of comprehensive small molecule databases have emerged including DrugBank (Wishart et al., 2006), ChEMBL (Bento et al., 2014), PharmGKB (Hewett et al., 2002), Zinc (Williams, 2008), and PubChem (Wang et al., 2012), which have improved the chances of success by enabling the pre-selection of active compounds to test *in vitro*. *In silico* prediction of interactions between drugs and target proteins provides a convenient method to predict the new drug–target interactions (DTIs) (Wang and Zeng, 2013). Molecular docking, ligand-based and network-based approaches have been commonly used in virtually screening for a large number of compounds against a target protein (Ekins et al., 2007; Wang and Zeng, 2013). Moreover, Li (Li et al., 2011) have obtained a high enrichment of true positives predictions by using known interaction docking, consensus scoring, and specificity criteria.

Nitro group is critical for the anti–infective activity of nitro-based antimicrobial drugs, including nitroimidazoles, nitrothiazoles, and nitrofurans (Stover et al., 2000; Torreele et al., 2010). Based on the antimicrobial activity of nitrofurans against *S.mutans*, Zhang (Zhang et al., 2019) synthesized a novel water–soluble hybrid of indolin-2-one and nitrofuran ZY354, which exhibited low cytotoxicity and remarkable antimicrobial activity against *S.mutans* in multi-species biofilms. Toremifene, an FDA-approved drug for treating breast cancer, has also shown good inhibitory effect on the growth of *S. mutans* (Gerits et al., 2017a). Kuang (Kuang et al., 2020) identified a natural anticancer compound napabucasin (NAP) showed antimicrobial activity against oral *streptococci*. Using NAP as a lead compound, Xiao (Lyu et al., 2021) redesigned and synthesized a novel molecule LCG-N25. LCG-N25 exhibited stronger antimicrobial activity toward *S.mutans* with lower cytotoxicity.

Vitamin C and vitamin D are essential nutrients to human health. Interestingly, increased evidence showed that salivary vitamin C and serum vitamin D levels were associated with the occurrence of dental caries (Syed et al., 2019). Vitamin C has been reported to inhibit the synthesis of EPSs *via* inhibition of the quorum sensing and other stationary phase regulatory mechanisms (Pandit et al., 2017). Moreover, there was a concentration-dependent inhibitory effect of vitamin C on *S. mutans* growth and biofilm formation (Eydou et al., 2020). Vitamin D plays a key role in tooth mineralization, and it can lead to the "rachitic tooth" if the levels are unregulated (Foster et al., 2014). Saputo (Saputo et al., 2018) had screened FDA-approved drugs to identify old drugs with new therapeutic effects against *S. mutans*, and identified the vitamin D derivative doxercalciferol could interfere with *S. mutans* wall synthesis. Doxercalciferol exhibited synergistic activity in combination with bacitracin and possessed lytic activity against *S. mutans* through a bacitracin resistance mechanism of MbrABCD. Ferumoxytol was an FDA approved nanoparticle to treat iron deficiency (Schwenk, 2010). Liu (Liu et al., 2018) proved that ferumoxytol could disrupt intractable oral biofilms and prevent dental caries *via* intrinsic peroxidase-like activity.

Other drugs, such as dihydrofolate reductase inhibitor, trimetrexate analogues (Zhang et al., 2015), antiasthmatic drug zafirlukast (Gerits et al., 2017b), antifungal azoles lotrimazole and econazole (Qiu et al., 2017), efflux inhibitors reserpine (Zeng et al., 2017) have also been shown as potential inhibitors against *S. mutans* growth (Cui et al., 2019). Dipeptidyl peptidase (DPP IV) is a well-known therapeutic target in Type II diabetes. Anti-human DPP IV drugs saxagliptin can affect *S. mutans* growth (De et al., 2016; De et al., 2018).

Although drug repositioning has advantages such as lower cost, shorter development timelines and higher safety, the side effects and adverse reactions are yet to be solved (Yang et al., 2021). Firstly, the cytotoxicity of the novel molecules, particularly for the synthetic molecules should be comprehensively evaluated before clinical translation. In addition, drug resistance by oral bacteria still requires long-term evaluation both *in vitro* and *in vivo* models (Saputo et al., 2018). And the indications of reused drugs are narrow compared to antibiotics due to their original effects.

Computer-aided drug design (CADD)

Rapid developments in computer technology makes it possible to investigate biomolecular interactions at the molecular level and design/redesign new chemical molecules through computer-aided drug design (CADD) (Dixon et al., 2006). High research costs and significant decrease in the number of new drug approvals have made commercial pharmaceutical companies hesitant to spend on drug discovery research to some extent (Kitchen et al., 2004). CADD provides information about the bioactive parts of compounds virtually and allow rapid examination of the synthesis processes in a resource-efficient, more reliable, and cost-effective way without actually manufacturing them (Kitchen et al., 2004; Thomford et al., 2018; Xu et al., 2022a). Structure-based virtual screening (SBVS) and ligand-based virtual screening (LBVS) are two main strategies commonly applied in computer-aided drug discovery (Khan et al., 2019). SBVS depends on the structure of the target

and interactions with the ligands, while LBVS relies on the central similarity-property principle which indicates that similar molecules should exhibit similar properties (Ekins et al., 2007). The chemical similarity calculations are the core of LBVS (Willett, 2003). The methods of LBVS include similarity and substructure searching, quantitative structure-activity relationships (QSAR), and pharmacophore and 3D shape matching (Lavecchia and Di Giovanni, 2013). On the other hand, SBVS employs the 3D structure of the biological target to dock the candidate molecules and ranks them based on their predicted binding affinity or complementarity to the binding site (Lavecchia and Di Giovanni, 2013). SBVS and LBVS significantly minimize the complexity of finding potential therapeutic compounds against the pathogenic bacterial (Tan et al., 2008). Carmen identified ALS-31 as a small molecule inhibitor of *S. mutans* superoxide dismutase (SOD) by LBVS and SBVS, which inhibited planktonic growth and biofilm formation of *S. mutans* (Cerchia et al., 2022). Pushkaran and his colleagues (Pushkaran et al., 2019) computationally evaluated repurposing of an FDA approved drug Diosmin (DIO) using structure-based drug design method. They identified Diosmin (DIO) targeting the active site residues of L, D-transpeptidase (Ldt) enzymes which involved in *Mycobacterium tuberculosis* (*M. bt*) cell wall biosynthesis.

The process of CADD usually includes the following steps. First, various compounds aimed at the target enzyme undergo high-throughput screening. Then an absorption, distribution, metabolism and excretion (ADME) analysis is performed to determine the pharmacokinetic properties of these screened compounds. Next, molecular docking is applied to investigate the mechanism of interaction between these compounds and the target enzyme structure at the molecular level. Finally, molecular dynamic (MD) simulations and binding free energy calculations are performed to analyze the structure stability (Kitchen et al., 2004; Thomford et al., 2018). Key virulence factors such as antigens I/II, Gtfs and SrtA are usually exploited as the targets for computer-aided drug design against *S. mutans* (Table 1).

Antigens I/II

The antigen I/II (Ag I/II) family of adhesins are widely distributed on the cell surface of many streptococci, which also involved in *S. mutans* adhesion to the tooth surface and the bacterial co-aggregation (Matsumoto-Nakano, 2018; Yang et al., 2018). Through virtual searching for inhibitors based on Ag I/II protein structures, Rivera (Rivera-Quiroga et al., 2020) found three molecules ZINC19835187 (ZI-187), ZINC19924939 (ZI-939) and ZINC19924906 (ZI-906) inhibited about 90% adhesion of *S. mutans*. *S. mutans* cell-surface-localized adhesin P1, is an amyloid-forming protein (Tang et al., 2016). The interactions between C123 (C-terminal segment) and P1 contribute to

biofilm-related events such as amyloid fibrils formation, suggesting that C3 would serve as a promising anti-amyloid target (Rivière et al., 2020). Chen (Chen et al., 2021) selected small molecules targeting C3 through structure-based virtual screening, and found that D25 selectively inhibited amyloid fibrils and *S. mutans* biofilms but had little influence on biofilms formed by *S. gordonii* and *S. sanguinis*.
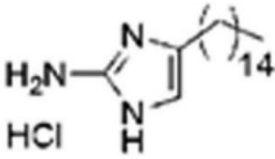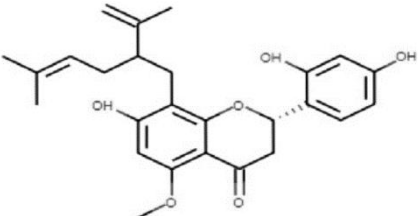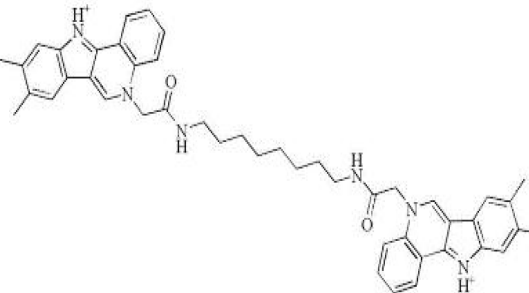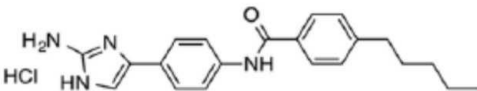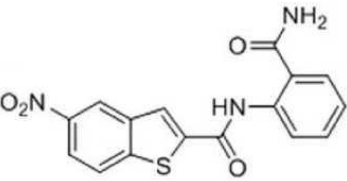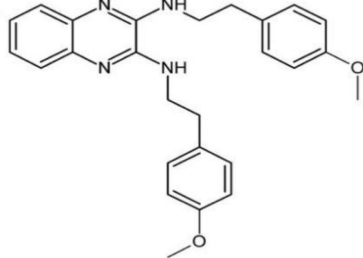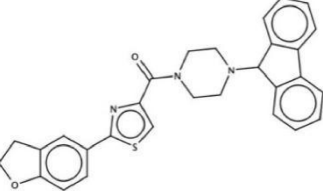
Sortase A

Sortase A (SrtA), one of the membrane-associated sortase enzymes, is responsible for anchoring of numerous virulence-associated surface proteins, including FruA, GbpC, Pac, WapA and Dex, and thus contributes to the biofilm formation of *S. mutans* (Luo et al., 2017). Although small molecules and natural products including trans-chalcone and flavonoid compounds exhibit effective inhibition against SrtA (Hu et al., 2013; Huang et al., 2014; Singh et al., 2014; Panche et al., 2016). The multi-drug resistance and side-effects make the discovery of new inhibitors for SrtA necessary (Luo et al., 2017). After high-throughput screening, CHEMBL243796 (kurarinone) was found to have especially good inhibitory activity against *S. mutans* SrtA (Salmanli et al., 2021). Luo (Luo et al., 2017) revealed that several similar compounds including acteoside (ZINC95098840) and oleuropein (ZINC98230413), with good affinities and appropriate pharmacokinetic parameters, were potential inhibitors to impede the catalysis of SrtA.

Glucosyltransferases
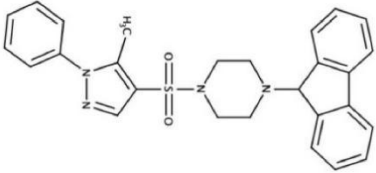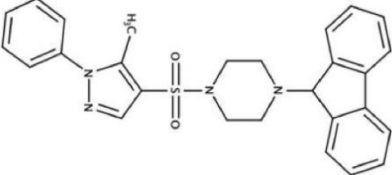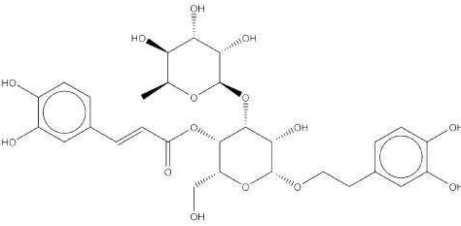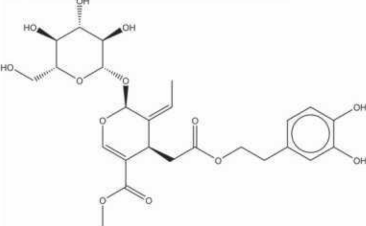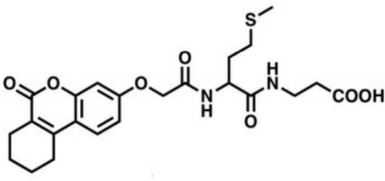
The glucosyltransferases (Gtfs) of *S. mutans* play essential roles in the etiology and pathogenesis of dental caries. The EPSs, mainly synthesized by Gtfs, provide binding sites that promote accumulation of microorganisms on the tooth surface and further establishment of pathogenic biofilms (Koo et al., 2010). Based on SBVS method, Zhang (Zhang et al., 2017) found two small-molecule compounds #G16 and #G43 specifically inhibited Gtfs and *S. mutans* biofilm formation. The compound #G43 showed great inhibitory effect on the activity of GtfB and GtfC than #G16. Ren (Ren et al., 2016) screened approximately 150,000 compounds from commercially available databases and identified a quinoxaline derivative, 2-(4-methoxyphenyl)-N-(3-{[2-(4-methoxyphenyl)ethyl]imino}-1,4-dihydro-2-quinoxalinylidene) ethanamine as a potential GtfC inhibitor. The computational techniques in drug design have improved the development and optimization of active compounds (Ejalonibu et al., 2021). Liu (Liu et al., 2011) screened a focused small-molecule library and found eight active compounds inhibit *S. mutans* production of Ag I/II and Gtf, sharing similar structural of 2-aminoimidazole (2-AI),

TABLE 1   Progress in computer-aided drug design (CADD) towards *S.mutans*.

Antimicrobial agents	Chemical Formula	Mechanisms	References
2A4		Selectively inhibit *S. mutans* adhesion.	(Liu et al., 2011)
CHEMBL243796		Inhibit *S. mutans* SrtA enzyme activity	(Salmanli et al., 2021)
D25		Selectively inhibit antigen I/II and *S. mutans* biofilms	(Chen et al., 2021)
3F1		Specifically target *S. mutans* biofilms independently of antigen I/II and Gtfs	(Garcia et al., 2017)
G43		Inhibit *S. mutans* Gtfs and biofilm formation	(Zhang et al., 2017)
2-(4-methoxyphenyl)-N-(3-{[2-(4-methoxyphenyl)ethyl]imino}-1,4-dihydro-2-quinoxalinylidene)ethanamine		Inhibit EPS synthesis and biofilm formation in *S. mutans* by target GtfC	(Ren et al., 2016)
ZINC19835187 (ZI-187),		Inhibit *S. mutans* adhesion by binding Ag I/II	(Rivera-Quiroga et al., 2020)
ZINC19924939 (ZI-939)			

(Continued)

TABLE 1 Continued

Antimicrobial agents	Chemical Formula	Mechanisms	References
ZINC19924906 (ZI-906)			
ZINC95098840		Interact with SrtA and impede SrtA catalysis	(Luo et al., 2017)
ZINC99230413			
ZLS-31		Inhibit *S. mutans* SOD	(Cerchia et al., 2022)

which helped to design the derivatives of marine natural products to inhibit both Gram-positive and Gram-negative bacteria.

The synthetic antimicrobial peptides

Antimicrobial peptides (AMPs) are small bioactive proteins that comprise a part of the body's first line to inactivate pathogens (Magana et al., 2020). AMPs can inhibit the growth of bacteria, disrupt bacterial cell membrane structure and compete with bacteria for adhesion (Jenssen et al., 2006; Guaní-Guerra et al., 2010; Magana et al., 2020). However, natural antimicrobial peptides generally have limitations, such as a short half-life, unstable in the variable oral environment,

and might lead to bacterial resistance (Torres et al., 2019; Niyonsaba et al., 2020). The synthetic AMPs has the advantages including slower emergence of resistance, increased selectivity, and decreased cytotoxicity toward healthy cells (Sullivan et al., 2011; Dalzini et al., 2016; Pletzer et al., 2016). The artificial antimicrobial peptides also have favorable pharmacokinetics and desirable stability (Niu et al., 2021a; Niu et al., 2021b). The synthesized antimicrobial peptide SET-M33D, an isomeric form with D amino acids, can kill multi-resistant pathogens, including Gram-positive *S. aureus*, *S. saprophyticus*, and various Gram-negative *Enterobacteriaceae* with high efficacy and low toxicity (Brunetti et al., 2020). The synthesized antimicrobial peptide GH12 induced low toxicity in human gingival fibroblasts and significantly reduce the cariogenic properties of *S. mutans* by decreasing the lactic acid

production and water-insoluble EPS synthesis (Wang et al., 2018). GH12 could make *S. sanguinis* and *S. gordonii* expand their ecological advantages by promoting hydrogen peroxide production, shifting the microbial composition to a more balanced one (Jiang et al., 2018; Jiang et al., 2020).

The methods of AMPs synthesis or discovery can be grouped into three approaches: rational design, computational design and high-throughput screening (Torres et al., 2019; Lei et al., 2021).

Rational design

The fusion of targeting and killing peptides is a common rational design strategy (Guo et al., 2015). A new class of pathogen-selective molecules, called selectively or specifically targeted antimicrobial peptides (STAMPs) was constructed (Eckert et al., 2006b; Huo et al., 2018). STAMP contains a pathogen-specific target peptide and antimicrobial peptide and/or connecting regions can selectively kill bacteria (Huo et al., 2018). *S. mutans* quorum-sensing (QS) system regulates the gene expression, bacteriocin production and biological behavior partially through competence stimulating peptide (CSP) (Huo et al., 2018). CSP serves as a STAMP targeting domain to mediate *S. mutans*-specific delivery of the antimicrobial peptide domain (Eckert et al., 2006a). When fused with broad antimicrobial peptide G2 at either the C terminus or N terminus, the CSP-derived STAMP C16G2, M8G2 and C16-33 showed robust, specific activity against *S. mutans* grown in planktonic cultures and biofilms in both single and multi-species biofilm states (Eckert et al., 2006a; Sullivan et al., 2011; De La Fuente-Nunez, 2019). The STAMPs C16G2, M8G2, C16-33, and M8-33 can target *S. mutans* without disturbing noncariogenic oral streptococci, indicating that they can maintain a normal ecological balance (Tan et al., 2008). Li (Li et al., 2010) synthesized *S. mutans*-specific targeting peptide 2_1G2, a derivative in which the *S. mutans*-specific CSPC16 targeting domain was replaced with peptide 2_1. The STAMP 2_1G2 could lead to protective biofilms formation with the ability to prevent secondary surface colonization by cariogenic *S. mutans*. A series of STAMPs C8H, C11H, C12H, C13H, and C14H were synthesized, and their selective antibacterial activity against *S. mutans* on single species and multi-species biofilms were studied, and a total of 21 protein spots were downregulated after C11H treatment.

Computational design

Advances in computational-resources have facilitated the discovery and synthesis of novel AMPs (Porto et al., 2017; De La Fuente-Nunez, 2019), including structure-activity relationships (SAR) study (Abdel Monaim et al., 2018), neural networks

(Müller et al., 2018), deep learning (Hamid and Friedberg, 2019). Since understanding the role and importance of each amino acid residue in a given sequence is fundamental for programming peptide, quantitative structure–activity relationship studies (QSAR) have been used to describe amino acid residues and their features (Torres et al., 2021). The approaches applied for the identification of AMPs from databases, including local alignments, regular expressions (REGEX), activity prediction by machine learning (Porto et al., 2017). By using supervised machine learning and a genetic algorithm, Boone (Boone et al., 2021) found a peptide active against *S. epidermidis*, with an improved ease of synthesis. Yazici (Yazici et al., 2016) analyzed the structures and predicted ternary conformations of the engineered chimeric peptides through computational modeling methods, which exhibited antimicrobial activity against *S. mutans*, *S. epidermidis*, and *E. coli*.

High-throughput screening

High-throughput screening of peptides is also an effective way. The main advantage of large screens is the higher probability of obtaining hits, which helping to select and optimize complex molecular descriptors, and obtain a more precise definition of simple molecular descriptors (Torres et al., 2021). Xie have developed an effective high-throughput screening system for designing and screening peptides that acted selectively on microbial membranes (Xie et al., 2006). However, the reported number of molecules needed to achieve conclusive SAR studies is higher than that required for structure-based screening approaches (Torres et al., 2021).

Conclusion and future prospects

Traditional anti-caries agents, such as fluoride, chlorhexidine, and antibiotics, are characterized by side-effects and low selectivity, which may destroy the homeostasis of oral microbiome. More attention is being directed to find alternative agents to control biofilm-related diseases. Drug repurposing of small molecule compounds lower drug development cost and risk. However, it has come to a consensus that preventing or treating dental biofilms are particularly challenging with small-molecule drugs due to low solubility, brief topical-exposure regimens, salivary clearance, and limited drug diffusion into EPS biofilm matrix (Sims et al., 2020; Osman et al., 2022). Nanoparticle carriers have shown good ability to increase small- molecule drug penetration to biofilms, improve drug stability, and enhance drug bioavailability (Sims et al., 2020; Zhang et al., 2021), which

may be potential candidates for clinical translation (Xu et al., 2022b). CADD provides information about the bioactive parts of compounds virtually and allow rapid examination of the synthesis processes. Using friendly and publicly accessible web-servers may be the future direction of prediction methods and computational tools development (Porto et al., 2018). And one of the limitations of computer-guided methods is the need for standardized and reliable biological data as input for designing process. The new synthesized antimicrobial peptide showed increased selectivity and decreased cytotoxicity, but AMPs perform poorly in the oral cavity due to low target specificity in solution, anionic protein adsorption and the diluting effects of saliva (Ramburrun et al., 2021). Designing hydroxyapatite-binding antimicrobial peptide (HBAMP), or incorporation into liquid crystalline systems (LCS) may be effective in the delivery of peptides, more strategies are still required to improve AMPs physiological *in vitro* and *in vivo* stability.

Moreover, it is noteworthy that current studies have mainly focused on *in vitro* or animal studies using single-species biofilms, which would limit the clinical translation of these approaches. The mechanism of small-molecule compounds' inhibitory effect on the biofilm is still unclear. The multi-species microbial, saliva, and enzyme make the oral cavity environment complex, affecting the efficacy of the novel agents *in vivo*. Combining these new methods, such as computational tools and algorithms, may be an effective way to synthesize novel antimicrobial agents. Further studies are also necessary to evaluate the antimicrobial activities, bioactivity, and biocompatibility of the novel drug more comprehensively and find effective drug delivery systems.

Conflict of interest

The authors declare that the research was conducted in the absence of any commercial or financial relationships that could be construed as a potential conflict of interest.

Publisher's note

All claims expressed in this article are solely those of the authors and do not necessarily represent those of their affiliated organizations, or those of the publisher, the editors and the reviewers. Any product that may be evaluated in this article, or claim that may be made by its manufacturer, is not guaranteed or endorsed by the publisher.

References

Abdel Monaim, S., Jad, Y. E., El-Faham, A., de la Torre, B. G., and Albericio, F. (2018). Teixobactin as a scaffold for unlimited new antimicrobial peptides: SAR study. *Bioorg. Med. Chem.* 26 (10), 2788–2796. doi: 10.1016/j.bmc.2017.09.040

Ashburn, T. T., and Thor, K. B. (2004). Drug repositioning: identifying and developing new uses for existing drugs. *Nat. Rev. Drug Discovery* 3 (8), 673–683. doi: 10.1038/nrd1468

Bento, A. P., Gaulton, A., Hersey, A., Bellis, L. J., Chambers, J., Davies, M., et al. (2014). The ChEMBL bioactivity database: an update. *Nucleic Acids Res.* 42 (Database issue), D1083–D1090. doi: 10.1093/nar/gkt1031

Bin Hafeez, A., Jiang, X., Bergen, P. J., and Zhu, Y. (2021). Antimicrobial peptides: An update on classifications and databases. *Int. J. Mol. Sci.* 22 (21), 11691–11742. doi: 10.3390/ijms222111691

Boone, K., Wisdom, C., Camarda, K., Spencer, P., and Tamerler, C. (2021). Combining genetic algorithm with machine learning strategies for designing potent antimicrobial peptides. *BMC Bioinf.* 22 (1), 239–255. doi: 10.1186/s12859-021-04156-x

Brookes, Z. L. S., Bescos, R., Belfield, L. A., Ali, K., and Roberts, A. (2020). Current uses of chlorhexidine for management of oral disease: a narrative review. *J. Dent.* 103, 103497–103505. doi: 10.1016/j.jdent.2020.103497

Brunetti, J., Carnicelli, V., Ponzi, A., Di Giulio, A., Lizzi, A. R., Cristiano, L., et al. (2020). Antibacterial and anti-inflammatory activity of an antimicrobial peptide synthesized with d amino acids. *Antibiot. (Basel)* 9 (12), 840–856. doi: 10.3390/antibiotics9120840

Cerchia, C., Roscetto, E., Nasso, R., Catania, M. R., De Vendittis, E., Lavecchia, A., et al. (2022). In silico identification of novel inhibitors targeting the homodimeric interface of superoxide dismutase from the dental pathogen *Streptococcus mutans*. *Antioxid. (Basel)* 11 (4), 785–803. doi: 10.3390/antiox11040785

Chen, Y., Cui, G., Cui, Y., Chen, D., and Lin, H. (2021). Small molecule targeting amyloid fibrils inhibits *Streptococcus mutans* biofilm formation. *AMB Express* 11 (1), 171–184. doi: 10.1186/s13568-021-01333-2

Coelho, A., Paula, A. B. P., Carrilho, T. M. P., Da Silva, M., Botelho, M., and Carrilho, E. (2017). Chlorhexidine mouthwash as an anticaries agent: A systematic review. *Quintessence Int.* 48 (7), 585–591. doi: 10.3290/j.qi.a38353

Cui, T., Luo, W., Xu, L., Yang, B., Zhao, W., and Cang, H. (2019). Progress of antimicrobial discovery against the major cariogenic pathogen *Streptococcus mutans*. *Curr. Issues Mol. Biol.* 32, 601–644. doi: 10.21775/cimb.032.601

Dalzini, A., Bergamini, C., Biondi, B., De Zotti, M., Panighel, G., Fato, R., et al. (2016). The rational search for selective anticancer derivatives of the peptide trichogin GA IV: a multi-technique biophysical approach. *Sci. Rep.* 6, 24000–24013. doi: 10.1038/srep24000

De La Fuente-Nunez, C. (2019). Toward autonomous antibiotic discovery. *mSystems* 4 (3), e00151–e00119. doi: 10.1128/mSystems.00151-19

De, A., Lupidi, G., Petrelli, D., and Vitali, L. A. (2016). Molecular cloning and biochemical characterization of xaa-pro dipeptidyl-peptidase from *Streptococcus*

mutans and its inhibition by anti-human DPP IV drugs. *FEMS Microbiol. Lett.* 363 (9), 066–072. doi: 10.1093/femsle/fnw066

De, A., Pompilio, A., Francis, J., Sutcliffe, I. C., Black, G. W., Lupidi, G., et al. (2018). Antidiabetic "gliptins" affect biofilm formation by *Streptococcus mutans*. *Microbiol. Res.* 209, 79–85. doi: 10.1016/j.micres.2018.02.005

Dixon, S. L., Smondyrev, A. M., and Rao, S. N. (2006). PHASE: a novel approach to pharmacophore modeling and 3D database searching. *Chem. Biol. Drug Des.* 67 (5), 370–372. doi: 10.1111/j.1747-0285.2006.00384.x

Eckert, R., He, J., Yarbrough, D. K., Qi, F., Anderson, M. H., and Shi, W. (2006a). Targeted killing of *Streptococcus mutans* by a pheromone-guided "smart" antimicrobial peptide. *Antimicrob. Agents Chemother.* 50 (11), 3651–3657. doi: 10.1128/aac.00622-06

Eckert, R., Qi, F., Yarbrough, D. K., He, J., Anderson, M. H., and Shi, W. (2006b). Adding selectivity to antimicrobial peptides: rational design of a multidomain peptide against *Pseudomonas* spp. *Antimicrob. Agents Chemother.* 50 (4), 1480–1488. doi: 10.1128/aac.50.4.1480-1488.2006

Ejalonibu, M. A., Ogundare, S. A., Elrashedy, A. A., Ejalonibu, M. A., Lawal, M. M., Mhlongo, N. N., et al. (2021). Drug discovery for *Mycobacterium tuberculosis* using structure-based computer-aided drug design approach. *Int. J. Mol. Sci.* 22 (24), 13259–13297. doi: 10.3390/ijms222413259

Ekins, S., Mestres, J., and Testa, B. (2007). In silico pharmacology for drug discovery: methods for virtual ligand screening and profiling. *Br. J. Pharmacol.* 152 (1), 9–20. doi: 10.1038/sj.bjp.0707305

Eydou, Z., Jad, B. N., Elsayed, Z., Ismail, A., Magaogao, M., and Hossain, A. (2020). Investigation on the effect of vitamin c on growth & biofilm-forming potential of *Streptococcus mutans* isolated from patients with dental caries. *BMC Microbiol.* 20 (1), 231–241. doi: 10.1186/s12866-020-01914-4

Flemming, H. C., Wingender, J., Szewzyk, U., Steinberg, P., Rice, S. A., and Kjelleberg, S. (2016). Biofilms: an emergent form of bacterial life. *Nat. Rev. Microbiol.* 14 (9), 563–575. doi: 10.1038/nrmicro.2016.94

Foster, B. L., Nociti, F. H.Jr., and Somerman, M. J. (2014). The rachitic tooth. *Endocr. Rev.* 35 (1), 1–34. doi: 10.1210/er.2013-1009

Garcia, S. S., Blackledge, M. S., Michalek, S., Su, L., Ptacek, T., Eipers, P., et al. (2017). Targeting of *Streptococcus mutans* biofilms by a novel small molecule prevents dental caries and preserves the oral microbiome. *J. Dent. Res.* 96 (7), 807–814. doi: 10.1177/0022034517698096

Gerits, E., Defraine, V., Vandamme, K., De Cremer, K., De Brucker, K., Thevissen, K., et al. (2017a). Repurposing toremifene for treatment of oral bacterial infections. *Antimicrob. Agents Chemother.* 61 (3), e01846–e01816. doi: 10.1128/aac.01846-16

Gerits, E., van der Massen, I., Vandamme, K., De Cremer, K., De Brucker, K., Thevissen, K., et al. (2017b). *In vitro* activity of the antiasthmatic drug zafirlukast against the oral pathogens *Porphyromonas gingivalis* and *Streptococcus mutans*. *FEMS Microbiol. Lett.* 364 (2), 005–011. doi: 10.1093/femsle/fnx005

Guaní-Guerra, E., Santos-Mendoza, T., Lugo-Reyes, S. O., and Terán, L. M. (2010). Antimicrobial peptides: general overview and clinical implications in human health and disease. *Clin. Immunol.* 135 (1), 1–11. doi: 10.1016/j.clim.2009.12.004

Guo, L., Mclean, J. S., Yang, Y., Eckert, R., Kaplan, C. W., Kyme, P., et al. (2015). Precision-guided antimicrobial peptide as a targeted modulator of human microbial ecology. *Proc. Natl. Acad. Sci. U.S.A.* 112 (24), 7569–7574. doi: 10.1073/pnas.1506207112

Hamid, M. N., and Friedberg, I. (2019). Identifying antimicrobial peptides using word embedding with deep recurrent neural networks. *Bioinformatics* 35 (12), 2009–2016. doi: 10.1093/bioinformatics/bty937

Hewett, M., Oliver, D. E., Rubin, D. L., Easton, K. L., Stuart, J. M., Altman, R. B., et al. (2002). PharmGKB: the pharmacogenetics knowledge base. *Nucleic Acids Res.* 30 (1), 163–165. doi: 10.1093/nar/30.1.163

Huang, P., Hu, P., Zhou, S. Y., Li, Q., and Chen, W. M. (2014). Morin inhibits sortase a and subsequent biofilm formation in *Streptococcus mutans*. *Curr. Microbiol.* 68 (1), 47–52. doi: 10.1007/s00284-013-0439-x

Huang, Y., Liu, Y., Shah, S., Kim, D., Simon-Soro, A., Ito, T., et al. (2021). Precision targeting of bacterial pathogen *via* bi-functional nanozyme activated by biofilm microenvironment. *Biomaterials* 268, 120581–120605. doi: 10.1016/j.biomaterials.2020.120581

Hu, P., Huang, P., and Chen, W. M. (2013). Curcumin inhibits the sortase a activity of the *Streptococcus mutans* UA159. *Appl. Biochem. Biotechnol.* 171 (2), 396–402. doi: 10.1007/s12010-013-0378-9

Huo, L., Huang, X., Ling, J., Liu, H., and Liu, J. (2018). Selective activities of STAMPs against *Streptococcus mutans*. *Exp. Ther. Med.* 15 (2), 1886–1893. doi: 10.3892/etm.2017.5631

Jakubovics, N. S., Goodman, S. D., Mashburn-Warren, L., Stafford, G. P., and Cieplik, F. (2021). The dental plaque biofilm matrix. *Periodontol.* 86 (1), 32–56. doi: 10.1111/prd.12361

Jenssen, H., Hamill, P., and Hancock, R. E. (2006). Peptide antimicrobial agents. *Clin. Microbiol. Rev.* 19 (3), 491–511. doi: 10.1128/cmr.00056-05

Jiang, W., Wang, Y., Luo, J., Chen, X., Zeng, Y., Li, X., et al. (2020). Antimicrobial peptide GH12 prevents dental caries by regulating dental plaque microbiota. *Appl. Environ. Microbiol.* 86 (14), e00527–e00520. doi: 10.1128/aem.00527-20

Jiang, W., Wang, Y., Luo, J., Li, X., Zhou, X., Li, W., et al. (2018). Effects of antimicrobial peptide GH12 on the cariogenic properties and composition of a cariogenic multispecies biofilm. *Appl. Environ. Microbiol.* 84 (24), e01423–e01418. doi: 10.1128/aem.01423-18

Kanwar, I., Sah, A. K., and Suresh, P. K. (2017). Biofilm-mediated antibiotic-resistant oral bacterial infections: mechanism and combat strategies. *Curr. Pharm. Des.* 23 (14), 2084–2095. doi: 10.2174/1381612822666161124154549

Khan, S. U., Ahemad, N., Chuah, L. H., Naidu, R., and Htar, T. T. (2019). Sequential ligand- and structure-based virtual screening approach for the identification of potential G protein-coupled estrogen receptor-1 (GPER-1) modulators. *RSC Adv.* 9 (5), 2525–2538. doi: 10.1039/c8ra09318k

Kitchen, D. B., Decornez, H., Furr, J. R., and Bajorath, J. (2004). Docking and scoring in virtual screening for drug discovery: methods and applications. *Nat. Rev. Drug Discovery* 3 (11), 935–949. doi: 10.1038/nrd1549

Koo, H., Xiao, J., Klein, M. I., and Jeon, J. G. (2010). Exopolysaccharides produced by *Streptococcus mutans* glucosyltransferases modulate the establishment of microcolonies within multispecies biofilms. *J. Bacteriol.* 192 (12), 3024–3032. doi: 10.1128/jb.01649-09

Kuang, X., Yang, T., Zhang, C., Peng, X., Ju, Y., Li, C., et al. (2020). Repurposing napabucasin as an antimicrobial agent against oral streptococcal biofilms. *BioMed. Res. Int.* 2020, 8379526–8379534. doi: 10.1155/2020/8379526

Lavecchia, A., and Di Giovanni, C. (2013). Virtual screening strategies in drug discovery: a critical review. *Curr. Med. Chem.* 20 (23), 2839–2860. doi: 10.2174/09298673113209990001

Lei, M., Jayaraman, A., Van Deventer, J. A., and Lee, K. (2021). Engineering selectively targeting antimicrobial peptides. *Annu. Rev. BioMed. Eng.* 23, 339–357. doi: 10.1146/annurev-bioeng-010220-095711

Li, Y. Y., An, J., and Jones, S. J. (2011). A computational approach to finding novel targets for existing drugs. *PloS Comput. Biol.* 7 (9), e1002139. doi: 10.1371/journal.pcbi.1002139

Li, L. N., Guo, L. H., Lux, R., Eckert, R., Yarbrough, D., He, J., et al. (2010). Targeted antimicrobial therapy against *Streptococcus mutans* establishes protective non-cariogenic oral biofilms and reduces subsequent infection. *Int. J. Oral. Sci.* 2 (2), 66–73. doi: 10.4248/ijos10024

Liu, Y., Naha, P. C., Hwang, G., Kim, D., Huang, Y., Simon-Soro, A., et al. (2018). Topical ferumoxytol nanoparticles disrupt biofilms and prevent tooth decay *in vivo via* intrinsic catalytic activity. *Nat. Commun.* 9 (1), 2920–2931. doi: 10.1038/s41467-018-05342-x

Liu, C., Worthington, R. J., Melander, C., and Wu, H. (2011). A new small molecule specifically inhibits the cariogenic bacterium *Streptococcus mutans* in multispecies biofilms. *Antimicrob. Agents Chemother.* 55 (6), 2679–2687. doi: 10.1128/aac.01496-10

Luo, H., Liang, D. F., Bao, M. Y., Sun, R., Li, Y. Y., Li, J. Z., et al. (2017). In silico identification of potential inhibitors targeting *Streptococcus mutans* sortase a. *Int. J. Oral. Sci.* 9 (1), 53–62. doi: 10.1038/ijos.2016.58

Lyu, X., Li, C., Zhang, J., Wang, L., Jiang, Q., Shui, Y., et al. (2021). A novel small molecule, LCG-N25, inhibits oral streptococcal biofilm. *Front. Microbiol.* 12. doi: 10.3389/fmicb.2021.654692

Magana, M., Pushpanathan, M., Santos, A. L., Leanse, L., Fernandez, M., Ioannidis, A., et al. (2020). The value of antimicrobial peptides in the age of resistance. *Lancet Infect. Dis.* 20 (9), e216–e230. doi: 10.1016/s1473-3099(20)30327-3

Mai, J., Tian, X. L., Gallant, J. W., Merkley, N., Biswas, Z., Syvitski, R., et al. (2011). A novel target-specific, salt-resistant antimicrobial peptide against the cariogenic pathogen *Streptococcus mutans*. *Antimicrob. Agents Chemother.* 55 (11), 5205–5213. doi: 10.1128/aac.05175-11

Matsumoto-Nakano, M. (2018). Role of *Streptococcus mutans* surface proteins for biofilm formation. *Jpn. Dent. Sci. Rev.* 54 (1), 22–29. doi: 10.1016/j.jdsr.2017.08.002

Müller, A. T., Hiss, J. A., and Schneider, G. (2018). Recurrent neural network model for constructive peptide design. *J. Chem. Inf. Model.* 58 (2), 472–479. doi: 10.1021/acs.jcim.7b00414

Niu, J. Y., Yin, I. X., Mei, M. L., Wu, W. K. K., Li, Q. L., and Chu, C. H. (2021a). The multifaceted roles of antimicrobial peptides in oral diseases. *Mol. Oral. Microbiol.* 36 (3), 159–171. doi: 10.1111/omi.12333

Niu, J. Y., Yin, I. X., Wu, W. K. K., Li, Q. L., Mei, M. L., and Chu, C. H. (2021b). Antimicrobial peptides for the prevention and treatment of dental caries: A concise review. *Arch. Oral. Biol.* 122, 105022–105033. doi: 10.1016/j.archoralbio.2020.105022

Niyonsaba, F., Song, P., Yue, H., Sutthammikorn, N., Umehara, Y., Okumura, K., et al. (2020). Antimicrobial peptide derived from insulin-like growth factor-binding protein 5 activates mast cells *via* mas-related G protein-coupled receptor X2. *Allergy* 75 (1), 203–207. doi: 10.1111/all.13975

Niyonsaba, F., Song, P., Yue, H., Sutthammikorn, N., Umehara, Y., Okumura, K., et al. (2020). Antimicrobial peptide derived from insulin-like growth factor-binding protein 5 activates mast cells *via* mas-related G protein-coupled receptor X2. *Allergy* 75 (1), 203–207. doi: 10.1111/all.13975

Osman, N., Devnarain, N., Omolo, C. A., Fasiku, V., Jaglal, Y, and Govender, T. (2016). Surface modification of nano-drug delivery systems for enhancing antibiotic delivery and activity. *Wiley Interdisc Rev Nanomed Nanobiotechnol*, 14 (1), e1758–e61. doi: 10.1002/wnan.1758

Pandit, S., Ravikumar, V., Abdel-Haleem, A. M., Derouiche, A., Mokkapati, V., Sihlbom, C., et al. (2017). Low concentrations of vitamin c reduce the synthesis of extracellular polymers and destabilize bacterial biofilms. *Front. Microbiol.* 8(2599). doi: 10.3389/fmicb.2017.02599

Pathak, J. L., Yan, Y., Zhang, Q., Wang, L., and Ge, L. (2021). The role of oral microbiome in respiratory health and diseases. *Respir. Med.* 185, 106475–106482. doi: 10.1016/j.rmed.2021.106475

Pitts, N. B., Zero, D. T., Marsh, P. D., Ekstrand, K., Weintraub, J. A., Ramos-Gomez, F., et al. (2017). Dental caries. *Nat. Rev. Dis. Primers* 3, 17030–17045. doi: 10.1038/nrdp.2017.30

Pletzer, D., Coleman, S. R., and Hancock, R. E. (2016). Anti-biofilm peptides as a new weapon in antimicrobial warfare. *Curr. Opin. Microbiol.* 33, 35–40. doi: 10.1016/j.mib.2016.05.016

Porto, W. F., Fensterseifer, I. C. M., Ribeiro, S. M., and Franco, O. L. (2018). Joker: An algorithm to insert patterns into sequences for designing antimicrobial peptides. *Biochim. Biophys. Acta Gen. Subj.* 1862 (9), 2043–2052. doi: 10.1016/j.bbagen.2018.06.011

Porto, W., Pires, A., and Franco, O. (2017). Computational tools for exploring sequence databases as a resource for antimicrobial peptides. *Biotechnol. Adv.* 35 (3), 337–349. doi: 10.1016/j.biotechadv.2017.02.001

Pushkaran, A. C., Vinod, V., Vanuopadath, M., Nair, S. S., Nair, S. V., Vasudevan, A. K., et al. (2019). Combination of repurposed drug diosmin with amoxicillin-clavulanic acid causes synergistic inhibition of mycobacterial growth. *Sci. Rep.* 9 (1), 6800–6813. doi: 10.1038/s41598-019-43201-x

Qiu, W., Ren, B., Dai, H., Zhang, L., Zhang, Q., Zhou, X., et al. (2017). Clotrimazole and econazole inhibit *Streptococcus mutans* biofilm and virulence *in vitro*. *Arch. Oral. Biol.* 73, 113–120. doi: 10.1016/j.archoralbio.2016.10.011

Ramburrun, P., Pringle, N. A., Dube, A., Adam, R. Z., D'souza, S., and Aucamp, M. (2021). Recent advances in the development of antimicrobial and antifouling biocompatible materials for dental applications. *Mater. (Basel)* 14 (12), 3167–3198. doi: 10.3390/ma14123167

Ren, Z., Cui, T., Zeng, J., Chen, L., Zhang, W., Xu, X., et al. (2016). Molecule targeting glucosyltransferase inhibits *Streptococcus mutans* biofilm formation and virulence. *Antimicrob. Agents Chemother.* 60 (1), 126–135. doi: 10.1128/aac.00919-15

Rivera-Quiroga, R. E., Cardona, N., Padilla, L., Rivera, W., Rocha-Roa, C., Diaz De Rienzo, M. A., et al. (2020). In silico selection and *in vitro* evaluation of new molecules that inhibit the adhesion of *Streptococcus mutants* through antigen I/II. *Int. J. Mol. Sci.* 22 (1), 377–393. doi: 10.3390/ijms22010377

Rivière, G., Peng, E. Q., Brotgandel, A., Andring, J. T., Lakshmanan, R. V., Agbandje-Mckenna, M., et al. (2020). Characterization of an intermolecular quaternary interaction between discrete segments of the *Streptococcus mutans* adhesin P1 by NMR spectroscopy. *FEBS J.* 287 (12), 2597–2611. doi: 10.1111/febs.15158

Roman, B. I. (2021). The expanding role of chemistry in optimizing proteins for human health applications. *J. Med. Chem.* 64 (11), 7179–7188. doi: 10.1021/acs.jmedchem.1c00294

Salmanli, M., Tatar Yilmaz, G., and Tuzuner, T. (2021). Investigation of the antimicrobial activities of various antimicrobial agents on *Streptococcus mutans* sortase a through computer-aided drug design (CADD) approaches. *Comput. Methods Programs BioMed.* 212, 106454–106461. doi: 10.1016/j.cmpb.2021.106454

Saputo, S., Faustoferri, R. C., and Quivey, R. G.Jr. (2018). Vitamin D compounds are bactericidal against Streptococcus mutans and target the bacitracin-associated efflux system. *Antimicrob. Agents Chemother.* 62 (1), e01675–e01617. doi: 10.1128/aac.01675-17

Schwenk, M. H. (2010). Ferumoxytol: a new intravenous iron preparation for the treatment of iron deficiency anemia in patients with chronic kidney disease. *Pharmacotherapy* 30 (1), 70–79. doi: 10.1592/phco.30.1.70

Simon, G., Bérubé, C., Voyer, N., and Grenier, D. (2019). Anti-biofilm and anti-adherence properties of novel cyclic dipeptides against oral pathogens. *Bioorg. Med. Chem.* 27 (12), 2323–2331. doi: 10.1016/j.bmc.2018.11.042

Sims, K. R.Jr., Maceren, J. P., Liu, Y., Rocha, G. R., Koo, H., and Benoit, D. S. W. (2020). Dual antibacterial drug-loaded nanoparticles synergistically improve treatment of *Streptococcus mutans* biofilms. *Acta Biomater.* 115, 418–431. doi: 10.1016/j.actbio.2020.08.032

Singh, P., Anand, A., and Kumar, V. (2014). Recent developments in biological activities of chalcones: a mini review. *Eur. J. Med. Chem.* 85, 758–777. doi: 10.1016/j.ejmech.2014.08.033

Sparks, T. C., Hahn, D. R., and Garizi, N. V. (2017). Natural products, their derivatives, mimics and synthetic equivalents: role in agrochemical discovery. *Pest Manag. Sci.* 73 (4), 700–715. doi: 10.1002/ps.4458

Stover, C. K., Warrener, P., Vandevanter, D. R., Sherman, D. R., Arain, T. M., Langhorne, M. H., et al. (2000). A small-molecule nitroimidazopyran drug candidate for the treatment of tuberculosis. *Nature* 405 (6789), 962–966. doi: 10.1038/35016103

Sullivan, R., Santarpia, P., Lavender, S., Gittins, E., Liu, Z., Anderson, M. H., et al. (2011). Clinical efficacy of a specifically targeted antimicrobial peptide mouth rinse: targeted elimination of *Streptococcus mutans* and prevention of demineralization. *Caries Res.* 45 (5), 415–428. doi: 10.1159/000330510

Syed, S., Yassin, S. M., Dawasaz, A. A., Amanullah, M., Alshahrani, I., and Togoo, R. A. (2019). Salivary 1,5-anhydroglucitol and vitamin levels in relation to caries risk in children. *BioMed. Res. Int.* 2019, 4503450–4503456. doi: 10.1155/2019/4503450

Tang, W., Bhatt, A., Smith, A. N., Crowley, P. J., Brady, L. J., and Long, J. R. (2016). Specific binding of a naturally occurring amyloidogenic fragment of *Streptococcus mutans* adhesin P1 to intact P1 on the cell surface characterized by solid state NMR spectroscopy. *J. Biomol. NMR* 64 (2), 153–164. doi: 10.1007/s10858-016-0017-1

Tan, L., Geppert, H., Sisay, M. T., Gütschow, M., and Bajorath, J. (2008). Integrating structure- and ligand-based virtual screening: comparison of individual, parallel, and fused molecular docking and similarity search calculations on multiple targets. *ChemMedChem* 3 (10), 1566–1571. doi: 10.1002/cmdc.200800129

Thomford, N. E., Senthebane, D. A., Rowe, A., Munro, D., Seele, P., Maroyi, A., et al. (2018). Natural products for drug discovery in the 21st century: innovations for novel drug discovery. *Int. J. Mol. Sci.* 19 (6), 1578–1606. doi: 10.3390/ijms19061578

Torreele, E., Bourdin Trunz, B., Tweats, D., Kaiser, M., Brun, R., Mazué, G., et al. (2010). Fexinidazole–a new oral nitroimidazole drug candidate entering clinical development for the treatment of sleeping sickness. *PloS Negl. Trop. Dis.* 4 (12), e923–e937. doi: 10.1371/journal.pntd.0000923

Torres, M. D. T., Cao, J., Franco, O. L., Lu, T. K., and de la Fuente-Nunez, C. (2021). Synthetic biology and computer-based frameworks for antimicrobial peptide discovery. *ACS Nano* 15 (2), 2143–2164. doi: 10.1021/acsnano.0c09509

Torres, M. D. T., Sothiselvam, S., Lu, T. K., and de la Fuente-Nunez, C. (2019). Peptide design principles for antimicrobial applications. *J. Mol. Biol.* 431 (18), 3547–3567. doi: 10.1016/j.jmb.2018.12.015

Wang, Y., Wang, X., Jiang, W., Wang, K., Luo, J., Li, W., et al. (2018). Antimicrobial peptide GH12 suppresses cariogenic virulence factors of *Streptococcus mutans*. *J. Oral. Microbiol.* 10 (1), 1442089–1442099. doi: 10.1080/20002297.2018.1442089

Wang, Y., Xiao, J., Suzek, T. O., Zhang, J., Wang, J., Zhou, Z., et al. (2012). PubChem's bioAssay database. *Nucleic Acids Res.* 40, D400–D412. doi: 10.1093/nar/gkr1132

Wang, Y., and Zeng, J. (2013). Predicting drug-target interactions using restricted Boltzmann machines. *Bioinformatics* 29 (13), i126–i134. doi: 10.1093/bioinformatics/btt234

Willett, P. (2003). Similarity-based approaches to virtual screening. *Biochem. Soc. Trans.* 31 (Pt 3), 603–606. doi: 10.1042/bst0310603

Williams, A. J. (2008). A perspective of publicly accessible/open-access chemistry databases. *Drug Discovery Today* 13 (11-12), 495–501. doi: 10.1016/j.drudis.2008.03.017

Wishart, D. S., Knox, C., Guo, A. C., Shrivastava, S., Hassanali, M., Stothard, P., et al. (2006). DrugBank: a comprehensive resource for in silico drug discovery and exploration. *Nucleic Acids Res.* 34, D668–D672. doi: 10.1093/nar/gkj067

Xia, M. Y., Xie, Y., Yu, C. H., Chen, G. Y., Li, Y. H., Zhang, T., et al. (2019). Graphene-based nanomaterials: the promising active agents for antibiotics-independent antibacterial applications. *J. Control Release* 307, 16–31. doi: 10.1016/j.jconrel.2019.06.011

Xie, X., Fu, Y., and Liu, J. (2017). Chemical reprogramming and transdifferentiation. *Curr. Opin. Genet. Dev.* 46, 104–113. doi: 10.1016/j.gde.2017.07.003

Xie, Q., Matsunaga, S., Wen, Z., Niimi, S., Kumano, M., Sakakibara, Y., et al. (2006). *In vitro* system for high-throughput screening of random peptide libraries for antimicrobial peptides that recognize bacterial membranes. *J. Pept. Sci.* 12 (10), 643–652. doi: 10.1002/psc.774

Xu, Y., Huang, H., Wu, M., Tian, Y., Wan, Q., Shi, B., et al. (2022a). Rapid additive manufacturing of a superlight obturator for Large oronasal fistula in pediatric patient. *Laryngoscope*, 1–6. doi: 10.1002/lary.30352

Xu, Y., Xu, Y., Zhang, W., Li, M., Wendel, H. P., Geis-Gerstorfer, J., et al. (2022b). Biodegradable zn-Cu-Fe alloy as a promising material for craniomaxillofacial implants: An *in vitro* investigation into degradation behavior, cytotoxicity, and hemocompatibility. *Front. Chem.* 10, 860040–860056. doi: 10.3389/fchem.2022.860040

Yang, C., Scoffield, J., Wu, R., Deivanayagam, C., Zou, J., and Wu, H. (2018). Antigen I/II mediates interactions between *Streptococcus mutans* and *Candida albicans*. *Mol. Oral. Microbiol.* 33 (4), 283–291. doi: 10.1111/omi.12223

Yang, S., Zhang, J., Yang, R., and Xu, X. (2021). Small molecule compounds, a novel strategy against *Streptococcus mutans*. *Pathogens* 10 (12), 1540–1555. doi: 10.3390/pathogens10121540

Yazici, H., O'neill, M. B., Kacar, T., Wilson, B. R., Oren, E. E., Sarikaya, M., et al. (2016). Engineered chimeric peptides as antimicrobial surface coating agents toward infection-free implants. *ACS Appl. Mater. Interfaces* 8 (8), 5070–5081. doi: 10.1021/acsami.5b03697

Zeng, H., Liu, J., and Ling, J. (2017). Efflux inhibitor suppresses *Streptococcus mutans* virulence properties. *FEMS Microbiol. Lett.* 364 (7), 033–041. doi: 10.1093/femsle/fnx033

Zhang, C., Kuang, X., Zhou, Y., Peng, X., Guo, Q., Yang, T., et al. (2019). A novel small molecule, ZY354, iInhibits dental caries-associated oral biofilms. *Antimicrob. Agents Chemother.* 63 (5), e02414–e02418. doi: 10.1128/aac.02414-18

Zhang, Q., Nguyen, T., Mcmichael, M., Velu, S. E., Zou, J., Zhou, X., et al. (2015). New small-molecule inhibitors of dihydrofolate reductase inhibit *Streptococcus mutans*. *Int. J. Antimicrob. Agents* 46 (2), 174–182. doi: 10.1016/j.ijantimicag.2015.03.015

Zhang, Q., Nijampatnam, B., Hua, Z., Nguyen, T., Zou, J., Cai, X., et al. (2017). Structure-based discovery of small molecule inhibitors of cariogenic virulence. *Sci. Rep.* 7 (1), 5974–5983. doi: 10.1038/s41598-017-06168-1

Zhang, M., Yu, Z., and Lo, E. C. M. (2021). A new pH-responsive nano micelle for enhancing the effect of a hydrophobic bactericidal agent on mature *Streptococcus mutans* biofilm. *Front. Microbiol.* 12. doi: 10.3389/fmicb.2021.761583

Check for updates

Ecological influence by colonization of fluoride-resistant *Streptococcus mutans* in oral biofilm

Yan Shen, Fangzheng Yu, Lili Qiu, Mengjia Gao, Puxin Xu, Lingjun Zhang, Xiangyan Liao, Min Wang, Xiangyu Hu, Yan Sun* and Yihuai Pan*

School and Hospital of Stomatology, Wenzhou Medical University, Wenzhou, China

Background: Dental caries is one of the oldest and most common infections in humans. Improved oral hygiene practices and the presence of fluoride in dentifrices and mouth rinses have greatly reduced the prevalence of dental caries. However, increased fluoride resistance in microbial communities is concerning. Here, we studied the effect of fluoride-resistant Streptococcus mutans (S. mutans) on oral microbial ecology and compare it with wild-type S. mutans in vitro.

Methods: Biofilm was evaluated for its polysaccharide content, scanning electron microscopy (SEM) imaging, acid-producing ability, and related lactic dehydrogenase (LDH), arginine deiminase (ADS), and urease enzymatic activity determination. Fluorescence in situ hybridization (FISH) and quantitative real-time polymerase chain reaction (qRT-PCR) were used to evaluate the S. mutans ratio within the biofilm. It was followed by 16S rRNA sequencing to define the oral microbial community.

Results: Fluoride-resistant S. mutans produced increased polysaccharides in presence of NaF (P < 0.05). The enzymatic activities related to both acid and base generation were less affected by the fluoride. In presence of 275 ppm NaF, the pH in the fluoride-resistant strain sample was lower than the wild type. We observed that with the biofilm development and accumulative fluoride concentration, the fluoride-resistant strain had positive relationships with other bacteria within the oral microbial community, which enhanced its colonization and survival. Compared to the wild type, fluoride-resistant strain significantly increased the diversity and difference of oral microbial community at the initial stage of biofilm formation (4 and 24 h) and at a low fluoride environment (0 and 275 ppm NaF) (P < 0.05). Kyoto Encyclopedia of Genes and Genomes (KEGG) analysis revealed that fluoride-resistant strain enhanced the metabolic pathways and glucose transfer.

Conclusions: Fluoride-resistant S. mutans affected the microecological balance of oral biofilm and its cariogenic properties in vitro, indicating its negative impact on fluoride's caries prevention effect.

Introduction

Dental caries is among the most challenging diseases globally. Untreated caries in permanent teeth affected 2.4 billion people worldwide (Peres et al., 2019). Generally, the occurrence of caries is associated with the imbalance of acid and alkali production by the biofilms at the tooth surface (Pitts et al., 2017; Peres et al., 2019). A recently proposed caries ecology hypothesis suggests that the disease is related to the ecological homeostasis (Takahashi and Nyvad, 2011; Marsh et al., 2015). Ecological pressure leads to the imbalance of microorganisms or the abundance of pathogenic microorganisms such as *Streptococcus mutans*, resulting in the swift development of diseases (Takahashi and Nyvad, 2011). This theory prompted that controlling dental plaque is a critical point for the prevention and treatment of caries. As fluoride is widely used for preventing dental caries (Anusavice et al., 2005; Pitts et al., 2017), it enables the protection of the hard tissue of teeth by suppressing demineralization and accelerating remineralization (Ten Cate, 2004). Moreover, it influences the growth and metabolism of the bacteria (Oh et al., 2017). When fed into bacterial cytoplasm, fluoride reduces the activity of enolase and F-ATPases, decreases synthesis of intercellular polysaccharides and exopolysaccharides directly or indirectly, and weakens the acid-producing ability in the shape of hydrogen fluoride (Marquis et al., 2003; Liao et al., 2017). Nevertheless, due to its widespread use, fluoride also causes some problems. Dental fluorosis, fluorosis of bone, and fluoride resistance in bacteria commonly occur (Jha et al., 2011; Srivastava and Flora, 2020). For example, the appearance of a fluoride-resistant strain of *S. mutans* (FR) has been noted.

The FR strain can be isolated from xerostomia patients under high-dose fluoride treatment or laboratories (Streckfuss et al., 1980; Brown et al., 1983; Van Loveren et al., 1991a). *S. mutans* resistance to fluoride is no less than three times when compared with the fluoride-sensitive strain. Accordingly, studies on FR strains usually focus on their phenotype and genetic changes. Typical characters, such as fluoride resistance, adaptation, and stability, were identified, but cariogenic properties like acidogenicity and acidurity need special attention, due to their link with caries sensitivity (Zhu et al., 2012; Liao et al., 2015; Cai et al., 2017; Liao et al., 2017; Liao et al., 2018; Lee et al., 2021). As stable fluoride resistance was attributed to genetic changes (Van Loveren et al., 1991b; Liao et al., 2015; Liao et al., 2018; Lee et al., 2021), specific genes or their regulation were identified in causing fluoride resistance (Liao et al., 2016; Men et al., 2016; Murata and Hanada, 2016; Tang et al., 2019; Lu et al., 2020; Yu et al., 2020). Therefore, whether the rise of fluoride resistance would impact oral microbial ecology or not remains a question.

Recently, it was reported that fluoride resistance influenced the development of competitive dual-species biofilms comprising *S. mutans* and *Streptococcus sanguinis* (*S. sanguinis*) under *in vitro* fluoride treatment (Zhang K. et al., 2022). Fluoride resistance acquired an edge in competitive dual-species biofilm formation, resulting in a more robust biofilm formation, and increased cariogenic virulence. Nonetheless, the dual-species biofilm model is circumscribed for the lack of common representativeness. The oral microbial community is a typical multispecies flora colonized by more than 700 microbe species. Saliva biofilms are composed of a variety of bacteria, have the potential to restore the complexity of dental plaque, and reduce the enormous cost of animal models (Brown et al., 2019). This research used saliva-derived oral biofilm models that are easier to operate and repeat, especially in controlling variables when compared with animal models (Brown et al., 2019). In our study, we aim to comprehend how the FR strain makes a difference to the oral microbial communities in the presence of fluoride within biofilm development. Consequently, we compared saliva-derived biofilm's cariogenic virulence caused by FR or wild-type *S. mutans* (WT) and characterized specific microbiome shifts regarding establishment and stability. Our findings provide systematic insight into the profound ecological influence of fluoride resistance.

Materials and methods

Microbial strains and culture conditions

Wild-type *S. mutans* UA159 (WT) and its fluoride-resistant strain (FR) were used in this study. The FR strain was generated *in vitro* as described previously (Zhu et al., 2012). Briefly, an overnight WT bacterial suspension was inoculated on brain heart infusion (BHI, Oxoid, Basingstoke, UK) agar plates containing varying concentrations of NaF (50 to 1000 ppm). Isolated colonies were picked and passaged on BHI agar without NaF for 50 generations. After passage, a clone growing on a BHI plate containing 1,000 ppm NaF was identified as an FR strain. Bacteria were cultured in BHI for multiplication in an atmosphere of 5% CO_2 at 37°C.

Saliva collection

Ethics was authorized by the School and Hospital of Stomatology, Wenzhou Medical University (WYKQ2020007). To eliminate the interference of other *S. mutans*, saliva was collected from a healthy donor, whose saliva did not contain any *S. mutans* (screened from 20 healthy volunteers) (Koopman et al., 2015; Uranga et al., 2021). Briefly, volunteers were informed to not brush their teeth for 24 h and prevent drink or food intake for 2 h, before the collection. Saliva was collected as previous study (Uranga et al., 2021). Total saliva DNA was

extracted, and the absence of *S. mutans* was verified using quantitative real-time polymerase chain reaction (qRT-PCR, details are shown below). The primers are described in Supplementary Table S1. The collected saliva was mixed with 60% glycerol and stored at -80°C for further use (Huang et al., 2017).

Biofilms were cultured in 24-well plates containing glass disks in each well. Mixtures of saliva and *S. mutans* (WT or FR) were used for biofilm formation. The saliva sample was diluted 50-fold and mixed with an overnight culture of *S. mutans* (1.25×10^6 cells per well) (Li et al., 2010). McBain medium with 0.2% sucrose was used to culture biofilms (McBain et al., 2005). Biofilms were incubated anaerobically (10% CO_2, 10% H_2, and 80% N_2) for 4, 24, and 72 h with 0, 275, and 1,250 ppm NaF, and the medium was changed daily (Huang et al., 2017).

Scanning electron microscopy

Biofilms were washed with PBS and fixed using 2.5% glutaraldehyde. Then, the biofilms were dehydrated using an ethanol gradient (50%, 60%, 70%, 80%, 90%, 95%, and absolute ethyl alcohol; 30 min incubation per concentration). Biofilms were dried, coated with gold-palladium, and imaged using a scanning electron microscope (SEM; Hitachi, Tokyo, Japan) at ×1,000 magnification (Zhang K. et al., 2022).

Polysaccharide analysis

Quantitative analysis of water-insoluble polysaccharides was done by the anthrone method (Zhang K. et al., 2022). Briefly, the biofilms were collected, washed with PBS, resuspended in 0.4 M NaOH, and incubated for 30 min before centrifuging at $4,000 \times g$ for 10 min, and the supernatant was collected. The 100-µl supernatant was mixed with 300 µl anthrone solution (2 mg/ml, in concentrated sulfuric acid) and incubated at 95°C for 6 min in a water bath. The absorbance was monitored at 625 nm. Standard curves were prepared using the dextran standard.

Further, confocal laser scanning microscopy (CLSM) was performed to observe the polysaccharide production. Alexa Fluor 647 Dextran conjugate (Molecular Probes, Invitrogen Corp., Carlsbad, CA) was used to label α-glucan. After 4, 24, and 72 h of biofilm formation, biofilms were dyed with SYTO 9 (Molecular Probes, Invitrogen Corp., Carlsbad, CA, USA) and concanavalin A (Con A, (Molecular Probes, Invitrogen Corp., Carlsbad, CA, USA) to label microorganisms and α-D-glucopyranose polysaccharides separately (Chen et al., 2007; Adav et al., 2010). A CLSM (Nikon Corporation, Tokyo, Japan) was used to obtain the image, with excitation/emission

spectrums of 650/668 nm for Alexa Fluor 647, 555/580 nm for conA, and 480/500 nm for SYTO 9 (Zhang L. et al., 2022).

Acid production analysis

The acid-producing ability of biofilms was studied by measuring the pH and lactic acid content. After 4, 24, and 72 h incubation of biofilms, the supernatant pH was measured using a pH meter (Mettler Toledo Instruments Co. Ltd., Shanghai, China).

After biofilm formation, the biofilms were washed with Cysteine Peptone Water (CPW) and transferred to a new 24-well plate. Buffered Peptone Water (BPW, 1 ml) containing 0.2% (v/v) sucrose was added to each well and incubated at 37°C for 3 h to produce acid. The lactic acid content was measured by an enzymatic method (Zhang L. et al., 2022).

Enzyme activity determination

Protein content was used to standardize arginine deiminase (ADS) and urease activity and defined as µmol/min/mg protein (Zheng et al., 2017). In brief, cells from saliva-derived biofilms were added into a mixture with 50 mM arginine hydrochloride (Sigma-Aldrich Canada, Oakville, Ontario, Canada) and 0.5 mM Tris-maleate buffer (pH 6.0) and then incubated together for 120 min at 37°C to allow ammonia generation. The ammonia production was monitored using Nessler's reagent (Sigma-Aldrich) based on a standard generated with ammonium sulfate. Simultaneously, protein content was measured using Bradford's assay and bovine serum albumin was used as standard. Lactic dehydrogenase (LDH) activity was determined using an LDH Activity Assay Kit (Sigma-Aldrich), as per the manufacturer's guidelines (Zheng et al., 2017). Further, a deviation between the fluoride group (275 and 1250 ppm NaF) and the control group (0 ppm NaF) for the FR strain and WT was calculated separately. Results were shown as the absolute value of the deviation of enzyme activities compared with corresponding 0 ppm (ΔLDH, ΔADS, and ΔUrease).

Fluorescence *in situ* hybridization

Fluorescence *in situ* hybridization (FISH) was used to monitor *S. mutans* within biofilms (Zhang K. et al., 2022). Briefly, biofilms were fixed with 4% paraformaldehyde, treated with lysozyme, and dehydrated using an ethanol gradient (50%, 80%, and 96%). *S. mutans* and whole bacteria were dyed using specific probes (Supplementary Table S2). Biofilm images were obtained and analyzed using a CLSM (Nikon A1, Nikon Corporation, Japan) equipped with an oil immersion lens at ×60.

qRT-PCR

The quantitative ratio of *S. mutans* within saliva-derived biofilms was determined by qRT-PCR (Zhang K. et al., 2022). Genomic DNA was extracted from biofilms using a QIAamp DNA Mini Kit (QIAamp, Germany), as per the manufacturer's instructions. For qRT-PCR, a 20-μl reaction mixture was used (primers and probes are listed in Supplementary Table S1). The assay reaction was run in a StepOnePlus Real-Time PCR System (Applied Biosystems, Waltham, MA) as follows: 95°C for 30 s, 40 cycles of 95°C for 10 s, and 58°C for 30 s (Yoshida et al., 2003).

16S rRNA gene sequencing and analyses

Sequencing was used to detect the FR's ecological impression. After biofilm formation, the biofilm was collected by centrifugation followed by its transportation to Shanghai Majorbio Bio-Pharm Technology Co., Ltd. (Shanghai, China). DNA was extracted, amplified, and sequenced based on standard procedures. In brief, DNA was extracted utilizing FastDNA$^{®}$ Spin Kit (MP Biomedicals, USA). Sense primer (5′-CCTAYGGGRBGCASCAG-3′) and anti-sense primer (5′-GGACTACHVGGGTWTCTAAT-3′) were used for PCR amplification (Liu et al., 2016). Sequencing procedures were run with an Illumina NovaSeq PE250 platform (Illumina, San Diego, USA). The analyses of sequence data were performed using fastp version 0.19.6, FLASH version 1.2.7, PICRUSt2 (Phylogenetic Investigation of Communities by Reconstruction of Unobserved States), and UPARSE 7.1, involving raw data quality control, taxonomic annotation based on the NCBI database (Wang et al., 2007; Magoc and Salzberg, 2011; Edgar, 2013; Chen et al., 2018; Douglas et al., 2020). Bioinformatics and statistical analyses were as follows. The relative abundance difference of microbic taxa was examined at species levels by the Kruskal–Wallis test. The α-diversity between groups was performed using the Shannon index (Schloss et al., 2009). Principal coordinate analyses (PCoAs) were generated to calculate the community difference between groups, along with two non-parametric analyses, involving analysis of similarities (ANOSIM) and non-parametric multivariate analysis of variance (Adonis) using distance matrices. The co-occurrence network at the species level was analyzed using the Spearman correlation matrix ($\rho > 0.6$ and $P < 0.01$) (Barberán et al., 2012). Microbial functions (pathway and enzyme) were predicted by phylogenetic investigation of communities to rebuild the unobserved states based on the 16S rRNA gene sequence data. The rarefaction curves of samples are shown in Supplementary Figure S1.

Statistical analysis

All the assays were repeated three times independently. The statistical analysis was done using Statistical Package for Social Sciences (SPSS 16.0, SPSS Inc., Chicago, IL, USA). ANOVA and Scheffé *post-hoc* comparison were applied for comparison. A statistically significant difference was observed with $P < 0.05$.

Results

FR-involved biofilms produced more polysaccharides under fluoride and affected biofilm architecture differently

An obvious alteration of EPS information and biofilm construction can be found in CLSM and SEM images. CLSM images confirmed that in EPS staining (Figures 1A-C), biofilms with FR had more thickness and EPS than the WT ones, at different time points. The difference was particularly pronounced at a high NaF concentration (1,250 ppm). As shown in Figures 1D-F, under fluoride exposure, water-insoluble exopolysaccharide of FR-related biofilms increased more visibly than WT, at each of the three time points ($P < 0.05$), except for the 4-h biofilm at 275 ppm, among which there was no significant difference though. The SEM images (Figure 2A) showed a somewhat similar tendency. Collectively, the existence of FR led to biochemical and structural alternation of biofilms, resulting in more robust biofilms with more biomass under fluoride when compared with the ones with WT.

FR-involved biofilms had lower pH at 275 ppm NaF and showed stronger acidogenicity after high fluoride treatment

FR groups had lower supernatant pH than WT groups at 275 ppm NaF (Figures 2B-D). The accessorial supernatant pH with the increase in fluoride implied a repressive effect by fluoride on the biofilm acid output. However, we observed that in lactic acid generation, the effect of fluorine was different. For each age of saliva-derived biofilms (4, 24, and 72 h), the lactic acid production increased with fluoride resistance to 1,250 ppm compared with its counterpart WT (Figures 2E-G; $P < 0.05$). It showed a similar tendency at 0 (24 h biofilms) and 275 ppm (72 h-biofilms) (Figures 2F, G; $P < 0.05$). Hence, the data showed that the acidogenicity advantage of saliva-derived biofilms with FR could appear after high fluoride treatment.
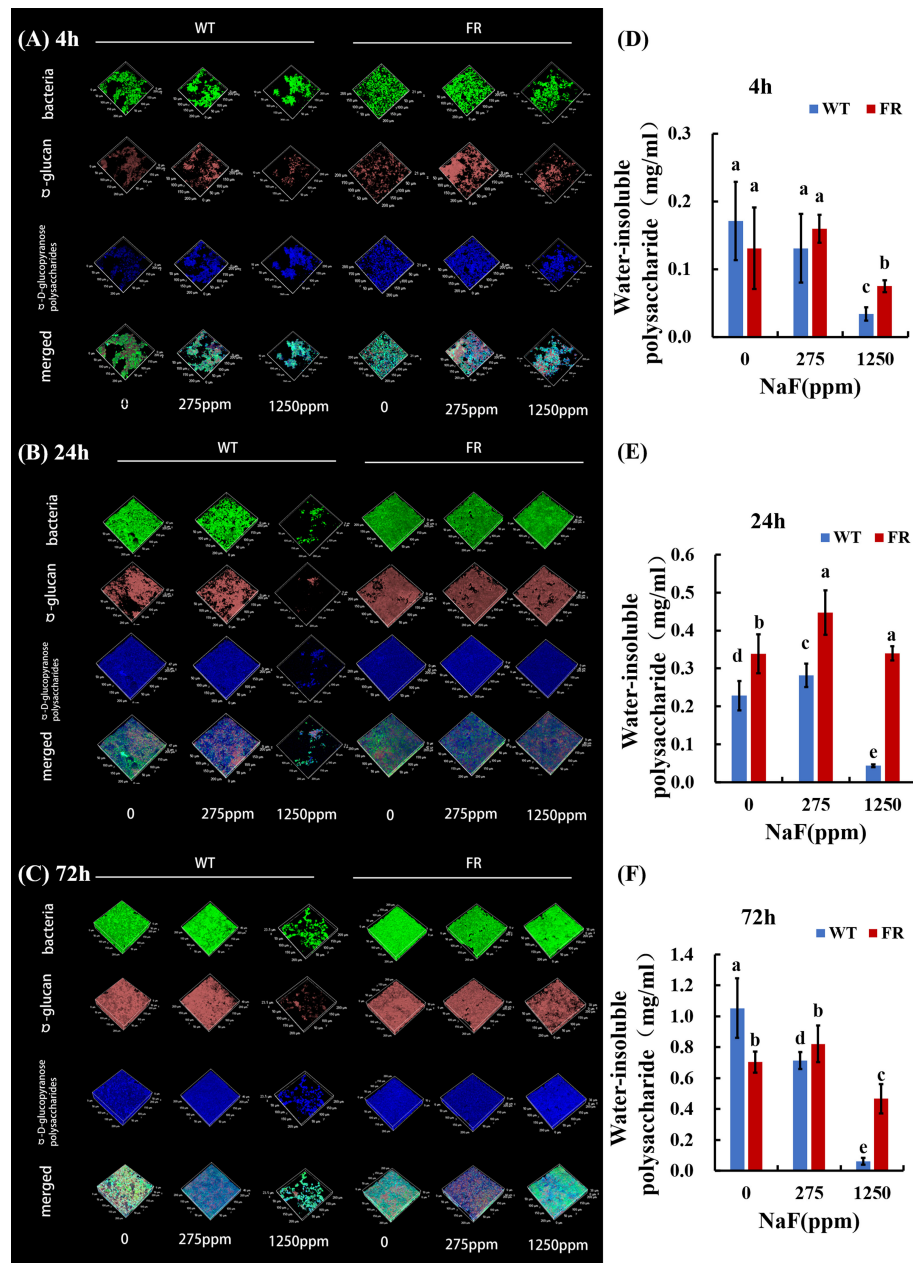
FIGURE 1

Polysaccharide analysis of biofilms. **(A-C)** Bacterial and polysaccharide staining of biofilms. Bacteria were labeled with green, dextran was stained red, and α-polysaccharides were dyed blue. **(D-F)** Water-insoluble polysaccharide of biofilms revealed by anthrone mensuration. Data are presented as mean ± standard deviation, and different letters demonstrate a significant difference between groups (P < 0.05).

FR-involved biofilms were more likely to maintain the primary acid–base metabolism of oral microorganisms facing fluoride stress

Enzyme activity related to acid–base metabolism was detected for its close connection with cariogenicity. For enzymatic activity, lactic dehydrogenase (LDH, acidogenic enzyme), arginine deiminase (ADS, alkali-producing enzyme), and urease (alkali-producing enzyme) activities were investigated and deviation was calculated between the fluoride group (275 and 1250 ppm NaF) and control group (0 ppm NaF) for the FR strain and WT separately (Figure 3). The deviations of FR groups were lower than WT groups in general (Figure 3),
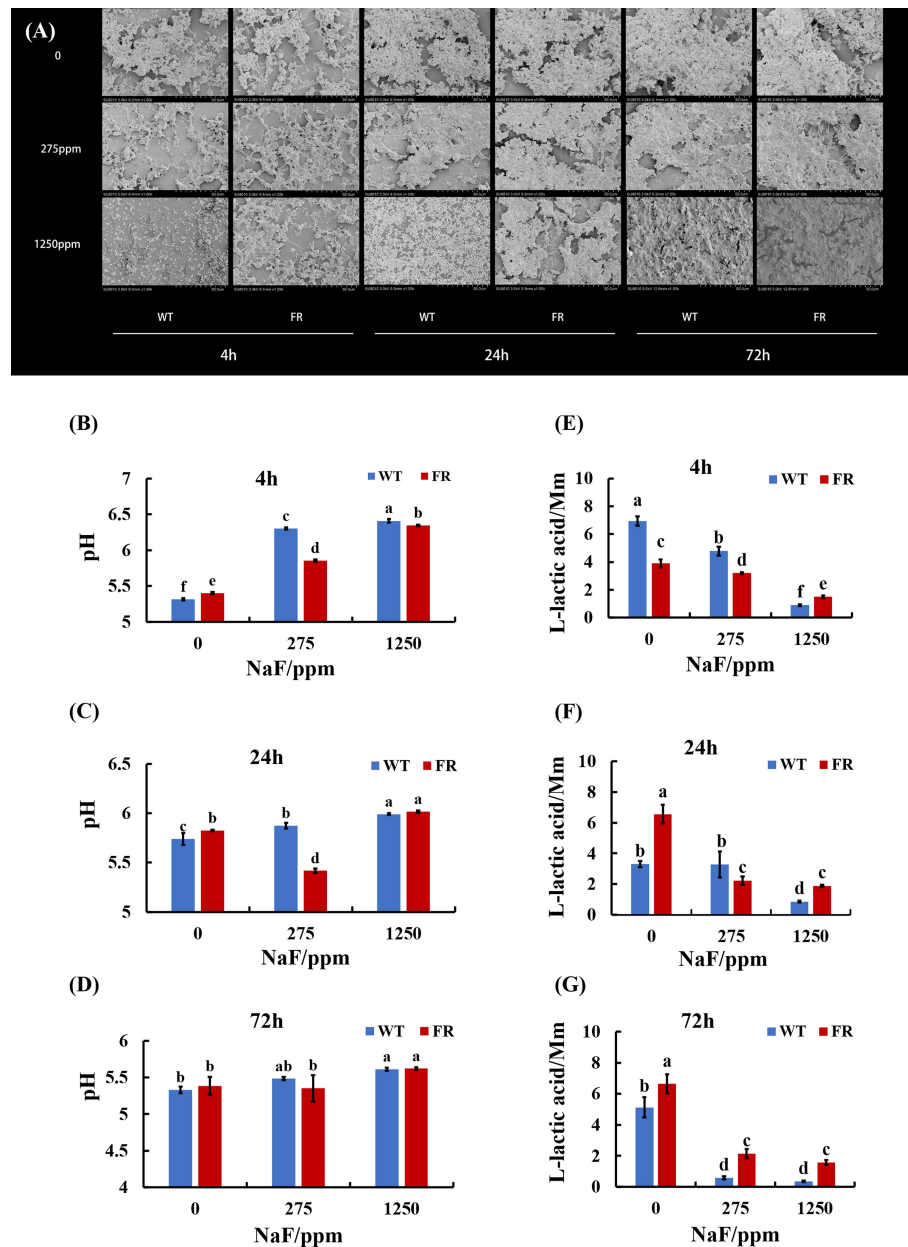
FIGURE 2
Biofilm structure and acid production. **(A)** SEM images of biofilms, scale bar 50 μm. **(B-D)** Supernatant pH of biofilms. **(E-G)** Lactic acid generation of biofilms. Data are presented as mean ± standard deviation, and different letters demonstrate a significant difference between groups (P < 0.05).

except ΔADS activity for 24-h biofilms at 1,250 ppm NaF and ΔUrease activity for 24-h biofilms at 275 ppm NaF, which showed a different trend but with no significant difference (Figures 3E, H, *P*>0.05). Although deviations of FR groups including ΔADS activity, ΔADS activity, and ΔUrease activity in all the remaining groups were lower than those of WT ones, no significant differences were observed between FR and WT groups for ΔLDH activity (72-h biofilms), ΔADS activity (24-h

biofilms at 275 ppm NaF and 72-h biofilms), and ΔUrease activity (72-h biofilms) (Figures 3C, E, F, I, *P*>0.05). A significant difference can be found in ΔLDH activity (4-h biofilms and 24-h biofilms), ΔADS activity (4-h biofilms at 275 and 1,250 ppm NaF), and ΔUrease activity (4-h biofilms at 275 ppm and 1,250 ppm NaF together with 24-h biofilms at 1,250 ppm) (Figures 3A, B, D, G, H, *P* < 0.05). These findings indicate that under fluoride exposure, FR groups held to
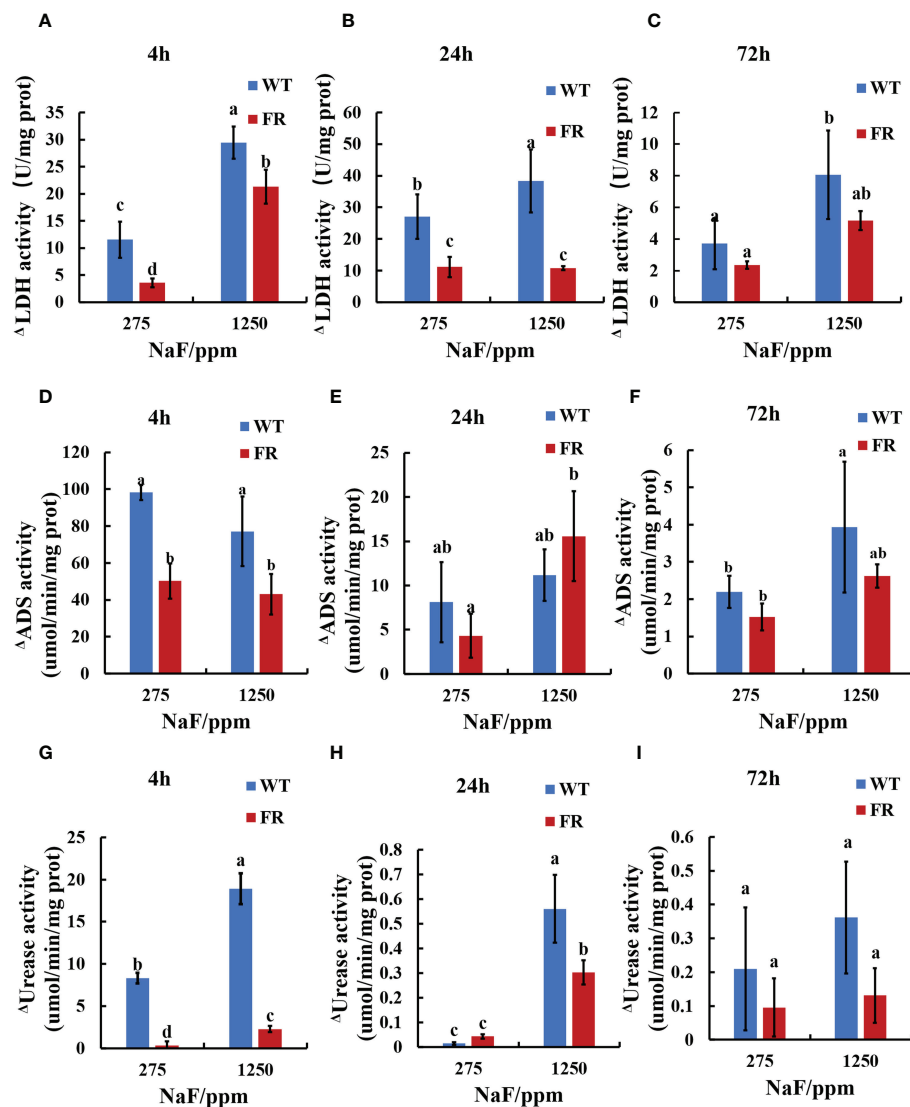
FIGURE 3

Enzyme activity in biofilms. **(A-C)** LDH activity. **(D-F)** ADS activity. **(G-I)** Urease activity. Δ represents shape of the absolute value of deviation of enzyme activities when compared with corresponding 0 ppm. Data are presented as mean ± standard deviation, and different letters demonstrate a significant difference between groups (P < 0.05).

previous acid–base metabolism rather than building a new one for oral microorganisms compared with the WT groups.

FR acquired a competitive advantage and changed microbial composition

To better delineate the influence of FR on the oral microbial community during the development of saliva-derived biofilm, we investigated the ratio of WT and FR by qRT-PCR and FISH and the percentages of community abundance on a species level

by 16S rRNA sequencing. Both FISH and qRT-PCR appeared at a similar ratio (Figures 4A-C, *P* < 0.05). In general, with increasing NaF concentrations (except group at 4 h and 275 ppm NaF), the WT proportion reduced in the biofilms and the FR proportion increased (Figures 4A-C, *P* < 0.05). A similar trend can be found in 16S rRNA sequencing results (Figure 4D). With time and the increasing concentration of NaF, FR exhibited a competitive advantage and its advantage was most remarkable in 24-h biofilms at 275 ppm (Figure 4D, *P* < 0.05). Surprisingly, despite the higher percentages of FR colonies than WT, the FR strains did not reach overwhelming superiority in
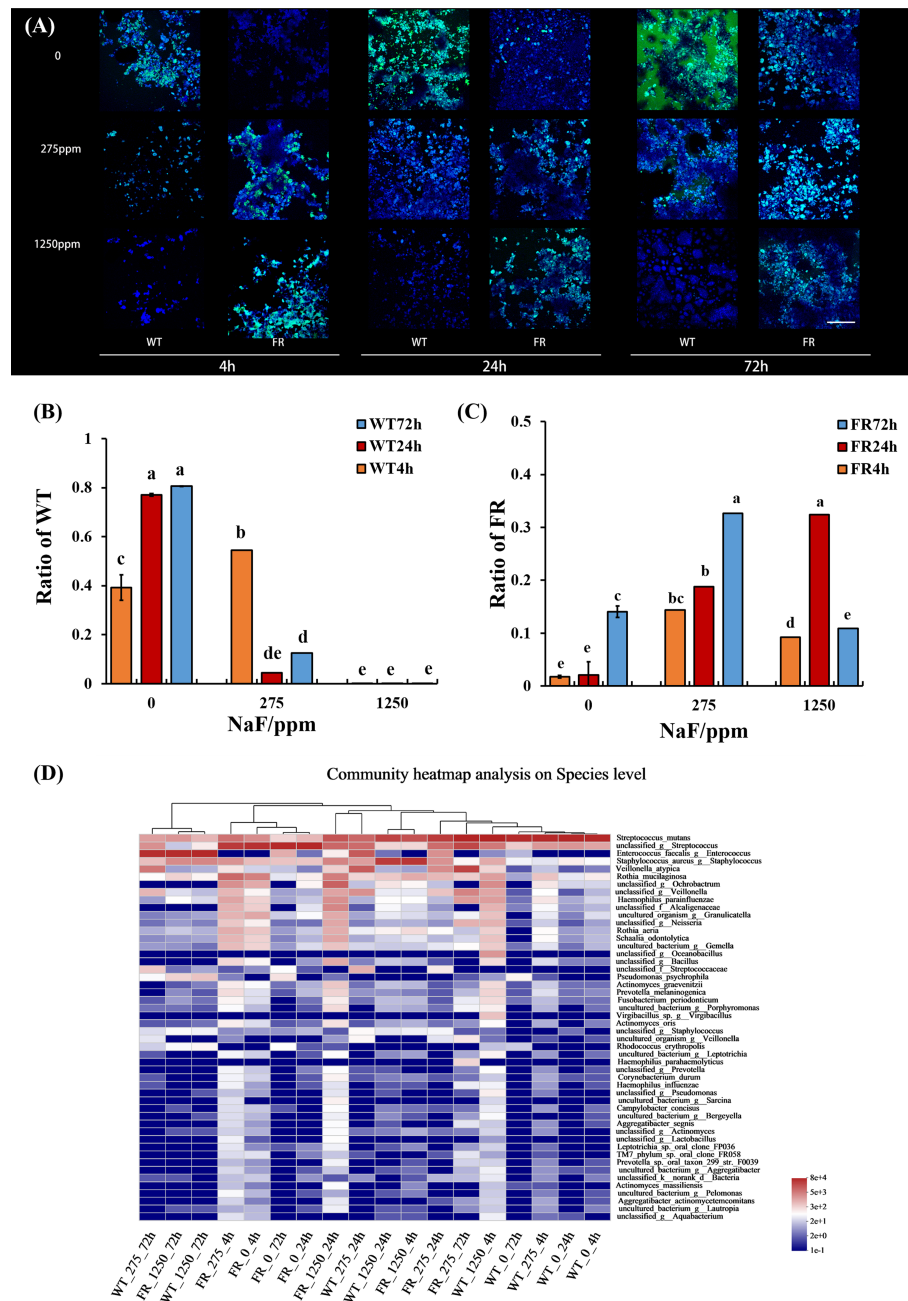
FIGURE 4

S. mutans ratio in biofilm and relative abundance of the 50 most predominant oral bacteria at the species level. **(A)** *S. mutans* within biofilms revealed by FISH; *S. mutans* was stained green, and all bacteria were stained blue, the scale bar 50 μm. **(B)** WT ratio revealed by qRT-PCR. **(C)** FR ratio revealed by qRT-PCR. **(D)** Relative abundance of the 50 most predominant oral bacteria at the species level. Data are presented as mean $\pm$ standard deviation, and different letters demonstrate a significant difference between groups (P < 0.05).

saliva-derived biofilms, under a high-fluorine environment (1,250 ppm NaF) in contrast to a low-fluoride environment (275 ppm NaF) (Figure 4D, *P* < 0.05), except in 24-h biofilms. Meanwhile, the percentage of WT gradually decreased with the increase in time and concentration of NaF (Figure 4D, *P* < 0.05).

The composition of microbial communities incubated with NaF was notably different from that with WT (Figure 4D). Given these, we documented that fluoride resistance obtained a competitive advantage under NaF and affected microbial composition.

FR made the microbe within biofilms more diverse and distinct in the early biofilm establishment phase at low fluoride

We examined the impression of FR on microbial ecology in saliva-derived biofilms by the method of 16S rRNA sequencing (values of Shannon index and PCoA of all groups are shown in

Supplementary Figure S2). As shown in Figure 5B, fluoride resistance played an important role on the microbial diversity in a low-fluoride environment (275 ppm), based on Shannon indices ($P < 0.05$). The case was similar at 0 ppm; at 275 ppm, the Shannon index of the group was higher than the 0-ppm group (Figures 5A, B; $P < 0.05$). PCoA showed that the oral microbial communities in the presence of FR were distinct from the WT; nevertheless, the difference was no longer so apparent with time
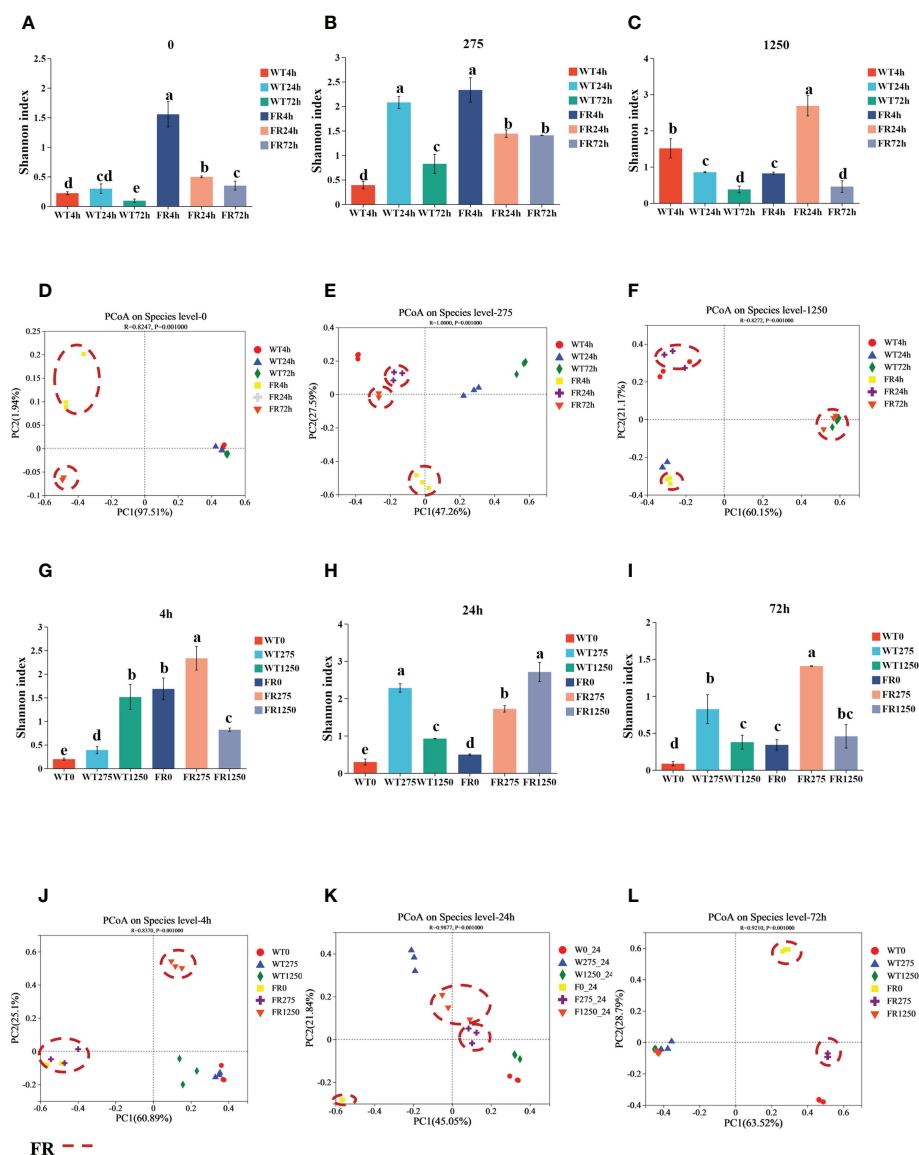
FIGURE 5

Shannon indices and PCoA of saliva-derived oral biofilms in the presence of WT/FR. **(A-C)** The Shannon indices separately at different incubating times of each concentration of NaF (0, 275, 1,250 ppm), standing at 4, 24, and 72 h. **(G-I)** The Shannon indices respectively at distinctive concentrations of NaF of each timepoint (4, 24, 72 h), representing 0, 275, and 1,250 ppm. **(D-F)** PCoA separately at different incubating times of each concentration of NaF (0, 275, 1,250 ppm), standing at 4, 24, and 72 h. **(J-L)** PCoA respectively at distinctive concentrations of NaF of each timepoint (4, 24, 72 h), representing 0, 275, and 1250 ppm. Data are presented as mean ± standard deviation, and different letters demonstrate a significant difference between groups (P < 0.05).

and increasing concentration of NaF, which is also indicated by the two dissimilarity tests including Adonis and ANOSIM (Figures 5D-F, J-L; Table 1; $P < 0.05$), whereas there was no significant difference between the figures of FR and WT at 1,250 ppm overall (Supplementary Figure S3F; $P > 0.05$). The community diversity of the 4- and 24-h biofilms altered with FR, and the values of the Shannon index were close in these two groups (Figures 5G, H; $P < 0.05$). With increasing incubation time (72 h), the values of the Shannon index became more similar between the WT and FR groups (Supplementary Figure S3I, $P > 0.05$). By contrast, no significant differences were observed between the WT and FR groups' Shannon indices for 275 ppm and 24 h (Supplementary Figures S3B, H, $P > 0.05$). There was no significant difference in the observations for FR and WT groups at 1,250 ppm and 72 h (Supplementary Figures S3C, I; $P > 0.05$), although its counterparts at different timepoints in the 1,250-ppm group and different concentrations of NaF in the 72-h group can distinguish respectively (Figure 5C; $P < 0.05$). These data show that during the early establishment of oral microbes (4 h, 24 h), FR played a role in adding diversity and distinction of communities, which was also present at low-fluoride concentrations (275 ppm). Nonetheless, the dissimilarities in diversity and distinction were gradually not so obvious with the increase in biofilm age (72 h) and concentration of NaF (1250 ppm).

FR obtained more help for colonization in microbial communities with biofilm development

Co-occurrence ecological networks concerning the top 10 abundant species-level taxa were constructed to further comprehend how saliva-derived biofilms assemble as incubation time and concentration of NaF increased and whether colonization of the FR strain impacted the oral microbial community network topology. With time, the positive relationship between the FR strain and other species

increased gradually and the negative was reduced (Figures 6D-F). The negative relationship in the WT group was most strengthened for the 24-h biofilm (Figures 6A-C). However, the situation changed when the concentration of NaF was considered. The negative links between *S. mutans* and other species decreased following the gradual increase of NaF (0, 275, and 1,250 ppm), whereas the positive one was the opposite (Figures 6G-I). The tendency of WT groups was similar to the one of the whole (Figures 6J-L). In contrast, for the FR groups, the relationship was slightly reduced (Figures 6M-O). Thus, it was documented that with biofilm development, the FR strain was easier to colonize in the communities and it can build a more positive relationship with other species, which increased the risk of caries. However, this situation may not be suitable under NaF.

FR might influence metabolism-related pathways and enhance glucosyl transfer within biofilms

Metabolism and biosynthesis related, ABC transporters involved, two-component system and quorum sensing associated as per Predicted Kyoto Encyclopedia of Genes and Genomes (KEGG) were upregulated in saliva-derived biofilms cultured with FR when compared with WT groups (Figure 7A). Similarly, most KEGG enzymes related to glucosyl transfer also enhanced within biofilms with FR when compared with WT groups (Figure 7B).

Discussion

Complex microbial communities inhabit the oral cavity, where the abundance and composition of microbial species shift resulting in ecological imbalance leading to polymicrobial diseases such as dental caries (Grice et al., 2008; Dewhirst et al., 2010; Fujimura et al., 2010; Hajishengallis, 2015; David et al.,

TABLE 1   Dissimilarity tests (Adonis and ANOSIM) for the biofilm microbiota.

	ANOSIM		Adonis	
	R	P	R^2	P
Overall	0.9024	0.001	0.9577	0.001
Saliva + FR *vs.* saliva + WT-0	0.8247	0.001	0.9954	0.001
Saliva + FR *vs.* saliva + WT-275	1	0.001	0.9738	0.001
Saliva + FR *vs.* saliva + WT-1250	0.8272	0.001	0.9056	0.001
Saliva + FR *vs.* saliva + WT-4h	0.837	0.001	0.9025	0.001
Saliva + FR *vs.* saliva + WT-24h	0.9877	0.001	0.9627	0.001
Saliva + FR *vs.* saliva + WT-72h	0.8272	0.001	0.9897	0.001
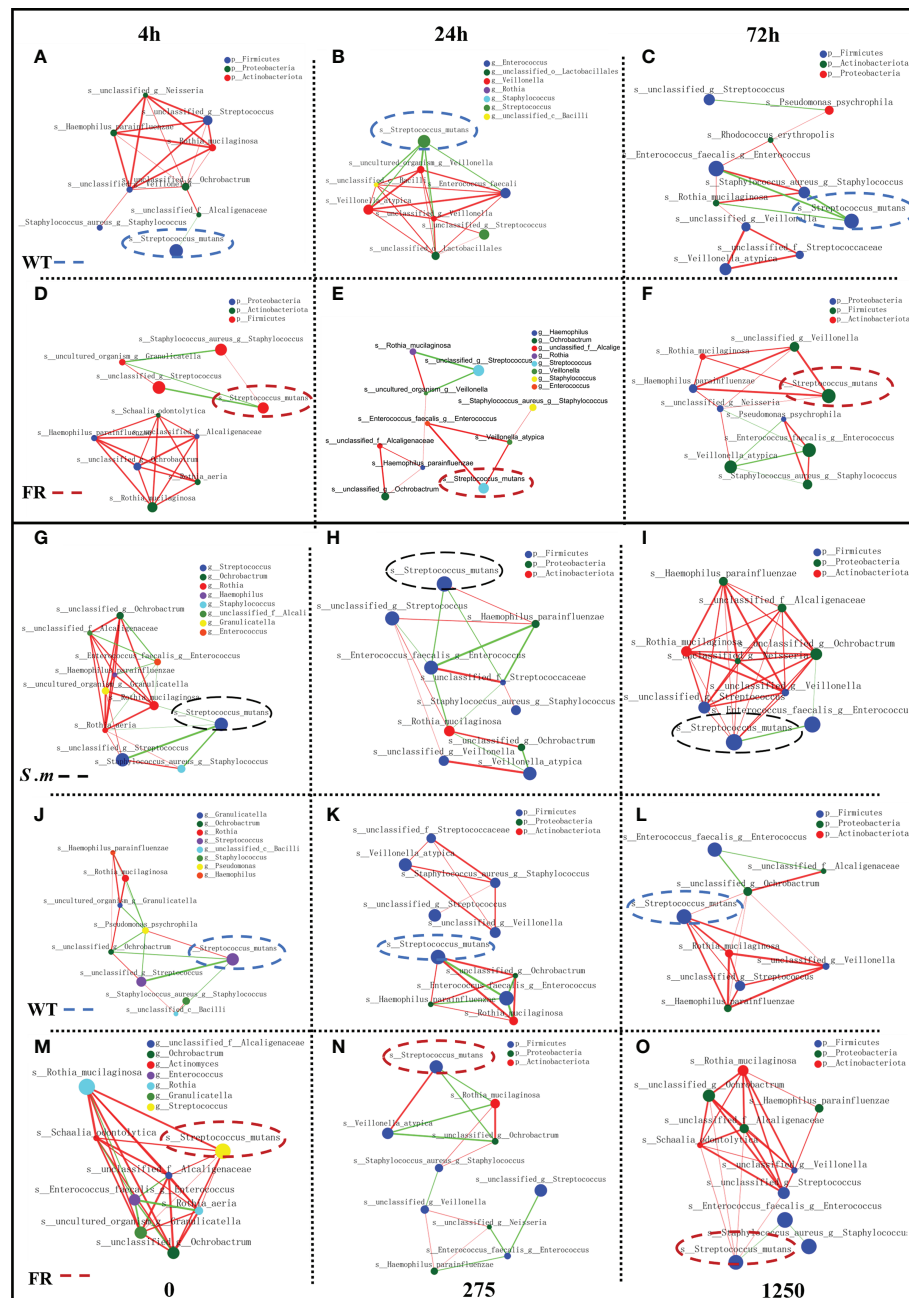
FIGURE 6

Network inferences of microbial relationships in oral biofilms with the presence of WT/FR. Each node represents an OTU, and each edge represents a significant pairwise association. Green lines represent negative relationships, and red lines represent positive relationships. **(A-C)** The network inferences of microbial relationships separately at different incubating times among biofilms with WT, standing at 4, 24, and 72 h. **(D-F)** The network inferences of microbial relationships separately at different incubating times among biofilms with FR, standing at 4, 24, and 72 h. **(G-I)** The network inferences of microbial relationships respectively at distinctive concentrations of NaF in biofilms with the presence of *S. mutans*, representing 0, 275, and 1,250 ppm. **(J-L)** The network inferences of microbial relationships respectively at distinctive concentrations of NaF in biofilms with the presence of WT, representing 0, 275, and 1,250 ppm. **(M-O)** The network inferences of microbial relationships respectively at distinctive concentrations of NaF in biofilms with the presence of FR, representing 0, 275, and 1,250 ppm.

2014; Levy et al., 2017). This study for the first time reveals the influence of FR on oral microbial communities under fluoride exposure *in vitro*. Our data indicated that the presence of FR impacted polysaccharide generation, acidogenicity, acid–base metabolism, enzyme activity, and microbial composition *in vitro*.

EPS is vital for the establishment of oral biofilms and the development of dental caries (Flemming and Wingender, 2010; Koo et al., 2013). Microbial communities of biofilm are wrapped in an extracellular matrix composed of polymers like EPS, which serves as 3D architecture, diffusion barrier, and cariogenic combining site (Flemming and Wingender, 2010; Xiao et al., 2012; Koo et al., 2013). EPS accelerates adherence of *S. mutans* on the surface of teeth by salivary glucosyltransferase (Vacca-Smith and Bowen, 1998; Bowen and Koo, 2011). One research reported that the cell surface polysaccharide biosynthesis-related genes in *Acidithiobacillus ferrooxidans* (*A. ferrooxidans*) can be expressed more under fluoride (Ma et al., 2016). Additionally, it has been observed that *malQ* genes in the *S. mutans* FR strain were upregulated, which is annotated as 4-alpha-glucanotransferase (Lee et al., 2021). Our findings illustrated that compared with the WT, more EPS was produced in FR groups under fluoride exposure (Figures 1 and 2A). In addition, the expression of glucosyltransferase was upregulated in saliva-derived biofilms with FR under fluoride exposure (Figure 7B). Given this, we guessed that owing to better adaptability under fluoride, FR enhanced the activity of glucosyltransferase, produced more EPS, and further contributed to the cariogenicity of an oral biofilm under NaF.

The accumulation of acid in an oral environment causes the demineralization of teeth directly and alters oral microbial flora indirectly (Takahashi and Nyvad, 2011; Pitts et al., 2017). *S. mutans* was identified to play an important role in caries not only for its EPS-matrix generation ability and aciduricity but also for its cariogenicity. FR biofilms had lower pH at 275 ppm NaF at three time points, which were consistent with a previous study in which FR-related dual-species biofilms had lower supernatant pH at 275 ppm NaF whereas less difference was found at 1,250 ppm NaF (Zhang K. et al., 2022). Under low fluoride, FR may be responsible for enhanced cariogenicity depending on its better survivability and acid production under NaF, whereas the inhibitory effect of NaF on acid generation may play a dominant role at high NaF concentrations, hence less difference between FR and WT groups in addition to higher pH when compared with 275 ppm NaF. Yet, these conjectures need to be studied. Lactic acid results showed higher acidogenicity at high fluoride (1,250 ppm NaF) treatment, whose additional acid production may increase the demineralization of teeth (Figures 2E-G) that may result from more total biomass and higher *S. mutans* ratio in FR groups at this concentration.

LDH, an oxidoreductase isoenzyme, acts as a catalyst for reaction of lactic acid and pyruvate. ADS can turn arginine to ammonia, and urease can hydrolyze urea to ammonia, to counteract the effects of biofilm acidification caused by bacterial glycolysis, which are the main alkaline-producing enzymes in oral bacteria (Colby and Russell, 1997). Interestingly, the data exhibited that changes in LDH, ADS, and urease activities in oral biofilms cultured with the FR strain were lower than WT or unchanged (Figure 3). Extremophiles such as fluoride-resistant strain have survival strategies to adjust themselves to suit an extreme environment (Raddadi et al., 2015). It has been reported that biofilm's maturation can affect the anticaries efficacy of fluoride including LDH activity (Ayoub et al., 2022). We speculate that in FR groups, the priority is to restore primary metabolic disequilibrium instead of establishing a new one under conditions of fluoride stress, so that it can enhance fluoride tolerance.

We find that FR strains would obtain overwhelmingly competitive advantage in oral microbial communities with biofilm development and fluoride, although it was less than WT at the beginning (Figure 4). It was apparent that the FR strain gradually showed its fluoride endurance in the colonizing process in the oral environment, especially with fluoride. A former study also reported that FR can acquire competitive advantage in dual-species biofilms in biofilm formation, which is consistent with our results. We see that with the application of oral care products with fluoride, FR can also result in some adverse impact. Its prosperous growth might lead to dental caries as one of major pathogenic bacteria.

In recent years, research has observed that there is a close connection between modern diseases and dysbiosis of oral microbiota (Hajishengallis, 2015; Levy et al., 2017). We documented that FR enables oral microbial communities to be more diverse and rich in the early formation phase (4 and 24 h) of biofilm and at low fluoride (275 ppm), which may lead to more severe dysbiosis than WT (Figures 5B, G, H) (Li et al., 2004). The reason may be the better fluoride tolerance of the FR strain during fluoride stress, and at 275 ppm, the diversity of communities was enhanced compared with those with no fluoride (Figures 5A, B). One research has reported that salivary microbiota was resistant to a microbial shift (Belstrøm et al., 2018). In other words, it is likely to restore to their original with time. As the current study showed, with the development of biofilms, oral microbial communities gradually established, and till 72 h, it may restore to their original. Thus, the 72-h saliva-derived biofilms cocultured with FR became similar to WT in diversity (Figure 5I). Fluoride toxicity is significant at high concentrations (Li et al., 2013). We speculate that during fluoride stress, limited species of bacteria could survive; hence, there was no significant diversity between two groups at 1,250 ppm NaF (Figure 5C). Likewise, it can also explain why with the
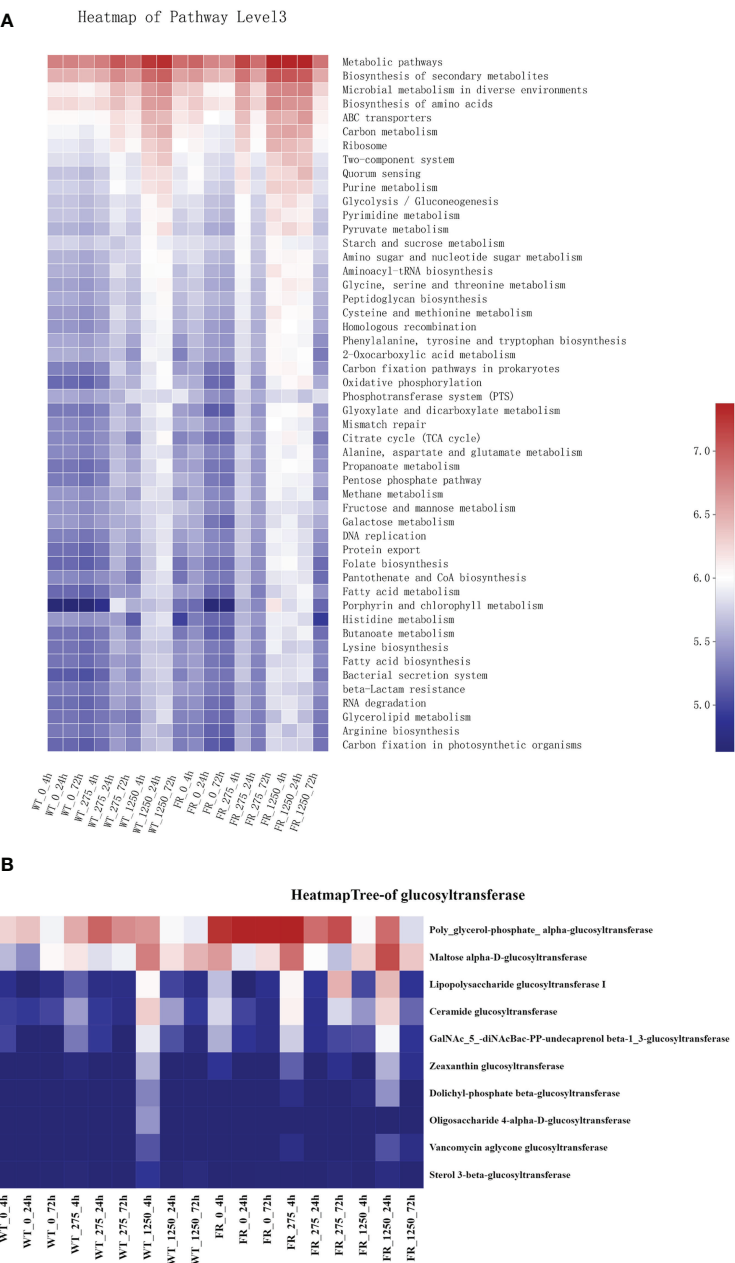
FIGURE 7
Prediction of Kyoto Encyclopedia of Genes and Genomes pathways and major glucosyltransferase of biofilms. **(A)** Prediction of KEGG pathways. The color gradient of the color block is used to display the changes in the abundance of different functions in the groups, and the legend indicates the value represented by the color gradient. **(B)** Major glucosyltransferase of biofilm in the presence of WT/FR. The color gradient of the color block is used to display the changes in the abundance of different functions in the groups, and the legend indicates the value represented by the color gradient.

increasing age of biofilm and NaF concentration, the distinction of oral microbial communities between the FR and WT groups was not so obvious as observed in the early colonization phase and under low NaF (Figures 5D-F, J-L).

An interesting phenomenon was revealed by co-occurring ecological networks with the increase in the biofilm's maturation; the positive relationship between FR and other species was reinforced, and the negative one was weakened. It

can exhibit the adaptation of FR faced with fluoride, especially compared with the case of WT (Figure 6). Adaptation is the most effective solution for environmental changes (Bowden, 1990), and it has been demonstrated that fluoride has the potential to provide some bacteria with the ecological benefits and some bacteria could adapt to fluoride (Hamilton and Bowden, 1982; Bowden, 1990). Thus, our results may also indicate the willingness of other species in the oral biofilm to adapt to the fluoride stress. We infer that the total environment can be considered favorable for the FR colony, due to the positive relationship between the FR strain and other species (Costello et al., 2009). With time, the relationship strengthened followed by the increased risk of caries. The abnormality in the case of NaF may be explained by the fluoride toxicity dimension (Li et al., 2013). The increase of NaF exhibits a toxic effect on the microorganisms; hence, the density and diversity of friendly species may decrease sharply. This result is consistent with other research that showed that the presence of FR in the oral environment would not necessarily reduce the anti-caries effect of fluoride.

Expressions of metabolism- and biosynthesis-related KEGG pathways were enhanced in the oral biofilms cultured with FR (Figure 7A). It has been reported that gene expression related to fluoride resistance upregulated the energy metabolism and protein synthesis (Ma et al., 2016). Metabolism-related pathways play an important role in physiological balance and protein biosynthesis and are crucial for cell growth under fluoride-like carbon metabolism (Xu et al., 2014; Joshua, 2019; Judge and Dodd, 2020). In addition, ABC transporter-related KEGG pathways were also heightened in FR groups, which was consistent with a previous study in which ABC transporters and permeases were enhanced in an FR strain (Lee et al., 2021). They hypothesized that upregulation of ABC transporters and permeases was to export fluoride ions (Lee et al., 2021). Furthermore, two-component system-related (involved in sensing and responding to environmental change) and quorum sensing-related (responsible for microbial communication and regulating associated physiological characteristics such as biofilm formation) KEGG pathways were upregulated in FR groups under NaF. Combining these results and upregulation of EPS-related genes as mentioned above, we speculated that the FR group can be superior to WT groups in coping with NaF stress in the following ways. FR groups showed more activity in sensing and communication within biofilms, followed by regulation of biofilms to adapt to stress by forming more robust biofilms and provide stronger protection simultaneously, pumping out fluoride ions and providing necessary energy and substances. However, these conjectures required further investigation. The inadequacy of the current investigation was the shortage of animal text to identify findings. In addition, using drugs such as arginine to regulate oral biofilm ecologically might be a noteworthy attempt to decrease adverse impacts resulting from FR.

Overall, the emergence of FR would affect the microecological balance of oral biofilms and their cariogenic properties *in vitro*. Their appearance may also affect the caries prevention effect of fluoride.

Data availability statement

The datasets of 16S rRNA gene sequencing presented in this study can be found in online repositories (https://www.ncbi.nlm.nih.gov/bioproject/PRJNA904954). Further inquiries can be directed to the corresponding authors.

Ethics statement

The studies involving human participants were reviewed and approved by School and Hospital of Stomatology, Wenzhou Medical University. The patients/participants provided their written informed consent to participate in this study.

Author contributions

YP and YSu designed this project. YSh, FY and LQ conducted experiments and acquired the data. MG, PX, XL, MW and XH analyzed and interpreted the data. YP and YSu polished the language. YSh wrote the main manuscript text. YP and YSu acquired funding. All authors contributed to the article and approved the submitted version.

Funding

Acknowledgments

Conflict of interest

The authors declare that the research was conducted in the absence of any commercial or financial relationships that could be construed as a potential conflict of interest.

Publisher's note

All claims expressed in this article are solely those of the authors and do not necessarily represent those of their affiliated organizations, or those of the publisher, the editors and the reviewers. Any product that may be evaluated in this article, or claim that may be made by its manufacturer, is not guaranteed or endorsed by the publisher.

Supplementary material

The Supplementary Material for this article can be found online at: https://www.frontiersin.org/articles/10.3389/fcimb.2022.1106392/full#supplementary-material

References

Adav, S. S., Lin, J. C., Yang, Z., Whiteley, C. G., Lee, D. J., Peng, X. F., et al. (2010). Stereological assessment of extracellular polymeric substances, exo-enzymes, and specific bacterial strains in bioaggregates using fluorescence experiments. *Biotechnol. Adv.* 28, 255–280. doi: 10.1016/j.biotechadv.2009.08.006

Anusavice, K. J., Zhang, N. Z., and Shen, C. (2005). Effect of CaF2 content on rate of fluoride release from filled resins. *J. Dent. Res.* 84, 440–444. doi: 10.1177/154405910508400508

Ayoub, H. M., Gregory, R. L., Tang, Q., and Lippert, F. (2022). The influence of biofilm maturation on fluoride's anticaries efficacy. *Clin. Oral. Investig.* 26, 1269–1282. doi: 10.1007/s00784-021-04100-6

Barberán, A., Bates, S. T., Casamayor, E. O., and Fierer, N. (2012). Using network analysis to explore co-occurrence patterns in soil microbial communities. *ISME J.* 6, 343–351. doi: 10.1038/ismej.2011.119

Belstrøm, D., Sembler-Møller, M. L., Grande, M. A., Kirkby, N., Cotton, S. L., Paster, B. J., et al. (2018). Impact of oral hygiene discontinuation on supragingival and salivary microbiomes. *JDR Clin. Trans. Res.* 3, 57–64. doi: 10.1177/2380084417723625

Bowden, G. H. (1990). Effects of fluoride on the microbial ecology of dental plaque. *J. Dent. Res.* 69, 653–683. doi: 10.1177/00220345900690S127

Bowen, W. H., and Koo, H. (2011). Biology of *Streptococcus mutans*-derived glucosyltransferases: role in extracellular matrix formation of cariogenic biofilms. *Caries. Res.* 45, 69–86. doi: 10.1159/000324598

Brown, J. L., Johnston, W., Delaney, C., Short, B., Butcher, M. C., Young, T., et al. (2019). Polymicrobial oral biofilm models: simplifying the complex. *J. Med. Microbiol.* 68, 1573–1584. doi: 10.1099/jmm.0.001063

Brown, L. R., White, J. O., Horton, I. M., Dreizen, S., and Streckfuss, J. L. (1983). Effect of continuous fluoride gel use on plaque fluoride retention and microbial activity. *J. Dent. Res.* 62, 746–751. doi: 10.1177/00220345830620061201

Cai, Y., Liao, Y., Brandt, B. W., Wei, X., Liu, H., Crielaard, W., et al. (2017). The fitness cost of fluoride resistance for different streptococcus mutans strains in biofilms. *Front. Microbiol.* 8. doi: 10.3389/fmicb.2017.01630

Chen, M. Y., Lee, D. J., Tay, J. H., and Show, K. Y. (2007). Staining of extracellular polymeric substances and cells in bioaggregates. *Appl. Microbiol. Biotechnol.* 75, 467–474. doi: 10.1007/s00253-006-0816-5

Chen, S., Zhou, Y., Chen, Y., and Gu, J. (2018). Fastp: an ultra-fast all-in-one FASTQ preprocessor. *Bioinformatics* 34, i884–i890. doi: 10.1093/bioinformatics/bty560

Colby, S. M., and Russell, R. R. (1997). Sugar metabolism by mutans streptococci. *Soc Appl. Bacteriol. Symp. Ser.* 26, 80S–88S. doi: 10.1046/j.1365-2672.83.s1.9.x

Costello, E. K., Laube, C. L., Hamady, M., Fierer, N., Gordon, J. I., and Knight, R. (2009). Bacterial community variation in human body habitats across space and time. *Science* 326, 1694–1697. doi: 10.1126/science.1177486

David, L. A., Materna, A. C., Friedman, J., Campos-Baptista, M. I., Blackburn, M. C., Perrotta, A., et al. (2014). Host lifestyle affects human microbiota on daily timescales. *Genome. Biol.* 15, R89. doi: 10.1186/gb-2014-15-7-r89

Dewhirst, F. E., Chen, T., Izard, J., Paster, B. J., Tanner, A. C., Yu, W. H., et al. (2010). The human oral microbiome. *J. Bacteriol.* 192, 5002–5017. doi: 10.1128/JB.00542-10

Douglas, G. M., Maffei, V. J., Zaneveld, J. R., Yurgel, S. N., Brown, J. R., Taylor, C. M., et al. (2020). PICRUSt2 for prediction of metagenome functions. *Nat. Biotechnol.* 38, 685–688. doi: 10.1038/s41587-020-0548-6

Edgar, R. C. (2013). UPARSE: highly accurate OTU sequences from microbial amplicon reads. *Nat. Methods* 10, 996–998. doi: 10.1038/nmeth.2604

Flemming, H. C., and Wingender, J. (2010). The biofilm matrix. *Nat. Rev. Microbiol.* 8, 623–633. doi: 10.1038/nrmicro2415

Fujimura, K. E., Slusher, N. A., Cabana, M. D., and Lynch, S. V. (2010). Role of the gut microbiota in defining human health. *Expert. Rev. Anti Infect. Ther.* 8, 435–454. doi: 10.1586/eri.10.14

Grice, E. A., Kong, H. H., Renaud, G., Young, A. C., Program, N. C. S., Bouffard, G. G., et al. (2008). A diversity profile of the human skin microbiota. *Genome. Res.* 18, 1043–1050. doi: 10.1101/gr.075549.107

Hajishengallis, G. (2015). Periodontitis: from microbial immune subversion to systemic inflammation. *Nat. Rev. Immunol.* 15, 30–44. doi: 10.1038/nri3785

Hamilton, I. R., and Bowden, G. H. (1982). Response of freshly isolated strains of streptococcus mutans and streptococcus mitior to change in pH in the presence and absence of fluoride during growth in continuous culture. *Infect. Immun.* 36, 255–262. doi: 10.1128/iai.36.1.255-262.1982

Huang, X., Zhang, K., Deng, M., Exterkate, R. A. M., Liu, C., Zhou, X., et al. (2017). Effect of arginine on the growth and biofilm formation of oral bacteria. *Arch. Oral. Biol.* 82, 256–262. doi: 10.1016/j.archoralbio.2017.06.026

Jha, S. K., Mishra, V. K., Sharma, D. K., and Damodaran, T. (2011). Fluoride in the environment and its metabolism in humans. *Rev. Environ. Contam. Toxicol.* 211, 121–142. doi: 10.1007/978-1-4419-8011-3_4

Joshua, C. J. (2019). Metabolomics: A microbial physiology and metabolism perspective. *Methods Mol. Biol.* 1859, 71–94. doi: 10.1007/978-1-4939-8757-3_3

Judge, A., and Dodd, M. S. (2020). Metabolism. *Essays Biochem.* 64, 607–647. doi: 10.1042/EBC20190041

Koo, H., Falsetta, M. L., and Klein, M. I. (2013). The exopolysaccharide matrix: a virulence determinant of cariogenic biofilm. *J. Dent. Res.* 92, 1065–1073. doi: 10.1177/0022034513504218

Koopman, J. E., Röling, W. F., Buijs, M. J., Sissons, C. H., ten Cate, J. M., and Keijser, B. J. (2015). Stability and resilience of oral microcosms toward acidification and candida outgrowth by arginine supplementation. *Microb. Ecol.* 69, 422–433. doi: 10.1007/s00248-014-0535-x

Lee, H. J., Song, J., and Kim, J. N. (2021). Genetic mutations that confer fluoride resistance modify gene expression and virulence traits of streptococcus mutans. *Microorganisms* 9, 849. doi: 10.3390/microorganisms9040849

Levy, M., Kolodziejczyk, A. A., Thaiss, C. A., and Elinav, E. (2017). Dysbiosis and the immune system. *Nat. Rev. Immunol.* 17, 219–232. doi: 10.1038/nri.2017.7

Liao, Y., Brandt, B. W., Li, J., Crielaard, W., Van Loveren, C., Deng, D. M., et al. (2017). Fluoride resistance in streptococcus mutans: a mini review. *J. Oral. Microbiol.* 9, 1344509. doi: 10.1080/20002297.2017.1344509

Liao, Y., Brandt, B. W., Zhang, M., Li, J., Crielaard, W., van Loveren, C., et al. (2016). A single nucleotide change in the promoter mutp enhances fluoride resistance of streptococcus mutans. *Antimicrob. Agents. Chemother.* 60, 7509–7512. doi: 10.1128/AAC.01366-16

Liao, Y., Chen, J., Brandt, B. W., Zhu, Y., Li, J., van Loveren, C., et al. (2015). Identification and functional analysis of genome mutations in a fluoride-resistant streptococcus mutans strain. *PloS One* 10, e0122630. doi: 10.1371/journal.pone.0122630

Liao, Y., Yang, J., Brandt, B. W., Li, J., Crielaard, W., van Loveren, C., et al. (2018). Genetic loci associated with fluoride resistance in streptococcus mutans. *Front. Microbiol.* 9. doi: 10.3389/fmicb.2018.03093

Li, J., Helmerhorst, E. J., Leone, C. W., Troxler, R. F., Yaskell, T., Haffajee, A. D., et al (2004). Identification of early microbial colonizers in human dental biofilm. *J. Appl. Microbiol.* 97 (6), 1311-1318. doi: 10.1111/j.1365-2672.2004.02420.x

Li, L. N., Guo, L. H., Lux, R., Eckert, R., Yarbrough, D., He, J., et al. (2010). Targeted antimicrobial therapy against streptococcus mutans establishes protective non-cariogenic oral biofilms and reduces subsequent infection. *Int. J. Oral. Sci.* 2, 66–73. doi: 10.4248/IJOS10024

Li, S., Smith, K. D., Davis, J. H., Gordon, P. B., Breaker, R. R., and Strobel, S. A. (2013). Eukaryotic resistance to fluoride toxicity mediated by a widespread family of fluoride export proteins. *Proc. Natl. Acad. Sci. U. S. A.* 110, 19018–19023. doi: 10.1073/pnas.1310439110

Liu, C., Zhao, D., Ma, W., Guo, Y., Wang, A., Wang, Q., et al. (2016). Denitrifying sulfide removal process on high-salinity wastewaters in the presence of halomonas sp. *Appl. Microbiol. Biotechnol.* 100, 1421–1426. doi: 10.1007/s00253-015-7039-6

Lu, M., Xiang, Z., Gong, T., Zhou, X., Zhang, Z., Tang, B., et al. (2020). Intrinsic fluoride tolerance regulated by a transcription factor. *J. Dent. Res.* 99, 1270–1278. doi: 10.1177/0022034520927385

Magoc, T., and Salzberg, S. L. (2011). FLASH: fast length adjustment of short reads to improve genome assemblies. *Bioinformatics* 27, 2957–2963. doi: 10.1093/bioinformatics/btr507

Ma, L., Li, Q., Shen, L., Feng, X., Xiao, Y., Tao, J., et al. (2016). Insights into the fluoride-resistant regulation mechanism of acidithiobacillus ferrooxidans ATCC 23270 based on whole genome microarrays. *J. Ind. Microbiol. Biotechnol.* 43, 1441–1453. doi: 10.1007/s10295-016-1827-6

Marquis, R. E., Clock, S. A., and Mota-Meira, M. (2003). Fluoride and organic weak acids as modulators of microbial physiology. *FEMS Microbiol. Rev.* 26, 493–510. doi: 10.1111/j.1574-6976.2003.tb00627.x

Marsh, P. D., Head, D. A., and Devine, D. A. (2015). Ecological approaches to oral biofilms: control without killing. *Caries. Res.* 49, 46–54. doi: 10.1159/000377732

McBain, A. J., Sissons, C., Ledder, R. G., Sreenivasan, P. K., De Vizio, W., and Gilbert, P. (2005). Development and characterization of a simple perfused oral microcosm. *J. Appl. Microbiol.* 98, 624–634. doi: 10.1111/j.1365-2672.2004.02483.x

Men, X., Shibata, Y., Takeshita, T., and Yamashita, Y. (2016). Identification of anion channels responsible for fluoride resistance in oral streptococci. *PloS One* 11, e0165900. doi: 10.1371/journal.pone.0165900

Murata, T., and Hanada, N. (2016). Contribution of chloride channel permease to fluoride resistance in streptococcus mutans. *FEMS Microbiol. Lett.* 363, fnw101. doi: 10.1093/femsle/fnw101

Oh, H. J., Oh, H. W., Lee, D. W., Kim, C. H., Ahn, J. Y., Kim, Y., et al. (2017). Chronologic trends in studies on fluoride mechanisms of action. *J. Dent. Res.* 96, 1353–1360. doi: 10.1177/0022034517717680

Peres, M. A., Macpherson, L. M. D., Weyant, R. J., Daly, B., Venturelli, R., Mathur, M. R., et al. (2019). Oral diseases: a global public health challenge. *Lancet* 394, 249–260. doi: 10.1016/s0140-6736(19)31146-8

Pitts, N. B., Zero, D. T., Marsh, P. D., Ekstrand, K., Weintraub, J. A., Ramos-Gomez, F., et al. (2017). Dental caries. *Nat. Rev. Dis. Primers* 3, 17030. doi: 10.1038/nrdp.2017.30

Raddadi, N., Cherif, A., Daffonchio, D., Neifar, M., and Fava, F. (2015). Biotechnological applications of extremophiles, extremozymes and extremolytes. *Appl. Microbiol. Biotechnol.* 99, 7907–7913. doi: 10.1007/s00253-015-6874-9

Schloss, P. D., Westcott, S. L., Ryabin, T., Hall, J. R., Hartmann, M., Hollister, E. B., et al. (2009). Introducing mothur: open-source, platform-independent, community-supported software for describing and comparing microbial communities. *Appl. Environ. Microbiol.* 75, 7537–7541. doi: 10.1128/AEM.01541-09

Srivastava, S., and Flora, S. J. S. (2020). Fluoride in drinking water and skeletal fluorosis: a review of the global impact. *Curr. Environ. Health Rep.* 7, 140–146. doi: 10.1007/s40572-020-00270-9

Streckfuss, J. L., Perkins, D., Horton, I. M., Brown, L. R., Dreizen, S., and Graves, L. (1980). Fluoride resistance and adherence of selected strains of streptococcus mutans to smooth surfaces after exposure to fluoride. *J. Dent. Res.* 59, 151–158. doi: 10.1177/00220345800590021501

Takahashi, N., and Nyvad, B. (2011). The role of bacteria in the caries process: ecological perspectives. *J. Dent. Res.* 90, 294–303. doi: 10.1177/0022034510379602

Tang, B., Gong, T., Zhou, X., Lu, M., Zeng, J., Peng, X., et al. (2019). Deletion of cas3 gene in streptococcus mutans affects biofilm formation and increases fluoride sensitivity. *Arch. Oral. Biol.* 99, 190–197. doi: 10.1016/j.archoralbio.2019.01.016

Ten Cate, J. M. (2004). Fluorides in caries prevention and control: empiricism or science. *Caries. Res.* 38, 254–257. doi: 10.1159/000077763

Uranga, C., Nelson, K. E., Edlund, A., and Baker, J. L. (2021). Tetramic acids mutanocyclin and reutericyclin a, produced by streptococcus mutans strain B04Sm5 modulate the ecology of an *in vitro* oral biofilm. *Front. Oral. Health* 2. doi: 10.3389/froh.2021.796140

Vacca-Smith, A. M., and Bowen, W. H. (1998). Binding properties of streptococcal glucosyltransferases for hydroxyapatite, saliva-coated hydroxyapatite, and bacterial surfaces. *Arch. Oral. Biol.* 43, 103–110. doi: 10.1016/s0003-9969(97)00111-8

Van Loveren, C., Spitz, L. M., Buijs, J. F., Ten Cate, J. M., and Eisenberg, A. D. (1991a). *In vitro* demineralization of enamel by f-sensitive and f-resistant mutans streptococci in the presence of 0, 0.05, or 0.5 mmol/L NaF. *J. Dent. Res.* 70, 1491–1496. doi: 10.1177/00220345910700120401

Van Loveren, C., Van de Plassche-Simons, Y. M., De Soet, J. J., De Graaff, J., and Ten Cate, J. M. (1991b). Acidogenesis in relation to fluoride resistance of streptococcus mutans. *Oral. Microbiol. Immunol.* 6, 288–291. doi: 10.1111/j.1399-302x.1991.tb00494.x

Wang, Q., Garrity, G. M., Tiedje, J. M., and Cole, J. R. (2007). Naive Bayesian classifier for rapid assignment of rRNA sequences into the new bacterial taxonomy. *Appl. Environ. Microbiol.* 73, 5261–5267. doi: 10.1128/AEM.00062-07

Xiao, J., Klein, M. I., Falsetta, M. L., Lu, B., Delahunty, C. M., Yates, J. R., et al. (2012). The exopolysaccharide matrix modulates the interaction between 3D architecture and virulence of a mixed-species oral biofilm. *PLoS Pathog.* 8, e1002623. doi: 10.1371/journal.ppat.1002623

Xu, M., Zhang, Q., Xia, C., Zhong, Y., Sun, G., Guo, J., et al. (2014). Elevated nitrate enriches microbial functional genes for potential bioremediation of complexly contaminated sediments. *ISME J.* 8, 1932–1944. doi: 10.1038/ismej.2014.42

Yoshida, A., Suzuki, N., Nakano, Y., Kawada, M., Oho, T., and Koga, T. (2003). Development of a 5′ nuclease-based real-time PCR assay for quantitative detection of cariogenic dental pathogens streptococcus mutans and streptococcus sobrinus. *J. Clin. Microbiol.* 41, 4438–4441. doi: 10.1128/jcm.41.9.4438-4441.2003

Yu, J., Wang, Y., Han, D., Cao, W., Zheng, L., Xie, Z., et al. (2020). Identification of streptococcus mutans genes involved in fluoride resistance by screening of a transposon mutant library. *Mol. Oral. Microbiol.* 35, 260–270. doi: 10.1111/omi.12316

Zhang, L., Shen, Y., Qiu, L., Yu, F., Hu, X., Wang, M., et al. (2022). The suppression effect of SCH-79797 on streptococcus mutans biofilm formation. *J. Oral. Microbiol.* 14, 2061113. doi: 10.1080/20002297.2022.2061113

Zhang, K., Xiang, Y., Peng, Y., Tang, F., Cao, Y., Xing, Z., et al. (2022). Influence of fluoride-resistant streptococcus mutans within antagonistic dual-species biofilms under fluoride *In vitro*. front. *Cell. Infect. Microbiol.* 12. doi: 10.3389/fcimb.2022.801569

Zheng, X., He, J., Wang, L., Zhou, S., Peng, X., Huang, S., et al. (2017). Ecological effect of arginine on oral microbiota. *Sci. Rep.* 7, 7206. doi: 10.1038/s41598-017-07042-w

Zhu, L., Zhang, Z., and Liang, J. (2012). Fatty-acid profiles and expression of the fabM gene in a fluoride-resistant strain of streptococcus mutans. *Arch. Oral. Biol.* 57, 10–14. doi: 10.1016/j.archoralbio.2011.06.011

In vitro versus *in situ* biofilms for evaluating the antimicrobial effectiveness of herbal mouthrinses

Nicole Schönbächler[1], Thomas Thurnheer[1], Pune Nina Paqué[1,2], Thomas Attin[1] and Lamprini Karygianni[1]*

[1]Clinic of Conservative and Preventive Dentistry, Center of Dental Medicine, University of Zurich, Zurich, Switzerland, [2]Clinic of Reconstructive Dentistry, Center of Dental Medicine, University of Zurich, Zurich, Switzerland

For centuries, diverse mouthrinses have been applied for medicinal purposes in the oral cavity. In view of the growing resistance of oral microorganisms against conventional antimicrobial agents e.g. chlorhexidine, the implementation of alternative treatments inspired by nature has lately gained increasing interest. The aim of the present study was to compare *in vitro* biofilm models with *in situ* biofilms in order to evaluate the antimicrobial potential of different natural mouthrinses. For the *in vitro* study a six-species supragingival biofilm model containing *A. oris*, *V. dispar*, *C. albicans*, *F. nucleatum*, *S. mutans* and *S. oralis* was used. Biofilms were grown anaerobically on hydroxyapatite discs and treated with natural mouthrinses Ratanhia, Trybol and Tebodont. 0.9% NaCl and 10% ethanol served as negative controls, while 0.2% CHX served as positive control. After 64h hours, biofilms were harvested and quantified by cultural analysis CFU. For the *in situ* study, individual test splints were manufactured for the participants. After 2h and 72h the biofilm-covered samples were removed and treated with the mouthrinses and controls mentioned above. The biofilms were quantified by CFU and stained for vitality under the confocal laser scanning microscope. In the *in vitro* study, 0.2% CHX yielded the highest antimicrobial effect. Among all mouthrinses, Tebodont (4.708 $\pm$ 1.294 log10 CFU, median 5.279, p<0.0001) compared with 0.9% NaCl showed the highest antimicrobial potential. After 72h there was no significant reduction in CFU after 0.2% CHX treatment. Only Trybol showed a statistically significant reduction of aerobic growth of microorganisms *in situ* (5.331 $\pm$ 0.7350 log10 CFU, median 5.579, p<0.0209). After treatment with the positive control 0.2% CHX, a significant percentage of non-vital bacteria (42.006 $\pm$ 12.173 log10 CFU, median 42.150) was detected. To sum up, a less pronounced effect of all mouthrinses was shown for the *in situ* biofilms compared to the *in vitro* biofilms.

1 Introduction

For centuries, diverse mouthrinses have been applied for medicinal purposes in the oral cavity. To date, numerous chemical ingredients and natural compounds, which are able to eliminate biofilms, have been subjects of current scientific research as potent ingredients of oral mouthrinses (Milleman et al., 2022). The reason for the increasing scientific interest is that biofilms cause serious infections in different parts of the human body and, especially in the oral cavity such as caries, periodontal disease or peri-implantitis (Spuldaro et al., 2021). Until now, several antimicrobial substances have been tested for the control of oral biofilms, including but not limited to chlorhexidine (CHX), essential oils, amine fluoride or triclosan. For over 40 years, CHX has been known as an excellent mouthrinse to control dental plaque and thereby prevent gingival inflammation (Cai et al., 2020). CHX is a cationic biguanide, which is bacteriostatic in low and bactericidal in higher concentrations is regarded as the gold standard (Abouassi et al., 2014). Yet, the use of CHX is associated with some well-known side effects, namely the reduction of human taste perception and discoloration of the tongue, composite fillings and teeth, which interfere with its application (Gürgan et al., 2006). It is also known that the antimicrobial activity of CHX is affected by the environment, also by the presence of organic compounds and food rests in the oral cavity (James et al., 2017). It is believed that the turnover rate of specific salivary proteins can decrease the activity of different agents with antimicrobial activity (Auschill et al., 2001; Auschill et al., 2005). In view of the growing resistance of oral microorganisms against conventional antimicrobial agents e.g. CHX, the implementation of alternative treatments inspired by nature has lately gained increasing interest (Karygianni et al., 2015; Shen et al., 2016; Cieplik et al., 2019). Due to the lack of secondary effects and a higher potential for long-term usage in the oral cavity, several natural plant extracts and plant-derived pure substances has been screened for the control of oral infections in recent studies (Karygianni et al., 2014; Tiwari et al., 2015; Cai et al., 2020; Kurz et al., 2021). Even the World Health Organization (WHO) published in 2014 recommendations to emphasize the importance of traditional and alternative phytomedicine for the well-being and presented many proposals to establish plant-based medicine (Kurz et al., 2021). In a systematic review on herbal interventions in the oral cavity was shown, that plant extracts as *Vitis vinifera*, *Camellia sinensis* or manuka honey exhibit high elimination rates of multispecies oral biofilms (Karygianni et al., 2015).

The oral cavity consisting of up to 700 different bacterial species is an enormously complex habitat, which is unique in the human body. The microbial cells, which are embedded in a matrix of extracellular polymeric substances, are irreversibly attached to epithelial- and tooth surfaces. Despite the dominance of adverse conditions (alternating temperatures, pH as well as oxygen and nutrient supplies) in the microenvironment of the oral cavity, biofilms survive thanks to commensal or mutualistic symbiotic relationships among different microbial species, allowing for the harmonic growth of both aerobic and anaerobic microorganisms (Wood et al., 2000). This physiochemical intercommunication pattern among oral microorganisms within a biofilm, can lead to extremely resistant biofilms, which can be up to 1000 times less susceptible to diverse antimicrobials when compared to planktonic microorganisms (Karygianni et al., 2014). Additionally, the heterogeneity and structural complexity of oral biofilms poses a great challenge for their treatment, which has been confirmed by the use of different biofilm models in several *in vitro* studies (Guggenheim et al., 2001). One of the most established models is a multispecies supragingival biofilm model, which consists of six different microbial species, was firstly established in Zurich and is widely known as "Zurich biofilm model" (Shapiro et al., 2002). The initial *in vitro* screening of potential antimicrobial substances is an important step for the selection of the agents to be applied in clinical trials. In such *in vitro* studies, several antimicrobial agents such as chlorhexidine (CHX), amine fluoride/stannous fluoride, triclosan and phenolic agents were shown to be effective against oral biofilms (Auschill et al., 2005). Furthermore, some clinical studies (Auschill et al., 2001; Auschill et al., 2005), examined the impact of antimicrobials on intact oral biofilms, suggesting that the antimicrobial agent-induced alterations within oral biofilms might considerably differ between *in situ* biofilms and *in vitro* biofilm models (Auschill et al., 2005). The aim of the present study was to compare *in vitro* biofilm models with *in situ* biofilms in order to evaluate the antimicrobial potential of different natural mouthrinses. The null hypothesis of the study was that *in vitro* and *in situ* biofilms yield comparable outcomes in terms of screening of potential plant-derived antimicrobial agents. The microbial growth was therefore quantified for the treated biofilms, which were visualized under the confocal laser scanning microscopy (CLSM) and finally analyzed using an image analysis software.

2 Materials and methods

2.1 *In vitro* biofilms

2.1.1 Strains and preparation of inoculum for *in vitro* biofilms

For this study, the following six representative supragingival microorganisms were used: *Veillonella dispar* (OMZ 493), *Fusobacterium nucleatum* (OMZ 598), *Streptococcus oralis* (OMZ 607), *Streptococcus mutans* (OMZ 918), *Actinomyces oris* (OMZ 745) and *Candida albicans* (OMZ 110) The microorganisms were obtained by cultivation on Columbia blood agar plates (CBA; Becton, Dickinsson and Company, Sparks, MD, USA) supplemented with 5% (v/v) hemolyzed human blood under anaerobic conditions at 37°C. For overnight cultures, the microorganisms were picked from the CBA plates and inoculated into 9 ml filter-sterilized fluid universal medium + 0.3% glucose supplemented with 67 mmol/L Sørensen's buffer, pH 7.2 ("modified fluid universal medium", mFUM). As nutrition for *V. dispar*, 0.1% (v/v) sodium lactate was added into mFUM (Guggenheim et al., 2001). The cultures were then incubated anaerobically at 37°C for 15 h. 500 μl of the grown cultures were transferred into 5 ml preequilibrated mFUM, whereas the strains were

again incubated for 5 h anaerobically at 37°C. After 5 h, the optical density (OD_{550}) was measured for each strain and adjusted with fresh mFUM at 1.0 +/- 0.05. To obtain a microbial suspension the density-adjusted culture was mixed in equal volume.

2.1.2 Collection of saliva

The saliva was collected in the morning between 9:00 and 10:00 o'clock, at least 1.5 h after eating, drinking or plaque control. Whole, unstimulated saliva was collected in sterile 50 ml tubes. Afterwards the collected saliva was pooled and centrifuged (30 min, 4°C, 27'500 x g). The supernatant was pasteurized (30 min, 60°C) and again centrifuged (30 min, 4°C, 27'500 x g). The supernatant was pipetted into 50 ml sterile tubes and stored at -20°C. For pellicle formation the hydroxyapatite discs (HA; Ø 9mm, Clarkson Chromatography Products, South Williamsport, PA, USA) were placed in 24-well polystyrene cell culture plates and covered with 800 µl of processed whole unstimulated pooled saliva from individual donors (Guggenheim et al., 2001).

2.1.3 *In vitro* biofilm formation

Biofilms were grown in 24-well polystyrene cell culture plates on pellicle coated HA discs for 64 h under anaerobic conditions at 37°C to initiate the biofilm formation. For the first 16 h, 1120 µl of saliva (diluted 1:2 with 0.25% NaCl), 480 µl mFum (Fum + 0.3% glucose) and 200 µl of the prepared microbial suspension were added to the preconditioned pellicle-coated discs. The growth medium consisting of diluted saliva and mFUM with a carbohydrate concentration of 0.15% glucose and 0.15% sucrose (w/v) instead of 0.3% glucose was renewed after 16 h and 40 h, respectively. The 1-minute treatments with three different mouthrinses (Table 1) and control solutions 0.9% NaCl (negative control), 10% EtOH (negative control) and 0.2% CHX (positive control) were conducted 3 times a day for 2 days: after 16 h, 20 h, 24 h, 40 h, 44 h and 48 h. After treatment, the discs were washed twice in 3 x 2 ml physiological saline (0.9% NaCl), transferred back to the growth medium and incubated anaerobically at 37°C.

2.1.4 Natural mouthrinses

Table 1 summarizes the tested mouthrinses along with their active agents. Tebodont (Dr. Wild & Co. AG, Muttenz, Switzerland), Ratanhia (Weleda, Schwäbisch Gmünd, Germany) and Trybol AG, Neuhausen, Switzerland) were tested. To evaluate the inhibitory effect of commercial mouthrinses on *in vitro* and *in situ* supragingival biofilms, Ratanhia and Trybol were diluted as recommended in the application instructions. Ratanhia was diluted to obtain final alcohol concentration of 10%, while Trybol was diluted with sterile water (1:20). All three of the chosen antimicrobial agents consist mainly of essential oils, as specified in Table 1. For the negative control,

physiological saline (0.9% NaCl) and 10% ethanol were used. The inhibitory effect of 0.2% chlorhexidine (CHX) served as positive control.

2.1.5 Biofilm harvesting

After 64 h the biofilms were rinsed three times in 0.9% NaCl to remove the non-adherent microorganisms. To harvest the biofilms, discs were transferred into 1 ml 0.9% NaCl, vortexed for 2 min and then sonicated for 5 s at 30 W (Sonifier B-12, Branson Ultrasonic, Urdorf, Switzerland). The resulting microbial suspensions were diluted in 0.9% NaCl by serial dilutions and plated on selective (Biggy Agar, Becton, Dickinsson and Company, Sparks, MD, USA) and non-selective agar plates (CBA) to assess the colony forming units (CFU). The plates were incubated for 72h under both aerobic ($10\%~CO_2$) and anaerobic conditions.

2.2 *In situ* biofilms

2.2.1 Subjects and specimens

Six volunteers from 25 to 59 years of age were selected. Prerequisites for participation in the study included (i) no use of antibiotics and mouthrinses three months prior to the wearing, (ii) no pregnancy or breastfeeding, (iii) no systemic diseases, and in addition, (iv) no oral hygiene was carried out in the 2 hours before wearing the appliance, (v) the consumption of food and liquids, as well as alcohol and nicotine, was prohibited during wearing the appliances and finally, (vi) the subjects had not participated in any other clinical examination up to 30 days before the start of the study. The written consent of the test persons to participate was given. The study was approved by the Ethics Committee of the University of Zurich (Basec-Number 2019-01324). After screening the patients' dental health, the DMFT scores retrieved were between 0 and 13.

2.2.2 Study design

The bovine enamel slabs (BES, d = 6 mm, h = 3 mm) were gained from freshly extracted bovine spongiform encephalopathy-free teeth. For each volunteer an individual, intraoral splint system was constructed for the upper jaw Figures 1. Six bovine enamel slabs were fixed towards the molar and premolar region with an A-silicon compound (President plus light body, Coltène/Whaledent AG, Altstätten, Switzerland). To avoid disturbing tongue and cheek movements the acrylic splint was rounded at the end and the BES margins were covered with silicon. During treatments the maxillary splint was not allowed to be brushed. During meals and oral hygiene, the splint system was stored in physiological saline for a maximum of 1 hour and then rinsed only with water before being put back into the

TABLE 1 Overview of the tested herbal mouthrinses, their active agents and the respective manufacturers.

Mouthrinses	Active ingredients	Manufacturer
Tebodont	*Melaleuca alternifolia*, sodium fluoride	Dr. Wild & Co. AG, Muttenz, Switzerland
Trybol	Chamomile, salvia, arnica	Trybol AG, Neuhausen, Switzerland
Rathania	Myrrhe, Ratanhia root, *Aesculus hippicastanum*, alcohol 57,6% diluted to 10% alcohol	Weleda, Schwäbisch Gmünd, Germany

FIGURE 1
Individual acrylic splints with six enamel slabs attached to different locations. The slabs were placed in the front, in the middle and in the back on both sides, right and left. All sides of the slabs, except the enamel surface were covered with silicone and embedded in the appliance. Due to the fact that biofilm formation can differ from molar to premolar, the treatment groups were shifted one position further at each subject. C/E: Back; B/F: Middle; A/D: Front.

oral cavity. Following the removal of the splint system after the given test periods of 2 h or 3 days, they were stored in 0.9% NaCl. Subsequently, the biofilms were treated and harvested for determining the microbial growth (CFU) or stained for assessing cell viability using confocal laser scanning microscopy (CLSM), respectively.

2.3 Determination of colony forming units

The colony-forming units (CFUs) for 2h and 72h were evaluated quantitatively. The patients had to wear the splint system first for 1 min, then the BES were treated for 1 min with the mouthrinse and control solutions respectively. After that the discs were rinsed three times in 1 ml 0.9% NaCl. Subsequently, the BES were worn for 2h and 72h, respectively. After the removal of the splints from the oral cavity, the silicon was detached from the samples and the discs were then treated for 2 min with the mouthrinses and again dipped in 1 ml NaCl three times. Afterwards the discs were transferred in 1 ml 0.9% NaCl. To harvest the biofilms, the BES were vortexed for 30 sec, sonicated for 2 min and again vortexed for another 30 sec. From the resulting microbial suspensions, serial dilutions were done and plated on CBA. The plates were incubated for 72h under aerobic (10% CO_2) and anaerobic conditions.

2.4 Biofilm staining

The obtained biofilms on the BES after 72 h were stained using nucleic acid stains. Following dyes from Invitrogen[TM] (ThermoFisher Scienfic, Reinach, Switzerland) were used for viability analysis and visualization of extracellular DNA (eDNA): SYTO 40 a cell-permeant nucleic acid stain, DRAQ7 and TOTO-1 cell impermeable DNA dyes. The BES were stained for 15 min at room temperature in the dark with a final concentration of 20 μM for SYTO 40 and DRAQ7 and 2 μM for TOTO-1. After staining, the discs were washed with H_2O and

then placed on upside down on chamber slides with a drop of Mowiol (Roth AG, Arlesheim, Switzerland).

2.5 Confocal laser scanning microscopy and image analysis

Subsequently, the stained biofilms were analyzed by confocal laser scanning microscopy using a Leica TCS SP5 microscope (Leica Microsystem, Wetzlar, Germany) with x 63/1.4 NA oil-immersion objective lens. Excitation of the dyes were carried out using the following wavelengths: UV laser 405 nm, Argon laser 488 nm and Helium-Neon laser 633 nm. Fluorescence emission was detected at the following wavelengths: 420-460 nm (SYTO 40), 515-570 nm (TOTO-1), and 687-770 nm (DRAQ7). The biofilms were scanned in sequential mode, and z-series were generated by vertical optical sectioning using a step size of 0.5 μm. Image acquisition was conducted in 6x line average mode. Each disc was measured at three different positions. Images were processed using IMARIS software (version 9.7.2, Bitplane, Zurich, Switzerland) and quantified by Fiji. The 3D data were collapsed into 2D by maximal z-projection and each channel was analyzed separately. Contrary to TOTO-1, the threshold of SYTO 40 and DRAQ7 stains was not modified. The measurements were set areas, min/max, gray value, area fraction, mean gray value and stack position and the size of the analyze particles were from 0.10 - infinity micron^2.

2.6 Statistical analysis

For the *in vitro* study three independent experiments were conducted and within each experiment every treatment group was represented in triplicate (n=9). For the *in situ* study independent experiments of 6 subjects were carried out and within each subject every treatment group was represented once. The data points of the treatment groups were summarized of all subjects (n=6). For the quantification of the cell viability, 18 data points were generated, as each biofilm sample was scanned at 3 positions. Two-way analysis of variance (ANOVA) was used to analyze the difference in microbial growth per biofilm between the control groups (CHX, ethanol, NaCl) and the different treatments with herbal mouthrinses. For correction Tukey's multiple comparisons test was used. Missing values were ascribed the lowest detection limit value of the assay to allow for logarithmic transformation. Statistics have been implemented using GraphPad Prism software (version 7; La Jolla, CA, USA). Significance level was set at p < 0.05.

3 Results

3.1 *In vitro* effects of mouthrinses

The antimicrobial effect of the tested mouthrinses on the microbial growth of supragingival biofilms consisting of six species grown for 64h *in vitro* is illustrated In Figure 2. The application of 0.2% CHX as positive control shows a significant decrease (0.000 ± 0.000 $\log_{10}$ CFU, median 0.000, *p< 0.0001*) on both aerobic and anaerobic
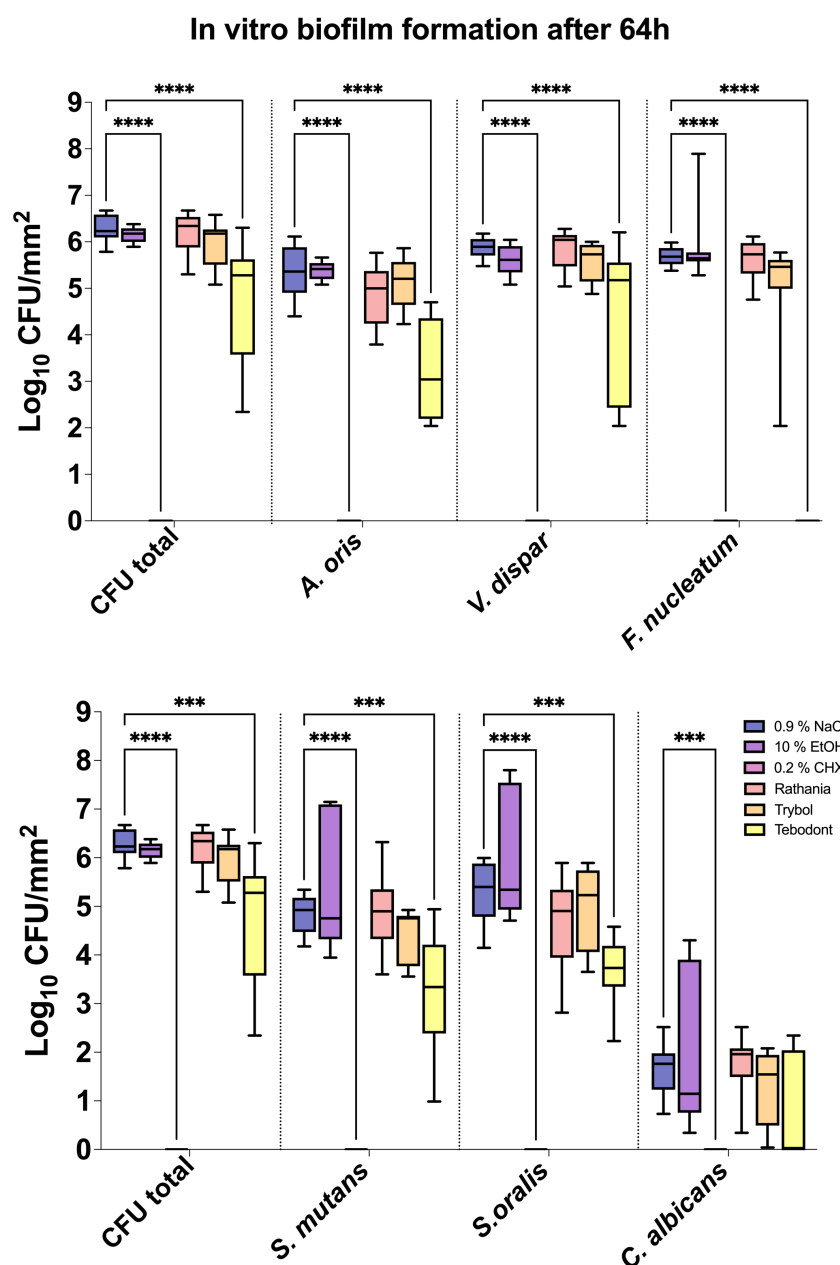
FIGURE 2
Box plots illustrating the colony-forming units (CFUs) of six-species oral biofilms after simultaneous exposure to the natural mouthrinses Ratanhia, Trybol, Tebodont. 0.2% CHX (positive control), 0.9% NaCl and 10% EtOH (negative control) were also used. The CFU values were shown on a $\log_{10}$ scale per mm^2 ($\log_{10}$/mm^2). The line dividing the box shows the median. The p-values of the significantly different data are plotted: ***= P-value <0.001, **** = P-value < 0.0001.

microorganisms compared to the two negative controls (0.9% NaCl; 6.289 ± 0.289 $\log_{10}$ CFU, median 6.230, *p< 0.0001* and 10% ethanol; 6.154 ± 0.170 $\log_{10}$ CFU, median 6.176, *p< 0.0001*). A significant antimicrobial effect was also found for Tebodont (4.708 ± 1.294 $\log_{10}$ CFU, median 5.279, *p< 0.0001*) compared to the negative controls (0.9% NaCl and 10% EtOH). In comparison with Trybol (5.971 ± 0.498 $\log_{10}$ CFU, median 6.176, *p< 0.0138*) and Ratanhia (6.208 ± 0.454 $\log_{10}$ CFU, median 6.342, *p< 0.0016*), Tebodont presented a significant antimicrobial activity. Treatment with Ratanhia (6.208 ± 0.454 $\log_{10}$ CFU, median 6.342, *p> 0.9999*) or Trybol (5.971 ± 0.498 $\log_{10}$ CFU,

median 6.176, *p> 0.9968*) failed to yield significant reduction of $\log_{10}$ CFU compared to the negative controls.

Furthermore, Tebodont induced a significant decrease of the bacterial counts of *A. oris* (3.260 ± 1.092 $\log_{10}$ CFU, median 3.041, *p> 0.0001*), *V. dispar* (4.342 ± 1.612 $\log_{10}$ CFU, median 5.176, *p> 0.0001*) and *F. nucleatum* (0.107 ± 0.319 $\log_{10}$ CFU, median 0.000, *p> 0.0001*). A substantial antibacterial effect of Tebodont was observed for *S. mutans* (3.239 ± 1.217 $\log_{10}$ CFU, median 3.342, *p> 0.0328*) and *S. oralis* (3.682 ± 0.683 $\log_{10}$ CFU, median 3.732, *p> 0.0011*). The microbial counts of *Candida albicans* solely (0.714 ± 1.074 $\log_{10}$ CFU,

median 0.000, $p > 0.2653$) were not affected by the treatment with the herbal mouthrinses. Treatment with 0.2% CHX ended to a significant decrease of microbial counts of all six supragingival species (0.000 ± 0.000 $\log_{10}$ CFU, median 0.000, $p < 0.0001$).

3.2 In situ effects of mouthrinses

The eradication rates of initially adherent oral aerobic and anaerobic microorganisms following treatment of in situ biofilms with different herbal mouthrinses are shown in Figure 3. Treatment with 0.2% CHX turned out to be very effective against the initial adhesion of aerobic (1.439 ± 1.219 $\log_{10}$ CFU, median 1.534) and anaerobic (anaerobic; 1.439 ± 0.9357 $\log_{10}$ CFU, median 1.361) microorganisms after 2h. In contrast, Tebodont, showed no killing effect in situ (aerobic; 3.467 ± 0.5111 $\log_{10}$ CFU, median 3.739, $p < 0.0336$ and anaerobic; 3.557 ± 0.4561 $\log_{10}$ CFU, median 3.764, $p < 0.0248$). Contrary to Tebodont, a significant reduction of the microbial counts was detected for Trybol under both aerobic (2.071 ± 1.142 $\log_{10}$ CFU, median 2.298, $p < 0.0308$) and anaerobic conditions (2.207 ± 0.8791 $\log_{10}$ CFU, median 2.338, $p < 0.0431$).

Regarding the adherent oral microorganisms after 72h in situ (Figure 4), there was no statistically significant reduction of CFUs ($\log_{10}$/mm^2) after treatment with 0.2 CHX (aerobic 5.525 ± 0.6452 $\log_{10}$ CFU, median 5.525, $p > 0.9999$ and anaerobic 5.549 ± 0.7243 $\log_{10}$ CFU, median 5.280, $p > 0.9999$). In comparison to Tebodont, only Trybol showed a statistically significant difference in CFU ($\log_{10}$/mm^2) of aerobic microorganisms in situ (5.331 ± 0.7350 $\log_{10}$ CFU, median 5.579, $p < 0.0209$). Interestingly, there was no significant difference between the negative controls 0.9% NaCl (aerobic 2.438 ± 1.562 $\log_{10}$ CFU, median 2.166, $p < 0.7711$ and anaerobic 2.553 ± 1.478 $\log_{10}$ CFU, median 2.325, $p > 0.9999$),10% ethanol (aerobic 2.338 ± 1.629 $\log_{10}$ CFU, median 2.747, $p < 0.7205$ and anaerobic 2.199 ± 0.8702 $\log_{10}$ CFU, median 2.1000, $p > 0.9999$) compared to the positive control (0.2% CHX) as shown in Figures 3 and 4 after 2h and 72h, respectively.

3.3 In vitro versus in situ effects of mouthrinses

An interesting difference between in vitro and in situ biofilms (72 h) in regard to the antimicrobial effects of the tested herbal mouthrinses is demonstrated in Figure 5. Interestingly, when comparing in vitro versus in situ, a significant CFU reduction was shown after treatment of the in vitro biofilms with 0.2% CHX (0.000 ± 0.000 $\log_{10}$ CFU, median 0.000, $p < 0.0001$) or Tebodont (4.708 ± 1.294 $\log_{10}$ CFU, median 5.279, $p < 0.0253$). Yet, no significant reduction of the microbial growth for both aerobic and anaerobic microorganisms was found after treatment of the in situ biofilms (72h) with 0.2% CHX (5.525 ± 0.645 $\log_{10}$ CFU, median 5.525, $p < 0.0001$) or Tebodont (6.400 ± 0.708 $\log_{10}$ CFU, median 6.161, $p < 0.0253$). Interestingly, treatment with the mouthrinse Ratanhia led to a less substantial microbial growth (aerobic, anaerobic) in situ after 72 h (5.485 ± 0.491 $\log_{10}$ CFU, median 5.517, $p < 0.0157$) when compared with the in vitro microbial growth (6.208 ± 0.454 $\log_{10}$ CFU, median 6.342, $p < 0.0157$). However, the mouthrinse Trybol yielded no significant reduction in both aerobic and anaerobic microbial growth both after 72 h in situ (5.331 ± 0.735 $\log_{10}$ CFU, median 5.579, $p > 0.1587$) and in vitro (5.971 ± 0.498 $\log_{10}$ CFU, median 6.176, $p > 0.1587$).

3.4 DNA staining and extracellular matrix

The quantification of stained nucleic acids following CLSM microscopy is shown in Figure 6, while Figure 7 demonstrates representative CLSM images after staining of extracellular DNA
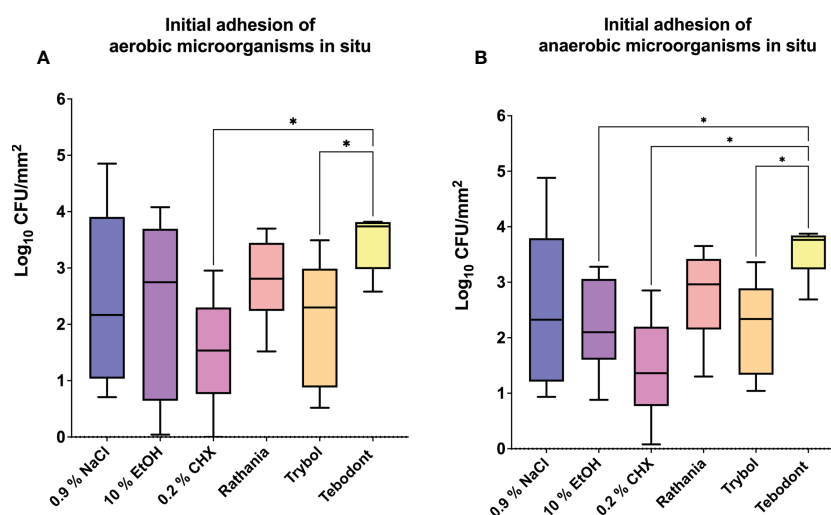
FIGURE 3
Box plots show the number of CFUs that demonstrate the antimicrobial effect of the tested substances on aerobic **(A)** and anaerobic **(B)** bacteria after an oral exposure time of 2 hours. A positive control (0.2% CHX), two negative controls (0.9% NaCl, 10% EtOH) and the natural mouthrinses Ratanhia, Trybol and Tebodont were also tested. The CFU values were shown on a $\log_{10}$ scale per mm^2 ($\log_{10}$/mm^2). The horizontal line within the box shows the median values. The p-values of the significantly different data are plotted: *= P-value <0.05.
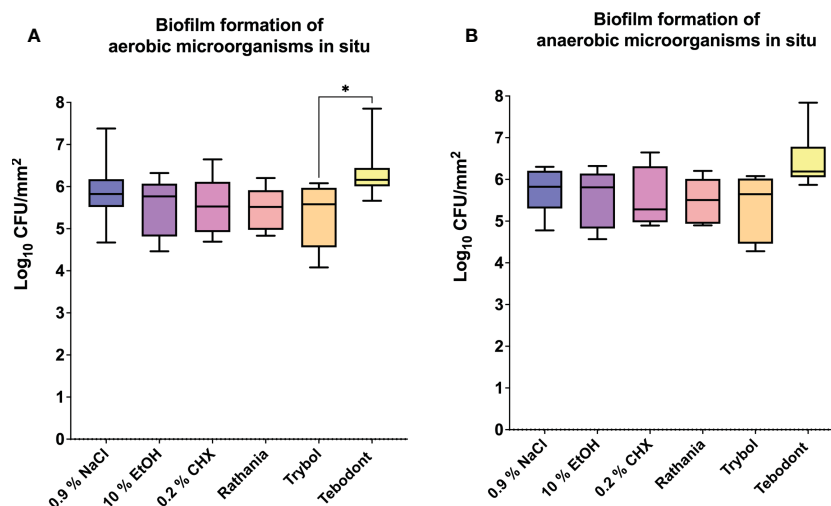
FIGURE 4
The graphs show the number of CFUs that demonstrate the antimicrobial effect of the tested substances on aerobic **(A)** and anaerobic **(B)** bacteria after an oral exposure time of 72 hours. A positive control (0.2% CHX), two negative controls (0.9% NaCl, 10% EtOH) and three different natural mouthrinses Ratanhia, Trybol and Tebodont were also used. The CFU values were shown on a $\log_{10}$ scale per mm^2 ($\log_{10}/mm^2$). The horizontal line within the box shows the median values. The p-values of the significantly different data are plotted: *= P-value <0.05.
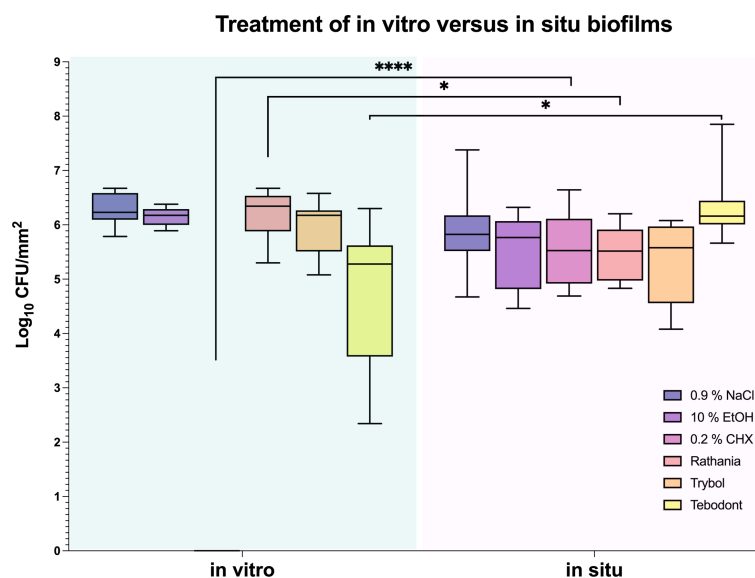
FIGURE 5
Box plots illustrating the comparison between the two treatment methods *in vitro* and *in situ*. It was measured by colony-forming units (CFUs) on a $\log_{10}$ scale per mm^2 ($\log_{10}/mm^2$). *In vitro* and *in situ* biofilms were treated with Ratanhia, Trybol, Tebodont. 0.2% CHX (positive control), 0.9% NaCl and 10% EtOH (negative control) were also used. The line dividing the box shows the median. The p-values of the significantly different data are plotted: *= P-value <0.05, **** = P-value < 0.0001.

(eDNA). Prior to the viability analysis and CLSM visualization, the biofilms had been treated with the natural mouthrinses Ratanhia, Trybol, Tebodont, as well as 0.2% CHX (positive control), 10% ethanol and 0.9% NaCl (negative controls). The biofilms were afterwards stained with SYTO 40, a cell-permeant nucleic acid stain in green, which can penetrate intact cells. On the other side, DRAQ7 (red) and TOTO-1 (blue) are cell impermeable DNA dyes. DRAQ7 was used to analyze the inactive (dead) bacteria within the biofilm. Nucleic acids within the extracellular matrix were stained blue by TOTO-1.

Although the percentage of stained nucleic acids varied for SYTO 40, no significant impact was observed following the treatment with the herbal mouthrinses. A similar diversity especially for 0.2% CHX is illustrated for TOTO-1 staining. Quantification of the DRAQ7-stained cells revealed that treatment with 0.2% CHX (42.006 ± 12.173 $\log_{10}$ CFU, median 42.150) significantly increased the proportions of the dead cells compared with the negative control groups 0.9% NaCl (18.878 ± 8.237 $\log_{10}$ CFU, median 19.450, *p> 0.0001*) and 10% ethanol (20.544 ± 6.882 $\log_{10}$ CFU, median 19.250, *p> 0.0001*).
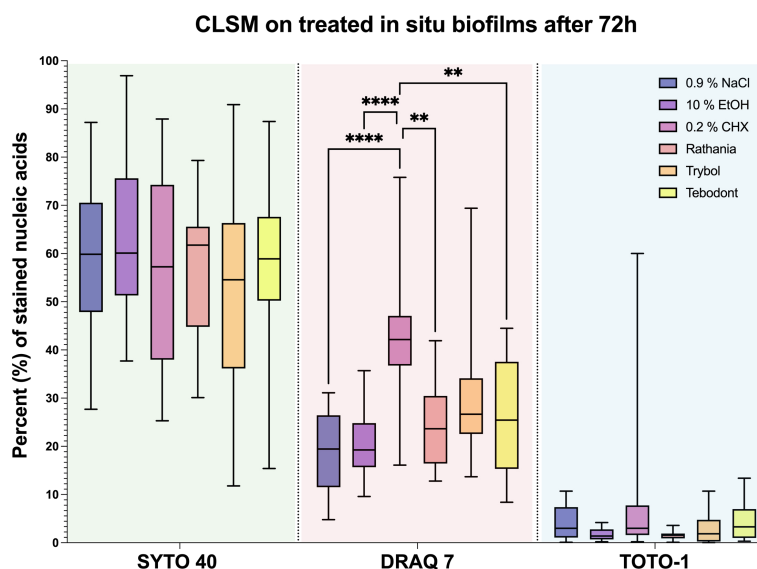
FIGURE 6
Boxplots illustrating the outcomes of image analysis. The *in situ* biofilm was grown 72 hours on HA discs and afterwards treated with different mouthrinses: 0.2% CHX, 10% EtOH, 0.9% NaCl, Ratanhia, Tebodont and Trybol. The visualization of nucleic acids was aided by SYTO 40, a cell-permeant nucleic acid stain, as well as DRAQ7 and TOTO-1, which cell impermeable DNA dyes. The percentage of stained nucleic acids was measured. The line dividing the box shows the median. The p-values of the significantly different data are plotted: ** = P-value < 0.01., **** = P-value < 0.0001.
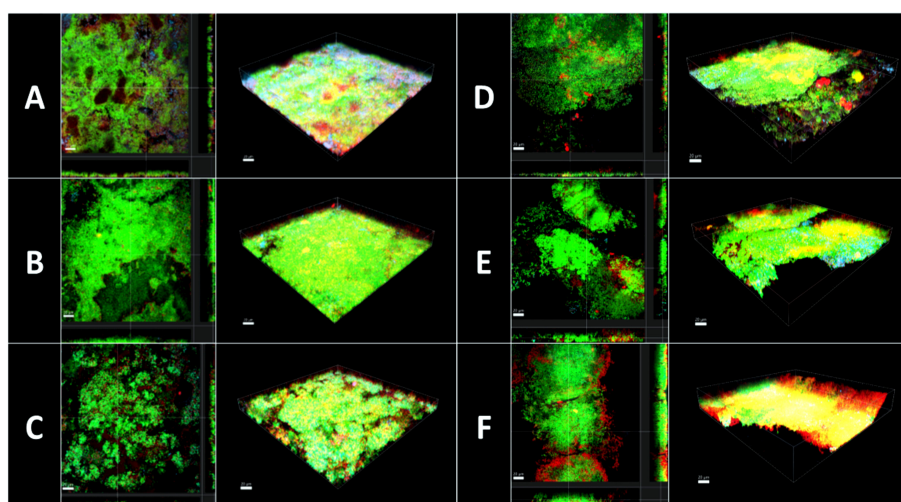
FIGURE 7
Confocal laser scanning microscopy (CLSM). 3D reconstructions and images sections of biofilm grown 3 days on HA discs and afterwards treated with different mouthrinse **(A)** 0.2% CHX, **(B)** 10% EtOH, **(C)** 0.9% NaCl, **(D)** Ratanhia, **(E)** Tebodont, **(F)** Trybol. The biofilms were used for viability analysis and visualization of extracellular DNA (eDNA): SYTO 40 a cell-permeant nucleic acid stain in green, DRAQ7 in red and TOTO-1 cell impermeable DNA dyes in blue.

Treatment with the herbal mouthrinses as Ratanhia (24.789 ± 8.914 $\log_{10}$ CFU, median 23.650, *p< 0.0015*) and Tebodont (26.711 ± 11.566 $\log_{10}$ CFU, median 25.450, *p< 0.0073*) yielded higher proportions of vital microorganisms compared to CHX (42.006 ± 12.173 $\log_{10}$ CFU, median 42.150). The mouthrinse Trybol yielded for both SYTO 40 and DRAQ7 a high variance in the percentages of stained nucleic acids. Yet, when Trybol was compared with both SYTO 40 (52.983 ± 23.271 $\log_{10}$ CFU, median 54.550, *p< 0.9123*) and DRAQ7 (30.150 ± 14.555 $\log_{10}$ CFU, median 26.650, *p< 0.1076*) compared to the negative control (0.9% NaCl) there is no statistically significant difference.

Illustrative series of confocal laser scanning microscopy (CLSM) images of biofilms after antimicrobial treatment are shown in Figure 7. The panels in Figure 7 indicated with A-F are images in sections of *in situ* biofilms after 72 h and 3D reconstructions in maximal Z-projections. The panels show the viable microorganisms in green due to staining with SYTO 40, while nucleic acid of dead microbial cells appears in red due to staining with DRAQ 7. Nucleic acids within the extracellular matrix were stained blue by TOTO-1. Panel A represents biofilms treated with 0.2% CHX and clearly shows a higher percentage of red- and blue-stained nucleic acids than panels

B and C, which demonstrate the negative controls. Treatment with 0.2% CHX resulted in less dense biofilms compared to treatment with 10% ethanol. Panels B, C, D show only a few microbial cells in red and blue. A fact that points out that treatment with the herbal mouthrinses like Panels B, C, D were less effective than the treatment with 0.2% CHX.

4 Discussion

Nowadays, the use of a toothbrush and fluoridated toothpaste is essential when oral hygiene is practiced. However, complete plaque removal is rather unrealistic, so a chemotherapeutic approach could be beneficial in some cases, in which antimicrobial control is mandatory (Zhang et al., 2019). The present study compares the effectiveness of diverse herbal mouthrinses on *in vitro* biofilms versus *in situ* biofilms. This allowed a better understanding of the differences in the outcomes between *in vitro* and *in situ* biofilms after treatment with plant-derived antimicrobial agents.

In vitro studies are necessary to evaluate the effectiveness of specific antimicrobial agents and to collect useful information for further *in situ* studies (Charles et al., 2004). For example, an excellent killing effect of 0.2% CHX was shown after the *in vitro* assays, since CHX was able to eradicate all six supragingival species of the *in vitro* biofilm after 64 h. To date, this excellent *in vitro* effect of CHX has been revealed in various reports (Guggenheim and Meier, 2011; Gränicher et al., 2021; Zhang et al., 2021). Interestingly, only Tebodont yielded a significant reduction of the *in vitro* biofilm growth compared to the negative controls. Tebodont yielded a significant reduction of *in vitro* bacterial growth of *A. oris*, *V. dispar*, *F. nucleatum*, *S. mutans* and *S. oralis*. Only for *C. albicans* there was no significant reduction detected *in vitro* after treatment with Tebodont. The same result was supported by another *in vitro* study, which also confirmed that Tebodont failed to eliminate *C. albicans*. An explanation could be that the strains of *C. albicans* might have been subjected to antifungal activity and become highly resistant to environmental stress (Francisconi et al., 2020). Although a significant reduction in oral microorganisms was detected, the antimicrobial effectivity of 0.2% CHX was much lower compared to that of Tebodont Similarly, the study of Shapiro et al., 1994 supported that sage and tea tree oil inhibited all laboratory strains used in the Zurich biofilm model (Shapiro et al., 1994). In *in vitro* studies it was shown that essential oils with low concentrations can disable enzymes, while essential oils in higher concentrations penetrate the biofilm, rupture the cell wall and thereby eliminate a wide range of microorganisms (Stoeken et al., 2007).

In the present *in situ* study, treatment with 0.2% CHX showed a significant impact against early biofilms after 2 h. Yet, there was no effect against biofilms after 72h compared to the negative controls. Interestingly, the essential oil Trybol achieved a significant outcome *in situ* compared to Tebodont. To confirm this, several clinical studies also concluded that a combination of brushing and rinsing with essential oil containing phenol, thymol, eucalyptol significantly reduced dental plaque and therefore gingivitis compared to only brushing (Stoeken et al., 2007). However, various earlier studies revealed that CHX allowed for a more efficient control of dental plaque compared to mouthrinses with essential oils (Charles et al.,

2004; Marchetti et al., 2011). It is surprising that the addition of plant extracts such as ratanhia, myrrh, chamomile, arnica, or sage can yield substantial antimicrobial, anti-inflammatory or epithelium-protecting properties (Shapiro et al., 1994). Especially mouthrinses containing chamomile flower extract contain a wide variety of active chemical nutrients and efficiently reduce dental plaque and gingivitis (Chen et al., 2014). Interestingly, flavonoids, including apigenin, chamazulene and alpha-bisabolol act as anti-inflammatory agents. Herbal ingredients such as sage, myrrh can displace the pH of saliva into the alkaline range and are therefore extremely effective against periodontal diseases (Willershausen et al., 1991). This is in accordance with a recent study which has shown that plant extracts can suppress the supragingival pathogens and thereby reduce plaque accumulation (Bosma et al., 2022). Another widely discussed ingredient of mouthwashes is ethanol, which is commonly used as a solvent in herbal mouthrinses. Ethanol at a high concentration of 40% can interfere with the growth of oral microorganisms, therefore it can be normally found at a concentration 5-27% in different mouthrinses (Brecx et al., 2003). Surprisingly, the mouthrinse Ratanhia contains 57.6% ethanol which when not correctly solved can reduce microorganisms, but can also have some side effects in oral cavity, notably a possible risk for oral cancer, xerostomia or mouth burning (Tiemann et al., 2007; Chen et al., 2014). In the present report, Ratanhia was solved to a final ethanol concentration of 10%. This may have led to non-beneficial outcome as expected for a natural mouthrinse, as the other active ingredients of the mouthwash were also diluted. A comparable outcome was also seen for the other tested mouthrinses, namely Trybol and Tebodont, which yielded a high variation of microbial growth both *in vitro* and *in situ*. One explanation could be that active bacterial communities are heterogenous, dynamic systems that are influenced by multiple internal and external factors, which constantly affect the viability process in the framework of homeostasis. Another fact is that there are individual differences in the microbial counts among the samples and probands which can also lead to high standard deviations (Kurz et al., 2021).

The main aim of our report was to demonstrate the differences between *in vitro* and *in situ* biofilms as study models. The *in vitro* supragingival multispecies "Zurich biofilm model" has been successfully applied for over 25 years for testing the effect of antimicrobial agents in the field of oral medicine (Guggenheim et al., 2004; Ten Cate, 2006). Nevertheless, modern molecular biological investigations have identified over 700 different bacterial species in oral biofilm. The bacteria in their extracellular polysaccharide matrix communicate through signaling molecules, and use an quorum-sensing system to enable their survival (Karygianni et al., 2020; Eick, 2021). These bacteria mainly live under nutrient limitation and are often in a dormant state. Such dormant bacteria react differently to antimicrobial agents than the bacteria that are in a metabolically active state. Furthermore, it has been found that many mouthrinses bind to the extracellular polysaccharide matrix initially before they even reach the bacteria in the deeper layers of the biofilm (Karygianni et al., 2020). Interestingly, in the present study, 0.2% CHX and tea tree oil (Tebodont) showed a statistically significant eradication of supragingival strains of *in vitro* biofilms, but there was no reduction of *in situ* biofilms after 2h and 72h. These findings

highlight the reason why 0.2% CHX as well as mouthwashes like Tebodont and Trybol are less effective *in situ* than *in vitro*. Interestingly, solely Ratanhia showed better inhibitory effects *in situ* than *in vitro*. The *in vitro* biofilm model allows for the standardized control of the antimicrobial potential of the mouthrinses, but does not adequately reflect the physiological intra-oral situation (Auschill et al., 2004).

The live/dead viability assay it enabled the visualization of the active and non-active cells of the initial and mature oral biofilm (Kurz et al., 2021). In order to better understand the metabolic process or the turnover rate of saliva it is necessary to choose biofilms which grow directly in the oral cavity and whose three-dimensional structure is not manipulated. Through the use of CSLM, the biofilm structure, thickness and the viability was analyzed *in situ* (Lukic et al., 2020; Sousa et al., 2022). In the present study, it was shown in Figure 7 that treatment with 0.2% CHX yielded a less dense biofilm compared with the negative control, even though there was no statistical antimicrobial effect. Extracellular DNA (eDNA) is of great importance for microbial adhesion in the early phase of biofilm formation. Thus, the desire to highlight eDNA's role in biofilm formation has encouraged the visualization of eDNA in the biofilm using the stain TOTO-1 (Schlafer and Meyer, 2017). The CLSM images revealed a wide range of stained nucleic acids (SYTO 40). The percentages of vital microorganisms declined significantly after the treatment with 0.2% CHX. The essential oil Trybol yielded for both SYTO 40 and DRAQ7 a high variability in the percentages of stained nucleic acids. The difference between the vital staining and the CFU values can be attributed to the fact that the microbial aggregates were vortexed and thus, falsify the results (Al-Ahmad et al., 2008). Various studies have proven the advantages of CHX to substantially reduce microbial vitality in oral cavity (Al-Ahmad et al., 2013; Quintas et al., 2015; Kensche et al., 2017). A systematic review showed still a beneficial antibiofilm behavior of different natural ingredients stating that that there is a positive correlation between therapy protocols based on the use of medicinal herbs and the eradication rates of the treated oral biofilm (Karygianni et al., 2015). However, in an earlier study, it was shown that the effectiveness of mouthrinses differed between *in vitro* and *in situ* studies depending on the treatment duration and repeated use of the antimicrobial agent (Auschill et al., 2005). These findings apply to our study, in which the biofilms were only treated once for 2 minutes with the different mouthrinses. The same data confirmed also an earlier study of Arweiler et al., 2004 with a less substantial effect of biofilm density reduction (Arweiler et al., 2004). Furthermore, if fluorescein is applied for a longer time than indicated, microorganisms will not survive and the staining DRAQ7 and TOTO-1 will penetrate the cells, a fact which could lead to a falsification of the results. The major limitation of the study are associated with the visualization of biofilms using CLSM and the subsequent image analysis. The visualization of representative areas on the enamel slabs, the self-fluorescence of the enamel and technical difficulties during quantification were the main challenges of the present study.

In conclusion, natural mouthrinses and 0.2% CHX have a less pronounced effect on *in situ* biofilms, than on *in vitro* biofilms. Both *in vitro* and *in situ* models used in these studies highlighted the efficacy of mouthrinses under short-term exposure, which can lead to different results compared to long-term exposure. More studies are required to clarify the biological mechanisms that contribute to the effect of herbal mouthrinses.

Data availability statement

The original contributions presented in the study are included in the article/supplementary material. Further inquiries can be directed to the corresponding author.

Ethics statement

The studies involving human participants were reviewed and approved by the Ethics Committee of the University of Zurich (Basec-Number 2019-01324). Written informed consent for participation was not required for this study in accordance with the national legislation and the institutional requirements.

Author contributions

Funding

Acknowledgments

Conflict of interest

The authors declare that the research was conducted in the absence of any commercial or financial relationships that could be construed as a potential conflict of interest.

Publisher's note

References

Abouassi, T., Hannig, C., Mahncke, K., Karygianni, L., Wolkewitz, M., Hellwig, E., et al. (2014). Does human saliva decrease the antimicrobial activity of chlorhexidine against oral bacteria? *BMC Res. Notes* 7, 711. doi: 10.1186/1756-0500-7-711

Al-Ahmad, A., Wiedmann-Al-Ahmad, M., Auschill, T. M., Follo, M., Braun, G., Hellwig, E., et al. (2008). Effects of commonly used food preservatives on biofilm formation of streptococcus mutans *in vitro. Arch. Oral. Biol.* 53, 765–772. doi: 10.1016/j.archoralbio.2008.02.014

Al-Ahmad, A., Wiedmann-Al-Ahmad, M., Fackler, A., Follo, M., Hellwig, E., Bächle, M., et al. (2013). *In vivo* study of the initial bacterial adhesion on different implant materials. *Arch. Oral. Biol.* 58, 1139–1147. doi: 10.1016/j.archoralbio.2013.04.011

Auschill, T. M., Arweiler, N. B., Netuschil, L., Brecx, M., Reich, E., and Sculean, A. (2001). Spatial distribution of vital and dead microorganisms in dental biofilms. *Arch. Oral. Biol.* 46, 471–476. doi: 10.1016/S0003-9969(00)00136-9

Auschill, T. M., Hein, N., Hellwig, E., Follo, M., Sculean, A., and Arweiler, N. B. (2005). Effect of two antimicrobial agents on early *in situ* biofilm formation. *J. Clin. Periodontol* 32, 147–152. doi: 10.1111/j.1600-051X.2005.00650.x

Auschill, T. M., Hellwig, E., Sculean, A., Hein, N., and Arweiler, N. B. (2004). Impact of the intraoral location on the rate of biofilm growth. *Clin. Oral. Investig.* 8, 97–101. doi: 10.1007/s00784-004-0255-6

Arweiler, N. B., Hellwig, E., Sculean, A., Hein, N., and Auschill, T. M. (2004). Individual vitality pattern of in situ dental biofilms at different locations in the oral cavity. *Caries Res* 38, 442–447.

Bosma, M. L., Mcguire, J. A., Sunkara, A., Sullivan, P., Yoder, A., Milleman, J., et al. (2022). Efficacy of flossing and mouthrinsing regimens on plaque and gingivitis: A randomized clinical trial. *J. Dent. Hyg* 96, 8–20.

Brecx, M., Netuschil, L., and Hoffmann, T. (2003). How to select the right mouthrinses in periodontal prevention and therapy. part II. clinical use and recommendations. *Int. J. Dent. Hyg* 1, 188–194. doi: 10.1034/j.1601-5037.2003.00046.x

Cai, H., Chen, J., Panagodage Perera, N. K., and Liang, X. (2020). Effects of herbal mouthwashes on plaque and inflammation control for patients with gingivitis: A systematic review and meta-analysis of randomised controlled trials. *Evid Based Complement Alternat Med.* 2020, 2829854. doi: 10.1155/2020/2829854

Charles, C. H., Mostler, K. M., Bartels, L. L., and Mankodi, S. M. (2004). Comparative antiplaque and antigingivitis effectiveness of a chlorhexidine and an essential oil mouthrinse: 6-month clinical trial. *J. Clin. Periodontol* 31, 878–884. doi: 10.1111/j.1600-051X.2004.00578.x

Chen, Y., Wong, R. W., Mcgrath, C., Hagg, U., and Seneviratne, C. J. (2014). Natural compounds containing mouthrinses in the management of dental plaque and gingivitis: a systematic review. *Clin. Oral. Investig.* 18, 1–16. doi: 10.1007/s00784-013-1033-0

Cieplik, F., Jakubovics, N. S., Buchalla, W., Maisch, T., Hellwig, E., and Al-Ahmad, A. (2019). Resistance toward chlorhexidine in oral bacteria - is there cause for concern? *Front. Microbiol.* 10, 587. doi: 10.3389/fmicb.2019.00587

Eick, S. (2021). Biofilms. *Monogr. Oral. Sci.* 29, 1–11. doi: 10.1159/000510184

Francisconi, R. S., Huacho, P. M. M., Tonon, C. C., Bordini, E., Correia, M. F., Sardi, J. C. O., et al. (2020). Antibiofilm efficacy of tea tree oil and of its main component terpinen-4-ol against candida albicans. *Braz. Oral. Res.* 34, e050. doi: 10.1590/1807-3107bor-2020.vol34.0050

Gränicher, K. A., Karygianni, L., Attin, T., and Thurnheer, T. (2021). Low concentrations of chlorhexidine inhibit the formation and structural integrity of enzyme-treated multispecies oral biofilms. *Front. Microbiol.* 12, 741863. doi: 10.3389/fmicb.2021.741863

Guggenheim, B., Giertsen, E., Schüpbach, P., and Shapiro, S. (2001). Validation of an *in vitro* biofilm model of supragingival plaque. *J. Dent. Res.* 80, 363–370. doi: 10.1177/00220345010800011201

Guggenheim, B., Guggenheim, M., Gmür, R., Giertsen, E., and Thurnheer, T. (2004). Application of the zürich biofilm model to problems of cariology. *Caries Res.* 38, 212–222. doi: 10.1159/000077757

Guggenheim, B., and Meier, A. (2011). *In vitro* effect of chlorhexidine mouth rinses on polyspecies biofilms. *Schweiz Monatsschr Zahnmed* 121, 432–441.

Gürgan, C. A., Zaim, E., Bakirsoy, I., and Soykan, E. (2006). Short-term side effects of 0.2% alcohol-free chlorhexidine mouthrinse used as an adjunct to non-surgical periodontal treatment: a double-blind clinical study. *J. Periodontol* 77, 370–384. doi: 10.1902/jop.2006.050141

James, P., Worthington, H. V., Parnell, C., Harding, M., Lamont, T., Cheung, A., et al. (2017). Chlorhexidine mouthrinse as an adjunctive treatment for gingival health. *Cochrane Database Syst. Rev.* 3, Cd008676. doi: 10.1002/14651858.CD008676.pub2

Karygianni, L., Al-Ahmad, A., Argyropoulou, A., Hellwig, E., Anderson, A. C., and Skaltsounis, A. L. (2015). Natural antimicrobials and oral microorganisms: A systematic review on herbal interventions for the eradication of multispecies oral biofilms. *Front. Microbiol.* 6, 1529. doi: 10.3389/fmicb.2015.01529

Karygianni, L., Cecere, M., Skaltsounis, A. L., Argyropoulou, A., Hellwig, E., Aligiannis, N., et al. (2014). High-level antimicrobial efficacy of representative Mediterranean natural plant extracts against oral microorganisms. *BioMed. Res. Int.* 2014, 839019. doi: 10.1155/2014/839019

Karygianni, L., Ren, Z., Koo, H., and Thurnheer, T. (2020). Biofilm matrixome: Extracellular components in structured microbial communities. *Trends Microbiol.* 28, 668–681. doi: 10.1016/j.tim.2020.03.016

Kensche, A., Holder, C., Basche, S., Tahan, N., Hannig, C., and Hannig, M. (2017). Efficacy of a mouthrinse based on hydroxyapatite to reduce initial bacterial colonisation in situ. *Arch. Oral. Biol.* 80, 18–26. doi: 10.1016/j.archoralbio.2017.03.013

Kurz, H., Karygianni, L., Argyropoulou, A., Hellwig, E., Skaltsounis, A. L., Wittmer, A., et al. (2021). Antimicrobial effects of inula viscosa extract on the *In situ* initial oral biofilm. *Nutrients* 13 (11), 4029. doi: 10.3390/nu13114029

Lukic, D., Karygianni, L., Flury, M., Attin, T., and Thurnheer, T. (2020). Endodontic-like oral biofilms as models for multispecies interactions in endodontic diseases. *Microorganisms* 8(5), 674. doi: 10.3390/microorganisms8050674

Marchetti, E., Mummolo, S., Di Mattia, J., Casalena, F., Di Martino, S., Mattei, A., et al. (2011). Efficacy of essential oil mouthwash with and without alcohol: a 3-day plaque accumulation model. *Trials* 12, 262. doi: 10.1186/1745-6215-12-262

Milleman, J., Bosma, M. L., Mcguire, J. A., Sunkara, A., Mcadoo, K., Delsasso, A., et al. (2022). Comparative effectiveness of toothbrushing, flossing and mouthrinse regimens on plaque and gingivitis: A 12-week virtually supervised clinical trial. *J. Dent. Hyg* 96, 21–34.

Quintas, V., Prada-López, I., Donos, N., Suárez-Quintanilla, D., and Tomás, I. (2015). *In situ* neutralisation of the antibacterial effect of 0.2% chlorhexidine on salivary microbiota: Quantification of substantivity. *Arch. Oral. Biol.* 60, 1109–1116. doi: 10.1016/j.archoralbio.2015.04.002

Schlafer, S., and Meyer, R. L. (2017). Confocal microscopy imaging of the biofilm matrix. *J. Microbiol. Methods* 138, 50–59. doi: 10.1016/j.mimet.2016.03.002

Shapiro, S., Giertsen, E., and Guggenheim, B. (2002). An in vitro oral biofilm model for comparing the efficacy of antimicrobial mouthrinses. *Caries Res.* 36, 93–100. doi: 10.1159/000057866

Shapiro, S., Meier, A., and Guggenheim, B. (1994). The antimicrobial activity of essential oils and essential oil components towards oral bacteria. *Oral. Microbiol. Immunol.* 9, 202–208. doi: 10.1111/j.1399-302X.1994.tb00059.x

Shen, Y., Zhao, J., de la Fuente-Núñez, C., Wang, Z., Hancock, R. E., Roberts, C. R., et al. (2016). Experimental and theoretical investigation of multispecies oral biofilm resistance to chlorhexidine treatment. *Sci. Rep.* 6, 27537. doi: 10.1038/srep27537

Sousa, V., Spratt, D., Davrandi, M., Mardas, N., Beltrán, V., and Donos, N. (2022). Oral microcosm biofilms grown under conditions progressing from peri-implant health, peri-implant mucositis, and peri-implantitis. *Int. J. Environ. Res. Public Health* 19(21), 14088. doi: 10.3390/ijerph192114088

Spuldaro, T. R., Rogério Dos Santos Júnior, M., Vicentis De Oliveira Fernandes, G., and Rösing, C. K. (2021). Efficacy of essential oil mouthwashes with and without alcohol on the plaque formation: A randomized, crossover, double-blinded, clinical trial. *J. Evid Based Dent. Pract.* 21, 101527. doi: 10.1016/j.jebdp.2021.101527

Stoeken, J. E., Paraskevas, S., and van der Weijden, G. A. (2007). The long-term effect of a mouthrinse containing essential oils on dental plaque and gingivitis: a systematic review. *J. Periodontol* 78, 1218–1228. doi: 10.1902/jop.2007.060269

Ten Cate, J. M. (2006). Biofilms, a new approach to the microbiology of dental plaque. *Odontology* 94, 1–9. doi: 10.1007/s10266-006-0063-3

Tiemann, P., Toelg, M., and Ramos, F. M. (2007). Administration of ratanhia-based herbal oral care products for the prophylaxis of oral mucositis in cancer chemotherapy patients: a clinical trial. *Evid Based Complement Alternat Med.* 4, 361–366. doi: 10.1093/ecam/nel070

Tiwari, V., Roy, R., and Tiwari, M. (2015). Antimicrobial active herbal compounds against acinetobacter baumannii and other pathogens. *Front. Microbiol.* 6, 618. doi: 10.3389/fmicb.2015.00618

Willershausen, B., Gruber, I., and Hamm, G. (1991). The influence of herbal ingredients on the plaque index and bleeding tendency of the gingiva. *J. Clin. Dent.* 2, 75–78.

Wood, S. R., Kirkham, J., Marsh, P. D., Shore, R. C., Nattress, B., and Robinson, C. (2000). Architecture of intact natural human plaque biofilms studied by confocal laser scanning microscopy. *J. Dent. Res.* 79, 21–27. doi: 10.1177/00220345000790010201

Zhang, J., Ab Malik, N., Mcgrath, C., and Lam, O. (2019). The effect of antiseptic oral sprays on dental plaque and gingival inflammation: A systematic review and meta-analysis. *Int. J. Dent. Hyg* 17, 16–26. doi: 10.1111/idh.12331

Zhang, T., Xia, L., Wang, Z., Hancock, R. E. W., and Haapasalo, M. (2021). Recovery of oral in vitro biofilms after exposure to peptides and chlorhexidine. *J. Endod.* 47, 466–471. doi: 10.1016/j.joen.2020.11.020

The application of mesoporous silica nanoparticles as a drug delivery vehicle in oral disease treatment

Lixin Fang[1,2], Huoxiang Zhou[3,4], Long Cheng[1], Yiyi Wang[1], Fei Liu[1]* and Suping Wang[1]*

[1]Stomatology Center, The First Affiliated Hospital of Zhengzhou University, Zhengzhou, China, [2]The Academy of Medical Sciences, Zhengzhou University, Zhengzhou, China, [3]Laboratory of Microbiology and Immunology, Institute of Medical and Pharmaceutical Sciences & the Beijing Genomics Institution (BGI) College, Zhengzhou University, Zhengzhou, China, [4]Henan Key Laboratory of Child Brain Injury and Henan Pediatric Clinical Research Center, The Third Affiliated Hospital and Institute of Neuroscience, Zhengzhou University, Zhengzhou, China

Mesoporous silica nanoparticles (MSNs) hold promise as safer and more effective medication delivery vehicles for treating oral disorders. As the drug's delivery system, MSNs adapt to effectively combine with a variety of medications to get over systemic toxicity and low solubility issues. MSNs, which operate as a common nanoplatform for the co-delivery of several compounds, increase therapy effectiveness and show promise in the fight against antibiotic resistance. MSNs offer a noninvasive and biocompatible platform for delivery that produces long-acting release by responding to minute stimuli in the cellular environmen. MSN-based drug delivery systems for the treatment of periodontitis, cancer, dentin hypersensitivity, and dental cavities have recently been developed as a result of recent unparalleled advancements. The applications of MSNs to be embellished by oral therapeutic agents in stomatology are discussed in this paper.

KEYWORDS

mesoporous silica nanoparticles (MSNs), drug delivery system, biofilm, dental caries, dentin hypersensitivity, oral squamous cell carcinoma, bone regeneration

1 Introduction

Mesoporous silica nanoparticles (MSNs) have drawn a lot of interest as novel therapeutic nanocarriers because of their ability to release a variety of drugs at the desired place in response to external stimuli. MSNs are more advantageous choices for drug loading as compared to other nanocarriers because of their tunable morphologies, mesostructures, and porosities, as well as their superior biocompatibility and simplicity of functionalization. Furthermore, mesoporous materials' high surface areas and large pore volumes enable them to hold more medications or molecules (Figure 1A, B). Thanks to their advantage in functionalization, they also provide new
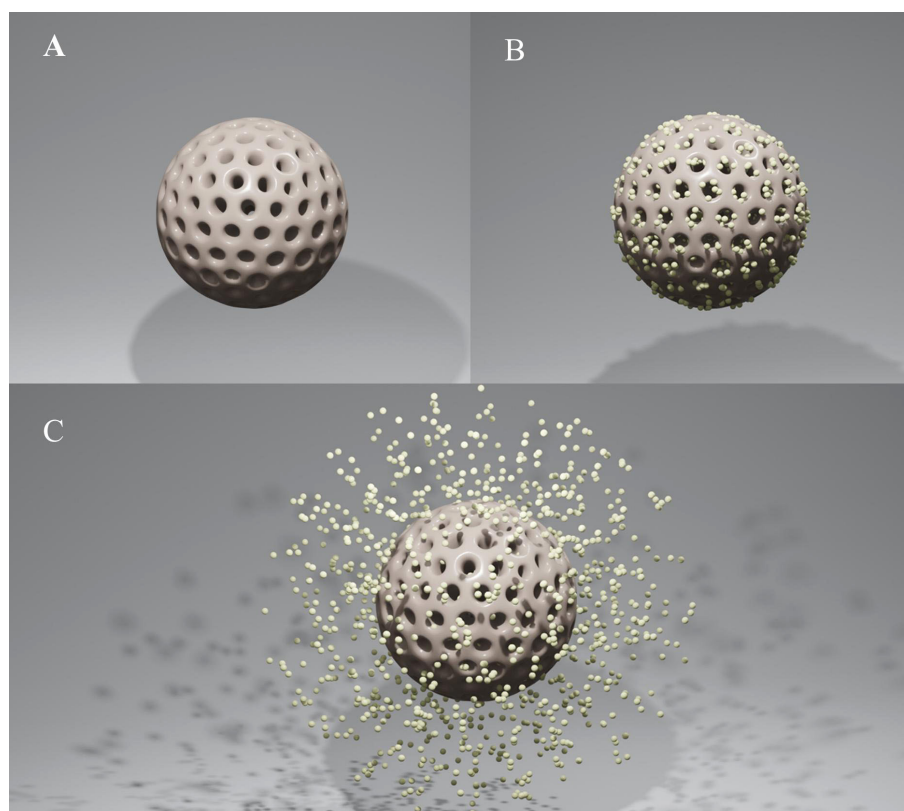
FIGURE 1
(A) Mesoporous silica nanoparticle (MSN). **(B)** MSN as a vehicle for drugs. **(C)** The agent's release of drug-loaded MSNs.

opportunities for medicinal synthesis in combination with other drugs. As a result, drug transfection into specific areas dramatically reduces side effects, and higher drug loading directly enhances therapeutic benefit. MSNs, one of the most promising nanocarriers, also have other exceptional benefits, including easy and affordable production, stability, dissolvability, biocompatibility, and biodegradability. With all of these attributes, MSNs give medications the needed solubility and stability in solution. This delivery system responds to particular micro-circumstances (such as pH, temperature, light, and magnetic and electric fields), which are the foundation of innovative treatment approaches in stomatology (Figure 1C). Targeted delivery also exhibits an effective and safe therapeutic strategy by greatly increasing the drug concentration in the treatment region and reducing the negative effects on adjacent normal tissue. Highly cytocompatible MSNs make it possible to load drugs in the following fields: 1) Combination with different drugs to improve their poor performance and allow responsive drug delivery simultaneously. 2) Provide the shared nanoplatform of drugs to control biofilm and cure infectious diseases synergistically while avoiding drug resistance. 3) Provide multiple medications with a shared nanoplatform to address conditions such as tumors and dental hypersensitivity. 4) MSNs with excellent surface properties and porosity have proven to be attractive bioactive materials for bone regeneration. Targeted delivery and biocompatibility extend the utilizing scope of MSNs. The recent research developments on MSNs and the biological uses of MSNs in stomatology, including antibiofilm, antitumor, reducing dentin sensitivity, and stimulating osteogenesis for bone regeneration, are summarized here.

2 Mesoporous silica nanoparticles as the vehicle for oral drugs

2.1 Mesoporous silica nanoparticle as a vehicle for chlorhexidine

As well as Gram-positive and Gram-negative organisms, chlorhexidine (CHX) is effective against a variety of fungi, facultative anaerobes, and aerobes. CHX adheres to the microorganism's cell wall and causes a leaking of internal components, which is how it works (Fardal and Turnbull, 1986). CHX is regarded as the "gold standard" to assess the antibacterial effect due to its broad-spectrum antibacterial activity, and its application has been thoroughly investigated, for instance, in mouthwash, dentin adhesives, and repair supplies. Previous *in vitro* and *in vivo* research has shown that MSNs have a promising capacity as a drug delivery vehicle for antibacterial agents (Hetrick et al., 2009; Slomberg et al., 2013). In order to enhance the antibiofilm efficiency and lengthen the antibacterial duration, CHX was encapsulated into MSNs. CHX@MSNs were able to penetrate the *Streptococcus mutans* biofilm matrix and closely interact with microbes to improve the antibiofilm efficiency (Li et al., 2016). CHX released from CHX@MSNs inhibited biofilms even after 50 h. Additionally, the bacterial resistance to CHX was overcome by adding additional drugs to MSNs to produce synergistic antibacterial effects (Lu et al., 2017; Lu et al., 2018). Moreover, CHX@MSNs were modified into dentin adhesives to reduce cariogenic bacteria and

impede biofilm permeation because a cariogenic bacteria-created acidic environment might cause pH-sensitive CHX@MSNs to release CHX (De Munck et al., 2009; Akram et al., 2021). According to recent findings, MSNs had great potential in dental restorative materials. CHX@MSNs could carry significant CHX when added to glass ionomer cement or composites, which boosted their antibacterial and antibiofilm activities without sacrificing their mechanical performance (Zhang et al., 2014; Yan et al., 2017). In contrast, directly mixing CHX into composites resulted in a burst release over a short period of time and produced a porous surface that encouraged bacterial adhesion and biofilm formation. Furthermore, MSNs can also serve as a co-delivery platform for simultaneously loading different agents to combat drug resistance. CHX-loaded silver (Ag)-decorated MSNs (Ag-MSNs@CHX) have been shown to exert more effective antibiofilm effects and remarkably reduce the toxicity of CHX in oral epithelial cells (Lu et al., 2017; Lu et al., 2018).

2.2 Mesoporous silica nanoparticle as a vehicle for silver nanoparticles

Ag nanoparticles (AgNPs) are frequently employed in stomatology because they can enter cells through their membranes and cause cell lysis. The electrostatic adsorption between the bacterial cell wall and AgNPs might kill bacteria by preventing the synthesis of proteins and deactivating respiratory enzymes (Santos-Beneit, 2015; Khubchandani et al., 2022). For a wider variety of applications, AgNPs were added to denture materials or orthodontic adhesives (Monteiro et al., 2009). For instance, Ag had been directly mixed into polymethylmethacrylate (PMMA); however, the addition did not confer materials with better mechanical properties and long-lasting antibacterial effects (Mohamed Hamouda, 2012). MSNs protected AgNPs from aggregation, and the controlled drug release lessened the cytotoxicity of AgNPs (Lok et al., 2007; Chen et al., 2016; Jin et al., 2018; Liu et al., 2018). Therefore, they were employed as nanocarriers to load AgNPs (Ag-MSNs) and then incorporated with PMMA, which showed sustained flexural strength and microbial anti-adhesive effects for 14 days (Jo et al., 2017). AgNPs had also worked with remineralization agents to stop dental caries (Carrouel et al., 2020). MSNs coated with bioactive glasses (BAGs) induced dentinal tubule occlusion and remineralization, and the addition of AgNPs would give BAG-coated MSNs antibacterial capabilities. Ag-MSN-based nanomaterials showed considerable promise in the treatment of dentin hypersensitivity and caries prevention, since Ag-BAG@MSN efficiently blocked the dentinal tubule following the acid challenge and inhibited the growth of bacteria (Tian et al., 2014; Jung et al., 2019). MSNs provide Ag with great stability, sustained antibacterial efficacy, and significant safety. The antimicrobial effectiveness of AgNPs is increased, and the utilization range is expanded after being loaded into MSNs.

2.3 Mesoporous silica nanoparticle as a vehicle for quaternary ammonium salts

Through electrostatic interaction, quaternary ammonium salts (QASs) cling to the negatively charged bacterial cell membrane and

kill bacteria in contact by integrating a hydrophobic alkyl tail into the lipid bilayer of the membrane (Zhang et al., 2018). They are frequently used in dental materials including dental adhesives, pit and fissure sealants, and dental implants. However, the contact-killing mechanism will not work if bacteria do not come into direct contact with materials, and the protein linked to the surface of the material will further reduce the killing effectiveness. A way to enhance the antibacterial activity is to exploit the synergistic effect by putting dual drugs on the same nanovehicle. MSNs are frequently employed in drug-loading fields because of their excellent drug-loading capacity and biocompatibility as well as their easily functionalized surface. MSNs decorated by Ag and QAS (Ag/QAS-MSNs) were created to combat head and neck cancers (HNCAs) and follow-up infections simultaneously in light of the antibiofilm and anticancer capability of Ag and QASs (Ito et al., 2009; Meena et al., 2017; Tang and Zheng, 2018; Deshmukh et al., 2019; Ahn and Park, 2020; Eid et al., 2020; Zhang et al., 2022). The findings showed that Ag/QAS-MSNs prevented the formation of bacterial colonies for at least 14 h mostly as a result of the sustained release of Ag+ and QAS from Ag/QAS-MSNs, which directly caused membrane damage and cell death. Comparing Ag/QAS-MSNs to QAS-MSNs, bare AgNPs, and pure QAS, Ag/QAS-MSNs also demonstrated the greatest antibacterial activity in a concentration-dependent manner (Zhang et al., 2022). AgNPs@MSNs treated with quaternary ammonium polyethyleneimine (QPEI), one of the QASs, were able to overcome the electrostatic repulsion between AgNPs and bacteria. Results revealed that compared to Ag@MSNs and QPEI alone, Ag@MSN-QPEI had greater antibacterial activity and a longer bactericidal duration (Niu et al., 2021; Zhou et al., 2021). MSNs have a potential future in the treatment of HNCA with higher antibacterial activity against follow-up infections as vehicles for QASs to co-deliver other drugs.

2.4 Mesoporous silica nanoparticle as a vehicle for curcumin

Curcumin has outstanding antibiofilm, anti-inflammatory, and antitumor activities. It prevents *S. mutans* from adhering to extracellular matrices and tooth surfaces, perturbing membrane integrity and inducing entocyte leakage of *Streptococcus* (Tyagi et al., 2015; Pamukcu et al., 2022). Curcumin was safe enough, and oral treatment did not cause reproductive toxicity in humans even at 500 mg twice daily for 30 days (Soleimani et al., 2018). However, the insolubility in water, limited bioavailability, and instability in the biological environment of curcumin hampered its therapeutic use. Recently, studies had focused on curcumin-loaded MSNs (Cur-MSNs) due to their abilities to overcome the mentioned constraints of curcumin with a high encapsulation efficiency, protecting curcumin from premature leakage and providing a controlled drug release (Ribeiro et al., 2022). Numerous studies had been conducted to demonstrate both their effect on the infections and their use in cancer therapy. Due to the MSNs' capacity to penetrate the matured biofilm matrix, curcumin can destroy the developed biofilms and suppress the development of biofilms with lower required doses and higher cytocompatibility after being repurposed by MSNs (Pamukcu et al., 2022). As the shared nanocarrier, MSNs could combine several

antimicrobial components to increase antimicrobial impact. The compounds that AgNPs decorated and curcumin-charged MSNs were characterized by low hemolytic action and persistent growth-inhibiting impact on *Staphylococcus aureus* and *Escherichia coli* (Song et al., 2020). Furthermore, curcumin reduced the proliferation of tumor cells *via* targeting molecules expressed by cancer-relevant genes and increasing the production of intracellular reactive oxygen species (ROS) (Shanmugam et al., 2015; Hafez Ghoran et al., 2022). MSNs easily enter cells through phagocytosis, and the numerous silanol groups on their surface enable the controllable curcumin release, showing greater potential in reducing tumor cell proliferation (Liu et al., 2018; Zhou et al., 2018). Compared with free curcumin, Cur-MSNs showed higher cytotoxicity in HNCA cells (Sharifi et al., 2022). Additionally, targeted distribution by hyaluronic acid (HA)-modified or -aminated MSNs had improved anticancer efficacy in breast cancer cells and colon cancer cells (Ghosh et al., 2021; Liu et al., 2022). These studies demonstrated that curcumin had a stronger effect on bacteria and tumor after loading into MSNs.

3 The prospective application of mesoporous silica nanoparticles in stomatology

3.1 Dental caries

S. mutans is the predominant etiological pathogen that firmly adheres to tooth surfaces and plays a critical role in generating an acidic environment. This environment ensures the development of biofilms, demineralization of the teeth, and the onset of dental caries. CHX@MSNs that were synthesized by loading CHX in functionalized MSNs showed a long-term and stimuli-responsive release of agents, meaning that the lactic acid produced by *S. mutans* might burst the release of CHX from MSNs (Zhang et al., 2014; Lu et al., 2018). Secondary caries is the primary cause of dental composite repair failure. Dental composites releasing antibacterial agents effectively reduced secondary caries and inhibited cariogenic biofilms, which could extend the service life of composite restorations. Therefore, incorporating CHX@MSNs into experimental resin-based dentin adhesives and dental composite showed potent inhibition of planktonic growth and biofilm formation with excellent bonding strength and least nanoleakage. Compared with directly mixing CHX into composites, composites containing CHX@MSNs largely kept their mechanical properties and smooth surfaces, resulting in the accumulation of very few planktonic bacteria with deformed membranes on the surface of composite resin (Zhang et al., 2014; Akram et al., 2021). Adding zinc (Zn) to dental resin composites has attracted more and more attention, since it has no adverse effects on the esthetic performance of the resins. However, the release of Zn from zinc oxide (ZnO) might lead to the destruction of the ZnO fillers and impair the composition's mechanical properties, and the difficulty in releasing Zn sustainably may have an impact on the composition's long-term antibacterial performance (Wang et al., 2019). The prepared Zn-MSNs effectively address the mentioned problems with improved the mechanical and antibacterial properties of the dental resin composites (Alvarez et al., 2021). In addition, the presence of Zn-MSNs has no detrimental effect on the conversion, shrinkage, curing depth, and biocompatibility of dental resins, indicating the potential of MSNs in dental compositions that transport agents (Bai et al., 2020).

3.2 Dentin hypersensitivity

Dentin hypersensitivity is characterized by rapid acute pain in response to thermal, chemical, and physical stimulation. Dentin exposure from abrasion, acid erosion, and gingival recession results in dentin hypersensitivity. According to the most widely recognized theory—hydrodynamic theory—obturating the exposed dentinal tubules with biomaterials to lessen the flux will be effective in treating dentin hypersensitivity.

Acid resistance is necessary for biomaterials to maintain their stability over time in the face of everyday acid erosion, which may be impacted by the depth of ions deposited in tubules. The biomedical fields have extensively used small and well-dispersed MSNs that were packed with remineralization agents and deeply infiltrated into dentinal tubules without compromising dentin bond strength (Zhang et al., 2018). Nano-hydroxyapatite (nHAp) acted as the Ca^{2+} and PO_4^{3-} reservoir that can facilitate crystal deposition and formation in demineralized portions of teeth. The dentinal tubules were blocked by the nHAp@MSN, which also prevented nHAp from dissolving without impairing the microtensile bond strength (MTBS) (Yu et al., 2016). However, applying remineralization agents alone would not be sufficient to manage the dentin surface, since exposed dentin was more prone to dental cavities. A natural extract derived from green tea called epigallocatechin-3-gallate (EGCG), which has versatile uses as an antibiofilm and anti-inflammatory agent, could be encapsulated into nHAp@MSNs to prevent caries by eradicating *S. mutans* biofilm. EGCG@nHAp@MSN was a multifunctional biomaterial for dentin hypersensitivity and caries by occluding dentinal tubules, reducing biofilm formation, and maintaining favorable acid-resistant stability (Yu et al., 2017). Bioactive glass nanoparticles (BGNs) relieved the discomfort of dentin hypersensitivity by occluding dentinal tubules and soft tissue regeneration (Jung et al., 2019). It was confirmed that the synthetic biocomposite material Ag-BGNs@MSN, which has a greater surface area, successfully induces remineralization, exerts antibacterial capability, and is a useful substance for the treatment of dentin hypersensitivity (Jung et al., 2019). Since tooth flaws frequently accompanied dentin discomfort, resin-based repair was required. Ag-BGNs@MSNs did not inhibit MTBS in *in vitro* research, but additional *in vivo* investigations are still needed to determine whether or not the material's characteristics alter.

3.3 Periodontitis

Dental plaque plays a role in the etiology of periodontitis, which finally results in tooth loss by destroying the tissues supporting the teeth. However, due to the intricate tooth anatomy, mechanical debridement by scaling and root planing (SRP) to remove the subgingival plaque does not entirely eradicate germs, especially in deep pockets (Warinner et al., 2014; Zupancic et al., 2019). The

unique therapeutic approach for periodontitis was made possible by MSNs, which enhanced medication concentration in the targeted tissue for the stimuli-responsive release and made it easier to kill bacteria in periodontal pockets (Hayes et al., 2018; Lin et al., 2020). In earlier research, MSNs were mechanically applied to prevent infections while being loaded with various chemicals, including CHX and antibiotics to eliminate biofilms (RR et al., 2019; AL et al., 2021). The host inflammatory response elicited by the subgingival dental biofilm also needs to be treated for the resultant irreversible destruction of the periodontium. Resveratrol (RSV; 3,5,4'-trihydroxy-trans-stilbene) has strong anti-inflammatory and antimicrobial effects, but its application is severely constrained by the poor water solubility, rapid decomposition, and short serum half-life (Bhattarai et al., 2016). The RSV-grafted MSN drug carrier could successfully extend its bioavailability in the local periodontal region, resulting in sustained pharmacological activity and removing RSV's inherent cytotoxicity (Tan et al., 2022). For RSV's anti-inflammatory effects and the ability to modulate glucose metabolism, MSN-RSV may also be able to alleviate diabetic periodontitis (DP) (El-Makaky and Shalaby, 2020). Diabetes mellitus (DM) impairs bone repair by increasing ROS production, which speeds up periodontal bone loss and makes bone regeneration in DP difficult (Hajishengallis et al., 2012; Mysak et al., 2014; Wang et al., 2023). Recent research used MSN-incorporated poly (D, L-lactide)-block-poly (ethylene glycol)-block-poly (D, L-lactide) (PPP) to achieve stepwise cargo release and emulate the cascade for diabetic periodontal bone regeneration, which can scavenge the overproduced ROS, regulate the diabetic microenvironment, and facilitate osteogenesis (Wang et al., 2023). In conclusion, MSNs offer flexible treatment plans for periodontitis that include elimination of the pathogens, reduction of inflammatory effects, and facilitation of osteogenesis.

3.4 Endodontic treatment failure

Endodontic treatment failure can be caused by a variety of factors, including the persistence of microorganisms, improperly cleaned root canals, and untreated canals (missing canals) (Alghamdi and Shakir, 2020). *Enterococcus faecalis* is the most common isolate from endodontic infections and is strongly linked to failed endodontic treatments because of its capacity to survive in extremely challenging conditions with limited nutrient availability and a high alkaline pH that can reach 11.5 (Stuart et al., 2006; Ozbek et al., 2009). Additionally, the mono-infection of *E. faecalis* in treated canals without synergistic assistance from other bacteria results in significant resistance to antimicrobial treatments. Incomplete removal of *E. faecalis* from the root canal by sodium hypochlorite (NaClO) and CHX highlights the need for more sophisticated strategies for thorough disinfection in endodontic treatments (Vianna et al., 2004; Eddy et al., 2005; Estrela et al., 2008). Sonodynamic therapy (SDT) relies on ultrasound (US) to activate the sonosensitizers and generate the ROS to obliterate bacterial infection (Serpe and Giuntini, 2015; Xu et al., 2017). MSNs are synthesized as the platform for conjugation with sonosensitizer protoporphyrin IX (PpIX) (MSNs@P) and Fe ions (MSNs@P-Fe) to

initiate a Fenton action in order to destroy bacteria without having to worry about resistance (Pang et al., 2019; Guo et al., 2021; Wang et al., 2021). Compared with the commonly used NaClO irrigant, this new strategy (MSNs@P-Fe + 0.01% H_2O_2 + US) is highly efficient in eliminating *E. faecalis* infection by exploiting low-concentration H_2O_2 to generate highly toxic ROS without inducing notable cell toxicity. This technique with excellent tissue penetrability is noninvasive and site-confined, showing the MSN platform's potential in the elimination of deeply ingrained infection. In addition, MSNs are selected as scaffolds in combination with hydrogel for the proliferation of human dental pulp stem cells (HDPSCs), and this new biopolymer scaffold improves the immigration and regeneration of HDPSCs to repair pulpitis (Wang et al., 2022).

3.5 Maxillofacial space infection

Fascial space infections are the common sequelae of odontogenic infections including periapical infection and pericoronitis (Singh et al., 2021). Patients with superficial dental infections typically experience localized pain and cellulitis, while those with deep infections or abscesses may experience swallowing and breathing issues. *S. aureus* is the dominating pathogenic bacterium of mouth floor cellulitis, a multispace infection that affects the sublingual, submental, and submandibular spaces with potentially life-threatening effects (Ogle, 2017). Selenium (Se) nanoparticles (SeNPs) are considered to be healthier and less toxic to healthy cells and have antibacterial effects. Incorporating Se into MSNs exhibits better antibacterial activity against *S. aureus*, and dispersibility is improved by preventing SeNP agglomeration (Chen et al., 2020). Methicillin-resistant *Staphylococcus aureus* (MRSA) biofilms pose a unique challenge in space infections due to the tolerance to various antibiotics. Proteins and environmental DNA (eDNA) make up the majority of the MRSA biofilm matrix, which makes it difficult for antibiotics to reach the deepest parts of the biofilm and precisely target cells (McCarthy et al., 2015). Meanwhile, immunosuppression increased the incidence of MRSA infection in patients with head and neck squamous cell carcinoma (HNSCC) following chemotherapy. Antibiotics delivered by nanoparticle-based carriers penetrate the biofilm better. In order to eliminate MRSA biofilms and target *S. aureus*, enzyme-functionalized MSNs are created. Results of cell viability and crystal violet staining demonstrate that the enzyme's efficiency against *S. mutans* was further enhanced after immobilizing into MSNs (Devlin et al., 2021). Sortase A (SrtA), a membrane-bound cysteine transpeptidase, binds virulence-associated proteins to the bacterial cell wall (Nitulescu et al., 2017). Naturally derived compounds with poor water solubility are classified as sortase A inhibitors (SrtAIs), including quercetin (QC) and berberine chloride (BR). With the help of MSNs, SrtAI's solubility can be increased, opening up new therapy options for superbugs with less hazardous side effects (Alharthi et al., 2022). When drugs are combined with MSNs, the antibacterial effect may be enhanced, the drug's release time may be prolonged, the inherent cytotoxicity may be eliminated, and bacterial resistance may be addressed with great physiochemical performance.

3.6 Oral squamous cell carcinoma

Oral squamous cell carcinoma (OSCC) has great probability of metastasis that may lead to poor prognosis or even death. The main medications used in OSCC treatment include paclitaxel (PTX), 5-fluorouracil (5-FU), methotrexate, and cisplatin (Molin and Fayette, 2011). With a lower pH and higher temperature than normal tissue, the tumor has different properties. MSNs are the prospective carriers to treat malignancies because of their perceptive response to pH and temperature (Lu et al., 2010; Meng et al., 2010). It is possible to destroy tumor cells by inhibiting the supply of glucose and causing a redox reaction because tumor cells have higher glucose requirements and endogenous reducing agents than normal cells (Chen et al., 2020). The combination of starving therapy with MSNs is prospective to increase the effectiveness in treating tumors. Glucose oxidase (GOx) and PTX can interrupt the intracellular energy supply and elevate the endogenous H_2O_2 level of tumor cells, exhibiting an amplified effect. Therefore, GOx and PTX were co-delivered *via* the MSNs as a nanoplatform to induce better therapeutic effects against cancer (Du et al., 2019). In addition, 5-FU, which is frequently used to treat OSCC, has hematologic and digestive side effects, including anemia, thrombocytopenia, and leukopenia (Bui et al., 2020). This nanoplatform of MSNs could preferentially accumulate 5-FU in tumors to suppress tumor growth and avoid side effects (Lee et al., 2010; Lu et al., 2010). The outer membrane vesicle (OMV)-MSN-5-FU overcomes the mentioned drawbacks by reducing the cumulative drug release and prolongs the targeted action time to inhibit tumor proliferation and metastasis (Huang et al., 2022). Consequently, MSNs can circumvent the challenges associated with administering anticancer medications by delivering them to specific tissues to improve biocompatibility.

3.7 Bone regeneration in the oromaxillofacial region

Periodontitis, maxillofacial infections, and tumors cause varying degrees of bone abnormalities. The main treatments for jaw abnormalities mainly include autologous bone graft, allogeneic bone graft, and artificial substitute implantation. Opening up the second surgical area is invasive, although clinical vascularized autologous bone graft is mature in repairing maxillofacial defects. Artificial replacements with a microporous structure, a particular hardness, and the ability to induce cell differentiation can be used to heal bone abnormalities. MSNs conveying biological cues in a targeted and regulated manner can improve the behavior of osteoclasts and the mechanical qualities of the biomaterial by attaching MSNs to the titanium substrate's surface (Rosenholm et al., 2016). MSNs are modified with a bone-forming peptide (BFP) to provide a slow-release mechanism for delivering osteogenic factors. Experiments demonstrate that BFP-laden MSNs (p-MSNs) with a sustained peptide release rate and better bioactivity could promote the osteogenic differentiation of mesenchymal stem cells (MSCs) and the spread of human osteoblast-like MG-63 for bone repair and regeneration (Luo et al., 2015). The MSNs were used to transmit genes and promote osteogenic differentiation. Bone morphogenetic protein-2 (BMP-2) plasmid DNA (pDNA) was combined with

aminated MSNs (MSN–NH$_2$), and the BMP-2 protein was produced by transfected MSCs, which demonstrated the potential of MSNs as a gene delivery system in bone regeneration (Kim et al., 2013). The *in vitro* cell cytotoxicity tests indicated that BMP-2 peptide-functionalized MSNs (MSNs-pep) is highly cytocompatible, and the osteoblast differentiation and bone regeneration of MSCs could be further enhanced after dexamethasone (DEX) was incorporated (Zhou et al., 2015). These systems also offer a nanoplatform on which to load various medications for efficient osteoblast development.

4 Conclusions and perspectives

MSNs offer interesting characteristics that can be used in combination with one another to enhance stomatology drug delivery. They also have significant potential for antibiofilm, tumor therapy, and combined therapy. Recent studies demonstrate that MSNs can improve the dissolution rate and bioavailability of the water-insoluble drugs by entrapping them in the mesopores and dispersing them with a large surface area. Moreover, MSNs functioning as nanoplatforms improve the antimicrobial effectiveness through combining various antimicrobial components. This co-delivery nanoplatform with several stimuli-responsive confers final compounds the abilities of antibacteria, antitumor, and bone regeneration of maxillofacial defects. The drug released from MSNs to targeted locations lowers the dosage with a longer half-life and improves the therapeutic effect (Esfahani et al., 2022). To help them evolve further, some important difficulties, such as the potential cytotoxicity and MSN excretion, must be resolved. Firstly, by raising the quantity of ROS, MSNs cause oxidative stress and apoptosis. Secondly, the therapeutic action will be limited by the residuals in the MSNs because only a portion of the medications will be released. Thirdly, due to the striking differences in the multistep MSN synthesis process, scaling up synthesis will face significant difficulties. The long-term therapeutic effect of MSN-based systems *in vivo* should be rigorously and extensively proven before the clinical translation of MSNs. Given the satisfactory resolution of these issues, MSN-based formulations may achieve exciting breakthroughs in the treatment of a variety of significant diseases and disorders.

Author contributions

All authors contributed to generate the ideas presented in this review. LF wrote the original draft and all the co-authors reviewed and complemented the text. All authors contributed to the article and approved the submitted version.

Funding

Project (Science and Technology Research) Project 212102310595 (S.W) and 222102310407 (FL).

Conflict of interest

The authors declare that the research was conducted in the absence of any commercial or financial relationships that could be construed as a potential conflict of interest.

Publisher's note

All claims expressed in this article are solely those of the authors and do not necessarily represent those of their affiliated organizations, or those of the publisher, the editors and the reviewers. Any product that may be evaluated in this article, or claim that may be made by its manufacturer, is not guaranteed or endorsed by the publisher.

References

Ahn, E. Y., and Park, Y. (2020). Anticancer prospects of silver nanoparticles green-synthesized by plant extracts. *Mater Sci. Eng. C. Mater. Biol. Appl.* 116, 111253. doi: 10.1016/j.msec.2020.111253

Akram, Z., Daood, U., Aati, S., Ngo, H., and Fawzy, A. S. (2021). Formulation of pH-sensitive chlorhexidine-loaded/mesoporous silica nanoparticles modified experimental dentin adhesive. *Mater Sci. Eng. C. Mater. Biol. Appl.* 122, 111894. doi: 10.1016/j.msec.2021.111894

AL, S. S., BinShabaib, M., Saad AlMasoud, N., Shawky, H. A., Aabed, K. F., Alomar, T. S., et al. (2021). Myrrh mixed with silver nanoparticles demonstrates superior antimicrobial activity against porphyromonas gingivalis compared to myrrh and silver nanoparticles alone. *Saudi Dent. J.* 33 (8), 890–896. doi: 10.1016/j.sdentj.2021.09.009

Alghamdi, F., and Shakir, M. (2020). The influence of enterococcus faecalis as a dental root canal pathogen on endodontic treatment: A systematic review. *Cureus* 12 (3), e7257. doi: 10.7759/cureus.7257

Alharthi, S., Ziora, Z. M., Janjua, T., Popat, A., and Moyle, P. M. (2022). Formulation and biological evaluation of mesoporous silica nanoparticles loaded with combinations of sortase a inhibitors and antimicrobial peptides. *Pharmaceutics* 14 (5), 986. doi: 10.3390/pharmaceutics14050986

Alvarez, E., Estevez, M., Jimenez-Jimenez, C., Colilla, M., Izquierdo-Barba, I., Gonzalez, B., et al. (2021). A versatile multicomponent mesoporous silica nanosystem with dual antimicrobial and osteogenic effects. *Acta Biomater.* 136, 570–581. doi: 10.1016/j.actbio.2021.09.027

Bai, X., Lin, C., Wang, Y., Ma, J., Wang, X., Yao, X., et al. (2020). Preparation of zn doped mesoporous silica nanoparticles (Zn-MSNs) for the improvement of mechanical and antibacterial properties of dental resin composites. *Dent. Mater.* 36 (6), 794–807. doi: 10.1016/j.dental.2020.03.026

Bhattarai, G., Poudel, S. B., Kook, S. H., and Lee, J. C. (2016). Resveratrol prevents alveolar bone loss in an experimental rat model of periodontitis. *Acta Biomater.* 29, 398–408. doi: 10.1016/j.actbio.2015.10.031

Bui, A. D., Grob, S. R., and Tao, J. P. (2020). 5-fluorouracil management of oculofacial scars: A systematic literature review. *Ophthalmic Plast. Reconstr. Surg.* 36 (3), 222–230. doi: 10.1097/IOP.0000000000001532

Carrouel, F., Viennot, S., Ottolenghi, L., Gaillard, C., and Bourgeois, D. (2020). Nanoparticles as anti-microbial, anti-inflammatory, and remineralizing agents in oral care cosmetics: A review of the current situation. *Nanomaterials (Basel)* 10 (1), 140. doi: 10.3390/nano10010140

Chen, M., Hu, J., Wang, L., Li, Y., Zhu, C., Chen, C., et al. (2020). Targeted and redox-responsive drug delivery systems based on carbonic anhydrase IX-decorated mesoporous silica nanoparticles for cancer therapy. *Sci. Rep.* 10 (1), 14447. doi: 10.1038/s41598-020-71071-1

Chen, J., Wei, Y., Yang, X., Ni, S., Hong, F., and Ni, S. (2020). Construction of selenium-embedded mesoporous silica with improved antibacterial activity. *Colloids Surf B. Biointerfaces* 190, 110910. doi: 10.1016/j.colsurfb.2020.110910

Chen, C. C., Wu, H. H., Huang, H. Y., Liu, C. W., and Chen, Y. N. (2016). Synthesis of high valence silver-loaded mesoporous silica with strong antibacterial properties. *Int. J. Environ. Res. Public Health* 13 (1), 99. doi: 10.3390/ijerph13010099

De Munck, J., Van den Steen, P. E., Mine, A., Van Landuyt, K. L., Poitevin, A., Opdenakker, G., et al. (2009). Inhibition of enzymatic degradation of adhesive-dentin interfaces. *J. Dent. Res.* 88 (12), 1101–1106. doi: 10.1177/0022034509346952

Deshmukh, S. P., Patil, S. M., Mullani, S. B., and Delekar, S. D. (2019). Silver nanoparticles as an effective disinfectant: A review. *Mater. Sci. Eng. C. Mater. Biol. Appl.* 97, 954–965. doi: 10.1016/j.msec.2018.12.102

Devlin, H., Fulaz, S., Hiebner, D. W., O'Gara, J. P., and Casey, E. (2021). Enzyme-functionalized mesoporous silica nanoparticles to target staphylococcus aureus and disperse biofilms. *Int. J. Nanomedicine* 16, 1929–1942. doi: 10.2147/IJN.S293190

Du, X., Zhang, T., Ma, G., Gu, X., Wang, G., and Li, J. (2019). Glucose-responsive mesoporous silica nanoparticles to generation of hydrogen peroxide for synergistic cancer starvation and chemistry therapy. *Int. J. Nanomedicine* 14, 2233–2251. doi: 10.2147/IJN.S195900

Eddy, R. S., Joyce, A. P., Roberts, S., Buxton, T. B., and Liewehr, F. (2005). An *in vitro* evaluation of the antibacterial efficacy of chlorine dioxide on e. faecalis in bovine incisors. *J. Endod.* 31 (9), 672–675. doi: 10.1097/01.don.0000155223.87616.02

Eid, A. M., Fouda, A., Niedbala, G., Hassan, S. E., Salem, S. S., Abdo, A. M., et al. (2020). Endophytic streptomyces laurentii mediated green synthesis of Ag-NPs with antibacterial and anticancer properties for developing functional textile fabric properties. *Antibiotics (Basel)* 9 (10), 641. doi: 10.3390/antibiotics9100641

El-Makaky, Y., and Shalaby, H. K. (2020). The effects of non-surgical periodontal therapy on glycemic control in diabetic patients: A randomized controlled trial. *Oral. Dis.* 26 (4), 822–829. doi: 10.1111/odi.13256

Esfahani, M. K. M., Alavi, S. E., Cabot, P. J., Islam, N., and Izake, E. L. (2022). Application of mesoporous silica nanoparticles in cancer therapy and delivery of repurposed anthelmintics for cancer therapy. *Pharmaceutics* 14 (8), 1579. doi: 10.3390/pharmaceutics14081579

Estrela, C., Silva, J. A., de Alencar, A. H., Leles, C. R., and Decurcio, D. A. (2008). Efficacy of sodium hypochlorite and chlorhexidine against enterococcus faecalis–a systematic review. *J. Appl. Oral. Sci.* 16 (6), 364–368. doi: 10.1590/S1678-77572008000600002

Fardal, O., and Turnbull, R. S. (1986). A review of the literature on use of chlorhexidine in dentistry. *J. Am. Dent. Assoc.* 112 (6), 863–869. doi: 10.14219/jada.archive.1986.0118

Ghosh, S., Dutta, S., Sarkar, A., Kundu, M., and Sil, P. C. (2021). Targeted delivery of curcumin in breast cancer cells *via* hyaluronic acid modified mesoporous silica nanoparticle to enhance anticancer efficiency. *Colloids Surf B. Biointerfaces* 197, 111404. doi: 10.1016/j.colsurfb.2020.111404

Guo, J., Xu, Y., Liu, M., Yu, J., Yang, H., Lei, W., et al. (2021). An MSN-based synergistic nanoplatform for root canal biofilm eradication *via* fenton-enhanced sonodynamic therapy. *J. Mater Chem. B* 9 (37), 7686–7697. doi: 10.1039/D1TB01031J

Hafez Ghoran, S., Calcaterra, A., Abbasi, M., Taktaz, F., Nieselt, K., and Babaei, E. (2022). Curcumin-based nanoformulations: A promising adjuvant towards cancer treatment. *Molecules* 27 (16), 5236. doi: 10.3390/molecules27165236

Hajishengallis, G., Darveau, R. P., and Curtis, M. A. (2012). The keystone-pathogen hypothesis. *Nat. Rev. Microbiol.* 10 (10), 717–725. doi: 10.1038/nrmicro2873

Hayes, R. B., Ahn, J., Fan, X., Peters, B. A., Ma, Y., Yang, L., et al. (2018). Association of oral microbiome with risk for incident head and neck squamous cell cancer. *JAMA Oncol.* 4 (3), 358–365. doi: 10.1001/jamaoncol.2017.4777

Hetrick, E. M., Shin, J. H., Paul, H. S., and Schoenfisch, M. H. (2009). Anti-biofilm efficacy of nitric oxide-releasing silica nanoparticles. *Biomaterials* 30 (14), 2782–2789. doi: 10.1016/j.biomaterials.2009.01.052

Huang, J., Wu, Z., and Xu, J. (2022). Effects of biofilm nano-composite drugs OMVs-MSN-5-FU on cervical lymph node metastases from oral squamous cell carcinoma. *Front. Oncol.* 12, 881910. doi: 10.3389/fonc.2022.881910

Ito, E., Yip, K. W., Katz, D., Fonseca, S. B., Hedley, D. W., Chow, S., et al. (2009). Potential use of cetrimonium bromide as an apoptosis-promoting anticancer agent for head and neck cancer. *Mol. Pharmacol.* 76 (5), 969–983. doi: 10.1124/mol.109.055277

Jin, C., Liu, X., Tan, L., Cui, Z., Yang, X., Zheng, Y., et al. (2018). Ag/AgBr-loaded mesoporous silica for rapid sterilization and promotion of wound healing. *Biomater Sci.* 6 (7), 1735–1744. doi: 10.1039/C8BM00353J

Jo, J. K., El-Fiqi, A., Lee, J. H., Kim, D. A., Kim, H. W., and Lee, H. H. (2017). Rechargeable microbial anti-adhesive polymethyl methacrylate incorporating silver sulfadiazine-loaded mesoporous silica nanocarriers. *Dent. Mater.* 33 (10), e361–e372. doi: 10.1016/j.dental.2017.07.009

Jung, J. H., Kim, D. H., Yoo, K. H., Yoon, S. Y., Kim, Y., Bae, M. K., et al. (2019). Dentin sealing and antibacterial effects of silver-doped bioactive glass/mesoporous silica nanocomposite: an *in vitro* study. *Clin. Oral. Investig.* 23 (1), 253–266. doi: 10.1007/s00784-018-2432-z

Jung, J. H., Park, S. B., Yoo, K. H., Yoon, S. Y., Bae, M. K., Lee, D. J., et al. (2019). Effect of different sizes of bioactive glass-coated mesoporous silica nanoparticles on dentinal tubule occlusion and mineralization. *Clin. Oral. Investig.* 23 (5), 2129–2141. doi: 10.1007/s00784-018-2658-9

Khubchandani, M., Thosar, N. R., Dangore-Khasbage, S., and Srivastava, R. (2022). Applications of silver nanoparticles in pediatric dentistry: An overview. *Cureus* 14 (7), e26956. doi: 10.7759/cureus.26956

Kim, T. H., Kim, M., Eltohamy, M., Yun, Y. R., Jang, J. H., and Kim, H. W. (2013). Efficacy of mesoporous silica nanoparticles in delivering BMP-2 plasmid DNA for *in vitro* osteogenic stimulation of mesenchymal stem cells. *J. BioMed. Mater. Res. A* 101 (6), 1651–1660. doi: 10.1002/jbm.a.34466

Lee, C. H., Cheng, S. H., Huang, I. P., Souris, J. S., Yang, C. S., Mou, C. Y., et al. (2010). Intracellular pH-responsive mesoporous silica nanoparticles for the controlled release of anticancer chemotherapeutics. *Angew. Chem. Int. Ed. Engl.* 49 (44), 8214–8219. doi: 10.1002/anie.201002639

Lin, J., He, Z., Liu, F., Feng, J., Huang, C., Sun, X., et al. (2020). Hybrid hydrogels for synergistic periodontal antibacterial treatment with sustained drug release and NIR-responsive photothermal effect. *Int. J. Nanomedicine* 15, 5377–5387. doi: 10.2147/IJN.S248538

Liu, C., Jiang, F., Xing, Z., Fan, L., Li, Y., Wang, S., et al. (2022). Efficient delivery of curcumin by alginate oligosaccharide coated aminated mesoporous silica nanoparticles and in vitro anticancer activity against colon cancer cells. *Pharmaceutics* 14 (6), 1166. doi: 10.3390/pharmaceutics14061166

Liu, R., Wang, X., Ye, J., Xue, X., Zhang, F., Zhang, H., et al. (2018). Enhanced antibacterial activity of silver-decorated sandwich-like mesoporous silica/reduced graphene oxide nanosheets through photothermal effect. *Nanotechnology* 29 (10), 105704. doi: 10.1088/1361-6528/aaa624

Liu, W., Wang, F., Zhu, Y., Li, X., Liu, X., Pang, J., et al. (2018). Galactosylated chitosan-functionalized mesoporous silica nanoparticle loading by calcium leucovorin for colon cancer cell-targeted drug delivery. *Molecules* 23 (12), 3082. doi: 10.3390/molecules23123082

Li, X., Wong, C. H., Ng, T. W., Zhang, C. F., Leung, K. C., and Jin, L. (2016). The spherical nanoparticle-encapsulated chlorhexidine enhances anti-biofilm efficiency through an effective releasing mode and close microbial interactions. *Int. J. Nanomedicine* 11, 2471–2480.

Lok, C. N., Ho, C. M., Chen, R., He, Q. Y., Yu, W. Y., Sun, H., et al. (2007). Silver nanoparticles: partial oxidation and antibacterial activities. *J. Biol. Inorg Chem.* 12 (4), 527–534. doi: 10.1007/s00775-007-0208-z

Lu, M. M., Ge, Y., Qiu, J., Shao, D., Zhang, Y., Bai, J., et al. (2018). Redox/pH dual-controlled release of chlorhexidine and silver ions from biodegradable mesoporous silica nanoparticles against oral biofilms. *Int. J. Nanomedicine* 13, 7697–7709. doi: 10.2147/IJN.S181168

Lu, J., Liong, M., Li, Z., Zink, J. I., and Tamanoi, F. (2010). Biocompatibility, biodistribution, and drug-delivery efficiency of mesoporous silica nanoparticles for cancer therapy in animals. *Small* 6 (16), 1794–1805. doi: 10.1002/smll.201000538

Luo, Z., Deng, Y., Zhang, R., Wang, M., Bai, Y., Zhao, Q., et al. (2015). Peptide-laden mesoporous silica nanoparticles with promoted bioactivity and osteo-differentiation ability for bone tissue engineering. *Colloids Surf B. Biointerfaces* 131, 73–82. doi: 10.1016/j.colsurfb.2015.04.043

Lu, M. M., Wang, Q. J., Chang, Z. M., Wang, Z., Zheng, X., Shao, D., et al. (2017). Synergistic bactericidal activity of chlorhexidine-loaded, silver-decorated mesoporous silica nanoparticles. *Int. J. Nanomedicine* 12, 3577–3589. doi: 10.2147/IJN.S133846

McCarthy, H., Rudkin, J. K., Black, N. S., Gallagher, L., O'Neill, E., and O'Gara, J. P. (2015). Methicillin resistance and the biofilm phenotype in staphylococcus aureus. *Front. Cell Infect. Microbiol.* 5, 1. doi: 10.3389/fcimb.2015.00001

Meena, R., Kumar, S., Kumar, R., Gaharwar, U. S., and Rajamani, P. (2017). PLGA-CTAB curcumin nanoparticles: Fabrication, characterization and molecular basis of anticancer activity in triple negative breast cancer cell lines (MDA-MB-231 cells). *BioMed. Pharmacother.* 94, 944–954. doi: 10.1016/j.biopha.2017.07.151

Meng, H., Xue, M., Xia, T., Zhao, Y. L., Tamanoi, F., Stoddart, J. F., et al. (2010). Autonomous *in vitro* anticancer drug release from mesoporous silica nanoparticles by pH-sensitive nanovalves. *J. Am. Chem. Soc.* 132 (36), 12690–12697. doi: 10.1021/ja104501a

Mohamed Hamouda, I. (2012). Current perspectives of nanoparticles in medical and dental biomaterials. *J. BioMed. Res.* 26 (3), 143–151. doi: 10.7555/JBR.26.20120027

Molin, Y., and Fayette, J. (2011). Current chemotherapies for recurrent/metastatic head and neck cancer. *Anticancer Drugs* 22 (7), 621–625. doi: 10.1097/CAD.0b013e3283421f7c

Monteiro, D. R., Gorup, L. F., Takamiya, A. S., Ruvollo-Filho, A. C., de Camargo, E. R., and Barbosa, D. B. (2009). The growing importance of materials that prevent microbial adhesion: antimicrobial effect of medical devices containing silver. *Int. J. Antimicrob. Agents* 34 (2), 103–110. doi: 10.1016/j.ijantimicag.2009.01.017

Mysak, J., Podzimek, S., Sommerova, P., Lyuya-Mi, Y., Bartova, J., Janatova, T., et al. (2014). Porphyromonas gingivalis: major periodontopathic pathogen overview. *J. Immunol. Res.* 2014, 476068. doi: 10.1155/2014/476068

Nitulescu, G., Nicorescu, I. M., Olaru, O. T., Ungurianu, A., Mihai, D. P., Zanfirescu, A., et al. (2017). Molecular docking and screening studies of new natural sortase a inhibitors. *Int. J. Mol. Sci.* 18 (10), 2217. doi: 10.3390/ijms18102217

Niu, J., Tang, G., Tang, J., Yang, J., Zhou, Z., Gao, Y., et al. (2021). Functionalized silver nanocapsules with improved antibacterial activity using silica shells modified with quaternary ammonium polyethyleneimine as a bacterial cell-targeting agent. *J. Agric. Food Chem.* 69 (23), 6485–6494. doi: 10.1021/acs.jafc.1c01930

Ogle, O. E. (2017). Odontogenic infections. *Dent. Clin. North Am.* 61 (2), 235–252. doi: 10.1016/j.cden.2016.11.004

Ozbek, S. M., Ozbek, A., and Erdorgan, A. S. (2009). Analysis of enterococcus faecalis in samples from Turkish patients with primary endodontic infections and failed endodontic treatment by real-time PCR SYBR green method. *J. Appl. Oral. Sci.* 17 (5), 370–374. doi: 10.1590/S1678-77572009000500004

Pamukcu, A., Erdogan, N., and Sen Karaman, D. (2022). Polyethylenimine-grafted mesoporous silica nanocarriers markedly enhance the bactericidal effect of curcumin against staphylococcus aureus biofilm. *J. BioMed. Mater. Res. B .Appl. Biomater.* 110 (11), 2506–2520. doi: 10.1002/jbm.b.35108

Pang, X., Xiao, Q., Cheng, Y., Ren, E., Lian, L., Zhang, Y., et al. (2019). Bacteria-responsive nanoliposomes as smart sonotheranostics for multidrug resistant bacterial infections. *ACS Nano* 13 (2), 2427–2438. doi: 10.1021/acsnano.8b09336

Ribeiro, T. C., Sabio, R. M., Luiz, M. T., de Souza, L. C., Fonseca-Santos, B., Cides da Silva, L. C., et al. (2022). Curcumin-loaded mesoporous silica nanoparticles dispersed in thermo-responsive hydrogel as potential Alzheimer disease therapy. *Pharmaceutics* 14 (9), 1976. doi: 10.3390/pharmaceutics14091976

Rosenholm, J. M., Zhang, J., Linden, M., and Sahlgren, C. (2016). Mesoporous silica nanoparticles in tissue engineering–a perspective. *Nanomedicine (Lond)* 11 (4), 391–402. doi: 10.2217/nnm.15.212

RR, H., Dhamecha, D., Jagwani, S., Rao, M., Jadhav, K., Shaikh, S., et al. (2019). Local drug delivery systems in the management of periodontitis: A scientific review. *J. Control Release* 307, 393–409. doi: 10.1016/j.jconrel.2019.06.038

Santos-Beneit, F. (2015). The pho regulon: a huge regulatory network in bacteria. *Front. Microbiol.* 6, 402. doi: 10.3389/fmicb.2015.00402

Serpe, L., and Giuntini, F. (2015). Sonodynamic antimicrobial chemotherapy: First steps towards a sound approach for microbe inactivation. *J. Photochem. Photobiol. B* 150, 44–49. doi: 10.1016/j.jphotobiol.2015.05.012

Shanmugam, M. K., Rane, G., Kanchi, M. M., Arfuso, F., Chinnathambi, A., Zayed, M. E., et al. (2015). The multifaceted role of curcumin in cancer prevention and treatment. *Molecules* 20 (2), 2728–2769. doi: 10.3390/molecules20022728

Sharifi, S., Dalir Abdolahinia, E., Ghavimi, M. A., Dizaj, S. M., Aschner, M., Saso, L., et al. (2022). Effect of curcumin-loaded mesoporous silica nanoparticles on the head and neck cancer cell line, HN5. *Curr. Issues Mol. Biol.* 44 (11), 5247–5259. doi: 10.3390/cimb44110357

Singh, A., Smriti, K., Nayak, S., and Gadicherla, S. (2021). MRSA infection of masticatory spaces in a paediatric patient. *BMJ Case Rep.* 14 (2), e236766. doi: 10.1136/bcr-2020-236766

Slomberg, D. L., Lu, Y., Broadnax, A. D., Hunter, R. A., Carpenter, A. W., and Schoenfisch, M. H. (2013). Role of size and shape on biofilm eradication for nitric oxide-releasing silica nanoparticles. *ACS Appl. Mater. Interfaces* 5 (19), 9322–9329. doi: 10.1021/am402618w

Soleimani, V., Sahebkar, A., and Hosseinzadeh, H. (2018). Turmeric (Curcuma longa) and its major constituent (curcumin) as nontoxic and safe substances: Review. *Phytother. Res.* 32 (6), 985–995. doi: 10.1002/ptr.6054

Song, Y., Cai, L., Tian, Z., Wu, Y., and Chen, J. (2020). Phytochemical curcumin-coformulated, silver-decorated melanin-like Polydopamine/Mesoporous silica composites with improved antibacterial and chemotherapeutic effects against drug-resistant cancer cells. *ACS Omega* 5 (25), 15083–15094. doi: 10.1021/acsomega.0c00912

Stuart, C. H., Schwartz, S. A., Beeson, T. J., and Owatz, C. B. (2006). Enterococcus faecalis: its role in root canal treatment failure and current concepts in retreatment. *J. Endod.* 32 (2), 93–98. doi: 10.1016/j.joen.2005.10.049

Tan, Y., Feng, J., Xiao, Y., and Bao, C. (2022). Grafting resveratrol onto mesoporous silica nanoparticles towards efficient sustainable immunoregulation and insulin resistance alleviation for diabetic periodontitis therapy. *J. Mater. Chem. B* 10 (25), 4840–4855. doi: 10.1039/D2TB00484D

Tang, S., and Zheng, J. (2018). Antibacterial activity of silver nanoparticles: Structural effects. *Adv. Healthc. Mater.* 7 (13), e1701503. doi: 10.1002/adhm.201701503

Tian, L., Peng, C., Shi, Y., Guo, X., Zhong, B., Qi, J., et al. (2014). Effect of mesoporous silica nanoparticles on dentinal tubule occlusion: an *in vitro* study using SEM and image analysis. *Dent. Mater. J.* 33 (1), 125–132. doi: 10.4012/dmj.2013-215

Tyagi, P., Singh, M., Kumari, H., Kumari, A., and Mukhopadhyay, K. (2015). Bactericidal activity of curcumin I is associated with damaging of bacterial membrane. *PLos One* 10 (3), e0121313. doi: 10.1371/journal.pone.0121313

Vianna, M. E., Gomes, B. P., Berber, V. B., Zaia, A. A., Ferraz, C. C., and de Souza-Filho, F. J. (2004). *In vitro* evaluation of the antimicrobial activity of chlorhexidine and sodium hypochlorite. *Oral. Surg. Oral. Med. Oral. Pathol. Oral. Radiol. Endod.* 97 (1), 79–84. doi: 10.1016/S1079-2104(03)00360-3

Wang, H., Chang, X., Ma, Q., Sun, B., Li, H., Zhou, J., et al. (2023). Bioinspired drug-delivery system emulating the natural bone healing cascade for diabetic periodontal bone regeneration. *Bioact. Mater.* 21, 324–339. doi: 10.1016/j.bioactmat.2022.08.029

Wang, D., Cheng, D. B., Ji, L., Niu, L. J., Zhang, X. H., Cong, Y., et al. (2021). Precise magnetic resonance imaging-guided sonodynamic therapy for drug-resistant bacterial deep infection. *Biomaterials* 264, 120386. doi: 10.1016/j.biomaterials.2020.120386

Wang, Y., Hua, H., Li, W., Wang, R., Jiang, X., and Zhu, M. (2019). Strong antibacterial dental resin composites containing cellulose nanocrystal/zinc oxide nanohybrids. *J. Dent.* 80, 23–29. doi: 10.1016/j.jdent.2018.11.002

Wang, W., Wang, X., Li, L., and Liu, Y. (2022). Anti-inflammatory and repairing effects of mesoporous silica-loaded metronidazole composite hydrogel on human dental pulp cells. *J. Healthc. Eng.* 2022, 6774075. doi: 10.1155/2022/6774075

Warinner, C., Rodrigues, J. F., Vyas, R., Trachsel, C., Shved, N., Grossmann, J., et al. (2014). Pathogens and host immunity in the ancient human oral cavity. *Nat. Genet.* 46 (4), 336–344. doi: 10.1038/ng.2906

Xu, F., Hu, M., Liu, C., and Choi, S. K. (2017). Yolk-structured multifunctional up-conversion nanoparticles for synergistic photodynamic-sonodynamic antibacterial resistance therapy. *Biomater. Sci.* 5 (4), 678–685. doi: 10.1039/C7BM00030H

Yan, H., Yang, H., Li, K., Yu, J., and Huang, C. (2017). Effects of chlorhexidine-encapsulated mesoporous silica nanoparticles on the anti-biofilm and mechanical properties of glass ionomer cement. *Molecules* 22 (7), 1225. doi: 10.3390/molecules22071225

Yu, J., Yang, H., Li, K., Lei, J., Zhou, L., and Huang, C. (2016). A novel application of nanohydroxyapatite/mesoporous silica biocomposite on treating dentin hypersensitivity: An *in vitro* study. *J. Dent.* 50, 21–29. doi: 10.1016/j.jdent.2016.04.005

Yu, J., Yang, H., Li, K., Ren, H., Lei, J., and Huang, C. (2017). Development of epigallocatechin-3-gallate-Encapsulated Nanohydroxyapatite/Mesoporous silica for therapeutic management of dentin surface. *ACS Appl. Mater Interfaces* 9 (31), 25796–25807. doi: 10.1021/acsami.7b06597

Zhang, L., Sun, H., Yu, J., Yang, H., Song, F., and Huang, C. (2018). Application of electrophoretic deposition to occlude dentinal tubules. *vitro. J. Dent.* 71, 43–48. doi: 10.1016/j.jdent.2018.01.012

Zhang, J., Tan, W., Zhang, Z., Song, Y., Li, Q., Dong, F., et al. (2018). Synthesis, characterization, and the antifungal activity of chitosan derivatives containing urea groups. *Int. J. Biol. Macromol.* 109, 1061–1067. doi: 10.1016/j.ijbiomac.2017.11.092

Zhang, J. F., Wu, R., Fan, Y., Liao, S., Wang, Y., Wen, Z. T., et al. (2014). Antibacterial dental composites with chlorhexidine and mesoporous silica. *J. Dent. Res.* 93 (12), 1283–1289. doi: 10.1177/0022034514555143

Zhang, H., Xu, J., Zhang, X., Wang, T., Zhou, D., Shu, W., et al. (2022). One-pot synthesis of Ag/Quaternary ammonium salt Co-decorated mesoporous silica nanoparticles for synergistic treatment of cancer and bacterial infections. *Front. Bioeng Biotechnol.* 10, 875317. doi: 10.3389/fbioe.2022.875317

Zhou, X., Feng, W., Qiu, K., Chen, L., Wang, W., Nie, W., et al. (2015). BMP-2 derived peptide and dexamethasone incorporated mesoporous silica nanoparticles for enhanced osteogenic differentiation of bone mesenchymal stem cells. *ACS Appl. Mater. Interfaces* 7 (29), 15777–15789. doi: 10.1021/acsami.5b02636

Zhou, Z., Gao, Y., Chen, X., Li, Y., Tian, Y., Wang, H., et al. (2021). One-pot facile synthesis of double-shelled mesoporous silica microcapsules with an improved soft-template method for sustainable pest management. *ACS Appl. Mater. Interfaces* 13 (33), 39066–39075. doi: 10.1021/acsami.1c10135

Zhou, Y., Quan, G., Wu, Q., Zhang, X., Niu, B., Wu, B., et al. (2018). Mesoporous silica nanoparticles for drug and gene delivery. *Acta Pharm. Sin. B.* 8 (2), 165–177. doi: 10.1016/j.apsb.2018.01.007

Zupancic, S., Casula, L., Rijavec, T., Lapanje, A., Lustrik, M., Fadda, A. M., et al. (2019). Sustained release of antimicrobials from double-layer nanofiber mats for local treatment of periodontal disease, evaluated using a new micro flow-through apparatus. *J. Control Release* 316, 223–235. doi: 10.1016/j.jconrel.2019.10.008

pH-activated antibiofilm strategies for controlling dental caries

Xiuqing Wang[1†], Jingling Li[1†], Shujun Zhang[1†], Wen Zhou[1], Linglin Zhang[2] and Xiaojing Huang[1*]

[1]Fujian Key Laboratory of Oral Diseases & Fujian Provincial Engineering Research Center of Oral Biomaterial & Stomatological Key Lab of Fujian College and University, School and Hospital of Stomatology, Fujian Medical University, Fuzhou, China, [2]State Key Laboratory of Oral Diseases, Department of Cariology and Endodontics, National Clinical Research Center for Oral Diseases, West China Hospital of Stomatology, Sichuan University, Chengdu, China

Dental biofilms are highly assembled microbial communities surrounded by an extracellular matrix, which protects the resident microbes. The microbes, including commensal bacteria and opportunistic pathogens, coexist with each other to maintain relative balance under healthy conditions. However, under hostile conditions such as sugar intake and poor oral care, biofilms can generate excessive acids. Prolonged low pH in biofilm increases proportions of acidogenic and aciduric microbes, which breaks the ecological equilibrium and finally causes dental caries. Given the complexity of oral microenvironment, controlling the acidic biofilms using antimicrobials that are activated at low pH could be a desirable approach to control dental caries. Therefore, recent researches have focused on designing novel kinds of pH-activated strategies, including pH-responsive antimicrobial agents and pH-sensitive drug delivery systems. These agents exert antibacterial properties only under low pH conditions, so they are able to disrupt acidic biofilms without breaking the neutral microenvironment and biodiversity in the mouth. The mechanisms of low pH activation are mainly based on protonation and deprotonation reactions, acids labile linkages, and H^+-triggered reactive oxygen species production. This review summarized pH-activated antibiofilm strategies to control dental caries, concentrating on their effect, mechanisms of action, and biocompatibility, as well as the limitation of current research and the prospects for future study.

KEYWORDS

biofilm, pH-responsive, antibiofilm agents, drug delivery systems, dental caries, *Streptococcus mutans*

1 Introduction

Oral biofilms are highly assembled microbial communities surrounded by an extracellular matrix (Bowen et al., 2018). After saliva glycoproteins cling to the tooth surface, oral microorganisms begin to gather and adhere, and form an orderly structured community wrapped in the extracellular matrix (Marsh et al., 2016). Under normal

conditions, the resident microbes, including commensal bacteria and opportunistic pathogens, coexist with each other to maintain relative dynamic balance, which plays an essential role in oral and whole-body health (Gao et al., 2018; Rosier et al., 2018). However, under hostile conditions such as high-carbonhydrate diet and poor oral hygiene, glycometabolic microorganisms in the biofilms can generate excessive organic acids from diet through a fermentation process (Simón-Soro and Mira, 2015; Hajishengallis et al., 2017). The organic acids are confined in the local biofilm by extracellular matrix, creating acidic niches (Benoit et al., 2019). The acidic environment affects the metabolic activity of oral microorganisms and exhibits an acid-induced selection, increasing the proportions of acidogenic and aciduric bacteria, such as *Streptococcus mutans* (*S. mutans*), the major cariogenic bacteria (Takahashi and Nyvad, 2011). Dental caries start with the break of the oral eubiosis, shifting from commensal biofilm to cariogenic biofilm with abundant acidogenic and aciduric microbes (Selwitz et al., 2007; Pitts et al., 2017; Tanner et al., 2018). There is a prolonged drop in pH value of cariogenic biofilm, leading to demineralization of dental hard tissue and development of dental caries when the value falls below 5.5 and lower (Margolis et al., 1999; Selwitz et al., 2007; Pitts et al., 2017; Xu et al., 2022b). Study confirmed that the pH at active caries niches was reduced to about 4.5 - 5.5 (Bowen, 2013). Therefore, it is tremendous significance to control acidic biofilm to prevent and treat dental caries.

Despite remarkable progress in the prevention of dental caries, especially with the application of fluoride, controlling acidic dental biofilms is still associated with serious challenges (Liu et al., 2018). Compared with planktonic bacteria, pathogens in the established biofilm are protected by extracellular matrix barriers (Kuang et al., 2018). Conventional drugs are incapable of degrading the matrix, resulting in far less effective against preformed acidic biofilm. Moreover, conventional broad-spectrum antimicrobials, such as chlorhexidine (CHX), kill oral microorganism effectively without selectivity, bringing challenges to long-term therapeutic use (Zhang et al., 2022a). Frequent use of antibacterial strategies without selectivity would potentially damage the ecological balance, which increases possibility of reinfection by opportunistic pathogens (Guo et al., 2015).

Efforts have been made to develop novel strategies to deal with these problems, including the following: 1) killing cariogenic pathogens specifically by *S. mutans*-specific targeting antimicrobial agents (Guo et al., 2015; Huo et al., 2018; Xiang et al., 2019); 2) modulating the biofilm pH *via* alkali production by alkali-producing bacteria to protect against plaque acidification and further dominance of cariogenic bacteria that thrive in acidic conditions (Liu et al., 2012); 3) digesting the protective extracellular matrix *via* enzymes to facilitate penetrability of antibacterial agent into mature biofilms (Gao et al., 2016; Liu et al., 2016); and 4) activating antimicrobial capacity smartly by components that can be activated by ambient stimuli (Gupta et al., 2002; Kost and Langer, 2012). Various stimuli are applied in stimuli-triggered antimicrobial strategies, such as thermal (Gopal et al., 2016; Imai et al., 2018), pressure (Montoya et al., 2021) and pH (Chen et al., 2022). pH is closely related to caries development, that is, dental hard tissues demineralize once the ambient pH

continuously drops below 5.5. As mentioned above, the pH of local niches of caries is about 4.5 - 5.5, while in the physiological conditions, salivary pH range 6.2 - 7.6 (Baliga et al., 2013). Therefore, acidic pH is the most promising stimuli that can be used to combat cariogenic biofilm smartly. Acidic-triggered strategies show antibacterial effect only under acidic conditions and do not function under neutral physiological conditions, exhibiting ability to maintain oral microecological homeostasis (Liu et al., 2018; Liang et al., 2020). In recent years, acidic-triggered strategies have attracted more and more attention in the prevention and treatment of caries, based on keeping balance and biodiversity of oral microecology (Liang et al., 2020; Naksagoon et al., 2021). This review summarizes the research progress of pH-responsive antibiofilm strategies to control dental caires in recent years, mainly focusing on antibiofilm effect, antimicrobial mechanism and biocompatibility, as well as the limitation of current research and the prospects for future research, in an attempt to provide reference for subsequent study.

2 pH-responsive antibiofilm strategies

The pH-activated antibiofilm strategy enhances the selectivity and efficacy of antimicrobial agents. Recent researches have focused on designing novel pH-activated strategies to control dental caries, including pH-responsive antimicrobial agents and pH-sensitive drug delivery systems.

2.1 pH-responsive antibiofilm agents

Several pH-responsive antibiofilm agents have been generated to inhibit the formation and development of cariogenic biofilm, and disrupt the unbalanced microbial composition. The agents include: 1) pH-responsive antimicrobial peptides; 2) organic compounds with amine groups; 3) iron oxide nanoparticles with peroxidase-like activity (Table 1).

2.1.1 pH-responsive antimicrobial peptides

Antimicrobial peptides (AMPs), a kind of pervasive natural peptides, exert the ability of antibiosis and antivirus and are present in both plants and animals as potent antibiotics for the inherent immune system (Zasloff, 2002; Reddy et al., 2004; Harris et al., 2009). These peptides have been reported to show the ability to inhibit the formation and development of pathogenic biofilm (Luo and Song, 2021), indicating that AMPs may be a promising antibiofilm strategy for dental caries control. Besides, AMPs are less likely to induce drug resistance since they target almost non-specific modes at multiple sites on microbial membranes (Malik et al., 2016; Steinbuch and Fridman, 2016). However, non-specific targeting to oral microorganism would potentially lead to ecological dysbiosis, which increases possibility of opportunistic infections (Eckert et al., 2006). In order to increase selectivity of AMPs, researchers developed novel kinds of AMPs with a targeting domain and an antimicrobial domain, such as C16G2 and C10-KKWW, which can selectively target *S. mutans* and kill them

TABLE 1 pH-responsive antibiofilm agents to control acidic biofilm.

Class	pH responsive antibiofilm agents	Antibiofilm activity	Mechanisms of action	Toxicity	Assay	Author, year
Antimicrobial peptide	Histatins-5	Inhibit the formation of *S. mutans* biofilm	Protonation of histidine residues under acid environment	–	*In vitro*	(Mochon and Liu, 2008; Krzyściak et al., 2015)
Antimicrobial peptide	Kappacin	Inhibit the growth of *S. mutans*, *P. gingivalis* and *A. naeslundii*	Membranolytic action at acidic pH	–	*In vitro*	(Malkoski et al., 2001; Dashper et al., 2007)
Antibacterial peptide nanoparticles	pHly-1 NPs	Inhibit formation of EPS and *S. mutans* biofilm and development of *S. mutans* biofilm	*Via* protonation of the histidine at low pH, peptide pHly-1 adopts random coil-helix conformation at low pH and forms nanoparticles	Low toxicity on the normal oral and gastric tissues	*In vitro & in vivo*	(Zhang et al., 2022a)
Antimicrobial peptide	AAPs	Inhibit the growth of *S. mutans* within the biofilm community	*Via* protonation of histidine residues at low pH, AAPs undergo a transition from a helical conformation to a random coil	–	*In vitro*	(Clark et al., 2021)
Antimicrobial peptide	GH12	Inhibit formation of EPS, water-insoluble glucan, and lactic acid in *S. mutans* biofilm as well as killing *S. mutans* within the multispecies biofilm	Due to protonation of histidine residues under acid environment, GH12 forms an amphipathic α-helix	Negligible cytotoxicity to human gingival fibroblast cells	*In vitro*	(Tu et al., 2016; Wang et al., 2017; Jiang et al., 2018; Jiang et al., 2021)
Antimicrobial peptide	LH12	Inhibit virulence and growth of cariogenic pathogens, as well as enhancing the competitiveness of commercial bacteria in the mixed-species microbiota	Via protonation of histidine residues under acid environment, LH12 forms an amphipathic α-helix	Show slight cytotoxicity to human gingival epithelial cells at a high concentration of 128 μg/mL	*In vitro*	(Jiang et al., 2022)
Quaternary pyridinium salt	Azo-QPS-C16	Inhibit acid-producing bacteria in multispecies biofilm	Weakly acid Azo-QPS-C16 and bases can assemble into inactive agglomerate at neutral pH, but the agglomerate will collapse at low pH	–	*In vitro*	(Yang et al., 2018)
Tertiary amine	DMAEM HMAEM	Inhibit formation of EPS and *S. mutans* biofilm and regulate oral microecological balance	Protonation of amine groups in tertiary amine under acid environment	Low cytotoxicity to human oral keratinocyte cells	*In vitro & in vivo*	(Liang et al., 2020; Shi et al., 2022)
Nanoparticles	Iron oxide nanoparticles	Kill bacteria in biofilm and break down EPS	The peroxidase-like activity of iron oxide nanoparticles	High biocompatibility	*In vitro & in vivo*	(Gao et al., 2016)

effectively (Guo et al., 2015; Xiang et al., 2019). These peptides exert efficacy in not only cariogenic but also healthy niches. Another strategy is pH-activated AMPs, which exert potent antimicrobial efficiency only in acidic environment and do not function under neutral physiological conditions, exhibiting ability to maintain oral microecological homeostasis (Liu et al., 2018; Liang et al., 2020). Some natural peptides have pH-responsive properties, and a number of researchers focus on designing novel pH-activated antimicrobial peptides.

Histatins, isolated from the human parotid salivary gland in 1988, is a group of pH-activated peptides rich in histidine residues (Fabian et al., 2012; Krzyściak et al., 2015; Khurshid et al., 2017). The antifungal activity of histatin-3 and histatin-5 have been proven to be enhanced by acidic pH (Mochon and Liu, 2008), and histatin-5 exhibits the ability to inhibit the formation of *S. mutans* biofilm

(Krzyściak et al., 2015). Kappacin, another natural antibacterial peptide, is the active form of Caseinomacropeptide, a heterogeneous C-terminal fragment from bovine milk (Malkoski et al., 2001). Kappacin has been proven to exhibit the antibacterial activity of inhibiting the growth of Gram-negative and Gram-positive bacteria in oral cavity, including *S. mutans*, *Porphyromonas gingivalis* (*P. gingivalis*) and *Actinomyces naeslundii* (*A. naeslundii*),which are components of supra gingival dental plaque (Malkoski et al., 2001; Dashper et al., 2007). An increase in antimicrobial activity against *S. mutans* and *A. naeslundii* has discovered under mildly acidic conditions.

Peptide pHly-1 forms into nanofibers at physiological pH, but can generate coil-helix conformation and turn into nanoparticles under an acid environment (Zhang et al., 2022a). It has been confirmed that pHly-1 nanoparticles were capable of suppressing

both formation and development of *S. mutans* biofilm at acidic pH, while negligible antibiofilm activity was found at neutral pH. The minimum inhibition concentration (MIC) and minimum bactericidal concentration (MBC) of pHly-1 nanoparticles against *S. mutans* were estimated to be 5.5 µM and 6.7 µM at pH 5.5, but > 44 µM and > 22 µM at pH 7.0, respectively. Besides, the agent exerted potent effects in inhibiting bacterial clusters and the formation of extracellular polymeric substances (EPS) in the preformed biofilms at pH 4.5 while negligible effects were observed at pH 7. Furthermore, initial, moderate, and severe dental caries lesions were significantly decreased by the use of pHly-1 NPs in the animal study with a rat carious model. It is worth mentioning that pHly-1 NPs exhibited a better anticaries effect than CHX *in vivo*.

Clavanins are a kind of a-helical amphipathic antimicrobial peptide with 23 amino acid residues, which were firstly purified from hemocytes of the invertebrate styela clava. It was found that Clavanin A was rich in both histidine and phenylalanine residues and had broad-spectrum antibacterial properties (Lee et al., 1997b). When the pH drops, the protonation of histidine residues enhances the ability to target bacterial membranes. At the same time, phenylalanine residues enable the AMP to form a flexible and hydrophobic structure to facilitate the interaction with membrane lipids (Lee et al., 1997a; van Kan et al., 2002; van Kan et al., 2003a; van Kan et al., 2003b). According to the structure of Clavanin A, two acid-activated peptides (AAPs), named AAP1 and AAP2, were designed to combat dental caries (Clark et al., 2021). It appeared that AAPs performed a more potent antibacterial ability than Clavanin A under a low pH value while overcoming Clavanin A's shortcoming of exhibiting antimicrobial efficacy at neutral pH. APP2 exerted more potent antibacterial activity at pH 5 than AAP1. In the test against microbes in *S. mutans* biofilms, AAP2 showed the potential to reduce the acid-producing flora within the biofilm community.

Inspired by the template (XXYY)n (X refers to a hydrophobic residue, Y refers to a hydrophilic residue, and n refers to the number of repeats) proposed by Wiradharma et al. as an appropriate structure of amphipathic, cationic α-helical AMPs, Wang et al. designed a peptide with 12 amino acid residues called GH12 against cariogenic bacteria (Wiradharma et al., 2011; Wang et al., 2017). Study showed that GH12 had much lower MIC against dental caries-associated bacteria (*S. mutans*, *Streptococcus sanguinis*, *Streptococcus gordonii* (*S. gordonii*), *Streptococcus mitis*, *Streptococcus salivarius*, *Streptococcus sobrinus*, *Actinomyces viscosus*, *Actinomyces naeslundii*, *Lactobacillus acidophilus*, *Lactobacillus casei*, and *Lactobacillus fermentum*) at pH 5.5 than at pH 7.2. The production of EPS component, water-insoluble glucan synthesis, and lactic acid in preformed *S. mutans* biofilm was also inhibited by GH12, and the inhibitory effects increased when pH dropped from 7.2 to 5.5 (Jiang et al., 2021). In addition to suppressing the formation and viability of *S. mutans* biofilm at pH 5.5, GH12 exhibited different antibacterial effect in killing different bacterial species in multispecies biofilm, which indicates that GH12 have the ability to change the microbiota composition of cariogenic biofilm (Jiang et al., 2018).

Another cationic amphiphilic α-helical AMP, named LH12, was also designed based on the (XXYY)n formula (Jiang et al., 2022). LH12 exhibited stronger antimicrobial activity against *S. mutans* in response to acidic environment. MIC and MBC of LH12 against *S. mutans* were about 12µg/ml and 16µg/ml at pH 5.5, but 21µg/ml and 32µg/ml at pH 7.2. In addition to kill *S. mutans*, 16 µg/mL and 32 µg/mL LH12 could reduce the production of lactic acid and EPS, as well as completely suppressing the biofilm formation. Furthermore, in the dual-species biofilm model, the proportion of *S. gordonii* was increased while the proportion of *S. mutans* was decreased, which indicated that LH12 could regulate the microbial composition.

2.1.2 Organic compounds with amine groups

A novel quaternary pyridinium salt with pH-controlled activity, (E)-1-hexadecyl-4-((4-(methacryloyloxy)phenyl)diazenyl)-pyridinium bromide (Azo-QPS-C16), was designed to curb the growth of acid-producing microbes (Yang et al., 2018). An 8-fold difference in efficacy against *S.mutans* was observed in acidic solutions than in neutral solutions. *Via* the saliva-derived multispecies biofilm model containing *Enterobacter* spp., *Klebsiella* spp. and *Streptococcus* spp., the ability of Azo-QPS-C16 to kill or inhibit acid-producing bacteria was monitored. The result showed that Azo-QPS-C16 could selectively eliminated sucrose-fermenting, acidogenic bacteria in biofilm while increasing the biomass of commensals. It is worth noting that the application of Azo-QPS-C16 was able to maintain the pH of culturing solutions above 5.5, below which demineralization of dental enamel happens (Kleinberg, 2002).

Liang et al. designed and synthesized two kinds of tertiary amine (TA) monomers: DMAEM (dodecylmethylaminoethyl methacrylate) and HMAEM (hexadecylmethylaminoethyl methacrylate). The MICs of DMAEM and HMAEM against the *Streptococci* species ranged from 0.18 to 5.95 µg/mL and 0.2 to 0.8 µg/mL, respectively at pH 5.0, while no antibacterial effect was detected even at the concentration up to 13.5 mg/ml at pH 7.0. Aimed at inhibiting secondary caries, the TAs with pH responsiveness were incorporated into adhesive resins, getting the TA-modified resin adhesives (TA@RAs) (Liang et al., 2020). There was no significant difference in antibiofilm activity between DMAEM@RAs and HMAEM@RAs. However, the pH of DMAEM@RAs and HMAEM@RAs when they started to exert antibacterial efficacy was 5.3 ± 0.03 and 4.1 ± 0.01, respectively, indicating that DMAEM-modified resin adhesives are more sensitive to pH than resin adhesives modified by HMAEM. Researchers in the same group further explored the antimicrobial effect of DMAEA@RA on dual-species biofilms of *S. mutans* and *Candida albicans* to prevent secondary caries (Shi et al., 2022). Results showed that DMAEM@RA were capable of inhibiting the development of dual-species biofilms as well as suppressing the production of EPS and acid when pH was below 5.5, while those activities at pH 6.0 were similar to negative control groups. *Via* down-regulating the expression of pH-regulated genes, virulence-associated, and cariogenic genes, DMAEA@RAs could reduce the mineral loss of teeth both *in vitro* and *in vivo* in a pH-dependent manner.

2.1.3 Iron oxide nanoparticles with peroxidase-like activity

Iron oxide nanoparticles, having been regarded as nanozymes, exert intrinsic enzyme mimetic efficiency to activate H_2O_2 which is similar to peroxidases (Gao et al., 2007). The nanoparticles have attracted great attention due to their antibacterial, antifungal, and anticancer abilities and low toxicity to human body (Dadfar et al., 2019). Gao et al. synthesized catalytic iron oxide nanoparticles (CAT-NP) containing Fe_3O_4 and found that there was an increase in catalytic efficiency of CAT-NP when pH dropped from 6.5 to 4.5 (Gao et al., 2016). CAT-NP exhibited potent efficacy to induce extracellular matrix degradation and kill bacteria within the acidic microenvironment of cariogenic biofilm. Moreover, it possessed an additional pH-dependent mechanism to control dental caries by directly decreasing the demineralization of enamel in acidic environment. A kind of dextran-coated iron oxide nanoparticles termed nanozymes (Dex-NZM) was designed to specifically target biofilms (Naha et al., 2019). Dextran, a polysaccharide with low toxicity, can be embedded into the matrix of growing biofilms by bacterial exoenzymes, resulting in high selectivity toward biofilms (Gibbons and Banghart, 1967; Xiao et al., 2012). Compared with uncoated NZM, Dex-NZM displayed a better role in controlling dental biofilms at pH 4.5. To go a step further, Huang et al. combined glucose oxidase (GOx) with dextran-coated iron oxide nanoparticles (Dex-IONP) (Huang et al., 2021). GOx can catalyze glucose in cariogenic biofilms to generate H_2O_2, which facilitates the pH-dependent production of reactive oxygen species (ROS) by Dex-IONP. Dex-IONP-GOx displayed greater catalytic activity at pH 4.5 and 5.5 than at pH 6.5. In the *in vitro* test with a mixed-species biofilm model, Dex-IONP-GOx was confirmed to inhibit the cariogenic *S. mutans* potently, but with negligible effects against the commensal *Streptococcus oralis*.

2.2 pH-responsive drug delivery systems

The downside of traditional antimicrobial drugs, such as fanasol and CHX, is the toxicity or side effects caused by low selectivity. Killing microorganisms without selectivity reduces the diversity of microbial communities, thus destroying the ecological balance of microbial communities and bringing great challenges for clinical treatment. Therefore, great importance has been attached to strategies by which drugs are delivered without disrupting the internal oral environment. Acid-triggered drug delivery systems are able to deliver the drug to acidogenic biofilms effectively without disrupting the commensal biofilms. The carriers used to fabricate pH-activated drug release systems often contain a specific functional group, which can respond to changes in the pH of the ambient environment. The mechanisms by which carriers respond to pH mainly includes the charge shifting of pH-responsive residues and the degradation of acid-degradable residues (Deirram et al., 2019) (Figure 1; Table 2).

2.2.1 pH-responsive charge and/or hydrophilicity shifting systems

To equip carriers with pH-dependent activity, one strategy is to add moieties that can change charge and/or hydrophilicity when pH

decreases. The acidic pH can trigger the protonation of those groups or the change from hydrophobicity to hydrophilicity of polymers, which leads to the degradation of carriers and the release of drugs (Deirram et al., 2019). In some cases, polymers are self-assembled into cationic hydrophilic exteriors and pH-responsive hydrophobic interiors. When pH decreases below their pKa, the inner groups become hydrophilic and the carriers cleave (Horev et al., 2015; Zhou et al., 2016; Zhang et al., 2021).

A kind of 21 nm, self-assembly cationic nanoparticles encapsulating farnesols were designed to achieve pH-responsive drug release and selective oral biofilm disruption (Horev et al., 2015; Zhou et al., 2016; Sims et al., 2018). The nanoparticles, consisting of 2-(dimethylamino)ethyl methacrylate (DMAEMA), butyl methacrylate (BMA), and 2-propylacrylic acid (PAA) (p (DMAEMA)-b-p(DMAEMA-co-BMA-co-PAA)), overcame the hydrophobicity-related bad effect of farnesols in conventional treatments against oral biofilms. The nanoparticle generated higher binding affinities to pellicle and EPS at acidic pH than physiological conditions and enhanced the antibiofilm activity of farnesol *via* promoting drug localization. Farnesol release rate at pH 4.5 was twice as fast as the rate at pH 7.2, indicating that farnesol release was activated by acidic pH. Compared to solely farnesol, 4-fold enhancement was discovered in *S. mutans* biofilms disruption in drug-loaded nanoparticles group at pH 4.5. The drug-loaded nanoparticles group compromised the mechanical stability of biofilms, thus displaying more than 2-fold biofilm removal ability compared to free farnesol when exposed to shear stress (Horev et al., 2015).

Zhou et al. synthesized pH-activated, doxycycline (DOX)-loaded nanoparticles that contained N,N,N-trimethyl chitosan (TMC) and liposomes (Lips) (Zhou et al., 2018). The data displayed that DOX release half-life was 0.75 h at pH 4.5, yet 2.3 h at pH 6.8. In addition to releasing the DOX, TMC processed an antibacterial effect itself. Hu et al. tested the antibiofilm activity of this nanoparticle and results indicated that TMC-Lip-DOX nanoparticles disrupted the biofilm architecture and reduced the number of bacteria significantly, compared with TMC group and DOX group (Hu et al., 2019). Both *in vivo* and *in vitro* tests showed that the nanoparticles were able to inhibit dental plaque effectively and had nontoxicity.

Glycol chitosan with pH-activated charge inversion is able to target acidic bacterial infection sites and exhibits better antimicrobial efficiency (Yu et al., 2019; Yan et al., 2020). Based on this, a novel kind of photothermal antimicrobial nanoagent with pH responsiveness, named FePAgPG, was synthesized (Xu et al., 2022a). Fe_3O_4 nanoparticles were modified by Ag and two polydopamine layers in sequence and then wrapped with glycol chitosan. When pH decreased, the zeta potential of FePAgPG shifted from anionic (-24.57 ± 1.31 mV) to cationic value (7.89 ± 0.48 mV) due to the protonation of glycol chitosan. Thus, at acidic pH, the positively charged nanoparticles could better attach to negative *S. mutans* and 1.7-fold enhancements in efficacy against *S. mutans* was observed at pH 5.4 than at pH 7.4. *Via* infrared irradiation at low temperature, FePAgPG nanoparticles exerted a potent antimicrobial rate of over 95% against planktonic *S. mutans* and inhibited the formation of *S. mutans* biofilm.
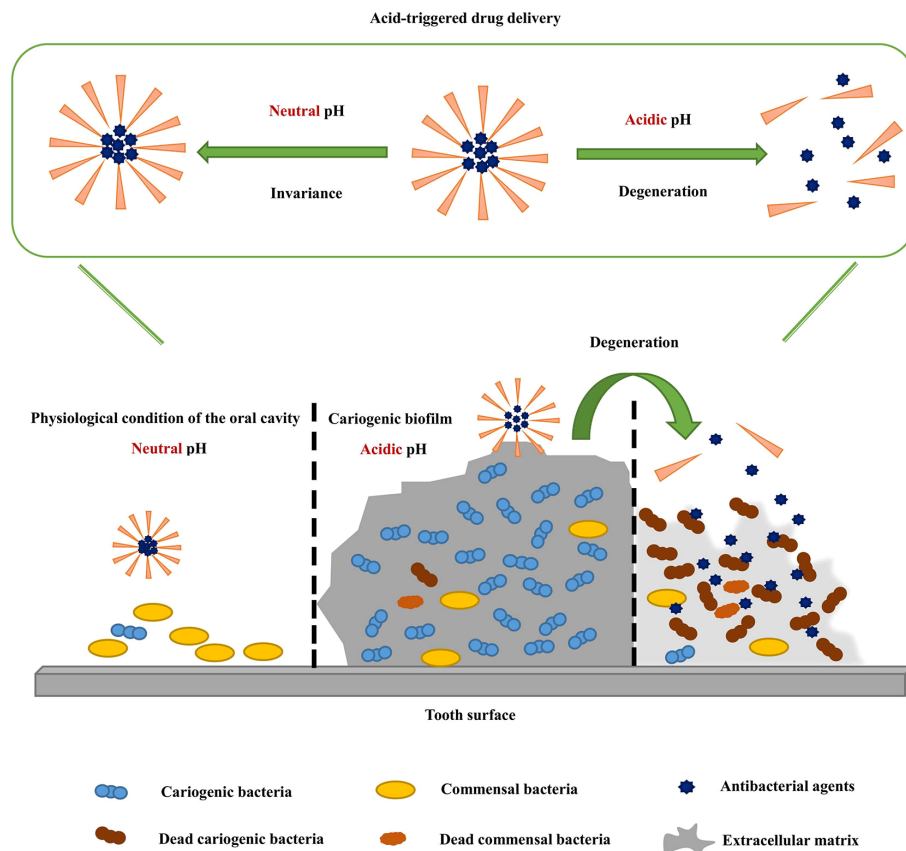
FIGURE 1
Acid-triggered drug delivery systems deliver the drug to acidogenic biofilms effectively.

Sun et al. designed a pH-responsive hydrogel coating which loaded antimicrobial peptides to capture and kill microbes. The pH-responsive coating, carboxybetaine methacrylate-dimethylaminoethyl methacrylate copolymer p(CBMA-co-DMAEMA), could capture bacteria and release antimicrobial peptides simultaneously, performing as a smart hunter (Sun et al., 2022). Zeta potentials of the surface shifted from -0.79 mV at pH 7 to 4.07 mV, 8.05 mV and 54.03 mV at pH 6, 5 and 4 respectively. When pH changed from 7.0 to 5.5, the number of dead bacteria on hydrogel layers loaded with antimicrobial peptides increase. The result indicated that the pH-activated capture of hydrogel layers mainly relied on cationic surface charge.

In order to inhibit cariogenic biofilms, Peng et al. designed a novel CHX-loaded pH-sensitive nanoparticle (p(DH)@CHX), composed of DMAEMA and hydroxyethyl methacrylate (HEMA) (Peng et al., 2022). According to data, the release of CHX was stable with low volume over time under physiological conditions, yet increased gradually at the acidic pH. In the test against cariogenic biofilm, researchers found that both p(DH)@CHX and CHX were capable of inhibiting the lactic acid production by biofilms, and no significant difference was found in the lactic acid production. CHX, an antibacterial agent with pronounced cytotoxicity while continuously used, exerted lower cytotoxicity against human oral keratinocytes when loaded into nanoparticles. Besides, p(DH)@CHX showed no effect on healthy saliva-derived biofilm while

exhibiting the same antimicrobial activities as free CHX on cariogenic biofilm.

An antibacterial agent, bedaquiline, exhibits high effects on killing planktonic bacteria but have limited efficacy in removing mature biofilm (Flemming et al., 2016; Bowen et al., 2018; Zhang et al., 2021). In order to improve permeability of bedaquiline to mature biofilm, Zhang et al. synthesized a novel pH-activated nano micelle, core-shell nano micelle (mPEG-b-PDPA), for loading hydrophobic antibacterial agents (Zhang et al., 2021). The release rate of bedaquiline was very gentle at pH 7, with about 35% in the first 12 h, while the amount released within 3 h reached 92.2% at pH 5. It has been confirmed that the bedaquiline-loaded micelles system could inhibit *S. mutans* biofilm formation and take antimicrobial effect against mature *S. mutans* biofilm.

2.2.2 pH-responsive systems with acid-degradable linkages

A simple and compelling strategy to design pH responsive polymers is to design nanocarriers including pH-responsive linkages with stabilization at neutral pH and activity at acidic pH. Those linkages mainly incorporate hydrazone linkages with ketone/aldehyde and hydrazide; imine linkages with an aldehyde (ketone) and amine; maleic acid amide linkages with amine and maleic anhydride; ortho ester linkages with alcohols and formate or ester (Deirram et al., 2019).

Aimed at reducing the side effect caused by the low selectivity of CHX, Zhao et al. designed a type of pH-responsive polymer that could release CHX in acid niches of cariogenic biofilms (Zhao et al., 2019). The whole system was named CA-PICMs. CHX was encapsulated in the core-shell polyionic complex micelles (PICMs) which were composed of cationic poly(ethylene glycol)-block-poly(2-((2-aminoethyl)carbamoyl)oxy)ethyl methacrylate (PEG-b-PAECOEMA) and anionic citraconic anhydride (CA). The citraconic amide is acid-degradable, and PEG block promotes the stability of the structure regardless of enzyme, pH, and temperature (Harris and Chess, 2003; Osada et al., 2005). While CA-PICMs reduced the toxicity of CHX, there was no statistical difference in antibacterial effects against *S. mutans* biofilms between

CA-PICMs and CHX, which indicates that the polymers may be a promising approach for dental caries therapy (Zhao et al., 2019).

In order to combat tooth decay and enhance enamel restoration, Xu et al. synthesized the micellars, 3-maleimidopropionic acid-poly(ethyleneglycol)-block-poly(L-lysine)/phyenylboronic acid (MAL-PEG-b-PLL/PBA), which contained pH-cleavable boronate ester bond (Xu et al., 2022b). The antibacterial agent tannic acid, NaF, and salivary-acquired peptide (SAP) were conjugated with MAL-PEG-b-PLL/PBA to form PMs@NaF-SAP. PMs@NaF-SAP exerted better performance against *S. mutans* biofilm under acidic environment, since there was an increase in drug release when pH dropped. When pH reached 5, the antibacterial potency of PMs@NaF-SAP was stronger than the

TABLE 2 pH-responsive drug delivery systems to control acidic biofilm.

Nanocarriers	Drug	Antibiofilm activity	Mechanisms of action	Toxicity	Assay	Author, year
p(DMAEMA)-b-p(DMAEMA-co-BMA-co-PAA)	Farnesol	Nanoparticles generate high binding affinities to pellicle and EPS surfaces and enhance antibiofilm activity of farnesol	Protonation of tertiary amines in DMAEMA and carboxyl groups in PAA at acidic pH	–	*In vitro & in vivo*	(Horev et al., 2015; Zhou et al., 2016; Sims et al., 2018)
TMC-Lip nanoparticles	Doxycycline	Nanoparticles disrupt the biofilm architecture and reduce the number of bacteria significantly	Protonation of amino groups	Good cytocompatibility on human periodontal ligament fibroblasts	*In vitro & in vivo*	(Zhou et al., 2018; Hu et al., 2019)
FePAgPG	Ag	Nanoparticles inhibit the formation of *S. mutans* biofilm	Protonation of amino groups in glycol chitosan	Good biocompatibility on human oral keratinocytes cells	*In vitro*	(Xu et al., 2022a)
p(CBMA-co-DMAEMA)	pH-switchable antibacterial octapeptides	The positively charged surface is able to capture cariogenic bacteria under acid environment and when pH decrease, the number of dead bacteria on hydrogel layers increase	Protonation of carboxyl groups in CMBA and tertiary amines in DMAEMA at low pH	Good biocompatibility on human oral keratinocyte cells	*In vitro*	(Sun et al., 2022)
poly (DMAEMA-co-HEMA)	Chlorhexidine	The whole system exhibits the same antimicrobial activities as free chlorhexidine on cariogenic biofilm	Protonation of tertiary amines in DMAEMA at low pH	Lower the cytotoxicity of chlorhexidine against human oral keratinocytes	*In vitro*	(Peng et al., 2022)
mPEG-b-PDPA	Bedaquiline	Inhibit *S. mutans* biofilm formation	Protonation of amine groups in PDPA segments under acid environment	No significant cytotoxicity	*In vitro*	(Zhang et al., 2021)
PEG-b-PAECOEMA/CA	Chlorhexidine	Respond to acid microenvironments of cariogenic biofilms and rapidly release chlorhexidine for efficient bacteria killing.	Degradation of citraconic amide groups at low pH	The carrier reduces the toxic of chlorhexidine	*In vitro*	(Zhao et al., 2019)
MAL-PEG-b-PLL/PBA	Tannic acid & sodium fluoride	PMs@NaF-SAP can suppress the growth of *S. mutans* biofilm and inhibit demineralization and facilitates remineralization in enamel slices	Cleavage of boronate ester bonds	The system exhibits much lower cytotoxicity than chlorhexidine	*In vitro & in vivo*	(Xu et al., 2022b)
PPi-Far-PMs	Farnesal	PPi-Far-PMs can inhibit the growth of *S. mutans* both *in vivo* and *in vitro*	Cleavage of hydrazone bonds	–	*In vitro & in vivo*	(Yi et al., 2020)
MSNs	Ag ions & chlorhexidine	Inhibit growth of *S. mutans* and *S. mutans* biofilm formation	Cleavage of disulfide bonds	Significantly reduce the toxicity of chlorhexidine	*In vitro & in vivo*	(Yue et al., 2018)
ZnO$_2$-Cu@RB NPs	Rose Bengal	Kill *S. mutans* in cariogenic biofilm and suppress the formation of EPS	Fenton reaction	–	*In vitro*	(Zhang et al., 2022b)

positive control treatment with CHX. In addition, PMs@NaF-SAP showed a significant inhibitory on bacterial adhesion compared with PMs@NaF, whilst NaF added inhibited demineralization and facilitated remineralization in enamel slices.

Farnesal (Far) was conjugated to PEG *via* acid-sensitive hydrazone bonds, which was then linked with pyrophosphate (PPi) and encapsulated into polymeric micelles to form a novel drug delivery system, PPi-Far-PMs (Yi et al., 2020). Far was released from its carriers much faster under an acidic condition (pH 4.5) than in a neutral environment (pH 7.4). PPi-Far-PMs could bind to dental enamel rapidly and inhibit the growth of *S. mutans*, while the antibacterial effects of free Far and farnesol groups showed no obvious difference from negative control. The *in vivo* test showed that PPi-Far-PMs facilitated the antibiofilm ability of Far, as well as restoring the microarchitecture of teeth with caries.

Yue et al. synthesized a novel kind of mesoporous silica nanoparticles (MSNs) with disulfide bonds introduced into the silica framework, which improved the degradable ability faced with environmental stimuli (Yue et al., 2018). To battle oral pathogens, Lu et al. loaded these MSNs with silver and CHX to form a novel kind of redox/pH dual-controlled nanoparticles (Lu et al., 2018). It has been confirmed that Ag-MSNs@CHX exhibited a glutathione- and pH-dependent release behavior of silver ions and CHX. Compared with CHX, Ag-MSNs@CHX exerted a more effective ability to inhibit the growth of *S. mutans* biofilms.

2.2.3 Others

Fenton reaction is a classical reaction that catalyzes H_2O_2 to generate strong oxidizing hydroxyl radical (•OH) and other reactive oxygen species under the effect of ferrous ion (Fe^{2+}) (Pignatello et al., 2006). It has been widely used to degrade organic matter that is difficult to be removed in sewage. In recent years, Fenton and Fenton-like reactions have been applied to other fields beyond the ecological environment, such as Chemodynamic therapy (CDT). CDT is a novel strategy to induce the apoptosis of cancer cells *via* catalyzing H_2O_2 to produce •OH and other strong oxidizing active species in the acidic microenvironment of tumor lesion areas (Li et al., 2021b). Since the pH of the cariogenic microenvironment is below physiological pH and ROS is capable of killing bacteria, researchers applied Fenton and Fenton-like reactions to antibiofilm. Based on Fenton and Fenton-like reaction, novel copper-doped zinc peroxide nanoparticles with the antibacterial agent Rose Bengal (ZnO_2-Cu@RB NPs) were created (Zhang et al., 2022b). H_2O_2 can be created by the reaction between ZnO_2 and hydrogen ions (H^+) in the acid environment, which triggers the Fenton-like reaction between Cu and H_2O_2. *In-vitro* results showed that ZnO_2-Cu@RB NPs performed potent inhibition against *S.mutans* in acidic biofilm. Reduction in the demineralization of apatite and suppression in the formation of EPS could also be found *in vitro* studies.

3 Mechanisms of action

Many antibacterial mechanisms of pH-responsive antibacterial strategies have been proposed, and can be summarized into the following three parts: (1) Protonation and deprotonation reactions.

Protonation reactions can transform the charge and structure of antimicrobial agents or drug carriers under an acid environment. (2) Acid labile linkages. Those linkages can cleave at low pH, contributing to the disassembly of carriers and drug release. (3) H^+-triggered ROS production. By generating ROS under low pH, ROS productive systems can kill bacteria in cariogenic acidic biofilm selectively with slight side effects (Deirram et al., 2019; Fu et al., 2021) (Figure 2).

3.1 Protonation and deprotonation reactions

Protonation is capturing protons to chemical species, such as atoms, molecules, or ions at low pH, while deprotonation is removing protons when pH increases. Properties of chemicals, such as charge and hydrophilic, change after protonation or deprotonation of specific groups. The low pH value in cariogenic microenvironment can trigger the protonation of chemicals and then result in the transformation of electric properties. In recent years, based on protonation and deprotonation mechanism, researchers have explored novel pH-activated antibiofilm strategies for dental caries control.

Via protonation reaction, pH-responsive antimicrobial peptides can change their electric properties and structures under low pH conditions. Histidine residue is the pH-responsive reactive site of most AMPs. Histidine is a basic amino acid with an imidazole side chain that can rapidly accept or provide protons when pH changes (Horch et al., 2014; Chen et al., 2019). The pK_a of histidine is about 6.5, which is closest to the normal oral physiological pH among the pKa of the 20 proteinogenic amino acids. Histidine is uncharged with hydrophobicity at neutral pH but can be protonated and turned into a hydrophilic residue when the ambient pH below its pK_a. Histidine has been widely utilized in the design of pH-sensitive antimicrobial peptides. *Via* the protonation of histidine residues at low pH, most antimicrobial peptides are positively charged and form an amphipathic structure. Positive charge enhances their binding ability to the anionic microbial cell membrane, and amphipathic structure facilitates the peptides to form pores in membrane bilayer or penetrate into cells to act on intracellular target points (Bechinger and Gorr, 2017). Hydrophobic surfaces help peptides insert into microbial membranes, mediating direct membrane disruption, which can be stabilized by the interaction between hydrophilic surfaces and the head group regions of the membranes *via* electrostatic adsorption (Thaker et al., 2013; Xiong et al., 2015). According to protonation reaction, scholars introduced histidine residues into antibacterial peptides to prepare pH-responsive antimicrobial peptide and carry out a series of studies.

Histatin-5 is one of eminent forms of human histatins, which has been reported to have potent activity against *Candida* organisms (Khurshid et al., 2017). Low pH can enhance the positive charge of histatin-5 *via* protonation of histidine residues, which facilitates the localization of histatin-5 on anionic membranes, thereby inducing perturbations on the cell surface that leads to a rapid translocation of the peptide into the cytoplasm (Mochon and Liu, 2008). Unlike typical pore-forming

FIGURE 2
Mechanism of pH-activated antibacterial strategies: **(A)** Protonation and deprotonation reaction, **(B)** Acid labile linkages and **(C)** H$^+$-triggered ROS production.
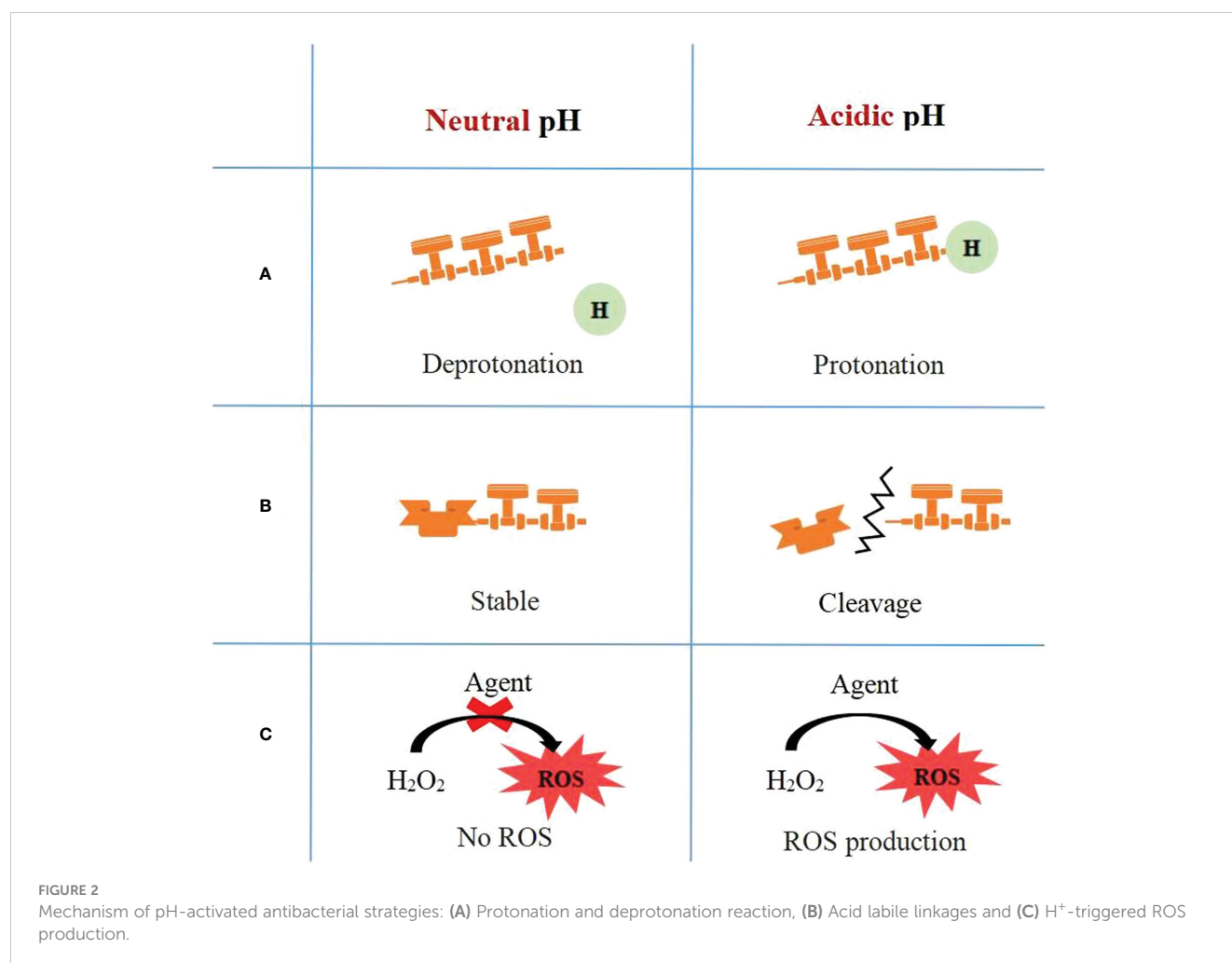
peptides, histatin-5 influences cell membrane functions by acting on intracellular targets. In addition, some researchers designed a novel pH-dependent peptide pHly-1 based on the structure of Lycosin-I, a cationic and amphiphilic peptide (Tan et al., 2013; Wang et al., 2014c). Aimed at enduing the peptide with the pH-responsive ability, researchers primarily exchanged lysine residues with histidine residues which increases positive charge and hydrophobicity of pHly-1; the anionic glutamic acid residues within lycosin-I were replaced by neutral glutamine residues which enabled pHly-1 to better interact with anionic microbial membranes; to improve hydrophobicity for membrane disruption, isoleucine with hydrophobicity substituted glycine and serine which are more hydrophilic (Zhang et al., 2022a). Especially, compared with the β-sheets and nanofibers structures at neutral pH, pHly-1 could adopt random coil-helix conformation and change into nanoparticles which promotes membrane permeation when pH decreased. Furthermore, inspired by the structure and pH-dependent ability of Clavanin A, other researchers designed two 14 aa long acid-activated peptides (AAPs) rich in histidine and phenylalanine residues to combat dental caries (Clark et al., 2021). Via protonation of histidine residues at low pH, positive charges of AAPs increased, and AAPs underwent a transition from a helical conformation to a random coil. Although the explicit antimicrobial

mechanism of AAPs is still unclear, the study confirmed that antimicrobial activity was closely associated with the increase in positive charges. Moreover, a 12 amino peptide, named GH12, with a large proportion of histidine residues and leucine residues, was synthesized (Wang et al., 2017). The protonation of histidine residues at low pH increased net positive charge of GH12, which led to the accumulation of cationic GH12 on negatively charged bacterial surfaces. Via the protonation reaction of histidine residues and increase of hydrophobicity around tryptophan sites, GH12 formed an amphipathic α-helix structure and killed bacteria by forming pores on cell membranes (Jiang et al., 2021). Similar to GH12, LH12 contains a histidine-rich sequence and can form an amphipathic α-helix structure to perturb microbial membranes (Jiang et al., 2022). Results showed that via reducing the gene expression of lactate dehydrogenase, alpha-subunit of F-type ATPase and glucosyltransferase, LH12 could inhibit acid production and biofilm formation.

Second strategy based on the protonation and deprotonation mechanism is the application of amine groups that exert switchable protonation and deprotonation ability along with the transformation of pH (Gannimani et al., 2020). Due to their pH switchable ability, amine groups have been widely applied to the design of antimicrobial agents. For example, DMAEM and

HMAEM, two novel kinds of tertiary amines, were incorporated into resin to modify its pH-responsive antibacterial property. DMAEM and HMAEM are composed of a long-chain alkane that could insert into bacterial membranes, a tertiary amine group, and a methacrylate-containing alkane. They have been confirmed to exhibit acid-activated antimicrobial and anticaries effects (Liang et al., 2020). In addition to the application in the design of antimrobial agents, amine groups can be ionizable moieties in drug delivery polymers, such as p(DMAEMA), trimethylamine, and polydopamine. Some researchers used poly(DMAEMA-co-HEMA) as a pH-sensitive drug carrier (Peng et al., 2022). DMAEMA contains tertiary amine with switchable protonation/deprotonation ability while responding to changes in pH (Brahim et al., 2003). Besides, the pKa of DMAEMA (around 7.5) is close to physiological pH. When pH is below the pKa, the monomer can be protonated and undergo structural changes, thus leading to swelling of the whole nanoparticle and delivery of drugs. HEMA, a hydrophilic polymer, can induce hydrophilicity on hydrophobic surfaces (Gulsen and Chauhan, 2005; Roointan et al., 2018). Moreover, amine groups in chitosan can be protonated when pH decreases (Yu et al., 2019; Yan et al., 2020). Researchers synthesized TMC-Lip nanoparticles consisting of negatively charged liposomes and positively charged TMC. Liposome, coated by TMC via electrostatic adsorption effect, was used to encapsulate DOX. The residual amines of TMC, as pH-responsive moieties, could protonate at low pH, which led to the charges of TMC-Lip nanoparticles shifting to the positive. The positive nanoparticles were able to selectively target anionic microbial cell surfaces and accumulate in biofilms. Besides, the protonation of TMC led to the instability of nanoparticles and drug release (Verheul et al., 2008; Mourya and Inamdar, 2009). Others grafted glycol chitosan with polydopamine which coated on the surface of nanoparticles. Via the protonation of amine groups in glycol chitosan at acid pH, the negatively charged nanoparticles turned positive, resulting in stronger adhesion with acidic biofilm (Xu et al., 2022a). Furthermore, some other researchers synthesized a pH-responsive core-shell nano micelle, mPEG-b-PDPA, which was capable of loading Bedaquiline. At low pH (below 6), the protonation of amine groups in PDPA segments shifted hydrophobicity in the core to hydrophilicity, and the spherical nanostructure of the micelle swelled and even disassembled, which resulted in drug release (Zhang et al., 2021).

Polymers with carboxyl groups, such as PAA and carboxybetaine methacrylate (CBMA), can also be protonated and applied to designs of drug release systems. Based on this, p(CBMA-co-DMAEMA) was fabricated as a pH-responsive hydrogel layer (Sun et al., 2022). Due to the protonation/deprotonation of carboxyl groups as pH changes, CBMA possesses the pH-activated property (Shao and Jiang, 2015). The protonation of amine groups and carboxyl groups in a carrier can exhibit synergistic pH-activated effects, so DMAEMA was incorporated as a synergistic pH switch. The protonation of the CBMA and DMAEMA at low pH accounted for the positive charges of hydrogel surface, which can capture negatively charged pathogens. With the transition of the layer's charge, the structure disassembles, accompanied by the release of antibacterial octapeptides (Sun et al., 2022). It is worth mentioning

that the octapeptide (Ac-Leu-Lys-Phe-Gln-Phe-His-Phe-Asp-NH2, IKFQFHFD) also processes pH-responsive properties (Wang et al., 2019). After the carboxylate groups were protonated, the IKFQFHFD formed a cationic amphiphilic structure similar to that of AMP, generating a potential pH-activated antimicrobial effect. In addition, other researchers designed the p(DMAEMA)-b-p(DMAEMA-co-BMA-co-PAA) that could self-assemble into ~21 nm cationic nanoparticles. The nanoparticle consisted of cationic coronas, p(DMAEMA), and p(DMAEMA-co-BMA-co-PAA) cores, which formed a structure with a hydrophilic surface and pH-activated hydrophobic interior. At acidic pH, DMAEMA and PAA residues protonated and the structure of carriers became unstable, accounting for drug release. It has been confirmed that cationic nanoparticles could selectively accumulate in the negatively charged bacterial biofilm surface and target anionic microorganisms (Ng et al., 2013).

3.2 Acid labile linkages

In addition to mechanisms based on protonation and deprotonation, pH-responsive antibiofilm systems with linkages that are labile at acidic environment are other promising strategies. pH responsive carriers incorporate citraconic amide, boric acid ester, hydrazone, disulfide bond, acid-base reaction, or ortho ester, into them as acid labile linkages, with which carriers are able to degrade when pH decreases (Huang et al., 2014; Lu et al., 2018; Deirram et al., 2019; Xu et al., 2022b).

Citraconic amide is formed by the reaction between citraconic anhydride and primary amines. At physiological pH, the citraconic amide is negatively charged and stable, but when pH decreases, it promptly cleaves back into the positively charged primary amine via degradation of linkage (Huang et al., 2014). When citraconic amide is incorporated into pH-sensitive drug delivery vehicles, the cleavage of citraconic amide at low pH can break the electrostatic balance and trigger the degradation of whole polymers (Lee et al., 2007; Lee et al., 2009), leading to drug release. Based on this mechanism, PEG-b-PAECOEMA/CA, the pH responsiveness of which comes from citraconic amide groups, was fabricated as a carrier of CHX (Zhao et al., 2019).

Boric acid ester bond, formed by the reaction between boric acid and hydroxy compound, is stable at physiological pH, but can degrade at low pH. MAL-PEG-b-PLL/PBA, the micelles carrier of tannic acid, conjugated tannic acid to PBA via boric acid ester bond. The micelles were pH-activated and capable of cleaving under cariogenic acidic conditions (Xu et al., 2022b). When the nanoparticles targeted the cariogenic dental plaque, boronate ester bonds responded to low pH and degraded, resulting in the release of tannic acid.

The hydrazone linkages are formed by condensation between hydrazide groups of carriers and aldehyde or ketones groups of the drugs (Sonawane et al., 2017). Those linkages can promptly hydrolysis when pH decreases below neutral physiological pH. Based on this, hydrazone linkages have been widely applied in conjugation between drugs and polymer backbones, aimed at reducing systemic toxicity by pH-triggered drug delivery (Yoshida

et al., 2013). For example, Far, derived from farnesol, was linked to PEG *via* hydrazone bonds. In acidic cariogenic microenvironment, the cleavage of hydrazine linkages leads to rapid release of Far, which improve the selectivity of Far (Chen et al., 2013; Mazzoni et al., 2015).

Disulfide bonds can cleave while reacting with H^+ and glutathione. Lu et al. introduced disulfide bonds into the silica framework of a novel kind of Mesoporous silica nanoparticles (MSNs), which was designed with redox/pH dual-controlled drug release ability (Lu et al., 2018). When pH decreases, the MSNs could degrade *via* the cleavage of disulfide bonds and glutathiones in the matrix could accelerate this process, resulting in the release of loaded Ag ions and CHX.

The chemical complexes assembled by the interaction of acid and base are unstable at low pH. Based on this, a novel kind of pH activated quaternary pyridinium salt was synthesized. The reversible control of antibacterial activity is achieved by acid-base interaction. Azo-QPS-C16 is a kind of antimicrobial agent. At physiological pH, alkaline triethanolamine interacted with weakly acid Azo-QPS-C16, and then two or more Azo-QPS-C16 assembled tightly into a sandwich stacking structure, which prevented Azo-QPS-C16 from exerting antibacterial efficiency. If pH decreases, the sandwich stacking structure will collapse and the Azo-QPS-C16 will come into effect. The active antimicrobial part of the Azo-QPS-C16 is the quaternary pyridinium salt and long alkyl chain, which can interact with the hydrophobic membrane and lyse the cell (Chen and Cooper, 2002). The quaternary pyridinium salt was able to adsorb on bacterial membranes by protonation in low pH while the long alkyl chain could insert into microbial membranes (Cheng et al., 2017; Gannimani et al., 2020).

3.3 H^+-triggered ROS production

ROS, an umbrella term referring to oxygen species with high reactivity, includes hydrogen peroxide (H_2O_2), singlet oxygen ($^1O_2$), hydroxyl radical (•OH), and superoxide anion radical ($O_2•^-$) (Nosaka and Nosaka, 2017; Cao et al., 2021). Besides directly damaging lipids, proteins, and DNA, ROS can destroy microbial membranes and cause the leakage of intracellular substances, which eventually results in the death of the bacteria (Li et al., 2021a). In addition, ROS production, as a major sterilization strategy, has higher antimicrobial efficacy and can reduce resistance of bacteria in contrast with traditional sterilization methods (Fu et al., 2021; Zhu et al., 2021). Therefore, H^+-triggered ROS production is a promising strategy for biofilm control.

CDT is a novel strategy to control cariogenic biofilm *via* ROS. The acid microenvironment can be used as a stimulus to trigger the production of H_2O_2. Metals ions such as Fe^{2+}, Mn^{2+}, and Cu^{2+} are able to react with H_2O_2 and promote the accumulation of ROS, mainly •OH, through the Fenton reaction or Fenton-like reaction (Bokare and Choi, 2014; Tang et al., 2019; Zhou et al., 2021), which leads to degradation of refractory organics (Chamarro et al., 2001; Pignatello et al., 2006) and inhibition of biofilm growth (Gao et al., 2016). ZnO_2-Cu@RB NPs are drug-loaded nanoparticles which achieves antibacterial responsiveness *via* the Fenton-like reaction

(Zhang et al., 2022b). ZnO_2 was added to produce H_2O_2 under acid environment by reaction $ZnO_2+2H^+ \rightarrow Zn^{2+}+H_2O_2$, enduing the nanoparticles with pH responsiveness. After that, copper ions could convert H_2O_2 into •OH with antibiofilm effects through the Fenton-like reaction ($2Cu^{2+}+H_2O_2 \rightarrow 2Cu^++O_2+2H^+$, $Cu^++H_2O_2 \rightarrow Cu^{2+}$ + OH^- +•OH).

CAT-NP can also produce ROS to control biofilms. Instead of relying on Fenton reactions, the catalytic activity has been confirmed to derive from the nanoparticles themselves (Wang et al., 2014a; Wang et al., 2014b). CAT-NP is able to perform a peroxidase-like activity that promptly catalyzes H_2O_2 at acid pH to form free radicals, which can both degrade EPS and kill bacteria (Gao et al., 2007). Aimed at enhancing the antibiofilm efficacy of iron oxide nanoparticles, some other researchers added GOx into iron oxide nanoparticles (Huang et al., 2021). GOx can catalyze glucose in EPS into H_2O_2 and H_2O_2 produced can react with iron oxide nanoparticles to produce ROS.

4 Biological safety

CHX is commonly used in clinical practice to prevent caries, but studies have shown that CHX has time-dependent and dose-dependent cytotoxic effects on gingival fibroblasts, and the concentration of 0.2% shows high toxicity. In addition, it kills oral microorganisms without selectivity and reduces the diversity of oral microbial community, thus destroying the ecological balance of microbial community and bringing great difficulties and challenges for clinical treatment (Mao et al., 2022). Studies have reported that pH-activated release of CHX and Ag-NPs biodegradable nanosystems (Ag-MSNs@CHX) can not only improve the anti-biofilm effect, compared to the CHX group showed significant cytotoxicity, Ag-MSNs@CHX also has a good safety at high concentrations (Lu et al., 2018). The smart pH-responsive agent, which only exerts antimicrobial action at acidic pH, is well suited for use in the uniquely acidic environment in which caries develop. It shows antibacterial effects during microbial dysregulation, rather than continuously killing all microorganisms, improving drug availability and maintaining microecological balance (Liang et al., 2020). pH-responsive drugs with targeted effects play their unique advantages in different fields, and their biocompatibility has attracted a lot of attention from scholars.

Many studies have designed pH activated antibacterial peptides, among which some scholars have reported that the antibacterial peptide GH12 has pH response characteristics, and this peptide shows stronger antibacterial and anti-biofilm activities under acidic pH. The peptide can not only maintain good stability in saliva, but also showed only a mild inhibitory effect at concentrations up to 128.0 µg/ml in a biotoxicity study, indicating a low cytotoxicity against human gingival fibroblasts (Jiang et al., 2021). Dual-sensitive antimicrobial peptide nanoparticles, pHly-1 NPs, showed reliable antimicrobial activity against Streptococcus pyogenes in acidic solutions mainly through cell membrane disruption. Compared with the clinically used mouthwash CHX, the development of dental caries in rats could be effectively inhibited with this nanoparticle. Moreover, by *in vitro* toxicity analysis, CHX

showed an IC_{50} value of 4.9 µM against human gingival fibroblasts, while pHly-1NPs exceeded 500µM. A concentration of 31.25 µM CHX induced approximately 40% of gastric-like organ death, but no significant effect was observed for treatments with pHly-1 NPs up to 500µM. It was shown that the nanoparticles exhibited a higher safety profile compared to the clinically used antimicrobial agent CHX (Zhang et al., 2022a).

In addition to pH activated antibacterial peptides, a series of nanomaterials were developed and designed to degrade the biofilm matrix by catalyzing the *in situ* generation of free radicals from hydrogen peroxide in an acidic environment, thereby destroying the caries biofilm. It is worth mentioning that the bio-safety of the materials was also verified while testing their antibiofilm effect. The experimental results show that the pH-responsive nanohybrid particles exhibit strong catalytic activity and antibiofilm properties at acidic pH, which do not cause harmful effects on mucosal tissues such as gingiva and palate *in vivo* and have good biocompatibility (Gao et al., 2016; Naha et al., 2019; Huang et al., 2021; Zhang et al., 2022b).

To improve the targeted antibacterial ability and reduce the side effects of broad-spectrum antimicrobial agents, scholars developed targeted negatively charged doxycycline (DOX) loaded nanocarriers (TMC-Lip DOX NPs). The experimental results showed that the material was effective in pH-activated removal of cariogenic biofilms and was biocompatible with non-toxicity to MC3T3-E1 cells (Zhou et al., 2018). Furthermore, a reactive multidrug delivery system (PMs@NaF-SAP) has been reported to effectively inhibit biofilm formation, which specifically adheres to tooth, identifies cariogenic conditions and intelligently releases drugs at acidic pH, thereby providing cariogenic biofilm resistance and restoring the microarchitecture and mechanical properties of demineralized teeth. Toxicological analysis showed that the nanosystem had little to no adverse effects on cells as well as gingival and palatal tissues (Xu et al., 2022b). In summary, pH-responsive antimicrobial materials, which play an antimicrobial role intelligently only at acidic pH, have been shown to be stable and biocompatible, and are a promising anti-biofilm agent.

5 Limitation and future prospects

Although pH-activated strategies have been widely explored, there are still some challenges that remain to be overcome. First, the antibiofilm researches are limited to one or several pathogenic microbes. Dental plaque is a highly diverse community of microorganism, containing about 500 types of bacteria (Paster et al., 2001; Wong and Sissons, 2001; Rasiah et al., 2005), so it is provincial to examine antimicrobial efficiency of agents only by uncomplicated *in vitro* model. A more sophisticated biofilm model *in vitro* and animal caries model *in vivo* should be included to better predict the efficacy of antimicrobial agents in future.

Besides, mature biofilms are highly assembled microbial communities surrounded by extracellular matrix, which protects the resident in deep layer from the antibacterial medicine. Digesting the extracellular matrix helps to improve penetrability of medicine into mature biofilms. At present, some pH-activated antimicrobial medicine are capable of digesting extracellular matrix or inhibiting the formation of EPS, such as pHly-1, GH12, LH12, DMAEM@RA, ZnO2-Cu@RB NPs, and CAT-NP, but most of agents lack ability to digest extracellular matrix. Synergistic combination of pH-activated bacterial killing and EPS digestion is regarded as a promising direction because of targeting specificity and eliminating efficacy.

Furthermore, the physical and biological complexity of the oral environment, such as saliva, should be taken into consideration. Due to the rapid clearance of saliva, topically applied medicine usually shows poor retention and a temporary effect. It is of tremendous significance to study pH-activated strategies with a long-term antibacterial effect. Some researches endow medicines with stronger adhesive ability by adding components which can selectively adhere to dental enamel, such as SAP and tris(tetran-butylammonium) hydrogen pyrophosphate (Yi et al., 2020; Xu et al., 2022b). Therefore, improving adhesion of antimicrobial agents may be a promising direction.

The pH-activated drug delivery system is used for controlling antimicrobials release, but the systems exhibit an ephemeral effect since it is hard to recharge the loaded drug once released. Accordingly, it is vital to develop pH-activated drug delivery systems which can re-captured agents when pH increases.

Although the researches on pH-activated antibiofilm strategies are flourishing, they are just carried out *in vitro* or in animal studies. More studies including clinical trials are needed to facilitate the wider acceptance of pH-activated antibiofilm strategies for controlling dental caries.

6 Conclusion

With the enhancement of microbial balance, pH-activated therapeutics, precision-guided to the acidic niches, have become novel strategies to control dental caries and aroused increasing attention among researchers. There are of tremendous significance and application potential for pH-activated antibiofilm materials to be adopted for clinical dental applications. Many studies indicate that pH-activated antibiofilm materials will be beneficial in cariostatic filed. But before them entering the market and reaching the dental chair, huge challenges related to long-term effects and cost-effectiveness need to be conquered, and the *in-vivo* effect should be further validated in clinical experiments.

Author contributions

XW, JL and SZ were involved in conceptualization, investigation, and writing original draft. WZ, LZ and XH were involved in review and editing. All authors contributed to the article and approved the submitted version.

Funding

Conflict of interest

The authors declare that the research was conducted in the absence of any commercial or financial relationships that could be construed as a potential conflict of interest.

Publisher's note

All claims expressed in this article are solely those of the authors and do not necessarily represent those of their affiliated organizations, or those of the publisher, the editors and the reviewers. Any product that may be evaluated in this article, or claim that may be made by its manufacturer, is not guaranteed or endorsed by the publisher.

References

Baliga, S., Muglikar, S., and Kale, R. (2013). Salivary pH: a diagnostic biomarker. *J. Indian. Soc Periodontol.* 17, 461–465. doi: 10.4103/0972-124X.118317

Bechinger, B., and Gorr, S. U. (2017). Antimicrobial peptides: mechanisms of action and resistance. *J. Dent. Res.* 96, 254–260. doi: 10.1177/0022034516679973

Benoit, D. S. W., Sims, K. R Jr, and Fraser, D. (2019). Nanoparticles for oral biofilm treatments. *ACS Nano.* 13, 4869–4875. doi: 10.1021/acsnano.9b02816

Bokare, A. D., and Choi, W. (2014). Review of iron-free fenton-like systems for activating H_2O_2 in advanced oxidation processes. *J. Hazard. Mater.* 275, 121–135. doi: 10.1016/j.jhazmat.2014.04.054

Bowen, W. H. (2013). The Stephan curve revisited. *Odontology* 101, 2–8. doi: 10.1007/s10266-012-0092-z

Bowen, W. H., Burne, R. A., Wu, H., and Koo, H. (2018). Oral biofilms: pathogens, matrix, and polymicrobial interactions in microenvironments. *Trends. Microbiol.* 26, 229–242. doi: 10.1016/j.tim.2017.09.008

Brahim, S., Narinesingh, D., and Guiseppi-Elie, A. (2003). Release characteristics of novel pH-sensitive p(HEMA-DMAEMA) hydrogels containing 3-(trimethoxy-silyl) propyl methacrylate. *Biomacromolecules* 4, 1224–1231. doi: 10.1021/bm034048r

Cao, Z., Li, D., Wang, J., and Yang, X. (2021). Reactive oxygen species-sensitive polymeric nanocarriers for synergistic cancer therapy. *Acta Biomater.* 130, 17–31. doi: 10.1016/j.actbio.2021.05.023

Chamarro, E., Marco, A., and Esplugas, S. (2001). Use of fenton reagent to improve organic chemical biodegradability. *Water. Res.* 35, 1047–1051. doi: 10.1016/s0043-1354(00)00342-0

Chen, H., Cheng, J., Cai, X., Han, J., Chen, X., You, L., et al. (2022). pH-switchable antimicrobial supramolecular hydrogels for synergistically eliminating biofilm and promoting wound healing. *ACS Appl. Mater. Interfaces.* 14, 18120–18132. doi: 10.1021/acsami.2c00580

Chen, C. Z., and Cooper, S. L. (2002). Interactions between dendrimer biocides and bacterial membranes. *Biomaterials* 23, 3359–3368. doi: 10.1016/s0142-9612(02)00036-4

Chen, F., Jia, Z., Rice, K. C., Reinhardt, R. A., Bayles, K. W., and Wang, D. (2013). The development of dentotropic micelles with biodegradable tooth-binding moieties. *Pharm. Res.* 30, 2808–2817. doi: 10.1007/s11095-013-1105-5

Chen, X., Ye, F., Luo, X., Liu, X., Zhao, J., Wang, S., et al. (2019). Histidine-specific peptide modification *via* visible-light-promoted c-h alkylation. *J. Am. Chem. Soc* 141, 18230–18237. doi: 10.1021/jacs.9b09127

Cheng, L., Zhang, K., Zhang, N., Melo, M. A. S., Weir, M. D., Zhou, X. D., et al. (2017). Developing a new generation of antimicrobial and bioactive dental resins. *J. Dent. Res.* 96, 855–863. doi: 10.1177/0022034517709739

Clark, S., Jowitt, T. A., Harris, L. K., Knight, C. G., and Dobson, C. B. (2021). The lexicon of antimicrobial peptides: a complete set of arginine and tryptophan sequences. *Commun. Biol.* 4, 605. doi: 10.1038/s42003-021-02137-7

Dadfar, S. M., Roemhild, K., Drude, N. I., von Stillfried, S., Knüchel, R., Kiessling, F., et al. (2019). Iron oxide nanoparticles: diagnostic, therapeutic and theranostic applications. *Adv. Drug Deliv. Rev.* 138, 302–325. doi: 10.1016/j.addr.2019.01.005

Dashper, S. G., Liu, S. W., and Reynolds, E. C. (2007). Antimicrobial peptides and their potential as oral therapeutic agents. *Int. J. Pept. Res. Ther.* 13, 505–516. doi: 10.1007/s10989-007-9094-z

Deirram, N., Zhang, C., Kermaniyan, S. S., Johnston, A. P. R., and Such, G. K. (2019). pH-responsive polymer nanoparticles for drug delivery. *Macromol Rapid Commun.* 40, e1800917. doi: 10.1002/marc.201800917

Eckert, R., He, J., Yarbrough, D. K., Qi, F., Anderson, M. H., and Shi, W. (2006). Targeted killing of *Streptococcus mutans* by a pheromone-guided "smart" antimicrobial peptide. *Antimicrob. Agents chemother.* 50, 3651–3657. doi: 10.1128/AAC.00622-06

Fabian, T. K., Hermann, P., Beck, A., Fejérdy, P., and Fábián, G. (2012). Salivary defense proteins: Their network and role in innate and acquired oral immunity. *Int. J. Mol. Sci.* 13, 4295–4320. doi: 10.3390/ijms13044295

Flemming, H. C., Wingender, J., Szewzyk, U., Steinberg, P., Rice, S. A., and Kjelleberg, S. (2016). Biofilms: An emergent form of bacterial life. *Nat. Rev. Microbiol.* 14, 563–575. doi: 10.1038/nrmicro.2016.94

Fu, Y., Yang, L., Zhang, J., Hu, J., Duan, G., Liu, X., et al. (2021). Polydopamine antibacterial materials. *Mater. Horiz.* 8, 1618–1633. doi: 10.1039/d0mh01985b

Gannimani, R., Walvekar, P., Naidu, V. R., Aminabhavi, T. M., and Govender, T. (2020). Acetal containing polymers as pH-responsive nano-drug delivery systems. *J. Control. Release* 328, 736–761. doi: 10.1016/j.jconrel.2020.09.044

Gao, L., Liu, Y., Kim, D., Li, Y., Hwang, G., Naha, P. C., et al. (2016). Nanocatalysts promote streptococcus mutans biofilm matrix degradation and enhance bacterial killing to suppress dental caries *in vivo*. *Biomaterials* 101, 272–284. doi: 10.1016/j.biomaterials.2016.05.051

Gao, L., Xu, T., Huang, G., Jiang, S., Gu, Y., and Chen, F. (2018). Oral microbiomes: more and more importance in oral cavity and whole body. *Protein. Cell.* 9, 488–500. doi: 10.1007/s13238-018-0548-1

Gao, L., Zhuang, J., Nie, L., Zhang, J., Zhang, Y., Gu, N., et al. (2007). Intrinsic peroxidase-like activity of ferromagnetic nanoparticles. *Nat. Nanotechnol.* 2, 577–583. doi: 10.1038/nnano.2007.260

Gibbons, R. J., and Banghart, S. B. (1967). Synthesis of extracellular dextran by cariogenic bacteria and its presence in human dental plaque. *Arch. Oral. Biol.* 12, 11–23. doi: 10.1016/0003-9969(67)90137-9

Gopal, J., Chun, S., and Doble, M. (2016). Attenuated total reflection fourier transform infrared spectroscopy towards disclosing mechanism of bacterial adhesion on thermally stabilized titanium nano-interfaces. *J. Mater. Sci-Mater M.* 27, 135. doi: 10.1007/s10856-016-5739-9

Gulsen, D., and Chauhan, A. (2005). Dispersion of microemulsion drops in HEMA hydrogel: A potential ophthalmic drug delivery vehicle. *Int. J. Pharm.* 292, 95–117. doi: 10.1016/j.ijpharm.2004.11.033

Guo, L., McLean, J. S., Yang, Y., Eckert, R., Kaplan, C. W., Kyme, P., et al. (2015). Precision-guided antimicrobial peptide as a targeted modulator of human microbial ecology. *Proc. Natl. Acad. Sci. U.S.A.* 16;112 (24), 7569–7574. doi: 10.1073/pnas.1506207112

Gupta, P., Vermani, K., and Garg, S. (2002). Hydrogels: from controlled release to pH-responsive drug delivery. *Drug Discov. Today* 15, 7(10):569–79. doi: 10.1016/s1359-6446(02)02255-9

Hajishengallis, E., Parsaei, Y., Klein, M. I., and Koo, H. (2017). Advances in the microbial etiology and pathogenesis of early childhood caries. *Mol. Oral. Microbiol.* 32, 24–34. doi: 10.1111/omi.12152

Harris, J. M., and Chess, R. B. (2003). Effect of pegylation on pharmaceuticals. *Nat. Rev. Drug Discov.* 2, 214–221. doi: 10.1038/nrd1033

Harris, F., Dennison, S. R., and Phoenix, D. A. (2009). Anionic antimicrobial peptides from eukaryotic organisms. *Curr. Protein Pept. Sci.* 10, 585–606. doi: 10.2174/138920309789630589

Horch, M., Pinto, A. F., Mroginski, M. A., Teixeira, M., Hildebrandt, P., and Zebger, I. (2014). Metal-induced histidine deprotonation in biocatalysis? Experimental and theoretical insights into superoxide reductase. *RSC Adv.* 4, 54091–54095. doi: 10.1039/c4ra11976b

Horev, B., Klein, M. I., Hwang, G., Li, Y., Kim, D., Koo, H., et al. (2015). pH-activated nanoparticles for controlled topical delivery of farnesol to disrupt oral biofilm virulence. *ACS. Nano.* 9, 2390–2404. doi: 10.1021/nn507170s

Hu, F., Zhou, Z., Xu, Q., Fan, C., Wang, L., Ren, H., et al. (2019). A novel pH-responsive quaternary ammonium chitosan-liposome nanoparticles for periodontal treatment. *Int. J. Biol. Macromol.* 129, 1113–1119. doi: 10.1016/j.ijbiomac.2018.09.057

Huang, H., Li, Y., Sa, Z., Sun, Y., Wang, Y., and Wang, J. (2014). A smart drug delivery system from charge-conversion polymer-drug conjugate for enhancing tumor therapy and tunable drug release. *Macromol. Biosci.* 14, 485–490. doi: 10.1002/mabi.201300337

Huang, Y., Liu, Y., Shah, S., Kim, D., Simon-Soro, A., Ito, T., et al. (2021). Precision targeting of bacterial pathogen *via* bi-functional nanozyme activated by biofilm microenvironment. *Biomaterials* 268, 120581. doi: 10.1016/j.biomaterials.2020.120581

Huo, L., Huang, X., Ling, J., Liu, H., and Liu, J. (2018). Selective activities of STAMPs against *Streptococcus mutans*. *Exp. Ther. Med.* 15 (2), 1886–1893. doi: 10.3892/etm.2017.5631

Imai, K., Shimizu, K., Kamimura, M., and Honda, H. (2018). Interaction between porous silica gel microcarriers and peptides for oral administration of functioptides. *Sci. Rep.* 8, 10971. doi: 10.1038/s41598-018-29345-2

Jiang, W., Luo, J., Wang, Y., Chen, X., Jiang, X., Feng, Z., et al. (2021). The pH-responsive property of antimicrobial peptide GH12 enhances its anticaries effects at acidic pH. *Caries. Res.* 55, 21–31. doi: 10.1159/000508458

Jiang, W., Wang, Y., Luo, J., Li, X., Zhou, X., Li, W., et al. (2018). Effects of antimicrobial peptide GH12 on the cariogenic properties and composition of a cariogenic multispecies biofilm. *Appl. Environ. Microbiol.* 84, e01423–e01418. doi: 10.1128/AEM.01423-18

Jiang, W., Xie, Z., Huang, S., Huang, Q., Chen, L., Gao, X., et al. (2022). Targeting cariogenic pathogens and promoting competitiveness of commensal bacteria with a novel pH-responsive antimicrobial peptide. *J. Oral. Microbiol.* 15, 2159375. doi: 10.1080/20002297.2022.2159375

Khurshid, Z., Najeeb, S., Mali, M., Moin, S. F., Raza, S. Q., Zohaib, S., et al. (2017). Histatin peptides: pharmacological functions and their applications in dentistry. *Saudi. Pharm. J.* 25, 25–31. doi: 10.1016/j.jsps.2016.04.027

Kleinberg, I. (2002). A mixed-bacteria ecological approach to understanding the role of the oral bacteria in dental caries causation: an alternative to *Streptococcus mutans* and the specific-plaque hypothesis. *Crit. Rev. Oral. Biol. Med.* 13, 108–125. doi: 10.1177/154411130201300202

Kost, J., and Langer, R. (2012). Responsive polymeric delivery systems. *Adv. Drug Deliv. Rev.* 64, 327–341. doi: 10.1016/j.addr.2012.09.014

Krzyściak, W., Jurczak, A., Piątkowski, J., Kościelniak, D., Gregorczyk-Maga, I., Kołodziej, I., et al. (2015). Effect of histatin-5 and lysozyme on the ability of *Streptococcus mutans* to form biofilms in *in vitro* conditions. *Postepy. Hig. Med. Dosw* 69, 1056–1066. doi: 10.5604/01.3001.0009.6575

Kuang, X., Chen, V., and Xu, X. (2018). Novel approaches to the control of oral microbial biofilms. *Biomed. Res. Int.* 2018, 6498932. doi: 10.1155/2018/6498932

Lee, I. H., Cho, Y., and Lehrer, R. I. (1997a). Effects of pH and salinity on the antimicrobial properties of clavanins. *Infect. Immun.* 65, 2898–2903. doi: 10.1128/iai.65.7.2898-2903.1997

Lee, Y., Fukushima, S., Bae, Y., Hiki, S., Ishii, T., and Kataoka, K. (2007). A protein nanocarrier from charge-conversion polymer in response to endosomal pH. *J. Am. Chem. Soc.* 129, 5362–5363. doi: 10.1021/ja071090b

Lee, Y., Ishii, T., Cabral, H., Kim, H. J., Seo, J. H., Nishiyama, N., et al. (2009). Charge-conversional polyionic complex micelles-efficient nanocarriers for protein delivery into cytoplasm. *Angew. Chem. Int. Ed. Engl.* 48, 5309–5312. doi: 10.1002/anie.200900064

Lee, I. H., Zhao, C., Cho, Y., Harwig, S. S., Cooper, E. L., and Lehrer, R. I. (1997b). Clavanins, alpha-helical antimicrobial peptides from tunicate hemocytes. *FEBS. Lett.* 400, 158–162. doi: 10.1016/s0014-5793(96)01374-9

Li, H., Zhou, X., Huang, Y., Liao, B., Cheng, L., and Ren, B. (2021a). Reactive oxygen species in pathogen clearance: the killing mechanisms, the adaption response, and the side effects. *Front. Microbial.* 11, 622534. doi: 10.3389/fmicb.2020.622534

Li, S. L., Jiang, P., Jang, F. L., and Liu, Y. (2021b). Recent advances in nanomaterial-based nanoplatforms for chemodynamic cancer therapy. *Adv. Funct. Mater.* 31, 2100243. doi: 10.1002/adfm.202100243

Liang, J., Liu, F., Zou, J., Xu, H. H. K., Han, Q., Wang, Z., et al. (2020). pH-responsive antibacterial resin adhesives for secondary caries inhibition. *J. Dent. Res.* 99, 1368–1376. doi: 10.1177/0022034520936639

Liu, Y., Kamesh, A. C., Xiao, Y., Sun, V., Hayes, M., Daniell, H., et al. (2016). Topical delivery of low-cost protein drug candidates made in chloroplasts for biofilm disruption and uptake by oral epithelial cells. *Biomaterials* 105, 156–166. doi: 10.1016/j.biomaterials.2016.07.042

Liu, Y. L., Nascimento, M., and Burne, R. A. (2012). Progress toward understanding the contribution of alkali generation in dental biofilms to inhibition of dental caries. *Int. J. Oral. Sci.* 4, 135–140. doi: 10.1038/ijos.2012.54

Liu, Y., Ren, Z., Hwang, G., and Koo, H. (2018). Therapeutic strategies targeting cariogenic biofilm microenvironment. *Adv. Dent. Res.* 29 (1), 86–92. doi: 10.1177/0022034517736497

Lu, M. M., Ge, Y., Qiu, J., Shao, D., Zhang, Y., Bai, J., et al. (2018). Redox/pH dual-controlled release of chlorhexidine and silver ions from biodegradable mesoporous silica nanoparticles against oral biofilms. *Int. J. Nanomed.* 13, 7697–7709. doi: 10.2147/IJN.S181168

Luo, Y., and Song, Y. (2021). Mechanism of antimicrobial peptides: antimicrobial, anti-inflammatory and antibiofilm activities. *Int. J. Mol. Sci.* 22, 11401. doi: 10.3390/ijms222111401

Malik, E., Dennison, S. R., Harris, F., and Phoenix, D. A. (2016). pH dependent antimicrobial peptides and proteins, their mechanisms of action and potential as therapeutic agents. *Pharm. (Basel).* 9, 67. doi: 10.3390/ph9040067

Malkoski, M., Dashper, S. G., O'Brien-Simpson, N. M., Talbo, G. H., Macris, M., Cross, K. J., et al. (2001). Kappacin, a novel antibacterial peptide from bovine milk. *Antimicrob. Agents. Chemother.* 45, 2309–2315. doi: 10.1128/AAC.45.8.2309-2315.2001

Mao, X., Hiergeist, A., Auer, D. L., Scholz, K. J., Muehler, D., Hiller, K. A., et al. (2022). Ecological effects of daily antiseptic treatment on microbial composition of saliva-grown microcosm biofilms and selection of resistant phenotypes. *Front. Microbiol.* 13. doi: 10.3389/fmicb.2022.934525

Margolis, H. C., Zhang, Y. P., Lee, C. Y., Kent, R. L.Jr., and Moreno, E. C. (1999). Kinetics of enamel demineralization *in vitro*. *J. Dent. Res.* 78 (7), 1326–1335. doi: 10.1177/00220345990780070701

Marsh, P. D., Do, T., Beighton, D., and Devine, D. A. (2016). Influence of saliva on the oral microbiota. *Periodontol. 2000.* 70, 80–92. doi: 10.1111/prd.12098

Mazzoni, A., Tjäderhane, L., Checchi, V., Di Lenarda, R., Salo, T., Tay, F. R., et al. (2015). Role of dentin MMPs in caries progression and bond stability. *J. Dent. Res.* 94, 241–251. doi: 10.1177/0022034514562833

Mochon, A. B., and Liu, H. (2008). The antimicrobial peptide histatin-5 causes a spatially restricted disruption on the *Candida albicans* surface, allowing rapid entry of the peptide into the cytoplasm. *PLoS. Pathog.* 4, e1000190. doi: 10.1371/journal.ppat.1000190

Montoya, C., Jain, A., Londoño, J. J., Correa, S., Lelkes, P. I., Melo, M. A., et al. (2021). Multifunctional dental composite with piezoelectric nanofillers for combined antibacterial and mineralization effects. *ACS Appl. Mater. Interfaces.* 13, 43868–43879. doi: 10.1021/acsami.1c06331

Mourya, V. K., and Inamdar, N. N. (2009). Trimethyl chitosan and its applications in drug delivery. *J. Mater. Sci. Mater. Med.* 20, 1057–1079. doi: 10.1007/s10856-008-3659-z

Naha, P. C., Liu, Y., Hwang, G., Huang, Y., Gubara, S., Jonnakuti, V., et al. (2019). Dextran-coated iron oxide nanoparticles as biomimetic catalysts for localized and pH-activated biofilm disruption. *ACS Nano.* 13, 4960–4971. doi: 10.1021/acsnano.8b08702

Naksagoon, T., Takenaka, S., Nagata, R., Sotozono, M., Ohsumi, T., Ida, T., et al. (2021). A repeated state of acidification enhances the anticariogenic biofilm activity of glass ionomer cement containing fluoro-zinc-silicate fillers. *Antibiotics* 10, 977. doi: 10.3390/antibiotics10080977

Ng, V. W., Ke, X., Lee, A. L., Hedrick, J. L., and Yang, Y. Y. (2013). Synergistic co-delivery of membrane-disrupting polymers with commercial antibiotics against highly opportunistic bacteria. *Adv. Mater.* 25, 6730–6736. doi: 10.1002/adma.201302952

Nosaka, Y., and Nosaka, A. Y. (2017). Generation and detection of reactive oxygen species in photocatalysis. *Chem. Rev.* 117, 11302–11336. doi: 10.1021/acs.chemrev.7b00161

Osada, K., Yamasaki, Y., Katayose, S., and Kataoka, K. (2005). A synthetic block copolymer regulates S1 nuclease fragmentation of supercoiled plasmid DNA. *Angew. Chem. Int. Ed. Engl.* 44, 3544–3548. doi: 10.1002/anie.200500201

Paster, B. J., Boches, S. K., Galvin, J. L., Ericson, R. E., Lau, C. N., Levanos, V. A., et al. (2001). Bacterial diversity in human subgingival plaque. *J. Bacteriol.* 183 (12), 3770–3783. doi: 10.1128/JB.183.12.3770-3783.2001

Peng, X., Han, Q., Zhou, X., Chen, Y., Huang, X., Guo, X., et al. (2022). Effect of pH-sensitive nanoparticles on inhibiting oral biofilms. *Drug Deliv.* 29, 561–573. doi: 10.1080/10717544.2022.2037788

Pignatello, J. J., Oliveros, E., and Mackay, A. (2006). Advanced oxidation processes for organic contaminant destruction based on the fenton reaction and related chemistry. *Crit. Rev. Env. Sci. Tec.* 36, 1–84. doi: 10.1080/10643380500326564

Pitts, N. B., Zero, D. T., Marsh, P. D., Ekstrand, K., Weintraub, J. A., Ramos-Gomez, F., et al. (2017). Dental caries. *Nat. Rev. Dis. Primers.* 3, 17030. doi: 10.1038/nrdp.2017.30

Rasiah, I. A., Wong, L., Anderson, S. A., and Sissons, C. H. (2005). V Ariation in bacterial DGGE patterns from human saliva: Over time, between individuals and in corresponding dental plaque microcosms. *Arch. Oral. Biol.* 50, 779–787. doi: 10.1016/j.archoralbio.2005.02.001

Reddy, K. V., Yedery, R. D., and Aranha, C. (2004). Antimicrobial peptides: premises and promises. *Int. J. Antimicrob. Agents.* 24 (6), 536–547. doi: 10.1016/j.ijantimicag.2004.09.005

Roointan, A., Farzanfar, J., Mohammadi-Samani, S., Behzad-Behbahani, A., and Farjadian, F. (2018). Smart pH responsive drug delivery system based on poly(HEMA-co-DMAEMA) nanohydrogel. *Int. J. Pharmaceut.* 552, 301–311. doi: 10.1016/j.ijpharm.2018.10.001

Rosier, B. T., Marsh, P. D., and Mira, A. (2018). Resilience of the oral microbiota in health: mechanisms that prevent dysbiosis. *J. Dent. Res.* 97, 371–380. doi: 10.1177/0022034517742139

Selwitz, R. H., Ismail, A. I., and Pitts, N. B. (2007). Dental caries. *Lancet* 369, 51–59. doi: 10.1016/S0140-6736(07)60031-2

Shao, Q., and Jiang, S. (2015). Molecular understanding and design of zwitterionic materials. *Adv. Mater.* 27, 15–26. doi: 10.1002/adma.201404059

Shi, Y., Liang, J., Zhou, X., Ren, B., Wang, H., Han, Q., et al. (2022). Effects of a novel, intelligent, pH-responsive resin adhesive on cariogenic biofilms *in vitro*. *Pathogens* 11 (9), 1014. doi: 10.3390/pathogens11091014

Simón-Soro, A., and Mira, A. (2015). Solving the etiology of dental caries. *Trends. Microbiol.* 23, 76–82. doi: 10.1016/j.tim.2014.10.010

Sims, K. R., Liu, Y., Hwang, G., Jung, H. I., Koo, H., and Benoit, D. S. W. (2018). Enhanced design and formulation of nanoparticles for anti-biofilm drug delivery. *Nanoscale* 11, 219–236. doi: 10.1039/c8nr05784b

Sonawane, S. J., Kalhapure, R. S., and Govender, T. (2017). Linkages in pH responsive drug delivery systems. *Eur. J. Pharm. Sci.* 99, 45–65. doi: 10.1016/j.ejps.2016.12.011

Steinbuch, K. B., and Fridman, M. (2016). Mechanisms of resistance to membrane-disrupting antibiotics in gram-positive and gram-negative bacteria. *Med. Chem. Commun.* 7, 86–102. doi: 10.1039/C5MD00389J

Sun, F., Hu, W., Zhao, Y., Li, Y., Xu, X., Li, Y., et al. (2022). Invisible assassin coated on dental appliances for on-demand capturing and killing of cariogenic bacteria. *Colloids Surf. B Biointerfaces.* 217, 112696. doi: 10.1016/j.colsurfb.2022.112696

Takahashi, N., and Nyvad, B. (2011). The role of bacteria in the caries process: ecological perspectives. *J. Dent. Res.* 90, 294–303. doi: 10.1177/0022034510379602

Tan, H., Ding, X., Meng, S., Liu, C., Wang, H., Xia, L., et al. (2013). Antimicrobial potential of lycosin-I, a cationic and amphiphilic peptide from the venom of the spider lycosa singorensis. *Curr. Mol. Med.* 13, 900–910. doi: 10.2174/15665240113139990045

Tang, Z., Liu, Y., He, M., and Bu, W. (2019). Chemodynamic therapy: tumour microenvironment-mediated fenton and fenton-like reactions. *Angew. Chem. Int. Ed. Engl.* 58, 946–956. doi: 10.1002/anie.201805664

Tanner, A. C. R., Kressirer, C. A., Rothmiller, S., Johansson, I., and Chalmers, N. I. (2018). The caries microbiome: implications for reversing dysbiosis. *Adv. Dent. Res.* 29 (1), 78–85. doi: 10.1177/0022034517736496

Thaker, H. D., Cankaya, A., Scott, R. W., and Tew, G. N. (2013). Role of amphiphilicity in the design of synthetic mimics of antimicrobial peptides with gram-negative activity. *ACS Med. Chem. Lett.* 4, 481–485. doi: 10.1021/ml300307b

Tu, H., Fan, Y., Lv, X., Han, S., Zhou, X., and Zhang, L. (2016). Activity of synthetic antimicrobial peptide GH12 against oral streptococci. *Caries Res.* 50, 48–61. doi: 10.1159/000442898

van Kan, E. J., Demel, R. A., Breukink, E., van der Bent, A., and de Kruijff, B. (2002). Clavanin permeabilizes target membranes *via* two distinctly different pH-dependent mechanisms. *Biochemistry* 41, 7529–7539. doi: 10.1021/bi012162t

van Kan, E. J., Demel, R. A., van der Bent, A., and de Kruijff, B. (2003a). The role of the abundant phenylalanines in the mode of action of the antimicrobial peptide clavanin. *Biochim. Biophys. Acta* 1615, 84–92. doi: 10.1016/s0005-2736(03)00233-5

van Kan, E. J., Ganchev, D. N., Snel, M. M., Chupin, V., van der Bent, A., and de Kruijff, B. (2003b). The peptide antibiotic clavanin a interacts strongly and specifically with lipid bilayers. *Biochemistry* 42, 11366–11372. doi: 10.1021/bi0349017

Verheul, R. J., Amidi, M., van der Wal, S., van Riet, E., Jiskoot, W., and Hennink, W. E. (2008). Synthesis, characterization and *in vitro* biological properties of O-methyl free N,N,N-trimethylated chitosan. *Biomaterials* 29, 3642–3649. doi: 10.1016/j.biomaterials.2008.05.026

Wang, J., Chen, X. Y., Zhao, Y., Yang, Y., Wang, W., Wu, C., et al. (2019). pH-switchable antimicrobial nanofiber networks of hydrogel eradicate biofilm and rescue stalled healing in chronic wounds. *ACS Nano.* 13, 11686–11697. doi: 10.1021/acsnano.9b05608

Wang, Y., Fan, Y., Zhou, Z., Tu, H., Ren, Q., Wang, X., et al. (2017). *De novo* synthetic short antimicrobial peptides against cariogenic bacteria. *Arch. Oral. Biol.* 80, 41–50. doi: 10.1016/j.archoralbio.2017.03.017

Wang, H., Jiang, H., Wang, S., Shi, W., He, J., Liu, H., et al. (2014a). Fe₃O₄-MWCNT magnetic nanocomposites as efficient peroxidase mimic catalysts in a fenton-like reaction for water purification without pH limitation. *RSC Adv.* 4, 45809–45815. doi: 10.1039/c4ra07327d

Wang, L., Min, Y., Xu, D., Yu, F., Zhou, W., and Cuschieri, A. (2014b). Membrane lipid peroxidation by the peroxidase-like activity of magnetite nanoparticles. *Chem. Commun.* 50, 11147–11150. doi: 10.1039/c4cc03082f

Wang, L., Wang, Y. J., Liu, Y. Y., Li, H., Guo, L. X., Liu, Z. H., et al. (2014c). *In vitro* potential of lycosin-I as an alternative antimicrobial drug for treatment of multidrug-resistant *Acinetobacter baumannii* infections. *Antimicrob. Agents. Chemother.* 58, 6999–7002. doi: 10.1128/AAC.03279-14

Wiradharma, N., Khoe, U., Hauser, C., Seow, S. V., Zhang, S., and Yang, Y. Y. (2011). Synthetic cationic amphiphilic α-helical peptides as antimicrobial agents. *Biomaterials* 32, 2204–2212. doi: 10.1016/j.biomaterials.2010.11.054

Wong, L., and Sissons, C. (2001). A comparison of human dental plaque microcosm biofilms grown in an undefined medium and a chemically defined artificial saliva. *Arch. Oral. Biol* 46 (6), 477–486. doi: 10.1016/s0003-9969(01)00016-4

Xiang, S. W., Shao, J., He, J., Wu, X. Y., Xu, X. H., and Zhao, W. H. (2019). A membrane-targeted peptide inhibiting PtxA of phosphotransferase system blocks *Streptococcus mutans*. *Caries Res.* 53 (2), 176–193. doi: 10.1159/000489607

Xiao, J., Klein, M. I., Falsetta, M. L., Lu, B., Delahunty, C. M., Yates, J. R., et al. (2012). The exopolysaccharide matrix modulates the interaction between 3D architecture and virulence of a mixed-species oral biofilm. *PLoS. Pathog.* 8, e1002623. doi: 10.1371/journal.ppat.1002623

Xiong, M., Lee, M. W., Mansbach, R. A., Song, Z., Bao, Y., Peek, R. M., et al. (2015). Helical antimicrobial polypeptides with radial amphiphilicity. *Proc. Natl. Acad. Sci. U.S.A.* 112, 13155–13160. doi: 10.1073/pnas.1507893112

Xu, X., Fan, M., Yu, Z., Zhao, Y., Zhang, H., Wang, J., et al. (2022a). A removable photothermal antibacterial "warm paste" target for cariogenic bacteria. *Chem. Eng. J.* 429, 132491. doi: 10.1016/j.cej.2021.132491

Xu, Y., You, Y., Yi, L., Wu, X., Zhao, Y., Yu, J., et al. (2022b). Dental plaque-inspired versatile nanosystem for caries prevention and tooth restoration. *Bioact. Mater.* 20, 418–433. doi: 10.1016/j.bioactmat.2022.06.010

Yan, L. X., Chen, L. J., Zhao, X., and Yan, X. P. (2020). pH switchable nanoplatform for *in vivo* persistent luminescence imaging and precise photothermal therapy of bacterial infection. *Adv. Funct. Mater.* 30, 1909042. doi: 10.1002/adfm.201909042

Yang, Y., Reipa, V., Liu, G., Meng, Y., Wang, X., Mineart, K. P., et al. (2018). pH-sensitive compounds for selective inhibition of acid-producing bacteria. *ACS. Appl. Mater. Interfaces.* 10, 8566–8573. doi: 10.1021/acsami.8b01089

Yi, Y., Wang, L., Chen, L., Lin, Y., Luo, Z., Chen, Z., et al. (2020). Farnesal-loaded pH-sensitive polymeric micelles provided effective prevention and treatment on dental caries. *J. Nanobiotechnol.* 18, 89. doi: 10.1186/s12951-020-00633-2

Yoshida, T., Lai, T. C., Kwon, G. S., and Sako, K. (2013). pH- and ion-sensitive polymers for drug delivery. *Expert. Opin. Drug Deliv.* 10, 1497–1513. doi: 10.1517/17425247.2013.821978

Yu, X., He, D., Zhang, X., Zhang, H., Song, J., Shi, D., et al. (2019). Surface-adaptive and initiator-loaded graphene as a light-induced generator with free radicals for drug-resistant bacteria eradication. *ACS Appl. Mater. Interfaces.* 11 (2), 1766–1781. doi: 10.1021/acsami.8b12873

Yue, J., Luo, S. Z., Lu, M. M., Shao, D., Wang, Z., and Dong, W. F. (2018). A comparison of mesoporous silica nanoparticles and mesoporous organosilica nanoparticles as drug vehicles for cancer therapy. *Chem. Biol. Drug Des.* 92, 1435–1444. doi: 10.1111/cbdd.13309

Zasloff, M. (2002). Antimicrobial peptides of multicellular organisms. *Nature* 415, 389–395. doi: 10.1038/415389a

Zhang, Y., Liu, W., and Huang, Y. (2022b). Bacterial biofilm microenvironment responsive copper-doped zinc peroxide nanocomposites for enhancing chemodynamic therapy. *Cheml. Eng. J.* 446, 137214. doi: 10.1016/j.cej.2022.137214

Zhang, P., Wu, S., Li, J., Bu, X., Dong, X., Chen, N., et al. (2022a). Dual-sensitive antibacterial peptide nanoparticles prevent dental caries. *Theranostics* 12, 4818–4833. doi: 10.7150/thno.73181

Zhang, M., Yu, Z., and Lo, E. C. M. (2021). A new pH-responsive nano micelle for enhancing the effect of a hydrophobic bactericidal agent on mature *Streptococcus mutans* biofilm. *Front. Microbiol.* 12. doi: 10.3389/fmicb.2021.761583

Zhao, Z., Ding, C., Wang, Y., Tan, H., and Li, J. (2019). pH-responsive polymeric nanocarriers for efficient killing of cariogenic bacteria in biofilms. *Biomater. Sci.* 7, 1643–1651. doi: 10.1039/c8bm01640b

Zhou, J., Horev, B., Hwang, G., Klein, M. I., Koo, H., and Benoit, D. S. (2016). Characterization and optimization of pH-responsive polymer nanoparticles for drug delivery to oral biofilms. *J. Mater. Chem. B.* 4 (18), 3075–3085. doi: 10.1039/C5TB02054A

Zhou, Z., Hu, F., Hu, S., Kong, M., Feng, C., Liu, Y., et al. (2018). pH-activated nanoparticles with targeting for the treatment of oral plaque biofilm. *J. Mater. Chem. B.* 6, 586–592. doi: 10.1039/c7tb02682j

Zhou, H., Li, X., Niu, D., Li, Y., Liu, X., Li, C., et al. (2021). Ultrasensitive chemodynamic therapy: bimetallic peroxide triggers high pH-activated, synergistic effect/H₂O₂ self-supply-mediated cascade fenton chemistry. *Adv. Healthc. Mater.* 10, e2002126. doi: 10.1002/adhm.202002126

Zhu, S., Yu, Q., Huo, C., Li, Y., He, L., Ran, B., et al. (2021). Ferroptosis: a novel mechanism of artemisinin and its derivatives in cancer therapy. *Curr. Med. Chem.* 28, 329–345. doi: 10.2174/0929867327666200121124404

OPEN ACCESS

*CORRESPONDENCE
Qi Han
✉ hanqi992011@163.com

†These authors have contributed equally to
this work

The effect of argon cold atmospheric plasma on the metabolism and demineralization of oral plaque biofilms

Haowei Zhao[1†], Xu Wang[2†], Zhuo Liu[3†], Ye Wang[4], Ling Zou[4], Yu Chen[1] and Qi Han[1*]

[1]State Key Laboratory of Oral Diseases and National Clinical Research Center for Oral Diseases, Department of Oral Pathology, West China Hospital of Stomatology, Sichuan University, Chengdu, China, [2]School of Mechanical Engineering, Sichuan University, Chengdu, China, [3]College of Intelligent Systems Science and Engineering, Huber Minzu University, Enshi, China, [4]State Key Laboratory of Oral Diseases and National Clinical Research Center for Oral Diseases, Department of Endodontics, West China Hospital of Stomatology, Sichuan University, Chengdu, China

Objective: The aim of this study was to design and optimize a cold atmospheric plasma (CAP) device that could be applied in an oral environment and to study its effects on plaque biofilm metabolism and regrowth, as well as microbial flora composition and enamel demineralization.

Method: CAP was obtained through a dielectric barrier discharge device; the optical properties were analyzed using emission spectroscopy. The electrochemical analysis of plasma devices includes voltametric characteristic curves and Lissajous. The *Streptococcus mutans* (UA159) and saliva biofilms were treated *in vitro*, and the effects of CAP on biofilm metabolism were investigated using MTT and lactate dehydrogenase assays. The duration of antibacterial activity on biofilms was examined, scanning electron microscopy was used to observe the morphology of biofilms, and 16S rRNA sequencing was used to explore the influence of CAP on the microbial flora composition of saliva biofilms. An *in vitro* model of biofilm-enamel demineralization was designed, and the effect of CAP on enamel demineralization was evaluated by micro surface hardness and micro-CT analysis.

Results: CAP had antibacterial proliferative ability toward *Streptococcus mutans* biofilms and saliva biofilms and was stronger than ultraviolet under the same tested conditions. After 24 h, the antibacterial effect disappeared, which proved the short-term timeliness of its bactericidal ability. CAP can inhibit the acid production of biofilms, and its inhibitory effect on saliva biofilms can be extended to 24 h. CAP had a strong ability to regulate the composition of plaque biofilms, especially for *Lactococcus* proliferation, a major acid-producing bacterium in microcosm biofilms. The CAP-treated enamels were more acid-tolerant than non-treated controls.

Conclusion: CAP had an explicit bactericidal effect on caries-related biofilms, which is a short-term antibacterial effect. It can inhibit the acid production of biofilms and has a downregulation effect on *Lactococcus* in saliva biofilms. CAP can help reduce demineralization of enamel.

1 Introduction

The oral cavity is a diverse microecological environment in which more than 700 microorganisms reside (Kitamoto et al., 2020). The imbalance of flora can lead to the proliferation of oral conditional pathogenic bacteria, which can cause the development of infectious diseases (Li et al., 2021a). Dental caries is this chronic endogenous infection caused by the proliferation of oral commensal flora, which is manifested by the proliferation of conditionally pathogenic bacteria contributing to the acidification of the microenvironment, resulting in an increase in the ratio of acid-producing and acid-tolerant bacteria (Bowen et al., 2018). Further acidification of the oral microenvironment disrupts the balance of mineralization and remineralization of the dental surface and disturbs calcium and phosphorus metabolism in the hard tissues, resulting in loss of inorganic material and destruction of organic collagen (Pandya and Diekwisch, 2019). Therefore, regulating the balance of flora, controlling the proliferation of conditionally pathogenic bacteria, and avoiding the acidification of the microenvironment are the key factors to reduce dental caries (Chen et al., 2020). Moreover, the high incidence of dental caries has a great impact on public health resources, thus regulating the flora balance, controlling the proliferation of conditionally pathogenic bacteria, and avoiding the acidification of the microenvironment also play a benign role in promoting public health resources (Peres et al., 2019).

Streptococcus mutans (S. mutans) has always been a highly detectable organism in the oral cavity of people with high risk of dental caries and is still considered as one of the main caries-causing organisms (Ramadugu et al., 2021; Zhang et al., 2022). Generally, the cariogenicity of *S. mutans* controlled by exogenous drugs is indirectly confirmed by the amount of bioaugmentation and metabolic acid production. Although the current demineralization-related tests do not fully reflect the degree of caries progression (Shahmoradi and Swain, 2017; Wang et al., 2019), the use of demineralization tests to evaluate the degree of caries progression is a valid evaluation method compared with the previously mentioned methods.

Exogenous antimicrobial drugs have always been an important part of the clinical approach to infectious diseases in dentistry, and traditional antimicrobial drugs have many undesirable side effects in use (Liang et al., 2020), making new antimicrobial modalities a research challenge and a hot topic in this field. Traditional oral antimicrobial drugs are mostly targeted at the bacterial envelope (Li et al., 2021b), increasing the permeability of the cell membrane, leading to leakage of intracellular material or penetration into the cell, and causing intracellular dehydration or denaturation of cellular

proteins, such as chlorhexidine, alcohol, or camphor (Wikén Albertsson et al., 2013). However, the residual problems associated with the use of traditional oral antimicrobial drugs have led to many limitations in clinical application, such as tooth staining, unpleasant taste, occasional allergic reactions, risk of oral microbial tolerance, cytotoxicity, and contraindications in pregnant and lactating patients (Nakanishi et al., 2018). Therefore, the development of new residue-free antimicrobial oral disinfection methods is of great clinical importance.

Plasma is the fourth state of matter and was discovered by Sir William Crookes in 1879 (Borges et al., 2021). Plasma can be divided into thermal plasma and cold atmospheric plasma (CAP) (Von Keudell and Schulz-Von Der Gathen, 2017). The source gases of CAP include helium, argon, nitrogen, helium oxygen (mixture of helium and oxygen), and air. CAP has a wide range of biomedical applications, such as modifying materials and promoting skin wound healing (Guo et al., 2022). Currently, CAP has started to be used in dentistry, such as surface modification of implant materials and tooth whitening (Khaledian et al., 2019; Nam et al., 2021). However, there are relatively few studies on whether CAP can control the acid-producing metabolism of oral biofilm to achieve a regulatory effect on oral microorganisms; secondly, studies on whether argon cryogenic plasma could inhibit the proliferation and metabolism of caries-causing or acid-producing microorganisms and affect tooth demineralization have not been reported. To this end, a low-temperature atmospheric plasma device was designed in this paper to investigate its effects on the proliferation of oral microorganisms and demineralization of tooth enamel.

2 Materials and method

2.1 Plasma device

An argon dielectric-barrier discharge (DBD) device equipped with double-ring electrodes was used, as shown in the Figure 1A. The plasma device consisted of gas supply system, mass flow controller, gas channel, and high-voltage AC power supply. The dielectric material (gas channel) was a quartz tube with an inner diameter of 4 mm, an outer diameter of 6 mm, and a length of 100 mm. The electrode was copper conductive tape with width of 8 mm. The distance between the low-voltage electrode and the outlet of the quartz tube was 8 mm. The center distance between the low-voltage electrode and the high-voltage electrode was 15 mm. Argon entered from the top of the quartz tube, and the purple plasma was
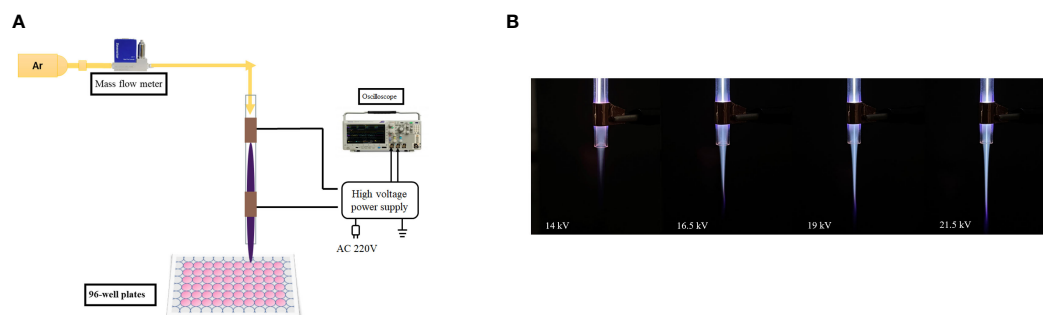
FIGURE 1
(A) Dielectric-barrier discharge plasma device. **(B)** Plasma appearance under different voltages.

ejected under the action of air flow, as shown in Figure 1B. The distance between the quartz tube outlet and targets was adjusted to 2 cm. The peak voltage was 19 kV, and gas flow was 2 l/min.

2.2 Electrical and spectral analyses

The volt–ampere characteristic curve, collected using an oscilloscope, can directly reflect the variation of the voltage and current of DBD. A Lissajous figure was obtained for calculating the discharge power. The optical characteristics of CAP were analyzed by the emission spectrum technique. The major group species in the process of discharge were deduced according to the position of the optical emission line.

2.3 Biofilm formation

2.3.1 *S. mutans* biofilms

S. mutans (UA159) was used in this study. The bacteria were diluted with a final concentration of 1×10^8 CFU/ml in brain heart infusion (BHI, Oxoid) media. For biofilm growth, 1% sucrose was added to BHI media and *S. mutans* was inoculated. Sterilized glass disks were placed into a 24-well plate. Then, 1.5 ml inoculum was

added to each well and incubated under anaerobic conditions (37°C, 5% CO_2). The disks were transferred into a new 24-well plate with fresh media after 8 h of incubation. After 24 h of incubation, the disks were washed with PBS before treatment. The workflow is shown in Figure 2.

2.3.2 Saliva biofilms

Saliva was collected from six healthy adult donors, who had natural dentition but no periodontal disease, had no active caries, and were not taking antibiotics in the past 3 months. Donors were instructed not to brush their teeth for 24 h or intake food or drink for 2 h before saliva donation. Non-stimulating saliva was collected and kept on ice. The saliva from each of the six donors were mixed and diluted in sterile glycerol to a concentration of 70%, then stored at −80°C.

The saliva-glycerol stock was added with 1: 50 final dilutions to SHI media as inoculum (Tian et al., 2010; Li et al., 2017). The SHI media contain proteose peptone 10 g/l, trypticase peptone (Oxoid) 5.0 g/l, yeast extract (Oxoid) 5.0 g/l, KCl 2.5 g/l, sucrose 5 g/l, hemin 5 mg/l, VitK 1 mg/l, urea 0.06 g/l, arginine 0.174 g/l, mucin (type II, Sigma) 2.5 g/l, sheep blood 5%, and N-acetylmuramic acid (Sigma) 10 mg/l. Sterilized glass disks were placed into a 24-well plate, and 1.5 ml of inoculum was added to each well, incubated under anaerobic conditions (37°C, 5% CO_2) for 8 h. Then, disks were transferred to
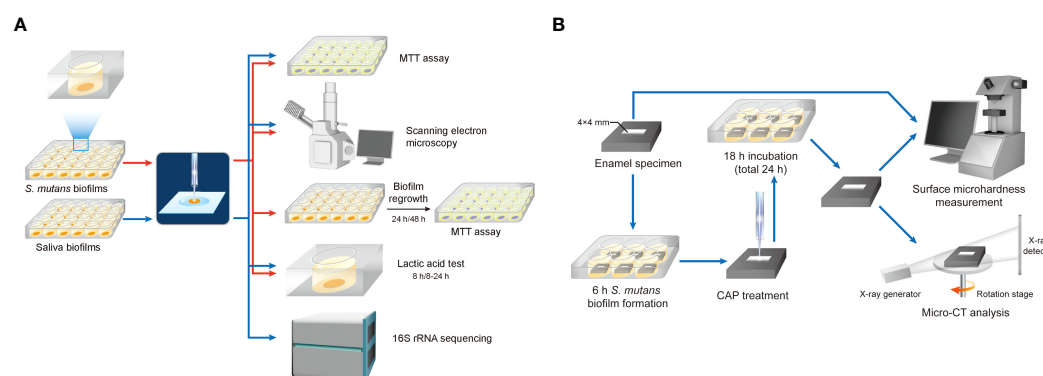
FIGURE 2
Workflow diagram. **(A)** Effects of CAP on the proliferation of oral microorganisms. **(B)** Effects of CAP on demineralization of tooth enamel.

new 24-well plates with fresh SHI media and incubated for another 16 h, for a total of 24 h.

2.4 MTT assay

The MTT assay is based on the cleavage of the yellow-colored tetrazolium salt, 3-(4,5-dimethylthiazol-2-yl)-2,5-diphenyl tetrazolium bromide, into a blue-colored formazan by the mitochondrial enzyme succinate-dehydrogenase[25]. Glass disks with 24-h biofilms were transferred to a new 24-well plate. The MTT solution (0.5 mg/ml MTT in PBS, BioFroxx, Germany) was added and followed by a 2-h incubation at 37°C in 5% CO_2. Metabolically active bacteria reduced the MTT to formazan. Disks were transferred to a new 24-well plate containing 1 ml of dimethyl sulfoxide (DMSO) to solubilize the formazan. The plate was placed on a gyratory shake for 20 min in the dark. The absorbance at 540 nm was measured *via* a microplate reader (SpectraMax M5). Experiments were performed in triplicates, and each group had three biofilm samples.

2.5 Biofilm image observation

The architecture of biofilms after CAP treatment was examined by scanning electron microscopy (SEM). Briefly, biofilms were fixed in 2.5% glutaraldehyde (v/v) at 4°C for 12 h then washed twice with PBS and dehydrated for 10 min using an increasing series of ethanol (30%, 50%, 70%, 80%, 85%, 90%, 95%, 100% (v/v)). Finally, biofilms were rinsed two times with hexamethyldisilane and coated with gold, followed by being observed after under SEM (Quanta 200, FEI, Hillsboro, OR, USA).

2.6 Biofilm regrowth

For biofilm regrowth, the 24-h-treated *S. mutans* biofilms were transferred to fresh BHI media (1% sucrose); the refreshing media were as described above. Bacterial viability was detected by MTT assay after 24 and 48 h of regrowth.

2.7 Lactic acid production

The level of lactic acid produced by biofilms was quantified to indicate the metabolic activity of biofilms. After CAP or UV treatment, biofilms on disks were gently transferred to fresh media and incubated for 24 h. The media were refreshed after 8 h, and the spent media were collected. The lactic acid concentration in the spent media was measured using an enzymatic spectrophotometric method (Deng et al, 2009). The principle of this method is based on the enzymatic conversion of L-lactate to pyruvate with the concomitant conversion of NAD^+ to NADH (Jiancheng, Nanjing, China). The absorbance at 530 nm was measured, and acid concentration was calculated based on the standard curve.

2.8 16S rRNA sequencing

The treated saliva biofilms were subjected to Personalbio (Shanghai, China), where DNA were extracted, amplified, and purified according to standard procedures and sequenced as described below. Briefly, total DNA were extracted using Omega M5635 Soil DNA Kit (USA) and stored at -20°C. For detecting the quantity and concentration of DNA, 0.8% agarose gel electrophoresis and a NanoDrop were performed. The highly variable regions (V3–V4) of the bacterial 16S rRNA gene with a length of around 468 bp were selected for sequencing. The forward and reverse primers for amplification were barcode+ ACTCCTACGGGAGGCAGCA and GGACTACHVGGGTWTCTAAT, respectively. Each 20-μl PCR reaction contains 1 μl template DNA, 5 μl 5× buffer, 0.25 μl FastPfu DNA Polymerase, 2 μl dNTPs, 1 μl of each primer, and 14.75 μl DDW. The thermal cycling conditions were composed of pre-denaturation at 98°C for 30 s, followed by 25 cycles of 98°C for 30 s, 50°C for 30 s, and 72 °C for 30 s, with a final extension cycle at 72°C for 5 min. The amplified products were extracted from 2% agarose gel electrophoresis and purified by AMPure XP beads (Beckman, USA). The qualified library was sequenced using the MiSeq v3 Reagent Kit (600 cycles) with a 2 × 250-bp base read profile.

2.9 Enamel specimen preparation and biofilm inoculation

Enamel blocks were obtained from bovine teeth and cut into sections measuring 8*8*5 mm. These specimens were stored in 0.1% thymol before use. After washing in an ultrasonic cleaner, enamel blocks were embedded with polymethylmethacrylate and coated with acid-tolerant nail varnish, leaving a window of 4*4 mm on the labial enamel surface (Figure 2B). The enamel surfaces were polished using #800, 1,000, 1,200, 1,500, 2,000, 3,000, and 50,000 silicon carbide paper (Struers) consecutively. The specimens were then sterilized using ultraviolet and placed into six-well plates. All animal experimental procedures were approved by the Animal Ethics Committee of West China Hospital of Sichuan University, China (No. WCHSIRB-D-2022-255). *S. mutans* was inoculated at a final concentration of 1×10^7 CFU/ml in 7 ml of BHI media with 1% sucrose per well. After 8 h of incubation in 5% CO_2 at 37°C, the specimen was treated with CAP for 1 or 3 min with the same parameters as described above. Ultraviolet light-C (UV-C) 254 nm was used for comparison. Specimens with no treatment were regarded as control. After treatment, enamel blocks were transferred to new six-well plates with fresh media and incubated for another 16 h. Enamel blocks were washed with flowing water for 30 min and rinsed with an ultrasonic machine for 30 min to remove the biofilms.

2.10 Surface microhardness measurement

The surface microhardness (SM) of each enamel block was measured before and after treatment, by using a microhardness tester (Struers) under a load of 50 g for 15 s. Five quadrilateral

indentations, spaced 100 µm apart from each other, were made in the center of each enamel block, arranged in a straight line. Enamel blocks with baseline surface microhardness (SM0) >300 was selected for further experiment. The surface microhardness of enamel after 16 h of incubation (SM1) was measured to calculate the surface microhardness loss percentage (SML%): SML%=(SM0-SM1)/SM0*100%

2.11 Micro-CT analysis

The micro-CT (Scanco Medical) analysis was performed at 90 kV and 155 µA on dry specimens. 0.5-mm-thick aluminum was used for hardware beam-hardening correction. Each specimen was scanned at 500proj/180° resolution with 5-µm precision. Data were analyzed using Scanco Evaluation. Lesion depth (LD) was calculated as follows: with the increase in demineralization depth, the corresponding mineral density of enamel increases. When the mineral density tended to be constant, it reached the normal enamel area. This point was regarded as the end of the lesion, and LD can be measured. Each sample were calculated triplicates.

2.12 Statistical analysis

Data were analyzed using the least significance difference test. Statistical analysis was performed using SPSS Statistics V.25.0 (IBM Corporation, USA) and a P-value of <0.05 was considered statistically significant.

3 Results

3.1 Electrical and optical analyses

When the applied voltage was 19 kV, volt–ampere characteristic curves in one cycle are shown in Figure 3A. The period was 116 µs, the peak voltage was 19 kV, the maximum current in the positive period was 0.12 mA, the waveform was a sine wave, and the phase difference was 90°.

When the applied voltage was 19 kV, the Lissajous figure of the plasma discharge device was as shown in Figure 3B. It was a closed parallelogram, and the power P of the discharge device can be calculated by the simplified formula $P = f\,CS$, where f stands for the

frequency of the applied voltage, C represents the capacitance of the applied voltage, and S is the area of the Lissajous figure. The area in the figure was 1.31, f was 8.634 kHz, and C was 0.47 pF, so the power was 5.3 W.

When the applied voltage was 19 kV, the spectrum of CAP collected at 2 cm from the outlet of the quartz tube was as shown in Figure 3C: the most obvious peaks of the emission spectrum corresponded to Ar, hydroxyl radicals (-OH), and N_2, respectively.

3.2 MTT assay

The lower the absorbance of OD540 in the MTT test, the lower the amounts of viable bacteria. As shown in Figure 4, compared with the control group, exposure to CAP and UV caused a decrease in biofilm activity right after treatments; both *S. mutans* and saliva biofilms by CAP treatment resulted in a greater reduction in biofilms activity than by UV under the same tested conditions.

3.3 Scanning electron microscopy

Figure 5 displays the representative biofilm images under SEM. Both *S. mutans* biofilms and saliva biofilms showed significant morphological alterations after CAP treatments when compared with the untreated controls, the contour of bacterial cells and biofilm structure vanished, whereas UV groups remained unchanged.

3.4 Biofilm regrowth

No significant difference of bacterial proliferation was observed after 24 or 48 h biofilm regrowth, as shown in Figure 6, suggesting that CAP had a short-term antibacterial effect.

3.5 The effect on acid production of biofilms

Lactic acid production of biofilms are plotted in Figure 7. Results showed that CAP can inhibit the acid production of *S. mutans* biofilms and saliva biofilms. The lactic production of *S. mutans* biofilms dropped after CAP treatments and recovered at 24 h, whereas the saliva biofilms remained statistically lower at 24 h.
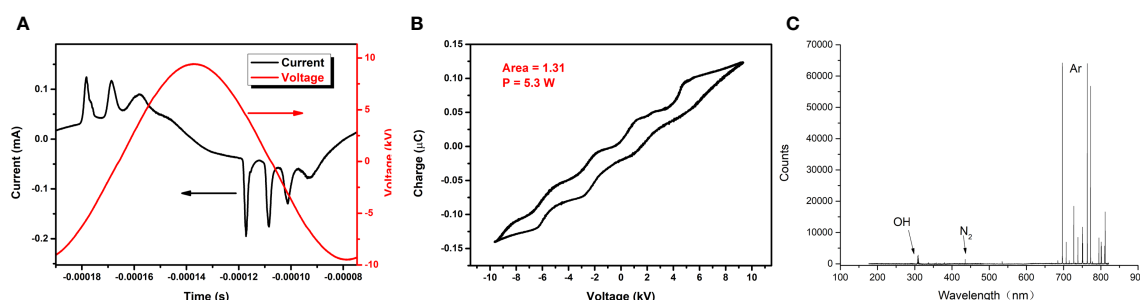
FIGURE 3
(A) Volt–ampere characteristic curve. **(B)** Lissajous diagram. **(C)** Diagram of optical emission spectroscopy.
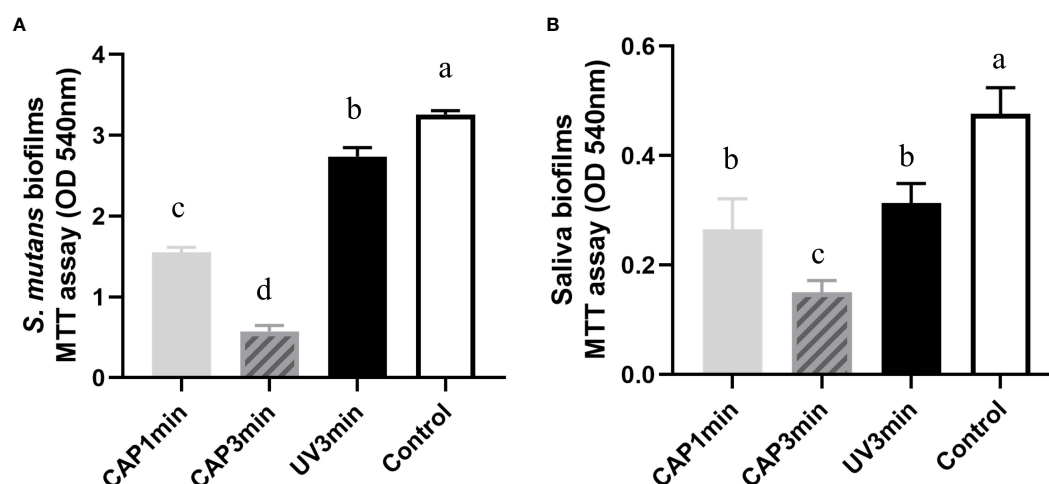
FIGURE 4
Comparison of the effects of CAP and UV on the biofilm activity. **(A)** *Streptococcus mutans* biofilm **(B)** saliva biofilm. Dissimilar letters indicate statistical differences between groups ($P < 0.05$).

3.6 16S rRNA sequencing

Figure 8 shows the average relative abundance of bacterial presence in saliva biofilms. At the genus level, the average relative abundance of *Streptococcus*, *Lactococcus*, *Lactobacillus*, *Leuconostoc*, *Neisseria*, *Weissella*, *Rothia*, *Haempophilus*, *Veillonella*, and *Ochrobactrum* were the top 10 in biofilms. The average relative abundance of *Lactococcus* decreased after CAP treatment, suggesting that CAP can repress the growth of low-pH *Lactococcus* species in saliva biofilms.

3.7 Surface microhardness measurement

Surface microhardness of enamel specimens is plotted in Figure 9A. Compared with untreated control, CAP-treated enamels (3 min) displayed less percentage of surface microhardness loss after 16 h of cariogenic challenge.

3.8 Micro-CT analysis

Figure 9B shows the lesion depth of enamel under micro-CT analysis. Results from micro-CT analysis showed the similar trend as surface microhardness loss. CAP 1- or 3-min treatment decreased enamel demineralization depth than non-treatment control (bacteria control). CAP demonstrated a protective effect in enamel demineralization, which was better than UV under the same tested condition.

4 Discussion

The present study investigated a CAP device, which is designed to be usable in the human oral environment. The aim of this study is the application of a CAP device in the intraoral environment, where the stability of the discharge is a prerequisite for safety. The device used a double-ring discharge structure with quartz tubes as the dielectric
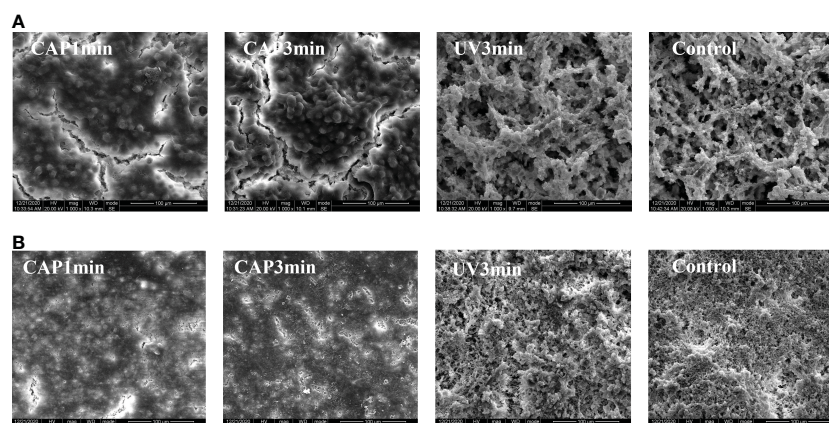
FIGURE 5
(A) SEM morphology observation of *Streptococcus mutans* biofilm (×1,000). **(B)** SEM morphology observation of saliva biofilm (×1,000).
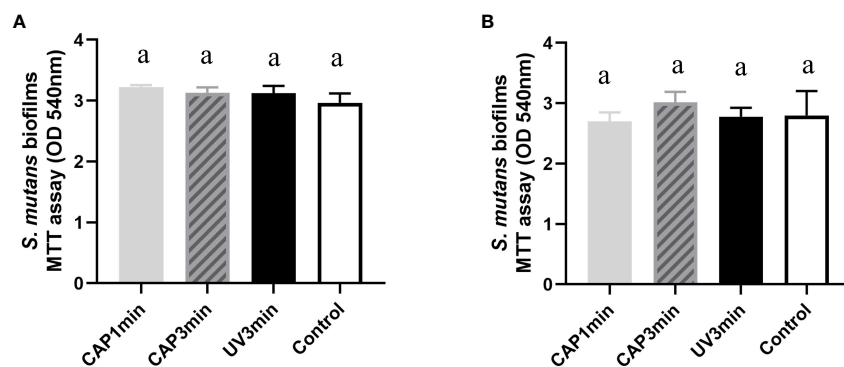
FIGURE 6
Bacterial activity after biofilm regrowth. **(A)** MTT value after 24 h of regrowth. **(B)** MTT value after 48 h of regrowth. Dissimilar letters indicate statistical differences between groups. There were no statistical differences between groups ($P > 0.05$).

material and argon as the discharge gas, which makes it easy to obtain plasma and provides discharge stability. The discharge temperature of the device was always below 40°, which is close to the temperature of the human oral cavity and does not cause burn damage to the soft tissues (Yazici et al., 2006). The voltametric characteristic curves and

Lissajous of the device were examined separately using oscilloscope acquisition and Lissa-like graphs.

The effect of CAP action on biofilm growth and regrowth were obtained by MTT assay, a method by which oral plaque biofilm activity can be demonstrated and which is widely used in the study of dental
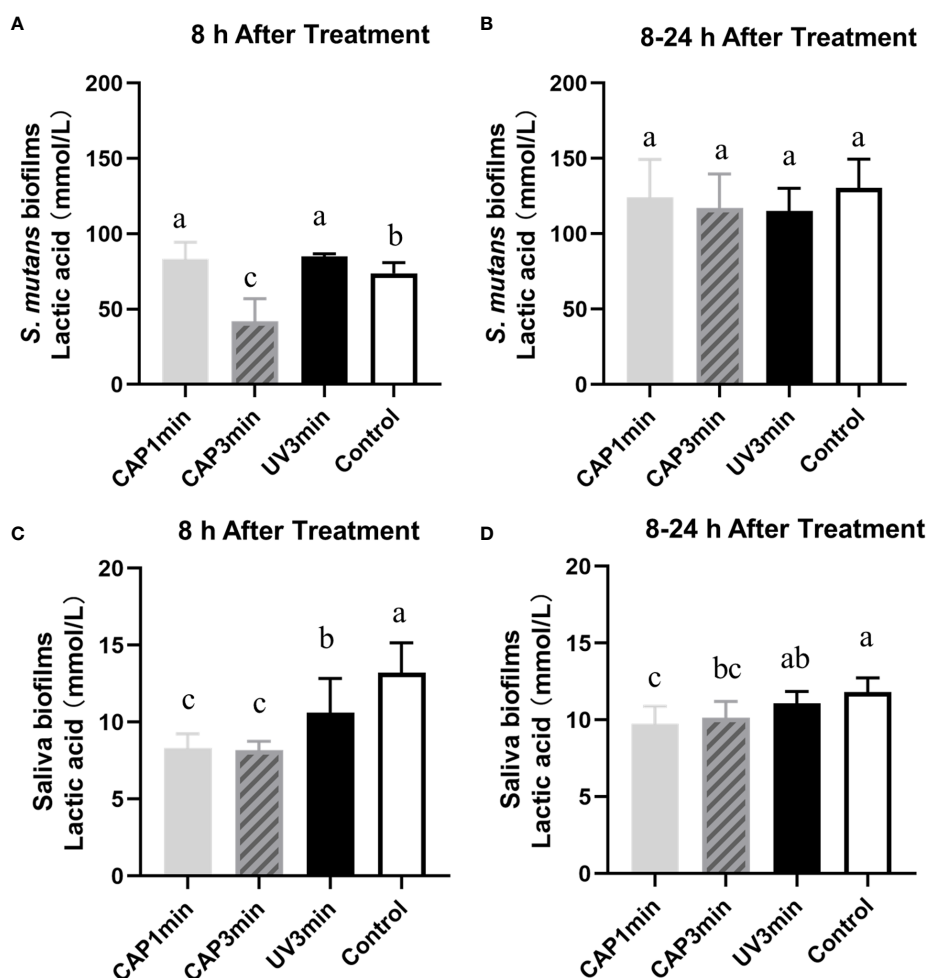
FIGURE 7
Lactic acid production of *Streptococcus mutans* biofilms **(A, B)** or saliva biofilms **(C, D)** at different times. A&C. The first 8 h after treatment. B&D. 8−24 h after treatment. Dissimilar letters indicate statistical differences between groups ($P < 0.05$).

FIGURE 8
Changes of bacterial composition of saliva biofilms after CAP treatment. (Average relative abundance−genus).

antimicrobial materials (Han et al., 2017; Liang et al., 2018). The data showed that the immediate killing effect of CAP was more pronounced for monospecies biofilms and microcosm biofilms, with significant immediate inhibition of biofilm growth activity and lactate metabolism. Other studies provided strong evidence that defined configurations of atmospheric pressure air plasmas can achieve rapid and highly effective bacterial killing in a biofilm model (Modic et al., 2017), which tends to be close to this study. Furthermore, the biofilm still had the ability to be regrown; for monospecies biofilms and microcosm biofilms, different biological characteristics were shown during regrowth (Rostami et al., 2017). The MTT data showed no difference between the two biofilms after 24 and 48 h, and the activity of bacterial mitochondrial succinate dehydrogenase in biofilms was shown to approach normal levels after 24 h of CAP action.

The metabolic effect of CAP on oral plaque biofilms was demonstrated by the amount of lactic acid produced. However, the recovery of biofilm metabolic lactate differed from the MTT changes, with *S. mutans* biofilms and microcosm biofilms maintaining the effects of CAP on them in 8 h. Between 8 and 24 h, lactic acid production from *S. mutans* biofilms did not differ between groups, but there were differences between microbial biofilm groups, with lower acid production in the CAP-treated group than untreated controls. Previous studies have tended to focus more on the immediate effect of the antimicrobial material and less on the regrowth state of the biofilm after the action of the antimicrobial material. Therefore, the state of the biofilm after antibacterial treatment and the bacterial activity exhibited during regrowth are matters of concern (Han et al.,

2019). Previously, oral disinfectants tended to leave residues in the mouth (Mikati et al., 2020), but the advent of CAP will make residue-free antimicrobial activity a reality. However, the CAP has a short time to exert its antimicrobial power, and the strong biofilm proliferation rebound after CAP stimulation is a drawback of the application, and how to improve this property will be the next step in this research.
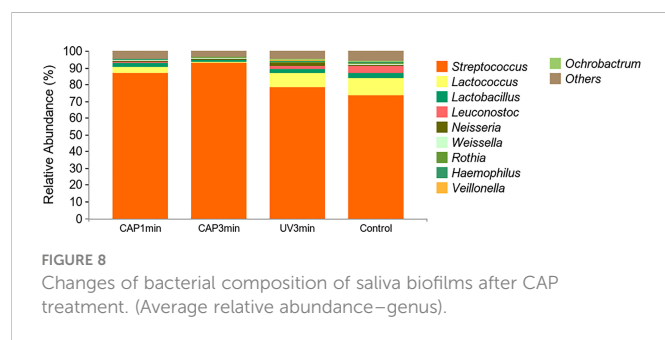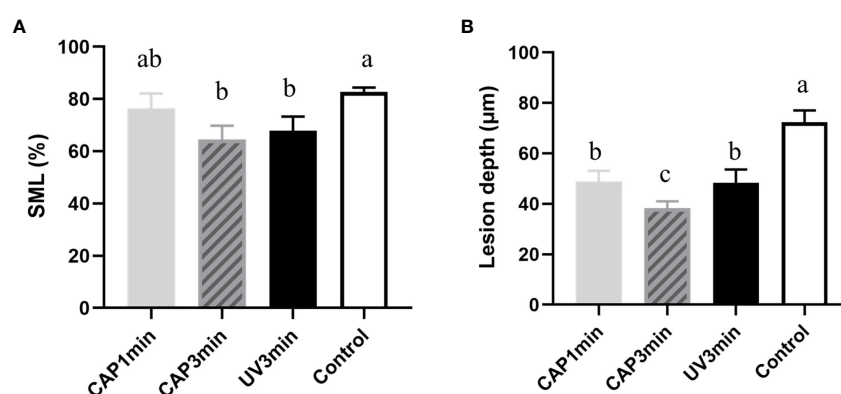
Changes in the oral microbial communities in response to CAP were obtained by 16S ribosomal RNA assay. There is evidence that information on oral microbial community structure and function has great potential in predicting the occurrence and treatment prognosis of oral diseases (Bowen et al., 2018; Valm, 2019), such as caries. Moreover, CAP has been less studied in improving the structural and functional information of oral microbial communities. The data revealed that on the basis of the overall microbial load being suppressed, the bioactivity of *Lactococcus* spp. was significantly suppressed whereas that of *Streptococcus* spp. was less influenced, suggesting that external stimuli have a weaker effect on the bioactivity of *Streptococcus* spp. or that the self-protection mechanism of *Streptococcus* spp. is more complete. This is different from previous studies of antimicrobial materials. The possible reason for this is that CAP is a gaseous molecule and its effect is immediate, transient, or too little after the action to have a sustained effect (Wu et al., 2011), as previous antimicrobial materials were contact antimicrobial, which was different from this experiment.

CAP's action on biofilms affecting enamel demineralization was obtained by surface hardness and cross-sectional micrographs. This study explored the future potential of plasma in the study of dental caries control through plaque microorganisms. In this part of the experiment plaque, biofilms were precultured on the enamel surface and the above biofilm culture process has been treated with this plasma to simulate the caries demineralization process *in vitro*. The CAP treatment leads to changes in the surface roughness and morphology of the hard tissues of the teeth and results in a reduction in the contact angle between water and glycol, as well as a significant reduction in carbon on the enamel surface, all of which have an effect on the mineralization and remineralization of the hard tissues of the teeth (Chen et al., 2013; Kermanshah et al., 2020).

This study provides an experimental basis for the development and application of CAP in the prevention and treatment of dental caries in the future. However, the present study was performed in *in*

FIGURE 9
(A) Surface microhardness loss of enamel blocks after treatment followed by a 16-h acid attack. (B) Lesion depth after treatment followed by the 16-h acid attack ($P < 0.05$).

vitro models, which is relatively ideal and cannot mimic the complex environment of human oral cavity. Thus, an *in vivo* animal experiment is needed for the further application of CAP.

5 Conclusion

In summary, CAP can reduce the cariogenicity of dental biofilms and inhibit enamel demineralization. This study provides an experimental basis for the development and application of CAP in the prevention and treatment of caries in the future.

Data availability statement

The data presented in the study are deposited in the NCBI SRA, accession number PRJNA938579.

Ethics statement

All animal experimental procedures were approved by the Animal Ethics Committee of West China Hospital of Sichuan University, China (NO.WCHSIRB-D-2022-255).

Author contributions

HZ: conceptualization; data curation; formal analysis; investigation; methodology; writing—original draft; writing—review and editing.

XW: device assembly; data curation; formal analysis. ZL: device design; conceptualization; methodology. YW: data curation; funding acquisition; methodology. LZ: methodology; writing—review. YC: conceptualization; funding acquisition; resources; supervision; validation. QH: conceptualization; funding acquisition; resources; supervision; validation; writing—review and editing. All authors contributed to the article and approved the submitted version.

Conflict of interest

The authors declare that the research was conducted in the absence of any commercial or financial relationships that could be construed as a potential conflict of interest.

Publisher's note

All claims expressed in this article are solely those of the authors and do not necessarily represent those of their affiliated organizations, or those of the publisher, the editors and the reviewers. Any product that may be evaluated in this article, or claim that may be made by its manufacturer, is not guaranteed or endorsed by the publisher.

References

Borges, A. C., Kostov, K. G., Pessoa, R. S., De Abreu, G. M. A., Lima, G. D. M. G., Figueira, L. W., et al. (2021). Applications of cold atmospheric pressure plasma in dentistry. *Appl. Sci* 11 (5), 1-15. doi: 10.3390/app11051975

Bowen, W. H., Burne, R. A., Wu, H., and Koo, H. (2018). Oral biofilms: Pathogens, matrix, and polymicrobial interactions in microenvironments. *Trends Microbiol.* 26, 229–242. doi: 10.1016/j.tim.2017.09.008

Chen, H., Yang, Y., Weir, M. D., Dai, Q., Lei, L., Homayounfar, N., et al. (2020). Regulating oral biofilm from cariogenic state to non-cariogenic state *via* novel combination of bioactive therapeutic composite and gene-knockout. *Microorganisms* 8 (9):E1410. doi: 10.3390/microorganisms8091410

Chen, M., Zhang, Y., Sky Driver, M., Caruso, A. N., Yu, Q., and Wang, Y. (2013). Surface modification of several dental substrates by non-thermal, atmospheric plasma brush. *Dent. Mater.* 29, 871–880. doi: 10.1016/j.dental.2013.05.002

Deng, D. M., Hoogenkamp, M. A., Ten Cate, J. M., and Crielaard, W. (2009). Novel metabolic activity indicator in streptococcus mutans biofilms. *J. Microbiol. Methods* 77 67–71. doi: 10.1016/j.mimet.2009.01.008a

Guo, P., Liu, Y., Li, J., Zhang, N., Zhou, M., Li, Y., et al. (2022). A novel atmospheric-pressure air plasma jet for wound healing. *Int. Wound J.* 19 (3), 538–552. doi: 10.1111/iwj.13652

Han, Q., Jiang, Y., Brandt, B. W., Yang, J., Chen, Y., Buijs, M. J., et al. (2019). Regrowth of microcosm biofilms on titanium surfaces after various antimicrobial treatments. *Front. Microbiol.* 10, 2693. doi: 10.3389/fmicb.2019.02693

Han, Q., Li, B., Zhou, X., Ge, Y., Wang, S., Li, M., et al. (2017). Anti-caries effects of dental adhesives containing quaternary ammonium methacrylates with different chain lengths. *Mater. (Basel)* 10, 643. doi: 10.3390/ma10060643

Kermanshah, H., Saeedi, R., Ahmadi, E., and Ranjbar Omrani, L. (2020). Efficacy of cavity liners with/without atmospheric cold helium plasma jet for dentin remineralization. *Biomater. Investig. Dent.* 7, 120–125. doi: 10.1080/26415275.2020.1803074

Khaledian, H. R., Zolfaghari, P., Elhami, V., Aghbolaghy, M., Khorram, S., Karimi, A., et al. (2019). Modification of Immobilized Titanium Dioxide Nanostructures by Argon plasma for photocatalytic removal of organic dyes. *Molecules* 24, 383. doi: 10.3390/molecules24030383

Kitamoto, S., Nagao-Kitamoto, H., Hein, R., Schmidt, T. M., and Kamada, N. (2020). The bacterial connection between the oral cavity and the gut diseases. *J. Dent. Res.* 99, 1021–1029. doi: 10.1177/0022034520924633

Liang, J., Li, M., Ren, B., Wu, T., Xu, H. H. K., Liu, Y., et al. (2018). The anti-caries effects of dental adhesive resin influenced by the position of functional groups in quaternary ammonium monomers. *Dent. Mater.* 34, 400–411. doi: 10.1016/j.dental.2017.11.021

Liang, J., Peng, X., Zhou, X., Zou, J., and Cheng, L. (2020). Emerging applications of drug delivery systems in oral infectious diseases prevention and treatment. *Molecules* 25 (3), 516. doi: 10.3390/molecules25030516

Li, Y., Qiao, D., Zhang, Y., Hao, W., Xi, Y., Deng, X., et al. (2021b). MapZ deficiency leads to defects in the envelope structure and changes stress tolerance of streptococcus mutans. *Mol. Oral. Microbiol.* 36, 295–307. doi: 10.1111/omi.12352

Li, L., Zhang, Y. L., Liu, X. Y., Meng, X., Zhao, R. Q., Ou, L. L., et al. (2021a). Periodontitis exacerbates and promotes the progression of chronic kidney disease through oral flora, cytokines, and oxidative stress. *Front. Microbiol.* 12, 656372. doi: 10.3389/fmicb.2021.656372

Li, B., Zhou, X., Zhou, X., Wu, P., Li, M., Feng, M., et al. (2017). Effects of different substrates/growth media on microbial community of saliva-derived biofilm. *FEMS Microbiol. Lett.* 364 (13), fnx123. doi: 10.1093/femsle/fnx123

Mikati, M. O., Miller, J. J., Osbourn, D. M., Barekatain, Y., Ghebremichael, N., Shah, I. T., et al. (2020). Antimicrobial prodrug activation by the staphylococcal glyoxalase GloB. *ACS Infect. Dis.* 6, 3064–3075. doi: 10.1021/acsinfecdis.0c00582

Modic, M., Mcleod, N. P., Sutton, J. M., and Walsh, J. L. (2017). Cold atmospheric pressure plasma elimination of clinically important single- and mixed-species biofilms. *Int. J. Antimicrob. Agents* 49, 375–378. doi: 10.1016/j.ijantimicag.2016.11.022

Nakanishi, Y., Yamamoto, T., Obana, N., Toyofuku, M., Nomura, N., and Kaneko, A. (2018). Spatial distribution and chemical tolerance of streptococcus mutans within dual-species cariogenic biofilms. *Microbes Environ.* 33, 455–458. doi: 10.1264/jsme2.ME18113

Nam, S. H., Choi, B. B. R., and Kim, G. C. (2021). The whitening effect and histological safety of nonthermal atmospheric plasma inducing tooth bleaching. *Int. J. Environ. Res. Public Health* 18 (9), 4714. doi: 10.3390/ijerph18094714

Pandya, M., and Diekwisch, T. G. H. (2019). Enamel biomimetics-fiction or future of dentistry. *Int. J. Oral. Sci.* 11, 8. doi: 10.1038/s41368-018-0038-6

Peres, M. A., Macpherson, L. M. D., Weyant, R. J., Daly, B., Venturelli, R., Mathur, M. R., et al. (2019). Oral diseases: A global public health challenge. *Lancet* 394, 249–260. doi: 10.1016/S0140-6736(19)31146-8

Ramadugu, K., Bhaumik, D., Luo, T., Gicquelais, R. E., Lee, K. H., Stafford, E. B., et al. (2021). Maternal oral health influences infant salivary microbiome. *J. Dent. Res.* 100, 58–65. doi: 10.1177/0022034520947665

Rostami, N., Shields, R. C., Yassin, S. A., Hawkins, A. R., Bowen, L., Luo, T. L., et al. (2017). A critical role for extracellular DNA in dental plaque formation. *J. Dent. Res.* 96, 208–216. doi: 10.1177/0022034516675849

Shahmoradi, M., and Swain, M. V. (2017). Micro-CT analysis of naturally arrested brown spot enamel lesions. *J. Dent.* 56, 105–111. doi: 10.1016/j.jdent.2016.11.007

Tian, Y., He, X., Torralba, M., Yooseph, S., Nelson, K. E., Lux, R., et al. (2010). Using DGGE profiling to develop a novel culture medium suitable for oral microbial communities. *Mol. Oral. Microbiol.* 25, 357–367. doi: 10.1111/j.2041-1014.2010.00585.x

Valm, A. M. (2019). The structure of dental plaque microbial communities in the transition from health to dental caries and periodontal disease. *J. Mol. Biol.* 431, 2957–2969. doi: 10.1016/j.jmb.2019.05.016

Von Keudell, A., and Schulz-Von Der Gathen, V. (2017). Foundations of low-temperature plasma physics–an introduction. *Plasma Sources Sci. Technol.* 26 (11). doi: 10.1088/1361-6595/aa8d4c

Wang, S., Wang, Y., Wang, Y., Duan, Z., Ling, Z., Wu, W., et al. (2019). Theaflavin-3,3'-Digallate suppresses biofilm formation, acid production, and acid tolerance in streptococcus mutans by targeting virulence factors. *Front. Microbiol.* 10, 1705. doi: 10.3389/fmicb.2019.01705

Wikén Albertsson, K., Persson, A., and Van Dijken, J. W. (2013). Effect of essential oils containing and alcohol-free chlorhexidine mouthrinses on cariogenic micro-organisms in human saliva. *Acta Odontol. Scand.* 71, 883–891. doi: 10.3109/00016357.2012.734414

Wu, Z., Chen, M., Li, P., Zhu, Q., and Wang, J. (2011). Dielectric barrier discharge non-thermal micro-plasma for the excitation and emission spectrometric detection of ammonia. *Analyst* 136, 2552–2557. doi: 10.1039/c0an00938e

Yazici, A. R., Müftü, A., Kugel, G., and Perry, R. D. (2006). Comparison of temperature changes in the pulp chamber induced by various light curing units, *in vitro*. *Oper. Dent.* 31, 261–265. doi: 10.2341/05-26

Zhang, K., Xiang, Y., Peng, Y., Tang, F., Cao, Y., Xing, Z., et al. (2022). Influence of fluoride-resistant streptococcus mutans within antagonistic dual-species biofilms under fluoride *In vitro*. *Front. Cell Infect. Microbiol.* 12, 801569. doi: 10.3389/fcimb.2022.801569

Current and prospective therapeutic strategies: tackling *Candida albicans* and *Streptococcus mutans* cross-kingdom biofilm

Yijun Li[1,2], Shan Huang[1], Jingyun Du[1], Minjing Wu[3] and Xiaojing Huang[1]*

[1]Fujian Key Laboratory of Oral Diseases and Fujian Provincial Engineering Research Center of Oral Biomaterial and Stomatological Key Lab of Fujian College and University, School and Hospital of Stomatology, Fujian Medical University, Fuzhou, China, [2]Department of Endodontics, Stomatological Hospital of Xiamen Medical College, Xiamen, China, [3]Stomatological Hospital, Southern Medical University, Guangzhou, China

Candida albicans (*C. albicans*) is the most frequent strain associated with cross-kingdom infections in the oral cavity. Clinical evidence shows the co-existence of *Streptococcus mutans* (*S. mutans*) and *C. albicans* in the carious lesions especially in children with early childhood caries (ECC) and demonstrates the close interaction between them. During the interaction, both *S. mutans* and *C. albicans* have evolved a complex network of regulatory mechanisms to boost cariogenic virulence and modulate tolerance upon stress changes in the external environment. The intricate relationship and unpredictable consequences pose great therapeutic challenges in clinics, which indicate the demand for *de novo* emergence of potential antimicrobial therapy with multi-targets or combinatorial therapies. In this article, we present an overview of the clinical significance, and cooperative network of the cross-kingdom interaction between *S. mutans* and *C. albicans*. Furthermore, we also summarize the current strategies for targeting cross-kingdom biofilm.

KEYWORDS

biofilm, *Candida albicans*, *Streptococcus mutans*, cross-kingdom interaction, therapeutic strategies

Introduction

Biofilms are highly organized communities of microorganisms attached to biotic and abiotic surfaces and surrounded by a protective extracellular matrix. The human oral cavity harbors nearly 700 species of microorganisms that live as biofilms (Valm, 2019). Generally, the composition, activities, and interactions among these microbial communities maintain

normal levels of fluctuation. Once endogenous dysbiosis of the oral microbial communities occurs due to some driven factors, these biofilms could transform into a pathogenic state to trigger infectious diseases such as caries, periodontitis and peri-implantitis and so on (Lamont et al., 2018; Sedghi et al., 2021). These driven factors include excessive carbohydrate consumption, reduced salivary flow, alcohol or tobacco overuse, poor oral hygiene, and so on (Sampaio-Maia et al., 2016; Rosier et al., 2018). In the past years, reports from governments and global health authorities have stated the seriousness of caries which occur in all ages especially in children and older adults (Gibney et al., 2021; Hugo et al., 2021). Dental caries, one of the most common diseases in the world, has been associated with a result of collective activities of dental biofilm. It refers to a process that cariogenic species metabolize external sugars and produce acids, thereby resulting in a lower pH local environment and the demineralization of the dental hard tissue over time.

Earlier studies have attributed bacterial biofilms not fungal biofilms to the main pathogenic factors of caries. Though the involvement of fungi like *Candida* species in oral mucosa infections is well recognized, the research about fungus in caries is poorly investigated owing to their small isolated populations from the human mouth (Nikawa et al., 1998; Maijala et al., 2007). In recent years, the role of *Candida* species infection in the etiology of caries has gained more attention. Some *Candida* species especially *Candida albicans* (*C. albicans*) is involved in the development of caries. *C. albicans* is a commensal fungus that colonizes the skin, oral mucosa, vaginal mucosa, and other anatomical parts. The virulence of *C. albicans* lies in its ability to form dense biofilms that comprise yeast cells, pseudo hyphae, and hyphae within the abundant matrix (Nobile and Johnson, 2015).

The cariogenic potential of *C. albicans* has been demonstrated in several parts. Firstly, *C. albicans* can not only adhere to hydroxyapatite-like substrates but also form co-adhesion with some pioneer bacteria to achieve tight adhesion to tooth surface (Montelongo-Jauregui and Lopez-Ribot, 2018; Thanh Nguyen et al., 2021). Secondly, even though *C. albicans* could not highly decompose sucrose due to the lack of α-glucosidase, it can still metabolize fructose, glucose, or lactose to produce short-chain carboxylic acids to lower the pH of the surrounding environment, thereby promoting the demineralization of hard tissue (Klinke et al., 2009). Thirdly, *C. albicans* shows peculiarities in terms of acid tolerance, which is related to the proton pump and H$^+$-ATPases on the cell membrane surface (Bowman and Bowman, 1986). It was proposed that the acid-producing and acid tolerance ability of *C. albicans* is superior to *Streptococcus mutans* (*S. mutans*) in some extreme conditions like lower pH environment. Fourthly, the most important cariogenic feature of *C. albicans* is its interspecies networks with different bacteria, whose consequences are associated with elevated virulence and more severe infection (Du et al., 2021; Fourie et al., 2021). The presence of *C. albicans* would undoubtedly alter the ecological niche shared with oral bacteria, which may encourage interspecies cooperation for the benefit of each other. For this review, we sought to update the readers concerning the clinical evidence, interaction relationship, and antimicrobial strategies advancements of cross-kingdom biofilms consisting of *C. albicans* and *S. mutans*.

Clinical evidence of the co-existence of *S. mutans* and *C. albicans*

Early childhood caries (ECC) is perhaps the most common form of dental caries that disproportionately affects millions of underprivileged preschool children worldwide. An earlier investigation found a higher amount of *C. albicans* in ECC children when compared to caries-free children, though the role of *C. albicans* in caries etiology has not been established yet at that time (de Carvalho et al., 2006). A clinical study has compared the microbial composition of caries plaque samples from 30 ECC children versus plaque samples from caries-free children and found a higher detection rate of *C. albicans* in ECC plaque sites (Srivastava et al., 2012). A number of clinical studies also supported the positive correlation between *C. albicans* carriage and ECC severity (Nascimento et al., 2016; Xiao et al., 2018b). Besides, two research teams pointed out that the genotypic distribution of *C. albicans* is also associated with the caries experience of children (Raja et al., 2010; Qiu et al., 2015). In addition to *C. albicans*, a high proportion of *S. mutans* was also detected in the plaque where *C. albicans* was co-isolated in ECC lesions (Bachtiar and Bachtiar, 2018; Sridhar et al., 2020). A previous study has reported that the total isolation frequency of *S. mutans* and *C. albicans* from plaque and saliva of ECC children was 66% and 18% respectively (Fragkou et al., 2016). Lately, a cohort study used 16s rRNA amplicon sequencing to identify the microbiota of saliva and supragingival plaque from severe early child caries (S-ECC) children (Xiao et al., 2018a). In comparison with data obtained from caries-free children, their results suggested that the presence of *C. albicans* in S-ECC children is responsible for bacterial composition change, which is characterized by an increased abundance of highly acidogenic and aciduric microbiota like *S. mutans*. In addition, as one of the virulence traits in S-ECC, the plaque glucosyltransferase (Gtf) enzymatic activity was significantly higher with the increased abundance of *C. albicans*. In addition to the above observations, it was found that the carriage of *C. albicans* and *S. mutans* in the infant oral cavity displayed positive associations with the mother's *C. albicans* carriage in a study of 101 mother-infant pairs (Ramadugu et al., 2020). Their results suggested the infant microbiota may have a prenatal origin. Based on the findings establishing the association of *S. mutans* and *C. albicans* in caries initiation and progression, a 2022 study of cross-sectional study wanted to investigate the association of *S. mutans* and *C. albicans* with ECC recurrence (Garcia et al., 2021). Taking a large sample from 143 children who were caries-free, treated for ECC with no recurrence, or treated for ECC and experiencing recurrence within 6 months, the study showed co-infection with *C. albicans* and *S. mutans* was strongly associated with caries recurrence.

Root caries is another subtype of severe caries except ECC, which mainly occurs in middle-aged and elderly people. *Streptococcus*, *Lactobacillus*, and *Actinomyces* species are recognized as the prominent pathogenic microorganisms in root caries. *C. albicans* was initially identified in root carious dentin (Fure, 2004), however, researchers did not find the reasons for its preference in colonizing the root surface. Another study reported higher counts of *C. albicans* in the root caries lesions of middle-aged

and old-aged patients with an incidence range from 27% to 31% (Zaremba et al., 2006), implying *C. albicans*'s colonization and the resulting acidification activities and activation of dentin tubule collagen dissolve may play essential roles in root caries. The co-existence and interaction of *S. mutans* and *C. albicans* in root caries were observed in recent researches via imaging and sequencing techniques. A recent clinical study of dental plaque composition analysis obtained from older Chinese people revealed that versus those without root caries, patients with root caries are abundant in *C. albicans* carriage and also positively correlated with increased *S. mutans* numbers (Du et al., 2020).

The above-mentioned clinical studies demonstrated the positive occurrence and correlation of *C. albicans* and *S. mutans* in the dental plaque of ECC and root caries. It can be inferred that their interaction contributes to the pathogenesis of caries.

Increased understanding of the complex cross-kingdom interactions of *C. albicans* and *S. mutans*

Pathogens in multi-species biofilms may act synergistically, antagonistically, and competitively during colonization. The co-infection of *C. albicans* and other bacteria could influence the expression of virulence traits, the human immune system response and antimicrobial resistance with consequences of increased morbidity, and health problems (Cavalcanti et al., 2015; Bernard et al., 2020). Considering the severities of co-infection due to the interaction of *C. albicans* and *S. mutans*, scientists have thoroughly investigated the interaction mechanisms in order to search for novel therapeutic solutions. Their interaction mechanisms lie in different stages of biofilm formation (Figure 1).

Physical interactions

The physical interaction between microorganisms is the prerequisite of coexistence, which promote co-adhesion and proximity, further contributing to chemical interactions and biofilm maturity. Scientists have attempted to reveal the exact mechanisms behind the interaction of *C. albicans* and oral bacteria in past decades (Jenkinson et al., 1990; Cavalcanti et al., 2017; Zhou et al., 2022). The agglutinin-like sequence family containing eight members is located in the cell wall of *C. albicans* and is the key to *C. albicans* in the interaction with other bacteria during biofilm development (Peters et al., 2012; von Ranke et al., 2018). For instance, evidence has shown the cell-to-cell contact between oral streptococci and *C. albicans* is mediated by bacterial surface adhesion SspA/SspB and hyphal cell wall ALS3 adhesins of *C. albicans* (Silverman et al., 2010). This suggests *S. mutans*, belonging to oral streptococci, may possess the same physical contact mode with *C. albicans* as *Streptococcus gordonii* (*S. gordonii*) and *Streptococcus oralis*. Indeed, antigen I/II of *S. mutans* mediates the interaction between *S. mutans* and *C. albicans*. Loss of *spaP* gene coding for antigen I/II could lead to a

significant reduction of *C. albicans* numbers in the dual-species biofilms both *in vitro* and *in vivo* (Yang et al., 2018). The required adhesin proteins in mediating the attachment to surfaces or cells of *C. albicans*, such as als1 and als3, are downstream targets of Efg1. The recent study has used *C. albicans* homozygous knockout strains including Δ*Δefg1* and Δ*Δals1*/Δ*Δals3* to investigate the role of adhesins in the interkingdom colonization between *S. mutans* and *C. albicans* (Ren et al., 2022). Notably, the Δ*Δefg1* and Δ*Δals1*/Δ*Δals3* deletion led to a severe reduction of coassembly between *C. albicans* and *S. mutans*. The findings indicated that *C. albicans* could directly bind to *S. mutans* through these surface proteins.

However, it seems that the co-adhesion between *C. albicans* and *S. mutans* is not just dependent on cell-cell physical direct binding, but is also mediated by Gtf enzymes secreted by *S. mutans*. Scanning electron microscope observation represented the co-adhesion of *C. albicans* and *S. mutans* within a dense matrix in the sucrose environment (Pereira-Cenci et al., 2008). Based on this finding, it has been hypothesized that the glucosyltransferase enzyme of *S. mutans* may contribute to the interaction of *C. albicans* and *S. mutans* during co-cultivation. Then Gregoire et al. explored the co-adhesion behaviors of *C. albicans* and *S. mutans* (Gregoire et al., 2011). The authors found that glucosyltransferase B, produced by *S. mutans*, binds tightly to the surface of *C. albicans* yeast cells and contributes to the *in situ* production of glucan by *C. albicans* cells. Interestingly, the *in situ*-formed glucans can provide adhesive sites for *S. mutans* binding, as well as enable the tight contact of *C. albicans* and *S. mutans*, and concomitantly enhance the attachment of *C. albicans* to the hydroxyapatite (HA) surface. The latter of the same research group used *gtfB* knock-out *S. mutans* strains, defective in regulating the formation of exopolysaccharides, to culture with *C. albicans* (Falsetta et al., 2014). The confocal laser scanning microscope (CLSM) image showed that the co-species biofilm of △*gtfB S. mutans* and *C. albicans* presented fairly small, random and sparse clusters, whose attachment force is too weak and mechanically easy to remove from HA disks. To further understand the exact locations of GtfB binding to *C. albicans* cell surface, another study has investigated the precise surface molecule of *C. albicans* when binding to GtfB (Hwang et al., 2017). *C. albicans* mutants with defects in genes encoding mannoprotein biosynthesis, including *och1* and *pmt4*, showed reduced abilities in binding with GtfB and robust biofilm formation. Atomic force microscopy (AFM) is an advanced tool for imaging and unveiling biophysical properties of the binding interactions between microorganisms. By using this technology, the binding force and dynamics of GtfB–*C. albicans* has been measured (Hwang et al., 2015). The data showed the bond between GtfB with *C. albicans* is highly stable with a low dissociation rate. Besides, the binding strength of GtfB to the *C. albicans* surface was ~2.5-fold higher and the binding stability was substantially higher (~20-fold), as compared with the GtfB adhesion to *S. mutans*. Another study also applied this method to evaluate the presence/absence of glucan on the binding forces of *S. mutans* to *C. albicans* (Wan et al., 2021). As a result, the glucan coating on *C. albicans* dramatically enhanced the binding between these two microorganisms. Notably, the binding force of *S. mutans* to glucan-coated *C. albicans* was substantially higher (~6-fold) than the one from *S. gordonii*–*C.*

Cross-kingdom interaction between *S. mutans* and *C. albicans*
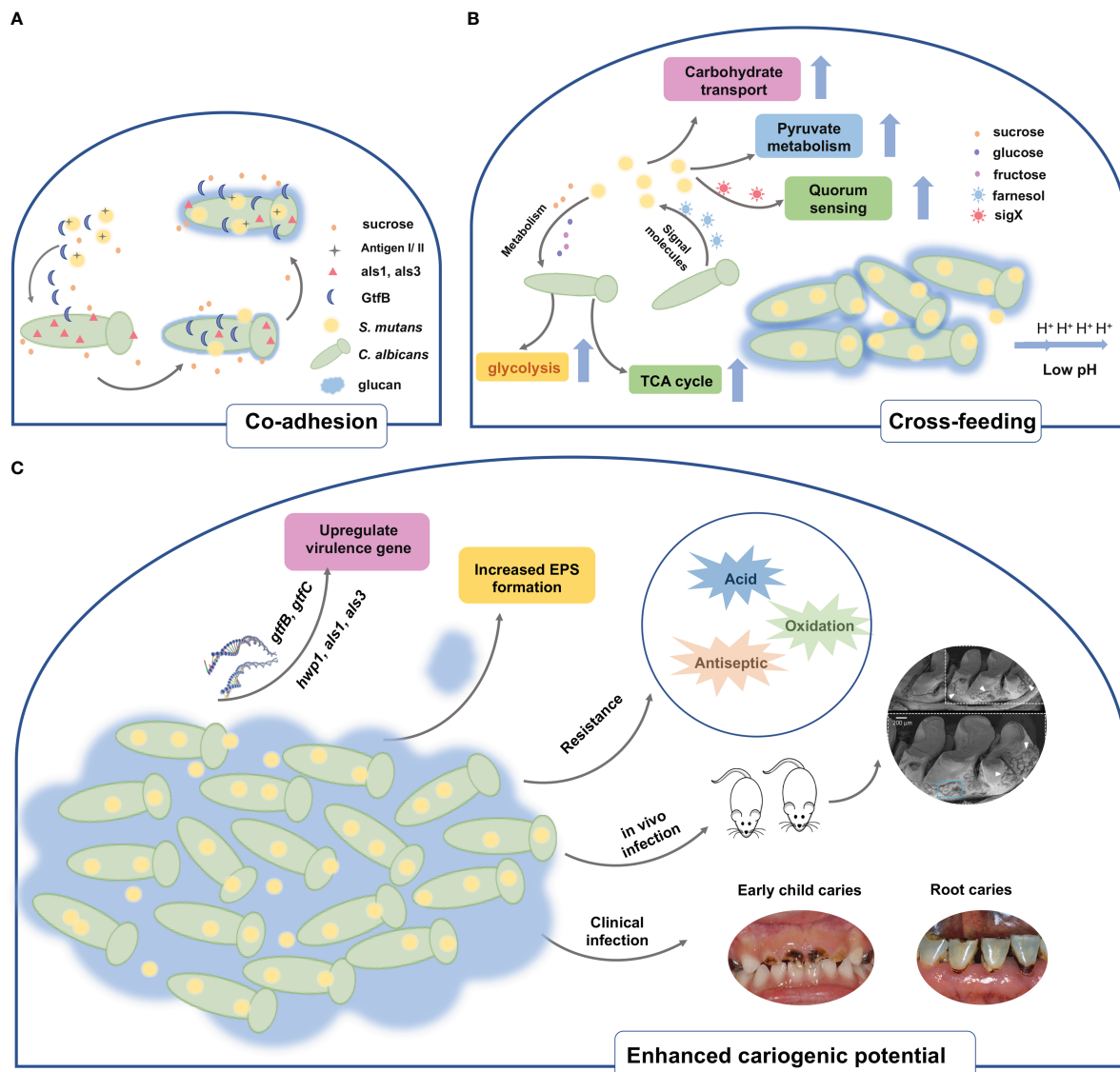
FIGURE 1

Schematic representation of the cross-kingdom interaction between *S. mutans* and *C. albicans*. **(A)** The physical interaction of *C. albicans* and *S. mutans* is mediated through antigenI/II and als adhesins. Under sucrose environment, *S. mutans*-derived GtfB binds to *C. albicans* cell surface, thereby producing glucans on the *C albicans* cell surfaces and in turn allowing *S. mutans* cells to adhere to the glucans. **(B)** In addition to physical interaction, cross-feeding metabolism occurs between *S. mutans* and *C. albicans*. *S. mutans* relies on sucrose as a nutrient source and metabolize sucrose into fructose and glucose, both of which are nutrient supply of *C. albicans*. Meanwhile, *S. mutans* significantly increases the biochemical activities of such as sugar transport systems, glycolysis, pyruvate degradation, and TCA cycle. Conversely, the presence of *C. albicans* contributes to carbohydrate transport and metabolic/catabolic process of *S. mutans*. The quorum sensing molecule of *C. albicans*, farnesol, could enhance cell growth, microcolony development, and Gtf activity of *S. mutans*. **(C)** Upregulated expressions of virulence factors both in *S. mutans* and *C. albicans* are observed when co-cultivating together. The interaction also stimulates the EPS matrix production and biofilm biomass formation. Owing to the increased virulence factors, the cross-kingdom biofilm of *S. mutans* and *C. albicans* displays resistance towards acid, oxidative, and antiseptic stress. Co-infection of *S. mutans* and *C. albicans in vivo* substantially increase biofilm accumulation, hard tissue demineralization, and carious lesions in rats. Clinical evidence demonstrated that the cross-kingdom relationship of *C. albicans* and *S. mutans* contributes to the progression of ECC and root caries.

albicans. This result indicated the higher binding force of *S. mutans-C. albicans* would help *S. mutans* boost competitiveness against *S. gordonii* under some cariogenic conditions.

Previous and current findings reveal *C. albicans* adhesins, *S. mutans*-derived GtfB and *C. albicans*-produced glucans are critical for the co-adhesion and subsequent co-species biofilm development. In addition, the strong binding force of *S. mutans* and *C. albicans* may account for, at least in part, the competitiveness of cross-kingdom biofilms. It is noteworthy that these findings are constructed in high sucrose conditions. However, the human saliva composition varies not comprising sucrose alone, therefore, further investigations of the different saliva components on the *S. mutans*

and *C. albicans* interaction are required to gain more knowledge of the pathogenesis of cross-kingdom biofilms.

Metabolic interaction

After the initial adhesion, the cells start to proliferate to form microcolonies, forming the basal layer of the biofilm. Different research groups have discovered that *S. mutans* and *C. albicans* stimulate each other's growth when co-cultivation with sucrose environment. Paradoxically, *C. albicans* is not capable of utilizing sucrose effectively (Williamson et al., 1993). It seems that complex signals, cross-feeding, and metabolic interactions between *S. mutans* and *C. albicans* influence the proliferation rate, growth pattern, and virulence of co-species biofilm. This was experimentally demonstrated by Wu et al., who observed that cell membrane vesicles of *S. mutans* decompose sucrose into glucose and fructose to offer nutrient supply for *C. albicans* from their Benedict's and Seliwanoff's tests (Wu et al., 2020). *C. albicans* grows at a much higher rate when supplemented with glucose or fructose than sucrose. For *S. mutans*, it has been shown that conditioned medium from *S. mutans* - *C. albicans* biofilm favors its growth, Gtf activity and microcolony development (Kim et al., 2017). In addition, some matrix components like α-Mannan and β-1,3-Glucan purified from *C. albicans* stimulate *S. mutans* adherence and biofilm formation (Khoury et al., 2020). These results implied that *S. mutans* and *C. albicans* could share metabolites and cooperatively metabolize complex molecules to complement the metabolic requirements for biosynthetic pathways. The latter two studies provide some evidence accounting for the complex mechanisms responsible for enhanced growth in *S. mutans* and *C. albicans* dual-species biofilm from the gene aspect. The first finding is proposed by Ellepola et al., showing *S. mutans* enhanced *C. albicans* gene expression related to carbohydrate metabolism, including sugar transport systems, glycolysis, pyruvate degradation to ethanol and acetate production, the tricarboxylic acid cycle, and the electron transport chain (Ellepola et al., 2019). Furthermore, the transcriptomic changes also somewhat influence the protein level, some proteins associated with carbohydrate metabolism of *C. albicans* were also significantly increased in mixed-species biofilms. Carbohydrate metabolism is a crucial part of dental caries development. Another research studied how *C. albicans* influences the transcriptome of *S. mutans* in an established co-cultivation biofilm model (He et al., 2017). Their transcriptome data suggested that significant difference in gene expression of *S. mutans* between single and dual-species biofilm. Gene ontology function analysis showed the genes of *S. mutans* is related to carbohydrate transport and metabolic/catabolic process were regulated. For instance, lac operon is responsible for lactose transport and metabolism, encoding the tagatose 6-phosphate pathway (Zeng and Burne, 2021). Conversely, the accelerated metabolism of lactose can also make *C. albicans* transform from yeast to virulent hyphae. Other small chemical molecules, including farnesol, competence-stimulating peptide (CSP) and *sigX*, are also involved in the mediation of the growth kinetics between *C. albicans* and *S. mutans* (Jarosz et al., 2009; Sztajer et al., 2014). Farnesol is a

lipophilic molecule that accumulates in cell membranes and mediates quorum sensing system of *C. albicans*. A low level of farnesol (25-50 μM) could boost *S. mutans* growth and stimulate *gtfB* expression, which is associated with the microcolony development of *S. mutans* (Kim et al., 2017). Though a higher level of farnesol inhibited *S. mutans* growth, interestingly, the presence of *S. mutans* appeared to reduce the farnesol production of *C. albicans*. *SigX* is an alternative sigma factor for genes that control the uptake of exogenous DNA in *S. mutans*, whose expression can be activated by the CSP and *sigX*-inducing peptide (XIP). Sztajer et al. demonstrated the induction of *sigX* and high activation of the complete quorum sensing regulon of *S. mutans* when in co-culture with *C. albicans* (Sztajer et al., 2014). These findings have evidenced that quorum sensing pathways of these two species participate in the cross-kingdom interaction between *S. mutans* and *C. albicans*. However, the exact mechanisms underlying how these molecules modulate competition and cooperation in cross-kingdom biofilms remain unclear, but their potential significance is high.

Impact on virulence traits

As soon as cells attach to the surface and grow, the biofilm continues to grow by a formation of extracellular polymeric substance (EPS) until it reaches the maturation phase. The EPS matrix, one of the biofilm virulence factors, contributes to intercellular interactions and biofilm stability (Flemming and Wingender, 2010). Mixed *C. albicans*-*S. mutans* biofilms display an abundance in EPS matrix compared to their monospecies biofilm format. The increased EPS matrix is conducive to nutrients retention, which in turn facilitates cross-feeding between them. However, very little is known about the exact compositions in the extracellular matrix of *S. mutans* and *C. albicans* cross-kingdom biofilms. Further work should be conducted to define the structure and functions of EPS matrix components in the cross-kingdom biofilm. Despite this, numerous genes associated with EPS matrix have been investigated, with the redundancy of these genes further complicating the structure of the biofilm. Multiple authors have ascribed the increase in EPS matrix to the upregulated *gtfB* expression in the *S. mutans*-*C. albicans* cross-kingdom biofilm. GtfB is responsible for the synthesis of water-insoluble glucose, which is linked by α-1,3 glucosidic linkages to form glucan, an essential fraction of the EPS matrix (Senadheera et al., 2007). In addition to *gtfB*, *S. mutans* also enhances the expression of *C. albicans hwp1*, *als1*, and *als3* in cross-kingdom biofilms (Ellepola et al., 2017). These upregulated genes are critical for the adherence, filamentous growth, and biofilm formation of *C. albicans* (Nobile et al., 2006; Lombardi et al., 2019).

S. mutans and *C. albicans* cross-kingdom biofilms are potent in acidogenicity owing to their metabolic mutualism relationship that facilitates the exchange of carbohydrates between partners. Sampaio et al. have assessed the acidogenicity of *S. mutans* and *C. albicans* cross-kingdom biofilm by measuring pH of culture medium and found the pH drops to an extreme value of 4.5 (Sampaio et al., 2019), collaborating with the findings of Kim (Kim et al., 2020).

This low pH condition made *S. mutans* and *C. albicans* be dominant species since this is a true "acid shock" for other oral commensals as they would cease growth or not survive below 5.5. Moreover, *ldh* gene expression related to acid production increased while *ureC* and *arcA* expression associated with acid counteraction decreased (Du et al., 2020). The distinct features of acidogenicity in cross-kingdom biofilm could result in more differential damage to mineralized tooth tissue. In addition to acidogenicity, the progression of caries is intertwined intimately with acid tolerance by caries pathogens. It is conceivable that EPS matrix in cross-kingdom biofilm would act as a physical and protective barrier for microorganisms. Several recent studies have also investigated the genetic regulation of acid tolerance in *S. mutans* and *C. albicans* co-species biofilm. For instance, the gene *PHR2*, which encodes putative glycosidases required for proper cross-linking of β-1,3-glucans and β-1,6-glucans *C. albicans*, was significantly upregulated in cross-kingdom biofilm (Matsushika et al., 2016). Another upregulated gene is *fabM*, which is responsible for monounsaturated fatty acids synthesis and is necessary for *S. mutans* survival in an acidic environment (Fozo and Quivey, 2004).

The cross-kingdom interaction may aid *C. albicans* or *S. mutans* to survive under some extreme conditions. It is well documented that the biological niches in which oral microorganisms reside are rich in physiological and molecular cues involving low pH, high expression of some specific enzymes, high concentration of hydrogen peroxide (H_2O_2), and so on. To mimic this situation, Lobo and co-workers have compared the survival rate of *C. albicans* or *S. mutans* dual-species biofilm with their corresponding single-species biofilm after exposure to different stress conditions (Lobo et al., 2019). They found that both *C. albicans* and *S. mutans* in dual-species biofilm displayed higher survival rate than single biofilm when responding to 3% H_2O_2 and 0.2% chlorhexidine (CHX), implying the dual-species biofilm has a higher tolerance ability. In addition, the increased resistance of *C. albicans* towards fluconazole was also observed when in co-culture with *S. mutans*. Kim et al. found that the *S. mutans*-derived EPS matrix, which is dramatically increased during co-existence, coats the fungal cell, thus hindering the uptake of fluconazole (Kim et al., 2018). For the phenomenon of the increased tolerance to disinfectants in *C. albicans*-bacterial cross-kingdom biofilm, several recent reviews have stated the possible mechanisms involved in interspecies protection (Nogueira et al., 2019; Yan et al., 2022). Regarding *S. mutans*-*C. albicans* cross-kingdom biofilm, the increased matrix proven before is responsible for the tolerance of the whole populations within the biofilm. As known, the disinfectants or antimicrobials may encounter limited penetration difficulties through the matrix and hardly reach the deepest layers of the biofilm in their active form. While the alterations like persister cell differentiation, upregulation of drug efflux pumps, or genetic resistance during *C. albicans* and *S. mutans* co-cultivation have not been explored.

Therapeutic strategies

Clinical and experimental evidence demonstrated that the cross-kingdom relationship of *C. albicans* and *S. mutans* contributes to the progression of ECC and root caries. The rising incidence of antimicrobial tolerance, as well as the involvement of the notorious cross-kingdom biofilms in caries, has raised an urgent need in the search for novel therapeutic strategies. The traditional treatments of carious lesions are done with mechanical removal by burs, hand excavators, or other techniques. Alternatively, Er: YAG laser ablation and fluorescence-aided caries excavation are also introduced in carious dentin removal following the notion of minimally invasive techniques. However, no matter how carefully done, healthy parts of the tooth will be removed, even causing pulp exposure and pulp complications. On account of the hardness of deciduous teeth and root cementum being low, the occurrence rate of pulp exposure increased. Additionally, *C. albicans* and *S. mutans* are still left behind in the dentine after excavation, which contributes to caries recurrence. In recent years, attempts have been made to treat cross-kingdom biofilms by utilizing natural products, developing new nanomaterials or applying laser therapy (Figure 2).

Natural compounds

Natural compounds, mainly phytochemicals, could be used as an alternative for complementing antibiotics in the treatment of multiple disorders (Mishra et al., 2020). A number of studies have been published where natural compounds were tested for antimicrobial efficacy against oral biofilms (Karygianni et al., 2015). The results have ascertained the role of these natural products in preventing microorganism adhesion, inhibiting the EPS matrix formation, and thus reducing the deleterious effects of the pathogenic biofilms. Several antimicrobial mechanisms of natural compounds are also identified, including inhibition of cell division, block of efflux pump activities, disruption of cell membrane, and quench of quorum sensing.

The most common type of natural compound in oral application is phenolics. For example, curcumin is a natural polyphenol extracted from the rhizomes of Curcuma longa, which has been extensively investigated due to its wide range of pharmacological properties (Zheng et al., 2020). Curcumin has been proven to reduce biofilm biomass and inhibit the EPS matrix formation of *C. albicans* and *S. mutans* cross-kingdom biofilm (Li et al., 2019). Besides, curcumin remarkably downregulated the expression of *gtfB* and *gtfC* in *S. mutans*, two essential genes for mediating the cross-kingdom interaction between *C. albicans* and *S. mutans*. Another finding of suppressing the expression levels of some quorum sensing genes was also observed in this study, which is consistent with the former studies on the functions of phytochemicals. Thymol, a phenol monoterpene compound, is a promising agent for the prevention of biofilms formed by gram-negative and gram-positive microbes. A recent study has investigated the effects of thymol on *C. albicans* and *S. mutans* dual-species biofilm (Priya et al., 2021). Their data revealed that 300 μg/mL thymol exhibits anti-biofilm activity in *C. albicans* and *S. mutans*, both single-species and dual-species biofilms. The antibacterial mechanism against *C. albicans* or *S. mutans* is through the inhibition of several physiological activities, including yeast-hyphal transformation, filamentation, acidogenicity

FIGURE 2
Different approaches for the treatment of the cross-kingdom biofilm. Biofilms could be inhibited by employing natural compounds, nanomedicine, antimicrobial peptides, antimicrobial photodynamic therapy, probiotics or combination therapy.
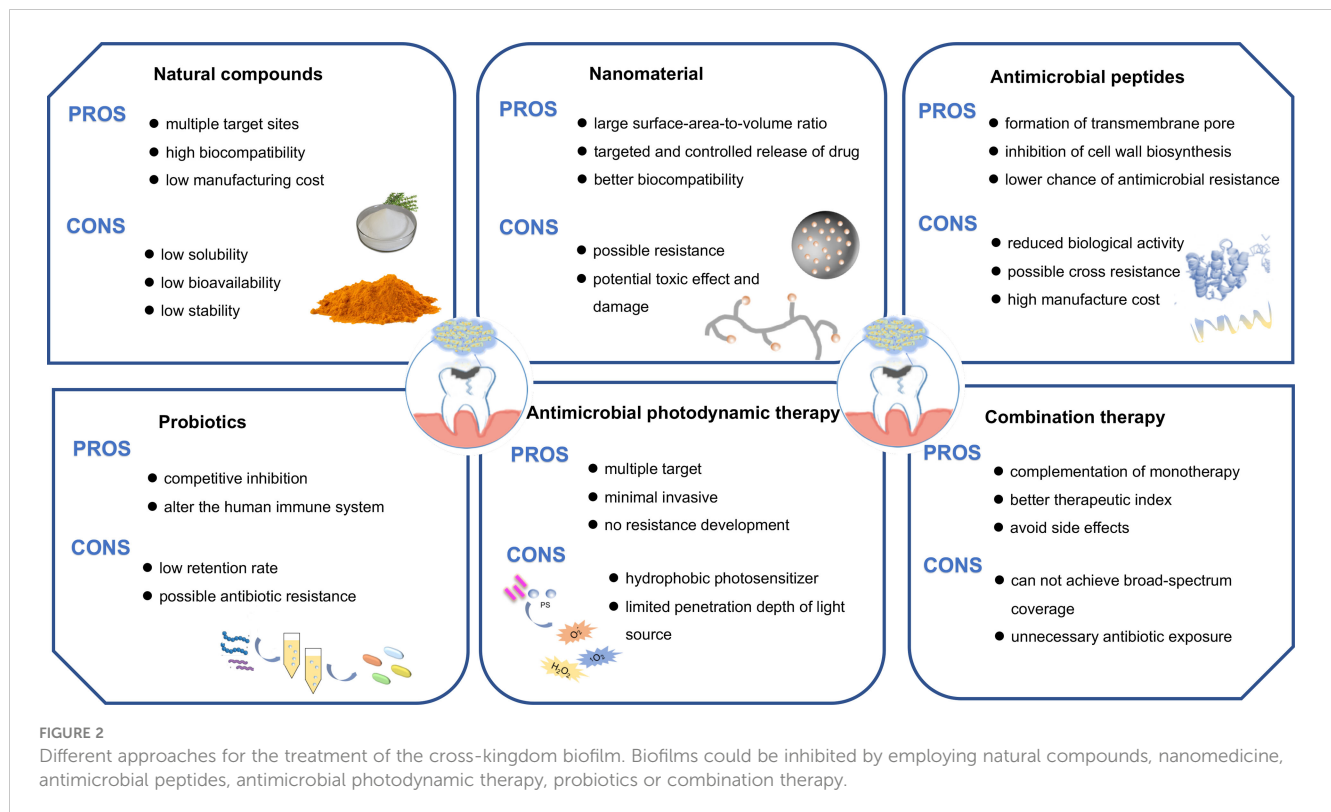
and acidurity. In the larvae infection model, the treatment with thymol led to reduced CFU counts of the infection site and significantly improved the survival of larvae. In addition, other types of natural compounds belonging to terpenoids or essential oils have been tested for their anti-biofilm capacity on the cross-kingdom biofilms. Caffeic acid phenethyl ester (CAPE), a classical type of terpenoids that extracts from propolis, exerts its potential in suppressing the growth, biofilm formation and EPS synthesis of *C. albicans* and *S. mutans* (Yin et al., 2022). The efficacy of CAPE is probably due to its down-regulation action in the expression level of *gtf* genes. Similarly, eugenol as a major component of essential oil, has been shown to inhibit the formation of *C. albicans* and *S. mutans* dual-species biofilm by reducing the viability of microorganisms and disrupting the biofilm structure. A few natural compounds with the potential of anti-biofilm activity are summarized in Table 1.

The wide exploration of the effects of these natural compounds is due to their unique characteristics like multiple target sites, high biocompatibility, low possibility of resistance and manufacturing cost. However, some drawbacks of natural extracts such as low solubility in water, low stability during storage, low bioavailability, and ingestion efficiency, hinder the full development of their use. One feasible method of improving the efficient delivery of natural compounds is to use nanotechnology in terms of increased bioavailability, targeting, and controlled release. The encapsulation of natural compounds by lipid-based nanoparticles is proven to be an efficient strategy to overcome those limitations. Additionally, the above-mentioned studies lack cytotoxicity evaluation, comparison with the current antimicrobials, and *in vivo* infection models to validate the drug efficacy. Thus, further

studies should be conducted in this regard to test the actual effectiveness of these natural compounds before entering into clinical application.

Nanomaterials

Nanomaterials, with dimensions generally in the 1–100 nm range, are versatile and bioactive and have received much attention in biomedical applications. They offer numerous advantages over conventional drugs, such as large surface-area-to-volume ratio, ultra-small sizes, and excellent chemical and physical properties (Benoit et al., 2019; Rubey and Brenner, 2021). Due to the intrinsic antimicrobial potential, organic and inorganic nanomaterials could act as biofilm-targeting agents or drug carriers. The antimicrobial mechanisms of nanomaterials on various microorganisms are not realized entirely. It is known that nanomaterials would penetrate microbial cell membrane easily and inhibit cell respiration and other essential biological processes. Additionally, nanomaterials could induce the burst of oxidative stress in microorganisms, leading to microbial death.

Chitosan is an excellent antimicrobial agent, a nontoxic polysaccharide, and nontoxic to various types of human cells. They show efficacy against *in vitro* and *in vivo* bacterial infections of a wide range of microbial species. Chitosan nanoparticles have been demonstrated to decrease the viability and the biofilm biomass of *C. albicans* and *S. mutans* biofilm after 18 h incubation (Ikono et al., 2019). However, treatment with chitosan nanoparticles for 3 hours did not affect the established dual-species biofilm. The results implied nanoparticles alone might have a limited effect on the cross-

TABLE 1 Summary of selected studies investigating antimicrobial effects of natural compounds on cross-kingdom biofilms.

Name	concentration	biofilm growth/ substrate	Treatment time	Microbial number reduction	Biofilm biomass reduction	Cytotoxicity	*In vivo* model	Proposed mechanisms	Reference
Curcumin	0.5 mM	48h/96-well plate	24 h	*Sm*: 69% *Ca*: 38%	24%	NM	NM	Inhibition of EPS formation and virulence factors	(Li et al., 2019)
Thymol	300 µg/mL	24h/ glass surface	24 h	*Sm*: 3.5 log *Ca*:2.5 log	50%	NM	larve infection	Inhibition of yeast-to-hyphal transition, hyphal-to-yeast transition, filamentation, and acidogenicity and acidurity of dual-species biofilms	(Priya et al., 2021)
CAPE	20, 40, 80µg/ mL	24 h/96-well plate	24 h	Reduced (No specific number)	Reduced (No specific number)	Human oral keratinocytes	NM	Inhibition of adhesion, EPS synthesis and cariogenic gene expression	(Yin et al., 2022)
GLE	0-7 mg/mL	24 h/96-well plate	24 h	NM	51 % (7 mg/ mL)	NM	NM	Inhibition of glucan formationof *S. m*	(Campbell et al., 2020)
GSE	0-7 mg/mL	24 h/96-well plate	24 h	NM	70 % (7 mg/ mL)	NM	NM	Inhibition of glucan formationof *S. m*	(Campbell et al., 2020)
PPFGT	0.0.1-0.63 mg/ mL	48 h/96-well plate	48h	NM	Reduced (No specific number)	NM	NM	Inhibition of growth and EPS	(Farkash et al., 2019)
Eugenol	50,100,200 µg/mL	48 h/glass coverslips	48 h	*Sm*:1.01 log (200 µg/mL) *Ca*:1.46 log (200 µg/mL)	NM	NM	NM	Disruption of cell membrane and matrix structure	(Jafri et al., 2019)
Tyrosol	50,100,200 mM	48 h/acrylic resin, hydroxyapatite	48 h	*Sm*:4 log (200 mM) *Ca*: 5log (200 mM)	NM	NM	NM	NM	(Arias et al., 2016)

Sm, *Streptococcus mutans*; *Ca*, *Candida albicans*; GSE, gesho stem extract; GLE, gesho leaf extract; NM, Not mentioned; EPS, Extracellular Polymeric Substance; ROS, Reactive oxygen species; PPFGT, polyphenon from green tea.

kingdom biofilms, which was consistent with the previous studies (Ikono et al., 2019; Aati et al., 2022). Therefore, scientists have worked on another way to take advantage of nano-sized materials. They could be engineered as drug carriers to transport promising drugs into the infection site, with the end goal of making the drug more efficient. Thanks to the encapsulation of the nanocarriers, the drug is protected from these threats and then taken up by the target cells to ensure the therapeutic effect. A representative example is the encapsulation of phloroglucinol into chitosan nanoparticles (CSNPs) via the ionic gelification method (Khan et al., 2022). Chitosan nanoparticles have been extensively employed to deliver different agents. The chitosan loaded with phloroglucinol (PG-CSNPs) exhibited inhibitory effects on the cross-kingdom biofilm of *C. albicans* and other bacteria in a concentration-dependent manner. Additionally, PG-CSNPs could enhance the effectiveness of several antibiotics in the mature cross-kingdom biofilms. CHX is regarded as a gold standard antimicrobial owing to its broad antimicrobial spectrum and excellent antimicrobial effectiveness. However, the higher concentration of CHX is toxic to the surrounding cells and likely to develop resistance. In order to solve this problem, iron oxide magnetic nanoparticles (IONPs) and chitosan (CS) have been synthesized, which protect CHX from

rapid degradation and reduce the dose required for therapeutic success (Vieira et al., 2019). The result also revealed that IONP-CS-CHX could effectively reduce the biofilm biomass of *C. albicans and S. mutans* dual-species biofilm. Moreover, INOP-CS-CHX showed a similar or superior effect in reducing viable microbial amounts and EPS matrix compared to free drugs. Both inorganic and organic nanoparticles can be modified to release the encapsulated drug under different stimuli, such as light, pH, and heat. Ito et al. formulated the multifunctional nanocarrier with a pH-responsive element, which achieved pH-triggered "smart release", to exert selective antibiofilm activity by targeting the specific pathogenic microenvironments (Ito et al., 2022). They studied the effects of the pH-responsive nanoparticles loaded with saturated farnesol (NPC-Far) on antibiofilm activity and teeth enamel demineralization. The NPC-Far could prevent local demineralization of tooth enamel by inhibiting biofilm formation on enamel. Table 2 summarizes the nanomaterials with inhibitory effects against cross-kingdom formed by *C. albicans* and *S. mutans*.

Overall, nanomaterials are characterized as a promising therapeutic platform for the treatment of cross-kingdom biofilms. However, two challenges threaten the wide application of nanomaterials for the eradication of biofilms: 1) the possible

TABLE 2 Summary of selected studies investigating antimicrobial effects of nanomaterials on cross-kingdom biofilms.

Name	concentration	biofilm growth/ substrate	Treatment time	Microbial number reduction	Biofilm biomass reduction	Cytotoxicity	*In vivo* model	Proposed mechanisms	Reference
CSNP	15%, 30%, 45%	18 h/96-well plate	3h,18h	Reduced (18h, 45%) Other groups no change	Reduced (18h, 45%) Other groups no change	NM	NM	NM	(Ikono et al., 2019)
PG-CSNP	512, 1024 μg/mL	72h/ silicon catheter	24 h	Complete inhibition	Complete inhibition	RAW.267	NM	Destruction of biofilm structure	(Khan et al., 2022)
INOP-CS-CHX	39, 78 μg/mL	24 h/96-well plate	24 h	*Sm*: 3.23, 3.24 $\log_{10}$ (39, 78μg/mL) *Ca*: 2.63, 5.91 $\log_{10}$ (39, 78μg/mL)	53 %(39 μg/mL) 68 % (78 μg/mL)	NM	NM	Inhibition of growth and metabolic activity of biofilms	(Vieira et al., 2019)
NPC-Far	0.5 mg/mL NPC+ 1mg/mL Far	44 h/ hydroxyapatite disks	Five times (0 h, 6 h, 20 h, 26 h, 32 h)	*Sm*: 2 log *Ca*:2 log	Reduced (No specific number)		NM	NM	Inhibition of 3D biofilm organization and disruption of acidification-related activities	(Ito et al., 2022)

Sm, *Streptococcus mutans*; *Ca*, *Candida albicans*, CSNP, chitosan nanoparticles; PG, phloroglucinol; INOP, iron oxide magnetic nanoparticles; CS, chitosan; CHX, chlorhexidine; NPC, nanoparticles; Far, farnesol.

resistance induced by repeated use of nanomaterials; 2) the potential toxic effect and damage from nanomaterials. The way to reduce the toxicity of nanomaterials is to synthesize nanomaterials by using some biodegradable biomaterials or by self-assembly. There still exists a widening gap between *in vitro* laboratory investigations and clinical practice. The current studies test the antibacterial efficacy through *in vitro* biofilms on polypropylene materials rather than tooth surfaces, which is far from the development of carious biofilms. The associated toxicities, potential side effects to surrounding cells, and lesser biocompatibility lack investigation. Furthermore, the underlying antimicrobial mechanisms and drug resistance possibility of nanoparticles should be revealed in the further work.

Probiotics

Probiotics refer to live cultures of microorganisms that could influence the composition of microbial communities and confer health benefits on the host when administered in adequate amounts. Probiotics have evolved as an alternative treatment of oral infectious disease owing to their reported beneficial effects in modulating the chronic inflammatory conditions of the gut. As the etiology of oral infection originates from the dysbiosis of microbial communities, the administration of probiotics may contribute to the clearance of pathogens, favor the growth of beneficial species and reduce the biofilm virulence. For instance, the consumption of probiotics in adequate amounts is effective in reducing cariogenic pathogen amounts through competing colonization sites in the mouth and secreting some harmful substance (Sivamaruthi et al., 2020).

Moreover, probiotics are participated in the interference of periodontitis via their inhibition of periodontopathogens and modulation of the immune response (Nguyen et al., 2021).

To date, *Lactobacilli* and *Bifidobacterium* are commonly studied probiotics, which produce lactic acid and other substances such as carbon peroxide and bacteriocins. The roles of *Lactobacillus plantarum* (*L. plantarum*) on the inhibition effect of *S. mutans* and *C. albicans* have been investigated. In a rat model, *L. plantarum* CCFM8724 decreased the carriage of *S. mutans* and reduced the caries score in rats (Zhang et al., 2020). The same group extended to investigate the disruption mechanisms of *L. plantarum* CCFM8724 by using metabolomics and transcriptomics analysis (Zhang et al., 2021). They found that some carbohydrates related to biofilm formation were decreased and virulence genes associated with adhesion were downregulated. Moreover, the supernatant of *L. plantarum* 108 could inhibit the biofilm formation of *S. mutans* and *C. albicans*, both in single-species and dual-species (Srivastava et al., 2020). In a recent study, Zeng et al. have assessed the effect of four Lactobacilli strains (*L. plantarum* ATCC 8014, *L. plantarum* ATCC 14917, *Lactobacillus rhamnosus* ATCC 2836, *Lactobacillus salivarius*) on the cross-kingdom biofilm of *S. mutans* and *C. albicans* (Zeng et al., 2022). The data suggested that *L. plantarum* possesses superior inhibition ability on the planktonic growth and biofilm formation of *S. mutans* and *C. albicans*, reduction in EPS matrix production, and microcolonies structure formation. *Streptococcus parasanguinis* is another beneficial commensal that could secrete antimicrobial substances to inhibit the growth of pathogens. The co-culture of a multi-species biofilm model of *S. parasanguinis*, *C. albicans*, and *S. mutans* presented a relative decrease in biofilm biomass compared to co-culture without *S.*

parasanguinis, indicating *S. parasanguinis* exert the disruption effect on *C. albicans* and *S. mutans* synergy (Huffines and Scoffield, 2020). Though *S. parasanguinis* reduces the viability of *S. mutans* in a H$_2$O$_2$ and nitrite-dependent manner, the lack of H$_2$O$_2$ production in *S. parasanguinis* did not affect the formation of *S. mutans* and *C. albicans* cross-kingdom biofilm. The results revealed that *S. parasanguinis* directly impaired the GTF activity of *S. mutans*, which prevents the GtfB-mediated binding to *C. albicans* mannan and glucan synthesis of *C. albicans*, thereby blocking the synergistic relationship between *C. albicans* and *S. mutans*.

In summary, probiotics examined using *in vitro* models show a promising method for the elimination of *C. albicans* and *S. mutans* cross-kingdom biofilm. Despite their potential effect on biofilm clearance, probiotics also have some drawbacks that constrain their application as a drug. On the one hand, most probiotics present a low retention rate in the oral cavity. Probiotics incorporated by fast-release formulations cannot ensure enough contact time between probiotic cells and the oral mucosa or dental surface. In addition, probiotics are not exempt from antibiotic resistance. Based on the dynamic condition of the caries biofilm development, more studies should extend the *in vitro* models to diverse and more biologically complex clinical situations. Besides, the effects of probiotics on long-term changes in microbiome composition merit further investigation.

Antimicrobial peptide

AMP has been considered as an alternative drug to antibiotics due to their several attractive properties, namely the ability to inhibit a broad spectrum of pathogens, the potential to downregulate virulence genes, and the low possibility to induce antimicrobial resistance. They are small-molecule polypeptides that can be divided into natural and synthetic antimicrobial peptides. There are several proposed mechanisms accounting for the direct killing of AMP. The most recognized antimicrobial mode of AMP is that they can insert into membrane bilayers and form transmembrane pores, which could be described by some models like 'barrel-stave' pore, 'carpet' or 'toroidal-pore' mechanism (Batoni et al., 2011; Niu et al., 2021). AMP could accumulate on cell surfaces of microbes, inhibit cell wall formation and induce cell membrane depolarization, leading to microbial death. Besides, AMP can also quickly penetrate microbial cell membranes to attack internal biological macromolecules and interfere with the normal metabolic activities of pathogens (Bechinger and Gorr, 2016).

The human cathelicidin AMP LL-37, has the potential for biofilm elimination, as demonstrated against *S. mutans* biofilm by inhibiting bacterial growth and biofilm formation (Wuersching et al., 2021). Another study has shown that LL-37 binds to the cell wall of *C. albicans*, alters the cell wall integrity, and affects cell adhesion of *C. albicans*, exerting anti-biofilm activity against *C. albicans* (Hsu et al., 2021). A clinical study also revealed the protective role of salivary LL-37 against ECC lesions (Colombo et al., 2016). Other AMPs including L18R, WMR-K, and gH625,

have been demonstrated to have antimicrobial capacity on *C. albicans* or *S. mutans* biofilm (Di Fermo et al., 2021; Galdiero et al., 2021; Maione et al., 2021). Simon and co-workers synthesized 75 kinds of cyclic dipeptides and found that cyclic dipeptides containing two aromatic amino acids have antibacterial activity and can effectively inhibit the adhesion of *C. albicans* and *S. mutans* to HA disk (Simon et al., 2019). The antibacterial mechanism may be related to interfering with the expression of quorum-sensing signal molecules. GERM CLEAN is a newly synthesized antibacterial peptide molecule with potent anti-biofilm activity. Xiong et al. have studied its effect on *C. albicans* and *S. mutans* biofilm, their results show that 50% GERM CLEAN can effectively reduce the formation of mixed biofilm, inhibit its acid production and prevent enamel demineralization (Xiong et al., 2021).

The advent of AMP has increased the availability of treatment in *C. albicans* and *S. mutans* cross-kingdom biofilm, however, some challenges still exist in their therapeutic utility. As most experiments were performed *in vitro* without mimicking the oral environment, the long-term stability of AMP in the oral cavity is still questionable. The caries biofilm often results in low pH of the local microenvironment, creating a harsh survival environment for AMP and making them lose biological activity. The antimicrobial and anti-biofilm performance of AMP may be dramatically affected. Several investigations have tried to use different chemical modification methods to extend the half-life of AMP, including the substitution of standard amino acids with non-natural amino acids, peptide cyclization or terminal modification via amidation, alkylation or acetylation. AMPs are expensive to manufacture under the scale of industrial production since their extraction, isolation, and purification processes are complex. Moreover, though AMP has a lower chance of inducing antimicrobial resistance than antibiotics, some bacteria harbor sensors that could activate AMP resistance mechanisms. Therefore, some aspects of AMP need to be explored further, such as the improvement of long-term stability, the controlled maintenance of bioactivity, and bacterial resistance.

Antimicrobial photodynamic therapy

aPDT is a process in which a non-toxic substance called photosensitizer interacts with the light source in the presence of oxygen. After receiving the appropriate wavelength of light illumination, the photosensitizer would undergo intersystem crossing to transform into a much longer-lived triplet photosensitizer. Then the triplet photosensitizer can interact with molecular oxygen via electron or energy transfer to produce reactive oxygen species (ROS) (Hu et al., 2018). These ROS are highly reactive and could target various cellular components leading to microbial death. Based on previous publications regarding antimicrobial mechanism of aPDT, it is proposed that aPDT undergoes two steps to fight against virulent biofilms. Firstly, the photosensitizer should penetrate the biofilm matrix and then bind to microbial cell surface or enter into the cellular cytoplasm. Once the photosensitizer is localized, the generated ROS could induce a series of attacks on adjacent molecules, including biofilms matrix components, cell wall or cell membrane, and inside the cells.

Due to this multi-target action of aPDT, it is reasonable to assume that aPDT can inactivate bacteria regardless of the level or mechanism of bacterial resistance. More importantly, aPDT has less opportunity to induce antimicrobial resistance when compared to antibiotics. Accumulating evidence has demonstrated the anti-planktonic and anti-biofilm effects of aPDT on gram-positive bacteria, gram-negative bacteria, and fungus (Pinto et al., 2018; Cai et al., 2019). Therefore, aPDT has been proposed to be a promising alternative in the treatment of oral infectious diseases. Gong et al. have investigated the effect of the combination of eosin and light-emitting diode on a multi-species biofilm including *S. mutans, C. albicans* and *Lactobacillus casei* (*L. casei*) (Gong et al., 2019). The CFU data showed the amount of *S. mutans*, *C. albicans* and *L. casei* was reduced by 96.64%, 97.59% and 83.33% respectively after aPDT treatment. Other articles also have investigated the antimicrobial effects of photosensitizers such as methylene blue and curcumin against *S. mutans* and *C. albicans* dual-species biofilm after irradiation (Pereira et al., 2010; Quishida et al., 2016). These results are hardly comparable due to multiple factors including bacteria species, photosensitizers, and aPDT parameters, but they all revealed that aPDT treatment alone is not enough to eradicate the cross-kingdom biofilm. Some photosensitizers are highly lipophilic and tend to aggregate in the aqueous environment, leading to the loss of photosensitizing activity and limited therapeutic index. Therefore, some endeavors have been made to overcome the situations and improve the efficiency of aPDT. As curcumin is water-insoluble, some studies have encapsulated curcumin in nanoformulations for increasing water solubility and antimicrobial effectiveness. The encapsulation of curcumin into Pluronics®-127 nanoparticles exhibited the antimicrobial effect against the *S. mutans* and *C. albicans* biofilms with more than 3 log steps of reduction (Dantas Lopes Dos Santos et al., 2021), which has achieved the bactericide effect stated by the USA Food and Drug Administration's Tentative Final Monograph. Though the enhancement of antimicrobial effectiveness was not observed compared to unloaded curcumin, the curcumin loaded with Pluronics®-127 exhibited adequate polydispersity index, stability, lower photodegradation, and autoaggregation compared to unloadedcurcumin. Another study has investigated the photodynamic action of chloroaluminium phthalocyanine in chitosan nanoparticles on cross-kingdom biofilm (Trigo-Gutierrez et al., 2018). Interestingly, the result showed that the encapsulated chloroaluminium phthalocyanine reduced the viable counts and metabolic activity of multi-species biofilm, whose antimicrobial effect is superior to 0.2% CHX.

The antimicrobial effectiveness of aPDT is dependent on multiple factors including the characteristics of photosensitizers, oxygen concentration, light dose and so on. aPDT is currently only proposed as an adjunct disinfection method in dental applications, mainly due to EPS matrix and efflux pumps of bacteria that hinder the binding capacity of photosensitizers and thus affect the antibacterial effect. Moreover, the generated ROS has a short lifespan and diffusion length in the biological environment. The specific structure and hypoxic environment of dentin tubule also confine the effect of aPDT. Further studies should concentrate on developing new photosensitizers with good hydrophilic properties

and high reactive oxygen species yields or improving the delivery efficiency of photosensitizers in order to achieve high antimicrobial efficacy.

Combination therapy

The complex structure of cross-kingdom biofilm and its elevated virulence pose major challenges to currently available antimicrobials (Ponde et al., 2021). As some antimicrobials have difficulties penetrating the dense matrix, the concentration of drug within the biofilm is too low to kill pathogens. Concerted efforts have been made to develop new antimicrobials, nonetheless, no new classes of antibiotics or their alternatives have been clinically approved in the last three decades. Given the recognition of the difficulties in drug innovation, combining the use of two or more antimicrobial agents may be a feasible and cost-effective strategy. Combination therapy has recently become optional for treating multidrug-resistant pathogens or complex cross-kingdom since it often leads to a more desirable outcome (Tyers and Wright, 2019; Zhang et al., 2022).

For example, aPDT has been paired with natural compounds, antibiotics, and chelating agents to enhance antimicrobial efficacy against refractory biofilms. These combinations possess many benefits, including less induced antimicrobial resistance, the reduction of side effects, the provision of alternative action pathways, and the improvement of the antimicrobial efficacy. Our previous work has compared the effects of toluidine blue O (TBO)-mediated aPDT in combination with H_2O_2 or not on *S. mutans* and *C. albicans* dual-species biofilm formed on polymethyl methacrylate disk and demonstrated that H_2O_2 administration followed by aPDT treatment displayed the highest capacity in disinfecting biofilm compared to either treatment alone (Li et al., 2021). Additionally, pretreatment with H_2O_2 could degrade EPS of biofilm and increase the outer membrane permeability of microbial cells, which are beneficial to the absorption of photosensitizers by microbial cells and further improves the effectiveness of aPDT treatment. The combination of antibiotics or antifungal drugs with chemotherapy is a feasible approach to treat difficult-to-treat infections and improve the therapeutic outcome. Kim et al. cultured *S. mutans* and *C. albicans* on HA disks for 43 h to form the cross-kingdom biofilms and investigated the combination effects of povidone iodine (PI) and fluconazole on biofilm (Kim et al., 2018). Interestingly, the combination exhibited higher antimicrobial efficacy than using PI or fluconazole and resulted in the complete elimination of *C. albicans* from HA disks. It has been documented that PI enhanced the uptake of fluconazole in *C. albicans* by disrupting the assembly of EPS matrix shield through inhibition of α-glucan synthesis by *S. mutans* bound on the *C. albicans* surface. Another example is the combination of Cis-2-decendnoic acid (C2DA) with CHX on dual-species biofilm (Rahmani-Badi et al., 2015). C2DA is a type of fatty acid secreted by *Pseudomonas aeruginosa* and could exert an anti-biofilm effect at nano-molar ranges. It was noteworthy that 100 nM C2DA and 0.06% CHX lead to the complete elimination of cross-kingdom biofilms, both of which decrease the dose required to achieve the same eradication

effect. Although the cooperative actions of H$_2$O$_2$ or CHX with some antimicrobial strategies have been proven previously, the side effects of high-concentration of H$_2$O$_2$ or CHX application should not be ignored. These side effects include taste alteration, tooth staining, burning sensation, and toxicity to oral mucosal cells. Therefore, it is not recommended to use H$_2$O$_2$ and CHX on children every day. However, there is one example where the combination of pH-responsive nanoparticles with three different drugs (tt-farnesol, myricetin, and compound 1771) showed limited efficiency against cross-kingdom biofilms (Roncari Rocha et al., 2022). Among them, tt-farnesol could target the cell membrane of microorganisms to exert an antibacterial effect; myricetin inhibits F-ATPase activity and suppresses the gene expression related to Gtfs; the compound 1771 inhibits the synthesis of lipoteichoic acid in Gram-positive bacteria to hinder the early coaggregation. The combination of three drugs had no efficacy on established *S. mutans* and *C. albicans* dual-species biofilms and only reduced the early colonization of microorganisms on the surface.

Antimicrobials reported to date do not meet the criteria of a "magic bullet", it is likely that we enter into the "post-antibiotic" era. The intricate interaction, spatial organization, and altogether behaviors of cross-kingdom biofilms reinforce the need to switch from monotherapy to combination therapy. From the studies we discussed, we could find the combination of two or more antimicrobials provides multiple sites of action to complement monotherapy, which is beneficial to the treatment of cross-kingdom biofilms formed by different structured microorganisms. Besides, the combination leads to a decrease in the antimicrobial concentration used and avoids some side effects. However, there are numerous questions left unanswered regarding standardized combination therapy. Firstly, the synergistic effect is not concluded from the enhancement of antimicrobial efficacy after applying combined antimicrobials. The synergistic interaction among antimicrobials should be evaluated through the assessment of fractional inhibitory concentration index. Secondly, the variables of combination therapy should be considered and reported in order to give a full comparison among studies. The treatment order, antimicrobial dosage and treatment frequency are linked to the final outcome. Additionally, several disadvantages of combination therapy should be considered. Not all combinations of antimicrobial methods could ultimately increase antimicrobial effectiveness. And, some combinations of antimicrobial strategies are only effective for certain species and cannot achieve broad-spectrum coverage. Under such circumstances, unnecessary antibiotic exposure that fuels resistance in the patient and the healthcare setting may occur.

Conclusion and future perspectives

Caries remain a tricky challenge worldwide, threatening individuals in developing and developed countries. The *S. mutans* and *C. albicans* cross-kingdom biofilm has been demonstrated to orchestrate the development and progression of caries. The specific features of the cross-kingdom biofilm, especially their mutual metabolic interaction, stability to mechanical forces, ability to produce EPS matrix, and resistance to current antimicrobials, make them an important clinical issue. However, many understandings regarding cross-kingdom biofilm are still uncovered such as resistance regulatory mechanisms and persistent cell development. There are also some new molecular targets needed to explore. The cognitions of the formation and regulation mechanisms of cross-kingdom biofilm, together with the validation in an *in vivo* model, are essential steps against cross-kingdom biofilm in caries treatment.

Over the past decade, there has been movement regarding innovative strategies against the cross-kingdom biofilm. The non-antibiotic therapeutic approaches, especially those natural extracts and nanomaterials, have shown significant potential in inactivating microorganisms and eliminating biofilm. Of the antimicrobials or strategies reviewed here, an efficient method to treat the cross-kingdom biofilm may be exploiting combinatory therapy. Combination therapy has shown advantages over standalone treatments such as reducing the concentration of the drug, enhancing selectivity and effectivity, and reducing the possibility of resistance. There are considerable uncertainties about these newly emerged treatments, which require further work to be done before implementing them in the clinic.

Herein, some considerations should be taken into account when developing new drugs or introducing new approaches for the elimination of *S. mutans* and *C. albicans* cross-kingdom biofilm. First, the toxicity profile of new antimicrobial agents should be concerned and thoroughly investigated before full-scale translation to the clinic. The main clearance route of oral topical treatment is via ingestion, which may lead to systemic circulation and tissue distribution. Several studies have reported systemic side effects due to the use of metal or metal-oxide-based nanoparticles (van der Zande et al., 2012; Lee et al., 2018). It is better to perform short-term and long-term evaluations to ensure the biosafety of new antimicrobial agents. Second, a concern of any new drug or strategy is the development of antimicrobial resistance, which should be explored in detail. Though the actions of some antimicrobial approaches like nanoparticles or aPDT are a combination of mechanisms, repeated exposure to any specific antimicrobial approach may result in variations of the targeted pathogens. Third, maintaining the balance of innate oral flora must be established during the use of a new drug or strategy. Indiscriminate use of antibiotics may lead to oral ecosystem dysbiosis again and aggravate the disease. The clinical goal of a new drug or strategy should not only aim to reduce pathogenic microbes but also to consolidate the harmonious balance of oral flora. Fourth, topical antibacterial agents are not maintained at the necessary level for a long duration due to the rapid clearance of saliva. To circumvent these problems, drug delivery systems like liposomes and micro particles are designed to target hydroxyapatite or bind with pellicle protein in order to enhance the bioavailability and retention of new compounds at dental surfaces and periodontal pockets. In addition, some studies have incorporated pH-responsive moieties into nanoparticles to ensure drug delivery in acidic pH within the cariogenic microenvironment. Fifth, patient compliance and motivation are essential in the prevention and treatment of caries. If child compliance is poor or the antimicrobial is discontinued

before the elimination of pathogenic microbes, recurrent caries may occur because remaining viable microorganisms will have the ability to grow and replicate. It therefore makes sense to develop new antimicrobial agents that do not require patient education for strict compliance. For instance, replacement therapy like probiotics may ensure lifelong protection after a single application without a need for long-term compliance. Besides, the other feasible method to improve patient compliance, it seems reasonable to move from local administrations by professionals to consumer products and home-care procedures, such as antimicrobial components incorporated into dentifrices and chewing gums. Sixth, economic consideration of new antibacterial compounds or strategies, in terms of production cost, is another important aspect in developing new drugs. It remains unclear whether the cost-benefit ratio of the new strategy will overcome traditional treatment regimens such as mechanical clearance, antiseptic use, or topical fluoride applications. The cost-effectiveness of the new strategy should be considered alongside the antimicrobial efficacy. Seventh, in addition to microbiological analysis, new antimicrobial drugs or approaches need further investigation on their practicality and feasibility. For instance, if the new drug is developed for daily use, examining the interaction of the new drug with currently available products like fluoride toothpaste may be required for compatible evaluation. Eighth, dental caries are caused by multi-species biofilms attaching to the dental surface or restorative materials. The artificial biofilm models range from monoculture to multi-species biofilm models. It is important to consider the shortcomings of biofilm models under *in vitro* and *ex vivo* conditions from clinical aspects. Single-species biofilm, predominantly *S. mutans*, is easy to grow and replicate in most experimental conditions. Although mono-species biofilm possesses high cariogenic potential, it cannot stimulate complex interspecies interactions related to high virulence and increased antimicrobial tolerance. Multi-species biofilm or naturally isolated biofilm are candidates for future studies to examine antimicrobial agents. In addition, substrates for biofilm culture are also an essential part of determining the effectiveness of antimicrobial agents. Synthetic surfaces like glass, polystyrene, or polydimethylsiloxane cannot reproduce the microanatomy of dentine and the interaction between the tooth surface and antimicrobial agent. It has been suggested that human dentin is a good choice for caries biofilm growth. Moreover, biofilm growth conditions, such as static or dynamic, will influence biofilm biomass, which in turn affects the evaluation of new antibacterial strategies against biofilms. Other factors like biofilm age, culture medium, and substrate size also influence the assessment of antimicrobial methods. However, there is no standardized protocol for biofilm model construction for antimicrobial assessment so far. Standardized biofilm models should be made to represent a similar oral environment, which will help researchers find potent therapeutic strategies.Therefore, future work is recommended to evaluate the overall aspects of the newly antimicrobials or strategies, which shall help in introducing effective approaches into clinical practice.

Apart from those strategies we reviewed here, we found that the physiological cell-to-cell interactions in *S. mutans* and *C.* *albicans* biofilm can indeed serve as another avenue worth exploring as the potential treatment target. Gtfs and glucans play a role in *S. mutans* and *C. albicans* interaction, which can be considered the primary targets for developing eradication strategies against cross-kingdom biofilms. Targeting Gtfs or glucans by hampering their activity and consequently inhibiting the production of EPS would impair the co-adhesion between *S. mutans* and *C. albicans*, which is an appealing strategy for cross-kingdom biofilm prevention. Another plausible strategy to treat *S. mutans* and *C. albicans* cross-kingdom biofilm is to inhibit the production of their adhesins, which are crucial to the formation and development of cross-kingdom biofilm. While some inhibitors of intercellular signaling of *S. mutans* or *C. albicans* biofilm have been identified in previous studies, little progress has been made in these inhibitors targeting *S. mutans* and *C. albicans* dual-species biofilm. Targeting metabolic pathway regulators such as farnesol, CSP, or XIP is anticipated to interfere with the cell-to-cell metabolic interaction and thus play a potential role in the treatment of dual-species biofilms.

Author contributions

YL, MW and XH contributed to the conception and design of the study. YL, SH and JD performed the data searching and wrote sections of the manuscript. YL wrote the first draft of the manuscript. XH performed the final corrections. All authors contributed to the manuscript revision and read and approved the submitted version.

Funding

Conflict of interest

The authors declare that the research was conducted in the absence of any commercial or financial relationships that could be construed as a potential conflict of interest.

Publisher's note

All claims expressed in this article are solely those of the authors and do not necessarily represent those of their affiliated organizations, or those of the publisher, the editors and the reviewers. Any product that may be evaluated in this article, or claim that may be made by its manufacturer, is not guaranteed or endorsed by the publisher.

References

Aati, S., Shrestha, B., and Fawzy, A. (2022). Cytotoxicity and antimicrobial efficiency of ZrO(2) nanoparticles reinforced 3D printed resins. *Dent. Mater* 38 (8), 1432–1442. doi: 10.1016/j.dental.2022.06.030

Arias, L. S., Delbem, A. C., Fernandes, R. A., Barbosa, D. B., and Monteiro, D. R. (2016). Activity of tyrosol against single and mixed-species oral biofilms. *J. Appl. Microbiol.* 120 (5), 1240–1249. doi: 10.1111/jam.13070

Bachtiar, E. W., and Bachtiar, B. M. (2018). Relationship between *Candida albicans* and *Streptococcus mutans* in early childhood caries, evaluated by quantitative PCR. *F1000Res* 7, 1645. doi: 10.12688/f1000research.16275.2

Batoni, G., Maisetta, G., Brancatisano, F. L., Esin, S., and Campa, M. (2011). Use of antimicrobial peptides against microbial biofilms: advantages and limits. *Curr. Med. Chem.* 18 (2), 256–279. doi: 10.2174/092986711794088399

Bechinger, B., and Gorr, S. U. (2016). Antimicrobial peptides: mechanisms of action and resistance. *J. Dental Res.* 96 (3), 254–260. doi: 10.1177/0022034516679973

Benoit, D. S. W., Sims, K. R.Jr., and Fraser, D. (2019). Nanoparticles for oral biofilm treatments. *ACS Nano* 13 (5), 4869–4875. doi: 10.1021/acsnano.9b02816

Bernard, C., Girardot, M., and Imbert, C. (2020). Candida albicans interaction with gram-positive bacteria within interkingdom biofilms. *J. Mycol. Med.* 30 (1), 100909. doi: 10.1016/j.mycmed.2019.100909

Bowman, B. J., and Bowman, E. J. (1986). H+-ATPases from mitochondria, plasma membranes, and vacuoles of fungal cells. *J. Membr Biol.* 94 (2), 83–97. doi: 10.1007/BF01871190

Cai, Z., Li, Y., Wang, Y., Chen, S., Jiang, S., Ge, H., et al. (2019). Disinfect *Porphyromonas gingivalis* biofilm on titanium surface with combined application of chlorhexidine and antimicrobial photodynamic therapy. *Photochem. Photobiol.* 95 (3), 839–845. doi: 10.1111/php.13060

Campbell, M., Fathi, R., Cheng, S. Y., Ho, A., and Gilbert, E. S. (2020). Rhamnus prinoides (gesho) stem extract prevents co-culture biofilm formation by *Streptococcus mutans* and *Candida albicans*. *Lett. Appl. Microbiol.* 71 (3), 294–302. doi: 10.1111/lam.13307

Cavalcanti, I. M., Del Bel Cury, A. A., Jenkinson, H. F., and Nobbs, A. H. (2017). Interactions between *Streptococcus oralis*, *Actinomyces oris*, and *Candida albicans* in the development of multispecies oral microbial biofilms on salivary pellicle. *Mol. Oral. Microbiol.* 32 (1), 60–73. doi: 10.1111/omi.12154

Cavalcanti, Y. W., Morse, D. J., da Silva, W. J., Del-Bel-Cury, A. A., Wei, X., Wilson, M., et al. (2015). Virulenceand pathogenicity of Candida albicans is enhanced in biofilms containing oral bacteria. *Biofouling* 31 (1), 27–38. doi: 10.1080/08927014.2014.996143

Colombo, N. H., Ribas, L. F., Pereira, J. A., Kreling, P. F., Kressirer, C. A., Tanner, A. C., et al. (2016). Antimicrobial peptides in saliva of children with severe early childhood caries. *Arch. Oral. Biol.* 69, 40–46. doi: 10.1016/j.archoralbio.2016.05.009

Dantas Lopes Dos Santos, D., Besegato, J. F., de Melo, P. B. G., Oshiro Junior, J. A., Chorilli, M., Deng, D., et al. (2021). Curcumin-loaded Pluronic((R)) f-127 micelles as a drug delivery system for curcumin-mediated photodynamic therapy for oral application. *Photochem. Photobiol.* 97 (5), 1072–1088. doi: 10.1111/php.13433

de Carvalho, F. G., Silva, D. S., Hebling, J., Spolidorio, L. C., and Spolidorio, D. M. (2006). Presence of mutans streptococci and candida spp. in dental plaque/dentine of carious teeth and early childhood caries. *Arch. Oral. Biol.* 51 (11), 1024–1028. doi: 10.1016/j.archoralbio.2006.06.001

Di Fermo, P., Ciociola, T., Di Lodovico, S., D'Ercole, S., Petrini, M., Giovati, L., et al. (2021). Antimicrobial peptide L18R displays a modulating action against inter-kingdom biofilms in the Lubbock chronic wound biofilm model. *Microorganisms* 9 (8), 1779. doi: 10.3390/microorganisms9081779

Du, Q., Ren, B., He, J., Peng, X., Guo, Q., Zheng, L., et al. (2020). *Candida albicans* promotes tooth decay by inducing oral microbial dysbiosis. *ISME J.* 15 (3), 894–908. doi: 10.1038/s41396-020-00823-8

Du, Q., Yuan, S., Zhao, S., Fu, D., Chen, Y., Zhou, Y., et al. (2021). Coexistence of *Candida albicans* and *Enterococcus faecalis* increases biofilm virulence and periapical lesions in rats. *Biofouling* 37 (9-10), 964–974. doi: 10.1080/08927014.2021.1993836

Ellepola, K., Liu, Y., Cao, T., Koo, H., and Seneviratne, C. J. (2017). Bacterial GtfB augments *Candida albicans* accumulation in cross-kingdom biofilms. *J. Dent. Res.* 96 (10), 1129–1135. doi: 10.1177/0022034517714414

Ellepola, K., Truong, T., Liu, Y., Lin, Q., Lim, T. K., Lee, Y. M., et al. (2019). Multi-omics analyses reveal synergistic carbohydrate metabolism in *Streptococcus mutans-Candida albicans* mixed-species biofilms. *Infect. Immun.* 87 (10), e00339–e00319. doi: 10.1128/IAI.00339-19

Falsetta, M. L., Klein, M. I., Colonne, P. M., Scott-Anne, K., Gregoire, S., Pai, C. H., et al. (2014). Symbiotic relationship between *Streptococcus mutans* and *Candida albicans* synergizes virulence of plaque biofilms *in vivo*. *Infect. Immun.* 82 (5), 1968–1981. doi: 10.1128/IAI.00087-14

Farkash, Y., Feldman, M., Ginsburg, I., Steinberg, D., and Shalish, M. (2019). Polyphenols inhibit *Candida albicans* and *Streptococcus mutans* biofilm formation. *Dent. J. (Basel)* 7 (2), 14. doi: 10.3390/dj7020042

Flemming, H.-C., and Wingender, J. (2010). The biofilm matrix. *Nat. Rev. Microbiol.* 8 (9), 623–633. doi: 10.1038/nrmicro2415

Fourie, R., Albertyn, J., Sebolai, O., Gcilitshana, O., and Pohl, C. H. (2021). *Candida albicans* SET3 plays a role in early biofilm formation, interaction with *Pseudomonas aeruginosa* and virulence in caenorhabditis elegans. *Front. Cell Infect. Microbiol.* 11. doi: 10.3389/fcimb.2021.680732

Fozo, E. M., and Quivey, R. G. (2004). The fabM gene product of *Streptococcus mutans* is responsible for the synthesis of monounsaturated fatty acids and is necessary for survival at low pH. *J. Bacteriol* 186 (13), 4152–4158. doi: 10.1128/jb.186.13.4152-4158.2004

Fragkou, S., Balasouli, C., Tsuzukibashi, O., Argyropoulou, A., Menexes, G., Kotsanos, N., et al. (2016). *Streptococcus mutans*, *Streptococcus sobrinus* and *Candida albicans* in oral samples from caries-free and caries-active children. *Eur. Arch. Paediatric Dentistry* 17 (5), 367–375. doi: 10.1007/s40368-016-0239-7

Fure, S. (2004). Ten-year cross-sectional and incidence study of coronal and root caries and some related factors in elderly Swedish individuals. *Gerodontology* 21 (3), 130–140. doi: 10.1111/j.1741-2358.2004.00025.x

Galdiero, E., Salvatore, M. M., Maione, A., Carraturo, F., Galdiero, S., Falanga, A., et al. (2021). Impact of the peptide WMR-K on dual-species biofilm *Candida albicans/Klebsiella pneumoniae* and on the untargeted metabolomic profile. *Pathogens* 10 (2), 214. doi: 10.3390/pathogens10020214

Garcia, B. A., Acosta, N. C., Tomar, S. L., Roesch, L. F. W., Lemos, J. A., Mugayar, L. R. F., et al. (2021). Association of *Candida albicans* and cbp(+) *Streptococcus mutans* with early childhood caries recurrence. *Sci. Rep.* 11 (1), 10802. doi: 10.1038/s41598-021-90198-3

Gibney, J. M., Naganathan, V., and Lim, M. (2021). Oral health is essential to the well-being of older people. *Am. J. Geriatr. Psychiatry* 29 (10), 1053–1057. doi: 10.1016/j.jagp.2021.06.002

Gong, J., Park, H., Lee, J., Seo, H., and Lee, S. (2019). Effect of photodynamic therapy on multispecies biofilms, including *Streptococcus mutans*, *lactobacillus casei*, and *Candida albicans*. *Photobiomodul Photomed Laser Surg.* 37 (5), 282–287. doi: 10.1089/photob.2018.4571

Gregoire, S., Xiao, J., Silva, B. B., Gonzalez, I., Agidi, P. S., Klein, M. I., et al. (2011). Role of glucosyltransferase b in interactions of *Candida albicans* with *Streptococcus mutans* and with an experimental pellicle on hydroxyapatite surfaces. *Appl. Environ. Microbiol.* 77 (18), 6357–6367. doi: 10.1128/AEM.05203-11

He, J., Kim, D., Zhou, X., Ahn, S. J., Burne, R. A., Richards, V. P., et al. (2017). RNA-Seq reveals enhanced sugar metabolism in *Streptococcus mutans* Co-cultured with *Candida albicans* within mixed-species biofilms. *Front. Microbiol.* 8, 1036. doi: 10.3389/fmicb.2017.01036

Hsu, C. M., Liao, Y. L., Chang, C. K., and Lan, C. Y. (2021). *Candida albicans* Sfp1 is involved in the cell wall and endoplasmic reticulum stress responses induced by human antimicrobial peptide LL-37. *Int. J. Mol. Sci.* 22 (19), 10633. doi: 10.3390/ijms221910633

Hu, X. Q., Huang, Y. Y., Wang, Y. G., Wang, X. Y., and Hamblin, M. R. (2018). Antimicrobial photodynamic therapy to control clinically relevant biofilm infections. *Front. Microbiol.* 9, 1299. doi: 10.3389/fmicb.2018.01299

Huffines, J. T., and Scoffield, J. A. (2020). Disruption of *Streptococcus mutans* and *Candida albicans* synergy by a commensal streptococcus. *Sci. Rep.* 10 (1), 19661. doi: 10.1038/s41598-020-76744-5

Hugo, F. N., Kassebaum, N. J., Marcenes, W., and Bernabe, E. (2021). Role of dentistry in global health: challenges and research priorities. *J. Dent. Res.* 100 (7), 681–685. doi: 10.1177/0022034521992011

Hwang, G., Liu, Y., Kim, D., Li, Y., Krysan, D. J., and Koo, H. (2017). *Candida albicans* mannans mediate *Streptococcus mutans* exoenzyme GtfB binding to modulate cross-kingdom biofilm development *in vivo*. *PLoS Pathog.* 13 (6), e1006407. doi: 10.1371/journal.ppat.1006407

Hwang, G., Marsh, G., Gao, L., Waugh, R., and Koo, H. (2015). Binding force dynamics of *Streptococcus mutans*-glucosyltransferase b to *Candida albicans*. *J. Dent. Res.* 94 (9), 1310–1317. doi: 10.1177/0022034515592859

Ikono, R., Vibriani, A., Wibowo, I., Saputro, K. E., Muliawan, W., Bachtiar, B. M., et al. (2019). Nanochitosan antimicrobial activity against *Streptococcus mutans* and *Candida albicans* dual-species biofilms. *BMC Res. Notes* 12 (1), 383. doi: 10.1186/s13104-019-4422-x

Ito, T., Sims, K. R.Jr., Liu, Y., Xiang, Z., Arthur, R. A., Hara, A. T., et al. (2022). Farnesol delivery via polymeric nanoparticle carriers inhibits cariogenic cross-kingdom biofilms and prevents enamel demineralization. *Mol. Oral. Microbiol.* 37 (5), 218–228. doi: 10.1111/omi.12379

Jafri, H., Khan, M. S. A., and Ahmad, I. (2019). *In vitro* efficacy of eugenol in inhibiting single and mixed-biofilms of drug-resistant strains of *Candida albicans* and *Streptococcus mutans*. *Phytomedicine* 54, 206–213. doi: 10.1016/j.phymed.2018.10.005

Jarosz, L. M., Deng, D. M., van der Mei, H. C., Crielaard, W., and Krom, B. P. (2009). *Streptococcus mutans* competence-stimulating peptide inhibits *Candida albicans* hypha formation. *Eukaryot Cell* 8 (11), 1658–1664. doi: 10.1128/EC.00070-09

Jenkinson, H. F., Lala, H. C., and Shepherd, M. G. (1990). Coaggregation of *Streptococcus sanguis* and other streptococci with *Candida albicans*. *Infect. Immun.* 58 (5), 1429–1436. doi: 10.1128/iai.58.5.1429-1436.1990

Karygianni, L., Al-Ahmad, A., Argyropoulou, A., Hellwig, E., Anderson, A. C., and Skaltsounis, A. L. (2015). Natural antimicrobials and oral microorganisms: a systematic review on herbal interventions for the eradication of multispecies oral biofilms. *Front. Microbiol.* 6, 1529. doi: 10.3389/fmicb.2015.01529

Khan, F., Oh, D., Chandika, P., Jo, D. M., Bamunarachchi, N. I., Jung, W. K., et al. (2022). Inhibitory activities of phloroglucinol-chitosan nanoparticles on mono- and dual-species biofilms of *Candida albicans* and bacteria. *Colloids Surf B Biointerfaces* 211, 112307. doi: 10.1016/j.colsurfb.2021.112307

Khoury, Z. H., Vila, T., Puthran, T. R., Sultan, A. S., Montelongo-Jauregui, D., Melo, M. A. S., et al. (2020). The role of *Candida albicans* secreted polysaccharides in augmenting *Streptococcus mutans* adherence and mixed biofilm formation: *In vitro* and *in vivo* studies. *Front. Microbiol.* 11, 307. doi: 10.3389/fmicb.2020.00307

Kim, D., Liu, Y., Benhamou, R. I., Sanchez, H., Simón-Soro, Á., Li, Y., et al. (2018). Bacterial-derived exopolysaccharides enhance antifungal drug tolerance in a cross-kingdom oral biofilm. *ISME J.* 12 (6), 1427–1442. doi: 10.1038/s41396-018-0113-1

Kim, H. E., Liu, Y., Dhall, A., Bawazir, M., Koo, H., and Hwang, G. (2020). Synergism of *Streptococcus mutans* and *Candida albicans* reinforces biofilm maturation and acidogenicity in saliva: an *In vitro* study. *Front. Cell Infect. Microbiol.* 10, 623980. doi: 10.3389/fcimb.2020.623980

Kim, D., Sengupta, A., Niepa, T. H. R., Lee, B.-H., Weljie, A., Freitas-Blanco, V. S., et al. (2017). *Candida albicans* stimulates *Streptococcus mutans* microcolony development via cross-kingdom biofilm-derived metabolites. *Sci. Rep.* 7 (1), 41332. doi: 10.1038/srep41332

Klinke, T., Kneist, S., de Soet, J. J., Kuhlisch, E., Mauersberger, S., Forster, A., et al. (2009). Acid production by oral strains of *Candida albicans* and lactobacilli. *Caries Res.* 43 (2), 83–91. doi: 10.1159/000204911

Lamont, R. J., Koo, H., and Hajishengallis, G. (2018). The oral microbiota: dynamic communities and host interactions. *Nat. Rev. Microbiol.* 16 (12), 745–759. doi: 10.1038/s41579-018-0089-x

Lee, J. H., Sung, J. H., Ryu, H. R., Song, K. S., Song, N. W., Park, H. M., et al. (2018). Tissue distribution of gold and silver after subacute intravenous injection of co-administered gold and silver nanoparticles of similar sizes. *Arch. Toxicol.* 92 (4), 1393–1405. doi: 10.1007/s00204-018-2173-4

Li, Y., Du, J., Huang, S., Wang, S., Wang, Y., Cai, Z., et al. (2021). Hydrogen peroxide potentiates antimicrobial photodynamic therapy in eliminating *Candida albicans* and *Streptococcus mutans* dual-species biofilm from denture base. *Photodiagnosis Photodyn. Ther.* 37, 102691. doi: 10.1016/j.pdpdt.2021.102691

Li, X., Yin, L., Ramage, G., Li, B., Tao, Y., Zhi, Q., et al. (2019). Assessing the impact of curcumin on dual-species biofilms formed by *Streptococcus mutans* and *Candida albicans*. *Microbiol. Open* 8 (12), e937. doi: 10.1002/mbo3.937

Lobo, C. I. V., Rinaldi, T. B., Christiano, C. M. S., De Sales Leite, L., Barbugli, P. A., and Klein, M. I. (2019). Dual-species biofilms of *Streptococcus mutans* and *Candida albicans* exhibit more biomass and are mutually beneficial compared with single-species biofilms. *J. Oral. Microbiol.* 11 (1), 1581520. doi: 10.1080/20002297.2019.1581520

Lombardi, L., Zoppo, M., Rizzato, C., Bottai, D., Hernandez, A. G., Hoyer, L. L., et al. (2019). Characterization of the candida orthopsilosis agglutinin-like sequence (ALS) genes. *PLoS One* 14 (4), e0215912. doi: 10.1371/journal.pone.0215912

Maijala, M., Rautemaa, R., Jarvensivu, A., Richardson, M., Salo, T., and Tjaderhane, L. (2007). *Candida albicans* does not invade carious human dentine. *Oral. Dis.* 13 (3), 279–284. doi: 10.1111/j.1601-0825.2006.01279.x

Maione, A., de Alteriis, E., Carraturo, F., Galdiero, S., Falanga, A., Guida, M., et al. (2021). The membranotropic peptide gH625 to combat mixed *Candida albicans/Klebsiella pneumoniae* biofilm: correlation between *In vitro* anti-biofilm activity and *In vivo* antimicrobial protection. *J. Fungi (Basel)* 7 (1), 26. doi: 10.3390/jof7010026

Matsushika, A., Negi, K., Suzuki, T., Goshima, T., and Hoshino, T. (2016). Identification and characterization of a novel issatchenkia orientalis GPI-anchored protein, IoGas1, required for resistance to low pH and salt stress. *PLoS One* 11 (9), e0161888. doi: 10.1371/journal.pone.0161888

Mishra, R., Panda, A. K., De Mandal, S., Shakeel, M., Bisht, S. S., and Khan, J. (2020). Natural anti-biofilm agents: strategies to control biofilm-forming pathogens. *Front. Microbiol.* 11, 566325. doi: 10.3389/fmicb.2020.566325

Montelongo-Jauregui, D., and Lopez-Ribot, J. L. (2018). Candida interactions with the oral bacterial microbiota. *J. Fungi (Basel)* 4 (4), 122. doi: 10.3390/jof4040122

Nascimento, M., Xiao, J., Moon, Y., Li, L., Rustchenko, E., Wakabayashi, H., et al. (2016). *Candida albicans* carriage in children with severe early childhood caries (S-ECC) and maternal relatedness. *PloS One* 11 (10), e0164242. doi: 10.1371/journal.pone.0164242

Nguyen, T., Brody, H., Radaic, A., and Kapila, Y. (2021). Probiotics for periodontal health-current molecular findings. *Periodontol 2000* 87 (1), 254–267. doi: 10.1111/prd.12382

Nikawa, H., H., T., and Yamamoto, T. (1998). Denture plaque - past and recent concerns. *J. Dent.* 26 (4), 299–304. doi: 10.1016/s0300-5712(97)00026-2

Niu, J. Y., Yin, I. X., Mei, M. L., Wu, W. K. K., Li, Q. L., and Chu, C. H. (2021). The multifaceted roles of antimicrobial peptides in oral diseases. *Mol. Oral. Microbiol.* 36 (3), 159–171. doi: 10.1111/omi.12333

Nobile, C. J., and Johnson, A. D. (2015). *Candida albicans* biofilms and human disease. *Annu. Rev. Microbiol.* 69, 71–92. doi: 10.1146/annurev-micro-091014-104330

Nobile, C. J., Nett, J. E., Andes, D. R., and Mitchell, A. P. (2006). Function of *Candida albicans* adhesin Hwp1 in biofilm formation. *Eukaryot Cell* 5 (10), 1604–1610. doi: 10.1128/EC.00194-06

Nogueira, F., Sharghi, S., Kuchler, K., and Lion, T. (2019). Pathogenetic impact of bacterial-fungal interactions. *Microorganisms* 7 (10), 459. doi: 10.3390/microorganisms7100459

Pereira, C. A., Romeiro, R. L., Costa, A. C. B. P., Machado, A. K. S., Junqueira, J. C., and Jorge, A. O. C. (2010). Susceptibility of *Candida albicans*, *Staphylococcus aureus*, and *Streptococcus mutans* biofilms to photodynamic inactivation: an *in vitro* study. *Lasers Med. Sci.* 26 (3), 341–348. doi: 10.1007/s10103-010-0852-3

Pereira-Cenci, T., Deng, D. M., Kraneveld, E. A., Manders, E. M., Del Bel Cury, A. A., Ten Cate, J. M., et al. (2008). The effect of *Streptococcus mutans* and *Candida glabrata* on *Candida albicans* biofilms formed on different surfaces. *Arch. Oral. Biol.* 53 (8), 755–764. doi: 10.1016/j.archoralbio.2008.02.015

Peters, B. M., Ovchinnikova, E. S., Krom, B. P., Schlecht, L. M., Zhou, H., Hoyer, L. L., et al. (2012). *Staphylococcus aureus* adherence to *Candida albicans* hyphae is mediated by the hyphal adhesin Als3p. *Microbiol. (Reading)* 158 (Pt 12), 2975–2986. doi: 10.1099/mic.0.062109-0

Pinto, A. P., Rosseti, I. B., Carvalho, M. L., da Silva, B. G. M., Alberto-Silva, C., and Costa, M. S. (2018). Photodynamic antimicrobial chemotherapy (PACT), using toluidine blue O inhibits the viability of biofilm produced by *Candida albicans* at different stages of development. *Photodiagnosis Photodyn. Ther.* 21, 182–189. doi: 10.1016/j.pdpdt.2017.12.001

Ponde, N. O., L., L., Ramage, G., Naglik, J. R., and Richardson, J. P. (2021). Candida albicans biofilms and polymicrobial interactions. *Crit. Rev. Microbiol.* 47 (1), 91–111. doi: 10.1080/1040841X.2020.1843400

Priya, A., Selvaraj, A., Divya, D., Karthik Raja, R., and Pandian, S. K. (2021). *In vitro* and *In vivo* anti-infective potential of thymol against early childhood caries causing dual species *Candida albicans* and *Streptococcus mutans*. *Front. Pharmacol.* 12. doi: 10.3389/fphar.2021.760768

Qiu, R., Li, W., Lin, Y., Yu, D., and Zhao, W. (2015). Genotypic diversity and cariogenicity of *Candida albicans* from children with early childhood caries and caries-free children. *BMC Oral. Health* 15 (1), 144. doi: 10.1186/s12903-015-0134-3

Quishida, C. C., De Oliveira Mima, E. G., Jorge, J. H., Vergani, C. E., Bagnato, V. S., and Pavarina, A. C. (2016). Photodynamic inactivation of a multispecies biofilm using curcumin and LED light. *Lasers Med. Sci.* 31 (5), 997–1009. doi: 10.1007/s10103-016-1942-7

Rahmani-Badi, A., Sepehr, S., and Babaie-Naiej, H. (2015). A combination of cis-2-decenoic acid and chlorhexidine removes dental plaque. *Arch. Oral. Biol.* 60 (11), 1655–1661. doi: 10.1016/j.archoralbio.2015.08.006

Raja, M., Hannan, A., and Ali, K. (2010). Association of oral candidal carriage with dental caries in children. *Caries Res.* 44 (3), 272–276. doi: 10.1159/000314675

Ramadugu, K., D.B., T., Gicquelais, R. E., Lee, K. H., Stafford, E. B., Marrs, C. F., et al. (2020). Maternal oral health influences infant salivary microbiome. *J. Dent. Res.* 100 (1), 58–65. doi: 10.1177/0022034520947665

Ren, Z., Jeckel, H., Simon-Soro, A., Xiang, Z., Liu, Y., Cavalcanti, I. M., et al. (2022). Interkingdom assemblages in human saliva display group-level surface mobility and disease-promoting emergent functions. *Proc. Natl. Acad. Sci. U.S.A.* 119 (41), e2209699119. doi: 10.1073/pnas.2209699119

Roncari Rocha, G., Sims, K. R.Jr., Xiao, B., Klein, M. I., and Benoit, D. S. W. (2022). Nanoparticle carrier co-delivery of complementary antibiofilm drugs abrogates dual species cariogenic biofilm formation *in vitro*. *J. Oral. Microbiol.* 14 (1), 1997230. doi: 10.1080/20002297.2021.1997230

Rosier, B. T., Marsh, P. D., and Mira, A. (2018). Resilience of the oral microbiota in health: mechanisms that prevent dysbiosis. *J. Dent. Res.* 97 (4), 371–380. doi: 10.1177/0022034517742139

Rubey, K. M., and Brenner, J. S. (2021). Nanomedicine to fight infectious disease. *Adv. Drug Delivery Rev.* 179, 113996. doi: 10.1016/j.addr.2021.113996

Sampaio, A. A., Souza, S. E., Ricomini-Filho, A. P., Del Bel Cury, A. A., Cavalcanti, Y. W., and Cury, J. A. (2019). *Candida albicans* increases dentine demineralization provoked by *Streptococcus mutans* biofilm. *Caries Res.* 53 (3), 322–331. doi: 10.1159/000494033

Sampaio-Maia, B., Caldas, I. M., Pereira, M. L., Perez-Mongiovi, D., and Araujo, R. (2016). The oral microbiome in health and its implication in oral and systemic diseases. *Adv. Appl. Microbiol.* 97, 171–210. doi: 10.1016/bs.aambs.2016.08.002

Sedghi, L., DiMassa, V., Harrington, A., Lynch, S. V., and Kapila, Y. L. (2021). The oral microbiome: role of key organisms and complex networks in oral health and disease. *Periodontol 2000* 87 (1), 107–131. doi: 10.1111/prd.12393

Senadheera, M. D., Lee, A. W., Hung, D. C., Spatafora, G. A., Goodman, S. D., and Cvitkovitch, D. G. (2007). The *Streptococcus mutans* vicX gene product modulates gtfB/C expression, biofilm formation, genetic competence, and oxidative stress tolerance. *J. Bacteriol* 189 (4), 1451–1458. doi: 10.1128/JB.01161-06

Silverman, R. J., Nobbs, A. H., Vickerman, M. M., Barbour, M. E., and Jenkinson, H. F. (2010). Interaction of *Candida albicans* cell wall Als3 protein with *Streptococcus gordonii* SspB adhesin promotes development of mixed-species communities. *Infect. Immun.* 78 (11), 4644–4652. doi: 10.1128/IAI.00685-10

Simon, G., Berube, C., Voyer, N., and Grenier, D. (2019). Anti-biofilm and anti-adherence properties of novel cyclic dipeptides against oral pathogens. *Bioorg Med. Chem.* 27 (12), 2323–2331. doi: 10.1016/j.bmc.2018.11.042

Sivamaruthi, B. S., Kesika, P., and Chaiyasut, C. (2020). A review of the role of probiotic supplementation in dental caries. *Probiotics Antimicrob. Proteins* 12 (4), 1300–1309. doi: 10.1007/s12602-020-09652-9

Sridhar, S., Suprabha, B. S., Shenoy, R., Suman, E., and Rao, A. (2020). Association of *Streptococcus mutans*, *Candida albicans* and oral health practices with activity status of caries lesions among 5-Year-Old children with early childhood caries. *Oral. Health Prev. Dent.* 18 (1), 911–919. doi: 10.3290/j.ohpd.a45411

Srivastava, B., Bhatia, H. P., Chaudhary, V., Aggarwal, A., Kumar Singh, A., and Gupta, N. (2012). Comparative evaluation of oral *Candida albicans* carriage in children with and without dental caries: a microbiological *in vivo* study. *Int. J. Clin. Pediatr. Dent.* 5 (2), 108–112. doi: 10.5005/jp-journals-10005-1146

Srivastava, N., Ellepola, K., Venkiteswaran, N., Chai, L. Y. A., Ohshima, T., and Seneviratne, C. J. (2020). Lactobacillus plantarum 108 inhibits *Streptococcus mutans* and *Candida albicans* mixed-species biofilm formation. *Antibiotics* 9 (8), 478. doi: 10.3390/antibiotics9080478

Sztajer, H., Szafranski, S. P., Tomasch, J., Reck, M., Nimtz, M., Rohde, M., et al. (2014). Cross-feeding and interkingdom communication in dual-species biofilms of *Streptococcus mutans* and *Candida albicans*. *ISME J.* 8 (11), 2256–2271. doi: 10.1038/ismej.2014.73

Thanh Nguyen, H., Zhang, R., Inokawa, N., Oura, T., Chen, X., Iwatani, S., et al. (2021). *Candida albicans* Bgl2p, Ecm33p, and Als1p proteins are involved in adhesion to saliva-coated hydroxyapatite. *J. Oral. Microbiol.* 13 (1), 1879497. doi: 10.1080/20002297.2021.1879497

Trigo-Gutierrez, J. K., Sanita, P. V., Tedesco, A. C., Pavarina, A. C., and Mima, E. G. O. (2018). Effect of chloroaluminium phthalocyanine in cationic nanoemulsion on photoinactivation of multispecies biofilm. *Photodiagnosis Photodyn. Ther.* 24, 212–219. doi: 10.1016/j.pdpdt.2018.10.005

Tyers, M., and Wright, G. D. (2019). Drug combinations: a strategy to extend the life of antibiotics in the 21st century. *Nat. Rev. Microbiol.* 17 (3), 141–155. doi: 10.1038/s41579-018-0141-x

Valm, A. M. (2019). The structure of dental plaque microbial communities in the transition from health to dental caries and periodontal disease. *J. Mol. Biol.* 431 (16), 2957–2969. doi: 10.1016/j.jmb.2019.05.016

van der Zande, M., Vandebriel, R. J., Van Doren, E., Kramer, E., Herrera Rivera, Z., Serrano-Rojero, C. S., et al. (2012). Distribution, elimination, and toxicity of silver nanoparticles and silver ions in rats after 28-day oral exposure. *ACS Nano* 6 (8), 7427–7442. doi: 10.1021/nn302649p

Vieira, A. P. M., Arias, L. S., de Souza Neto, F. N., Kubo, A. M., Lima, B. H. R., de Camargo, E. R., et al. (2019). Antibiofilm effect of chlorhexidine-carrier nanosystem based on iron oxide magnetic nanoparticles and chitosan. *Colloids Surf B Biointerfaces* 174, 224–231. doi: 10.1016/j.colsurfb.2018.11.023

von Ranke, N. L., Bello, M. L., Cabral, L. M., Castro, H. C., and Rodrigues, C. R. (2018). Molecular modeling and dynamic simulations of agglutinin-like family members from *Candida albicans*: new insights into potential targets for the treatment of candidiasis. *J. Biomol Struct. Dyn* 36 (16), 4352–4365. doi: 10.1080/07391102.2017.1417159

Wan, S. X., J.T., Y., Dhall, A., Koo, H., and Hwang, G. (2021). Cross-kingdom cell-to-Cell interactions in cariogenic biofilm initiation. *J. Dent. Res.* 100 (1), 74–81. doi: 10.1177/0022034520950286

Williamson, P. R., Huber, M. A., and Bennett, J. E. (1993). Role of maltase in the utilization of sucrose by *Candida albicans*. *Biochem. J.* 291 (Pt 3), 765–771. doi: 10.1042/bj2910765

Wu, R., Tao, Y., Cao, Y., Zhou, Y., and Lin, H. (2020). *Streptococcus mutans* membrane vesicles harboring glucosyltransferases augment *Candida albicans* biofilm development. *Front. Microbiol.* 11. doi: 10.3389/fmicb.2020.581184

Wuersching, S. N., Huth, K. C., Hickel, R., and Kollmuss, M. (2021). Inhibitory effect of LL-37 and human lactoferricin on growth and biofilm formation of anaerobes associated with oral diseases. *Anaerobe* 67, 102301. doi: 10.1016/j.anaerobe.2020.102301

Xiao, J., Grier, A., Faustoferri, R. C., Alzoubi, S., Gill, A. L., Feng, C., et al. (2018a). Association between oral candida and bacteriome in children with severe ECC. *J. Dent. Res.* 97 (13), 1468–1476. doi: 10.1177/0022034518790941

Xiao, J., Huang, X., Alkhers, N., Alzamil, H., Alzoubi, S., Wu, T. T., et al. (2018b). *Candida albicans* and early childhood caries: a systematic review and meta-analysis. *Caries Res.* 52 (1-2), 102–112. doi: 10.1159/000481833

Xiong, K., Chen, X., Zhu, H., Ji, M., and Zou, L. (2021). Anticaries activity of GERM CLEAN in *Streptococcus mutans* and *Candida albicans* dual-species biofilm. *Oral. Dis.* 28 (3), 829–839. doi: 10.1111/odi.13799

Yan, K., Yin, H., Wang, J., and Cai, Y. (2022). Subtle relationships between pseudomonas aeruginosa and fungi in patients with cystic fibrosis. *Acta Clin. Belg* 77 (2), 425–435. doi: 10.1080/17843286.2020.1852850

Yang, C., Scoffield, J., Wu, R., Deivanayagam, C., Zou, J., and Wu, H. (2018). Antigen I/II mediates interactions between *Streptococcus mutans* and *Candida albicans*. *Mol. Oral. Microbiol.* 33 (4), 283–291. doi: 10.1111/omi.12223

Yin, W., Zhang, Z., Shuai, X., Zhou, X., and Yin, D. (2022). Caffeic acid phenethyl ester (CAPE) inhibits cross-kingdom biofilm formation of *Streptococcus mutans* and *Candida albicans*. *Microbiol. Spectr.* 10 (5), e0157822. doi: 10.1128/spectrum.01578-22

Zaremba, M. L., S., W., Klimiuk, A., Daniluk, T., Rozkiewicz, D., Cylwik-Rokicka, D., Waszkiel, D., et al. (2006). Microorganisms in root carious lesions in adults. *Adv. Med. Sci.* 51 (Suppl 1), 237–240. doi: 10.1177/0022034520950286

Zeng, L., and Burne, R. A. (2021). Molecular mechanisms controlling fructose-specific memory and catabolite repression in lactose metabolism by *Streptococcus mutans*. *Mol. Microbiol.* 115 (1), 70–83. doi: 10.1111/mmi.14597

Zeng, Y., Fadaak, A., Alomeir, N., Wu, T. T., Rustchenko, E., Qing, S., et al. (2022). Lactobacillus plantarum disrupts *S. mutans–C. albicans* cross-kingdom biofilms. *Front. Cell. Infection Microbiol.* 12, 872012. doi: 10.3389/fcimb.2022.872012

Zhang, L., Bera, H., Wang, H., Wang, J., Guo, Y., Shi, C., et al. (2022). Combination and nanotechnology based pharmaceutical strategies for combating respiratory bacterial biofilm infections. *Int. J. Pharm.* 616, 121507. doi: 10.1016/j.ijpharm.2022.121507

Zhang, Q., Li, J., Lu, W., Zhao, J., Zhang, H., and Chen, W. (2021). Multi-omics reveals the inhibition of lactiplantibacillus plantarum CCFM8724 in *Streptococcus mutans-Candida albicans* mixed-species biofilms. *Microorganisms* 9 (11), 2368. doi: 10.3390/microorganisms9112368

Zhang, Q., Qin, S., Xu, X., Zhao, J., Zhang, H., Liu, Z., et al. (2020). Inhibitory effect of lactobacillus plantarum CCFM8724 towards *Streptococcus mutans-Candida albicans*-induced caries in rats. *Oxid. Med. Cell Longev* 2020, 4345804. doi: 10.1155/2020/4345804

Zheng, D., Huang, C., Huang, H., Zhao, Y., Khan, M. R. U., Zhao, H., et al. (2020). Antibacterial mechanism of curcumin: a review. *Chem. Biodivers* 17 (8), e2000171. doi: 10.1002/cbdv.202000171

Zhou, Z., Ren, B., Li, J., Zhou, X., Xu, X., and Zhou, Y. (2022). The role of glycoside hydrolases in *S. gordonii* and *C. albicans* interactions. *Appl. Environ. Microbiol.* 88 (10), e0011622. doi: 10.1128/aem.00116-22

Roles of *Streptococcus mutans-Candida albicans* interaction in early childhood caries: a literature review

Yifei Lu[1†], Yifan Lin[1†], Mingyun Li[1*] and Jinzhi He[2*]

[1]State Key Laboratory of Oral Diseases and National Clinical Research Center for Oral Diseases, Sichuan University, Chengdu, China, [2]Department of Cariology and Endodontics, West China Hospital of Stomatology, Sichuan University, Chengdu, China

As one of the most common oral diseases in kids, early childhood caries affects the health of children throughout the world. Clinical investigations show the copresence of *Candida albicans* and *Streptococcus mutans* in ECC lesions, and mechanistic studies reveal co-existence of *C. albicans* and *S. mutans* affects both of their cariogenicity. Clearly a comprehensive understanding of the interkingdom interaction between these two microorganisms has important implications for ECC treatment and prevention. To this end, this review summarizes advances in our understanding of the virulence of both *C. albicans* and *S. mutans*. More importantly, the synergistic and antagonistic interactions between these two microbes are discussed.

KEYWORDS

early-childhood caries, *Candida albicans*, *Streptococcus mutans*, interkingdom interaction, symbiosis, antagonism

1 Introduction

Early childhood caries is defined as "the presence of one or more decayed (non-cavitated or cavitated lesions), missing (due to caries) or filled tooth surfaces in any primary tooth" in a child under the age of six (American Academy of Pediatric Dentistry, 2021). Although significant progress against ECC has been made in pediatric dentistry, it still affects kids throughout the world. According to 72 global studies which measured the prevalence of ECC in preschoolers between 1998 and 2018, the average prevalence of ECC in kids at 1-year-old was 17%, while the prevalence of ECC in toddlers at 2-year-old sharply rose to 36% (Tinanoff et al., 2019). Worse still, the prevalence of ECC increases with the development of children. Specifically, the prevalence of ECC in 3, 4 and 5-year-old preschoolers was 43%, 55% and 63%, respectively (Tinanoff et al., 2019). ECC impacts children and their parents or caregivers in different ways. Apart from dental pain and abscess, children with ECC suffer a higher risk of hospitalization and emergency room visits, treatment costs, school time loss, poor learning ability and life quality, low growth parameters (weight, height), sleep disorders, self-esteem setbacks and negative social

interactions (Sachdev et al., 2016; Vieira-Andrade et al., 2016; Xiao et al., 2018a; Pierce et al., 2019).

ECC is a multifactorial disease. The prerequisites of ECC include the synchronized appearance of susceptible hosts, cariogenic microbes, and cariogenic substrate from food present for a sufficient length of time. Microbes are the initial factor of ECC. For quite a long time, oral microbiologists focused on the role of oral bacteria in the pathogenesis of ECC. *Streptococcus mutans*, a gram-positive facultative anaerobe, has long been taken as the main etiological factor of ECC. It is important to keep in mind that, the oral cavity is colonized by microbes from different domains, including eukaryotic cells, prokaryotic cells, archaea, and viruses. Although bacteria-targeting studies provide important clues to understand how microbes destroy the hard tissues of mammalian teeth, the roles of other microorganisms should not be ignored. In recent years, *Candida albicans*, a eukaryote and an opportunistic fungus, has been frequently detected in children with ECC. Studies revealed that the detection of *C. albicans* is positively related to the severity and incidence of ECC (Cui et al., 2021), suggesting its role in the occurrence of ECC. Importantly however, within the oral cavity, *S. mutans* and *C. albicans* actively interact with each other, and their inter-kingdom interactions mediate both of their cariogenicity (Falsetta et al., 2014; Kim et al., 2017; Xiao et al., 2018b; Sridhar et al., 2020). In this review, the virulence of *S. mutans* and *C. albicans* is present first, and then their complicated interactions as well as the influence of these interspecies interactions on the occurrence of ECC are discussed.

2 Streptococcus mutans

S. mutans is naturally present in the human oral cavity. To survive in the harsh environment of the human mouth, *S. mutans*, as well as other oral microbes, forms a highly organized microbial community termed as biofilm (Marsh and Zaura, 2017). Biofilm is a complex structure composed of aggregated microbial cells and microbially produced extracellular polymeric substances (EPS) (Marsh and Zaura, 2017). The construction of biofilm begins when saliva components selectively adsorb to the tooth surfaces, forming a thin acellular homogeneous organic membrane termed as acquired enamel pellicle. Acquired enamel pellicle provides binding sites for oral microorganisms including *S. mutans*. The surface proteins P1 (also known as PAc, SpaP, Ag I/II protein) of *S. mutans* can selectively bind to salivary lectins in acquired enamel pellicle, and this binding process enable the initial colonization of *S. mutans*. After initial binding, microbes including *S. mutans* start to proliferate and produce EPS, forming a stable three-dimensional community that contains channels to effectively distribute nutrients, oxygen and signaling molecules. *S. mutans* significantly promotes biofilm formation through sucrose-dependent and -independent ways. The sucrose-dependent mechanism mainly relies on extracellular glucose transferase secreted by itself. There are three extracellular glucose transferases secreted by *S. mutans*, including GtfB, GtfC, and GtfD. GtfB mostly produces viscous water-insoluble polysaccharides from sucrose, while GtfC synthesizes a mixture of insoluble and soluble polysaccharides

from sucrose. GtfD predominantly catalyzes sucrose to be soluble polysaccharides (Bowen and Koo, 2011; Krzyściak et al., 2014). Water-insoluble polysaccharides are the major component of EPS. Water-insoluble polysaccharides work as glue to facilitate bacterial adherence and accumulation. They also constitute the protective barrier for residing microbes, and provide the biofilm with mechanical stability (Cugini et al., 2019).

S. mutans promote the occurrence of dental caries including ECC by generating organic acids through carbohydrate metabolization. Carbohydrates including sugars from the environment are transported into *S. mutans* cells mainly through the phosphoenolpyruvate dependent phosphotransferase system (PEP-PTS). This system catalyzes the transportation and phosphorylation of monosaccharides, disaccharides, amino sugars, polyols, and other sugar derivatives. The bacteria ferment the phosphorylated sugar into pyruvate by glycolysis. Pyruvate then is catalyzed to be organic acids such as lactic acid and formic acid through a series of branched chain pathways. These organic acids lower the pH of the local microenvironment, which is the direct cause of tooth surface demineralization. Majority of sucrose (> 95%) is internalized through the PEP-PTS system, and the rest is extracellularly metabolized by Gtfs and fructose transferases (Ftfs) (Vadeboncoeur and Pelletier, 1997; Lemos et al., 2019). Other two binding protein-dependent carbohydrate transport systems, the multiple-sugar metabolism system (Msm) and maltose/maltodextrin ABC transporter, are also involved in the sucrose uptake of *S. mutans* (Zeng and Burne, 2013).

Acid resistance is a significant survival advantage and virulence factor of *S. mutans*. *S. mutans* utilizes a series of adaptation mechanisms to respond to the acid-damage. One of these mechanisms is called acid tolerance response. ATR helps *S. mutans* maintain the cytoplasm at a neutral level compared to extracellular space when the environment becomes acidic (Baker et al., 2017). First, the F1F0-ATPase system within the *S. mutans* cells serves as the proton pump and the primary mechanism to maintain pH homeostasis. In an acidic condition, the F1F0-ATPase system is activated, consequently, protons are pumped out of the cell (Bender et al., 1986). Second, in response to the acidification of its environment, *S. mutans* increases the proportion of monounsaturated membrane fatty acids. The monounsaturated membrane fatty acids decrease the permeability of extracellular protons (Fozo and Quivey, 2004; Matsui and Cvitkovitch, 2010). *S. mutans* also secretes cardiolipin (Macgilvray et al., 2012), an important acid resistant substance. In terms of alkali production to cope with acid stress, *S. mutans* is urease and ADS negative, both of which are utilized by oral streptococci to synthesize neutralizing molecules urea and/or ammonia. Instead, *S. mutans* has an agmatine deiminase system (AgDS) encoded by the agmatine-inducible *aguBDAC* operon. The AgDS catalyzes ammonia, CO_2, and ATP production (Chakraborty and Burne, 2017). Although AgDS does not seem to have a significant effect on environmental alkalization, the ammonia produced internally may contribute to the neutralization of cytoplasmic pH. In addition, Malolactic fermentation (MLF) could be also helpful for the alkalization of cytoplasm. MLF converts malate to less acidic lactate and CO_2 (Chakraborty and Burne, 2017). Interestingly, this fermentation

process can also lead to ATP synthesis through the reversible action of the F1−F0-ATPase (Chakraborty and Burne, 2017). In addition, when growing at low pH, the branched-chain amino acid (BCAA) biosynthesis of *S. mutans* was up-regulated. Pyruvate, the key metabolic intermediate, can be redirected to BCAA biosynthesis, therefore reducing acid end products, and maintaining the intracellular pH to alleviate acid stress (Len et al., 2004). Meanwhile, amino acids biosynthetic genes such as *ilvC* and *ilvE* related to the biosynthesis/degradation of branched-chain amino acids and the production of branched-chain fatty acids were identified as being up-regulated (Santiago et al., 2012). Last but not the least, *S. mutans* encodes DNA/protein repairing enzymes, proteases and chaperones that can fix protein and DNA damages in an acidic environment.

3 Candida albicans

Candida is the most detected fungal species in the oral cavity, especially *C. albicans* (Witherden et al., 2017; Delaney et al., 2019). It is a polymorphic organism that grows in yeast or filamentous fungal filament or pseudo-hyphae. The ability to switch between yeast and filamentous forms is critical for its virulence. External environmental signals and internal regulation are involved in the regulation of yeast filamentous transformation of *C. albicans*. External signals include temperature, pH, CO_2 concentration, serum, and malnutrition. Acidic pH, low temperature and rich nutritional conditions are conducive to *C. albicans* into yeast form (Lopes and Lionakis, 2022). Internal regulation includes signaling pathways and the phenotype conversion system called as white -opaque transition (Huang, 2012; Tao et al., 2022). *C. albicans* can adhere to the tooth enamel, and initial adhesion occurs through a strong interaction between yeast cell wall-associated adhesins and the salivary pellicle (Gunaratnam et al., 2021). Children with ECC had higher rates of *C. albicans* in saliva, dental plaque and infected dentin samples compared to kids without carious lesions (Moalic et al., 2001). Children with oral *C. albicans* have a higher risk for ECC (> 5 times) than children without *C. albicans* (Xiao et al., 2018b). The detection frequency of *C. albicans* in ECC was higher than that in caries cases not belonging to ECC and caries-free groups (Carvalho et al., 2006). The total loads of *C. albicans and S. mutans* in the supragingival dental plaque of children with ECC increase with the percentage of active carious lesions and the severity of dental caries (Sridhar et al., 2020). These studies, combined with others suggested there is a strong correlation between *C. albicans* and ECC.

It has been proved that *C. albicans* can produce acid (Klinke et al., 2011). *C. albicans* metabolized carbohydrates such as glucose from food, which causes the reduction of the pH in the growing environment from pH 7 to 4 (Fakhruddin et al., 2021). When the pH is below 5.5, the acidification of *S. mutans* decreased greatly and stopped at pH 4.2 (De Soet et al., 1991). However, *C. albicans* still maintains its acid production ability even at pH 4.0 (Klinke et al., 2009). The main organic acid synthesized by *C. albicans* were pyruvate and acetate (Klinke et al., 2009). *C. albicans* has a

greater ability to dissolve hydroxyapatite, which is about 20 times higher than that of *S. mutans* (Nikawa et al., 2003).

C. albicans has a high affinity to acquired enamel pellicle. Scanning electron microscopy showed that *C. albicans* initially combined with the *in-situ* pellicles on enamel, indicating that yeast cells attached to the enamel surface were in close contact with the salivary pellicle (Rocha et al., 2018; Gunaratnam et al., 2021). *C. albicans* adheres to hydroxyapatite through electrostatic interaction (Nikawa et al., 2003). In recent years, two different patterns of *Candida* colonization have been found. One is the establishment of a mycelial network with bacteria, and the other is forming a spatial arrangement with *Streptococcus* (Dige and Nyvad, 2019).

Secretory aspartyl proteases (Sap) is a vital virulence factor of *C. albicans*. Sap1 may play important roles in the development of severe early childhood caries (S-ECC) (Li et al., 2014). *C. albicans* is the main producer of hydrolase, secreting enzymes such as protease, hemolysin, phospholipase, collagenase and so on, et al. *C. albicans* also has significantly higher protease activity and phospholipase activity. The study also showed that the phospholipase activity of isolated *C. albicans* was may be positively correlated with protease activity.

4 Interactions between S. mutans and C. albicans

The copresence of *S. mutans* and *C. albicans* is frequently observed in oral samples from ECC patients (Xiao et al., 2018a). In recent years, the way how *S. mutans* and *C. albicans* interacts with each other as well as the effect of these interactions on the progress of dental caries including ECC has been intensively explored as summarized in Figure 1.

4.1 Synergism in metabolic activities

C. albicans promotes the carbohydrate intake of *S. mutans*. The glucose metabolic rate of *S. mutans* co-cultured with *C. albicans* was higher than those in the pure culture group (He et al., 2017; Oliveira et al., 2021). Further mechanism studies show that *C. albicans* affects the transcription of *S. mutans* genes associated with the transportation and metabolization of carbohydrates (He et al., 2017; Oliveira et al., 2021). Comparing to *C. albicans* or *S. mutans* single-species biofilms, dual species biofilms exhibited unique transcriptome profiles and most up-regulated genes were related to carbohydrate transport and metabolic/catabolic processes (Xiao et al., 2022). Specifically, when coexistence, many up-regulated genes of *S. mutans* are these participating in carbohydrate metabolism, galactose metabolism and glycolysis/gluconeogenesis (Xiao et al., 2022). Meanwhile, coculturing of *C. albicans* and *S. mutans* is a double win in terms of sugar utilization. Genes of *C. albicans* associating with carbohydrate metabolism were also significantly enhanced by co-culturing, including those involved in sugar transport, aerobic respiration, pyruvate breakdown, and
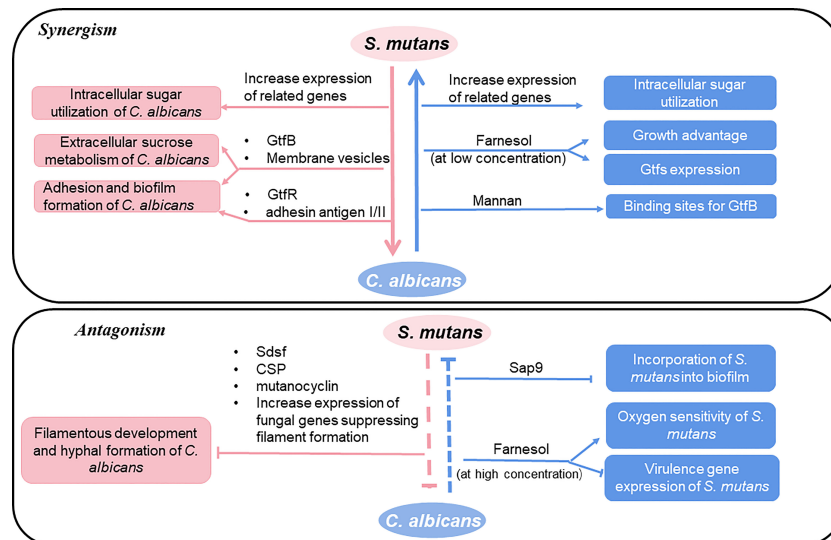
FIGURE 1
Interactions between *S. mutans* and *C. albicans*.

the glyoxylate cycle (He et al., 2017; Oliveira et al., 2021). Moreover, a new cross-feeding mechanism between these two species were identified to be mediated by GtfB. GtfB secreted by *S. mutans* enhances *C. albicans* carbohydrate utilization (Ellepola et al., 2019). Membrane vesicles (MVs) are subcellular parts secreted by *S. mutans* cells. MVs containing the Gtf enzyme can locate in the extracellular matrix of *C. albicans* biofilm, which contributes to the sucrose metabolism of *C. albicans* (Wu et al., 2020).

4.2 Synergism through signal molecules

The quorum sensing molecule farnesol secreted by *C. albicans* is generally considered as a bacteriostatic substance (Fernandes et al., 2018). However, farnesol can promote the growth of *S. mutans*, the expression of *gtfs*, the formation of biofilm and biological colonies and the activity of transferrin (Kim et al., 2017). It is worth noting that the effect of farnesol on *S. mutans* is concentration-dependent. This molecule inhibits a series of life activities of *S. mutans* at a high concentration (> 100μM) (Kim et al., 2017). The specific action mechanism of farnesol on *S. mutans* is still unknown, and further study is needed.

4.3 Synergism during biofilm formation

The *C. albicans-S. mutans* dual biofilm is characterized by the interweaving of expanded *S. mutans* microcolonies with Candida yeasts, hyphae, and pseudo-hyphae to form a three-dimensional inter-kingdom superstructure (Negrini et al., 2022). Compared to *C. albicans* or *S. mutans* single species biofilm, dual-species biofilm shows increased biomass, viable cells, EPS and protein content, acid resistance, oxidation, and antibacterial stress resistance, and larger microcolonies as well as much more complex 3D structure (Falsetta

et al., 2014; Lobo et al., 2019). The unique physical and chemical properties of *C. albicans-S. mutans* dual biofilm are resulted from the inter-kingdom synergistic interactions between these two microbes.

Polysaccharides are the major EPS components of biofilm playing important roles in the colonization of microorganisms. Polysaccharides produced by *S. mutans* are mainly β-1,3-glucan and β-1,6-glucan through the activity of Gtfs (Gregoire et al., 2011), and α-mannan is the most abundant EPS component of *C. albicans* biofilm, followed by β-1,6-glucan and β-1,3-glucan (Pierce et al., 2017). *S. mutans*-secreted Gtfs can bind strongly and stably to the mannan layer of *C. albicans*. This binding converts *C. albicans* into a de facto glucan producer and consequently promotes the assembly of the EPS-rich matrix scaffold. At present, it is known that three kinds of Gtfs can bind to the cell surface of *C. albicans in vitro*, among which GtfB has the strongest affinity. The binding of Gtfs to *C. albicans* affects the physical and chemical properties of dual biofilm significantly because, first, polysaccharides present in the biofilm directly affect the formation and size of the microcolony (Xiao et al., 2012). Second, the production of this 3D EPS-matrix contributes to form an intricate network of exopolysaccharide-enmeshed bacterial-islets (microcolonies) through localized cell-to-matrix interactions. Third, as a diffusion-limiting barrier, the EPS-matrix prevents acid within the biofilm from diffusing outward, thus prolonging and intensifying the acid attack. It helps to create spatial heterogeneities and acidic regions at specific locations at the surface of biofilm attachment (despite exposure to buffered neutral pH) (Xiao et al., 2017; Kim et al., 2018). Fourth, EPS-producing bacterial GtfB exoenzymes can directly modulate antifungal drug tolerance both at a single-cell level and within multicellular biofilms, even if *C. albicans* is defective in producing its own protective matrices (Liu et al., 2022). In addition, the binding of Gtfs to *C. albicans* enables the fungus to colonize EPS-coated surfaces readily, therefore recruiting more fungal cells into the biofilm. Finally, it enhances fungal-bacterial coherence (Falsetta

et al., 2014). Consistent with this, mutants of *S. mutans* lacking glucosyltransferase gene showed the ability to seriously disrupt the colonization, accumulation, and formation of cospecies biofilms of *C. albicans* (Carvalho et al., 2006; Wan et al., 2021). *BCR1* is the key gene to develop the biofilm of *C. albicans*, whose major functional downstream targets include *HWP1*, *ALS1*, and *ALS3* genes that encode cell surface proteins. Interestingly, GtfB augments the *C. albicans* counterpart in mixed-species biofilms through a *BCR1*-independent mechanism (Ellepola et al., 2017). In addition, GtfR of *S. mutans* can provide adhesion conditions to increase the biomass of *C. albicans* and biofilm matrix (Souza et al., 2020). Membrane vesicles (MVs) are subcellular parts secreted by cells and are of significance in disease progression and intercellular communication. MVs containing the Gtf enzyme can locate in the extracellular matrix of *C. albicans* biofilm, which contributes to the sucrose metabolism of *C. albicans* (Wu et al., 2020). *S. mutans* can also mediate the recruitment of *C. albicans* into biofilm through its adhesin antigen I/II. *S. mutans* antigen I/II promotes the adhesion of *both S. mutans* and *C. albicans* (Yang et al., 2018). Antigen I/II mediated process is independent of the streptococcal receptors of *C. albicans* (such as Als1 and Als3 proteins).

5 Antagonism between *C. albicans* and *S. mutans*

Not only "peace" but also "war" exists between *C. albicans* and *S. mutans*. The *S. mutans*-*C. albicans* association has pleiotropic effects that could be both cooperative and antagonistic. *S. mutans* exerts an inhibitory effect on the morphogenesis, pathogenicity and biofilm formation of *C. albicans* (Vílchez et al., 2010; Barbosa et al., 2016). *S. mutans* inhibits the hyphal formation of *C. albicans* through streptococcus diffusible signal factor (Sdsf) and competence stimulating peptide (CSP). Sdsf is a fatty acid signaling molecule and an intermediate product of unsaturated fatty acid synthesis. It decreases the expression of *HWP1* and *SAP5* and therefore suppresses the transformation of *C. albicans* from yeast to hypha at a concentration that does not affect fungal growth (Lee et al., 2017). CSP not only inhibits the formation of germ tube but stimulates the transformation of mycelium to yeast (Satala et al., 2021). When mixed culturing, *S. mutans* also increases the expression of fungal genes which are known to suppress filament formation such as *tup1* and *nrg1* (Jarosz et al., 2009). CSP is a quorum sensing molecule produced by *S. mutans* at the beginning of the exponential growth stage. *S. mutans* affect the filamentous development of *C. albicans* also by secreting a secondary metabolite mutanocyclin (a tetra acid). It is well-known that the conserved camp/protein kinase A (PKA) pathway plays a central role in many life activities of *C. albicans* (Tao et al., 2022). Mutanocyclin can metabolize the subunit TPK2 in *C. albicans* in a dose-dependent manner by regulating the PKA pathway to inhibit the growth of filaments, and the inactivation of TPK2 also leads to an increase in the sensitivity of *C. albicans* to mutanomycin. Meanwhile, mutanocylin shows a global impact on the transcriptional profile of *C. albicans*, which mainly regulates cell wall components through the Ras1 camp/PKA signaling pathway and EFG1 as well as the

subset of filamentous regulators regulated by SFL1. In addition, anchor protein genes related to cell wall biogenesis and remodeling may be involved in the regulation of mutanocyclin response, and anchor protein plays a key role in mutanocyclin regulated inflammation (Dutton et al., 2016).

C. albicans also has an inhibitory effect on *S. mutans*. For example, farnesol, the signaling molecule secreted by *C. albicans* at higher concentrations increases the oxygen sensitivity of *S. mutans* and down-regulated the expression of bacterial virulence-related genes including *luxS*, *brpA*, *ffh*, *recA*, *nth*, *smx*, *comC*, *comYB* as well as genes encoding bacteriocin. In addition, farnesol inhibits biofilm formation of biofilm (Rocha et al., 2018) and water-soluble EPS production (Wang et al., 2020). From this aspect, C. *albicans* suppress the cariogenic ability of *S. mutans* in specific situations. *C. albicans* that have the deletion of *Sap9* (encoding a secreted aspartyl protease) caused an increase in the incorporation of *S. mutans* into dual species biofilms, suggesting that *Sap9* may act as a key module to influence the competition between *C. albicans* and *S. mutans* (Dutton et al., 2016).

6 Summary and prospective

S. mutans has long been taken as the key etiological factor of dental caries, and the oral opportunistic fungus *C. albicans* also played an important role in promoting *S. mutans* to cause dental caries. At the same time, the studies related to ECC also reflect the correlation between them, but the specific interaction is unknown. Most of the released studies focus on gene regulation, adhesion, and metabolism interactions between these two microbes. With the innovation and development of technology, we need to explore the cariogenic mechanism and interaction of *S. mutans* and *C. albicans* in order to expand more ideas for the prevention and treatment of dental caries, formulate more detailed treatment strategies, and improve better oral health.

Author contributions

YLu and YLin drafted the manuscript. ML and JH designed, edited, and added valuable insights to the manuscript. All authors contributed to the article and approved the submitted version.

Funding

Conflict of interest

The authors declare that the research was conducted in the absence of any commercial or financial relationships that could be construed as a potential conflict of interest.

Publisher's note

All claims expressed in this article are solely those of the authors and do not necessarily represent those of their affiliated organizations, or those of the publisher, the editors and the reviewers. Any product that may be evaluated in this article, or claim that may be made by its manufacturer, is not guaranteed or endorsed by the publisher.

References

American Academy of Pediatric Dentistry (2021). "Policy on early childhood caries (ECC): consequences and preventive strategies," in *The reference manual of pediatric dentistry* (Chicago, III: American Academy of Pediatric Dentistry), 81–84.

Baker, J. L., Faustoferri, R. C., and Quivey, R. G.Jr (2017). Acid-adaptive mechanisms of *Streptococcus mutans*-the more we know, the more we don't. *Mol. Oral. Microbiol.* 32, 107–117. doi: 10.1111/omi.12162

Barbosa, J. O., Rossoni, R. D., Vilela, S. F., De Alvarenga, J. A., Velloso Mdos, S., Prata, M. C., et al. (2016). *Streptococcus mutans* can modulate biofilm formation and attenuate the virulence of *Candida albicans*. *PloS One* 11, e0150457. doi: 10.1371/journal.pone.0150457

Bender, G. R., Sutton, S. V., and Marquis, R. E. (1986). Acid tolerance, proton permeabilities, and membrane ATPases of oral *streptococci*. *Infect. Immun.* 53, 331–338. doi: 10.1128/iai.53.2.331-338.1986

Bowen, W. H., and Koo, H. (2011). Biology of *Streptococcus mutans*-derived glucosyltransferases: role in extracellular matrix formation of cariogenic biofilms. *Caries Res.* 45, 69–86. doi: 10.1159/000324598

Carvalho, F. G. D., Silva, D. S., Hebling, J., Spolidorio, L. C., and Spolidorio, D. M. P. (2006). Presence of *mutans streptococci* and *Candida* spp. in dental plaque/dentine of carious teeth and early childhood caries. *Arch. Oral. Biol.* 51, 1024–1028. doi: 10.1016/j.archoralbio.2006.06.001

Chakraborty, B., and Burne, R. A. (2017). Effects of arginine on *Streptococcus mutans* growth, virulence gene expression, and stress tolerance. *Appl. Environ. Microbiol.* 83, e00496–e00417. doi: 10.1128/AEM.00496-17

Cugini, C., Shanmugam, M., Landge, N., and Ramasubbu, N. (2019). The role of exopolysaccharides in oral biofilms. *J. Dent. Res.* 98, 739–745. doi: 10.1177/0022034519845001

Cui, Y., Wang, Y., Zhang, Y., Pang, L., Zhou, Y., Lin, H., et al. (2021). Oral mycobiome differences in various spatial niches with and without severe early childhood caries. *Front. Pediatr.* 9. doi: 10.3389/fped.2021.748656

Delaney, C., O'donnell, L. E., Kean, R., Sherry, L., Brown, J. L., Calvert, G., et al. (2019). Interkingdom interactions on the denture surface: implications for oral hygiene. *Biofilm* 1, 100002. doi: 10.1016/j.bioflm.2019.100002

De Soet, J. J., Van Loveren, C., Lammens, A. J., Pavicić, M. J., Homburg, C. H., Ten Cate, J. M., et al. (1991). Differences in cariogenicity between fresh isolates of *Streptococcus sobrinus* and *Streptococcus mutans*. *Caries Res.* 25, 116–122. doi: 10.1159/000261353

Dige, I., and Nyvad, B. (2019). Candida species in intact *in vivo* biofilm from carious lesions. *Arch. Oral. Biol.* 101, 142–146. doi: 10.1016/j.archoralbio.2019.03.017

Dutton, L. C., Jenkinson, H. F., Lamont, R. J., and Nobbs, A. H. (2016). Role of *Candida albicans* secreted aspartyl protease Sap9 in interkingdom biofilm formation. *Pathog. Dis.* 74, ftw005. doi: 10.1093/femspd/ftw005

Ellepola, K., Liu, Y., Cao, T., Koo, H., and Seneviratne, C. J. (2017). Bacterial GtfB augments *Candida albicans* accumulation in cross-kingdom biofilms. *J. Dent. Res.* 96, 1129–1135. doi: 10.1177/0022034517714414

Ellepola, K., Truong, T., Liu, Y., Lin, Q., and Seneviratne, C. J. (2019). Multi-omics analyses reveal synergistic carbohydrate metabolism in *Streptococcus mutans-candida albicans* mixed-species biofilms. *Infect. Immun.* 87, e00339–e00319. doi: 10.1128/IAI.00339-19

Fakhruddin, K. S., Samaranayake, L. P., Egusa, H., Ngo, H. C., and Pesee, S. (2021). Profuse diversity and acidogenicity of the candida-biome of deep carious lesions of severe early childhood caries (S-ECC). *J. Oral. Microb.* 13, 1964277. doi: 10.1080/20002297.2021.1964277

Falsetta, M. L., Klein, M. I., Colonne, P. M., Scott-Anne, K., Gregoire, S., Pai, C. H., et al. (2014). Symbiotic relationship between *Streptococcus mutans* and *Candida albicans* synergizes virulence of plaque biofilms *in vivo*. *Infect. Immun.* 82, 1968–1981. doi: 10.1128/IAI.00087-14

Fernandes, R. A., Monteiro, D. R., Arias, L. S., Fernandes, G. L., Delbem, A., and Barbosa, D. B. (2018). Virulence factors in *Candida albicans* and *Streptococcus mutans* biofilms mediated by farnesol. *Indian J. Microbiol.* 58, 138–145. doi: 10.1007/s12088-018-0714-4

Fozo, E. M., and Quivey, R. G.Jr (2004). The fabM gene product of *Streptococcus mutans* is responsible for the synthesis of monounsaturated fatty acids and is necessary for survival at low pH. *J. Bacteriol* 186, 4152–4158. doi: 10.1128/JB.186.13.4152-4158.2004

Gregoire, S., Xiao, J., Silva, B. B., Gonzalez, I., Agidi, P. S., Klein, M. I., et al. (2011). Role of glucosyltransferase b in interactions of *Candida albicans* with *Streptococcus mutans* and with an experimental pellicle on hydroxyapatite surfaces. *Appl. Environ. Microbiol.* 77, 6357–6367. doi: 10.1128/AEM.05203-11

Gunaratnam, G., Dudek, J., Jung, P., and Hannig, M. (2021). Quantification of the adhesion strength of *Candida albicans* to tooth enamel. *Microorganisms* 9, 2213. doi: 10.3390/microorganisms9112213

He, J., Dongyeop, K., Zhou, X., Sang-Joon, A., Burne, R. A., Richards, V. P., et al. (2017). RNA-Seq reveals enhanced sugar metabolism in *Streptococcus mutans* Co-cultured with *Candida albicans* within mixed-species biofilms. *Front. Microbiol.* 8. doi: 10.3389/fmicb

Huang, G. (2012). Regulation of phenotypic transitions in the fungal pathogen *Candida albicans*. *Virulence* 3, 251–261. doi: 10.4161/viru.20010

Jarosz, L. M., Deng, D. M., van der Mei, H. C., Crielaard, W., and Krom, B. P. (2009). *Streptococcus mutans* competence-stimulating peptide inhibits *Candida albicans* hypha formation. *Eukaryot Cell* 8, 1658–1664. doi: 10.1128/EC.00070-09

Kim, D., Liu, Y., Benhamou, R. I., Sanchez, H., Simón-Soro, Á., Li, Y., et al. (2018). Bacterial-derived exopolysaccharides enhance antifungal drug tolerance in a cross-kingdom oral biofilm. *Isme J.* 12, 1427–1442. doi: 10.1038/s41396-018-0113-1

Kim, D., Sengupta, A., Niepa, T. H., Lee, B. H., Weljie, A., Freitas-Blanco, V. S., et al. (2017). *Candida albicans* stimulates *Streptococcus mutans* microcolony development *via* cross-kingdom biofilm-derived metabolites. *Sci. Rep.* 7, 41332. doi: 10.1038/srep41332

Klinke, T., Guggenheim, B., Klimm, W., and Thurnheer, T. (2011). Dental caries in rats associated with *Candida albicans*. *Caries Res.* 45, 100–106. doi: 10.1159/000324809

Klinke, T., Kneist, S., De Soet, J. J., Kuhlisch, E., Mauersberger, S., Forster, A., and Klimm, W. (2009). Acid production by oral strains of *Candida albicans* and *Lactobacilli*. *Caries Res.* 43, 83–91. doi: 10.1159/000204911

Krzyściak, W., Jurczak, A., Kościelniak, D., Bystrowska, B., and Skalniak, A. (2014). The virulence of *Streptococcus mutans* and the ability to form biofilms. *Eur. J. Clin. Microbiol. Infect. Dis.* 33, 499–515. doi: 10.1007/s10096-013-1993-7

Lee, K. H., Park, S. J., Choi, S. J., and Park, J. Y. (2017). Proteus Vulgaris and Proteus mirabilis decrease *Candida albicans* biofilm formation by suppressing morphological transition to its hyphal form. *Yonsei Med. J.* 58, 1135–1143. doi: 10.3349/ymj.2017.58.6.1135

Lemos, J. A., Palmer, S. R., Zeng, L., Wen, Z. T., Kajfasz, J. K., Freires, I. A., et al. (2019). The biology of *Streptococcus mutans*. *Microbiol. Spectr.* 7, 10. doi: 10.1128/microbiolspec.GPP3-0051-2018

Len, A. C. L., Harty, D. W. S., and Jacques, N. A. (2004). Proteome analysis of *Streptococcus mutans* metabolic phenotype during acid tolerance. *Microbiology* 150, 1353–1366. doi: 10.1099/mic.0.26888-0

Li, W., Yu, D., Gao, S., Lin, J., Chen, Z., and Zhao, W. (2014). Role of *Candida albicans*-secreted aspartyl proteinases (Saps) in severe early childhood caries. *Int. Jo Mol. Sci.* 15, 10766–10779. doi: 10.3390/ijms150610766

Liu, Y., Wang, Z., Zhou, Z., Ma, Q., Li, J., Huang, J., et al. (2022). *Candida albicans CHK1* gene regulates its cross-kingdom interactions with *Streptococcus mutans* to promote caries. *Appl. Microbiol. Biotechnol.* 106, 7251–7263. doi: 10.1007/s00253-022-12211-7

Lobo, C. I. V., Rinaldi, T. B., Christiano, C. M. S., De Sales Leite, L., Barbugli, P. A., and Klein, M. I. (2019). Dual-species biofilms of *Streptococcus mutans* and *Candida albicans* exhibit more biomass and are mutually beneficial compared with single-species biofilms. *J. Oral. Microbiol.* 11, 1581520. doi: 10.1080/20002297.2019.1581520

Lopes, J. P., and Lionakis, M. S. (2022). Pathogenesis and virulence of *Candida albicans*. *Virulence* 13, 89–121. doi: 10.1080/21505594.2021.2019950

Macgilvray, M. E., Lapek, J. D., Friedman, A. E., and Quivey, R. G. (2012). Cardiolipin biosynthesis in *Streptococcus mutans* is regulated in response to external pH. *Microbiol. (Reading)* 158, 2133–2143. doi: 10.1099/mic.0.057273-0

Marsh, P. D., and Zaura, E. (2017). Dental biofilm: ecological interactions in health and disease. *J. Clin. Periodontol.* 44, S12–S22. doi: 10.1111/jcpe.12679

Matsui, R., and Cvitkovitch, D. (2010). Acid tolerance mechanisms utilized by *Streptococcus mutans*. *Future Microbiol.* 5, 403–417. doi: 10.2217/fmb.09.129

Moalic, E., Gestalin, A., Quinio, D., Gest, P. E., Zerilli, A., and Le Flohic, A. M. (2001). The extent of oral fungal flora in 353 students and possible relationships with dental caries. *Caries Res.* 35, 149–155. doi: 10.1159/000047447

Negrini, T. C., Ren, Z., Miao, Y., Kim, D., Simon-Soro, Á., Liu, Y., et al. (2022). Dietary sugars modulate bacterial-fungal interactions in saliva and inter-kingdom biofilm formation on apatitic surface. *Front. Cell Infect. Microbiol.* 12. doi: 10.3389/fcimb.2022.993640

Nikawa, H., Yamashiro, H., Makihira, S., Nishimura, M., and Hamada, T. (2003). *In vitro* cariogenic potential of *Candida albicans*. *Mycoses* 46, 471–478. doi: 10.1046/j.0933-7407.2003.00888.x

Oliveira, B., Filho, A., Burne, R. A., and Lin, Z. (2021). The route of sucrose utilization by *Streptococcus mutans* affects intracellular polysaccharide metabolism. *Front. Microbiol.* 12. doi: 10.3389/fmicb.2021.636684

Pierce, A., Singh, S., Lee, J., Grant, C., Cruz De Jesus, V., and Schroth, R. J. (2019). The burden of early childhood caries in Canadian children and associated risk factors. *Front. Public Health* 7. doi: 10.3389/fpubh.2019.00328

Pierce, C. G., Vila, T., Romo, J. A., Montelongo-Jauregui, D., Wall, G., Ramasubramanian, A., et al. (2017). The *Candida albicans* biofilm matrix: composition, structure and function. *J. Fungi (Basel)* 3 (1), 14. doi: 10.3390/jof3010014

Rocha, G. R., Florez Salamanca, E. J., De Barros, A. L., Lobo, C. I. V., and Klein, M. I. (2018). Effect of tt-farnesol and myricetin on *in vitro* biofilm formed by *Streptococcus mutans* and *Candida albicans*. *BMC Complement Altern. Med.* 18, 61. doi: 10.1186/s12906-018-2132-x

Sachdev, J., Bansal, K., and Chopra, R. (2016). Effect of comprehensive dental rehabilitation on growth parameters in pediatric patients with severe early childhood caries. *Int. J. Clin. Pediatr. Dent.* 9, 15–20. doi: 10.5005/jp-journals-10005-1326

Santiago, B., Macgilvray, M., Faustoferri, R. C., and Quivey, R. G. (2012). The branched-chain amino acid aminotransferase encoded by *ilvE* is involved in acid tolerance in *Streptococcus mutans*. *J. Bact.* 194, 2010–2019. doi: 10.1128/JB.06737-11

Satala, D., Gonzalez-Gonzalez, M., Smolarz, M., Surowiec, M., Kulig, K., Wronowska, E., et al. (2021). The role of *Candida albicans* virulence factors in the formation of multispecies biofilms with bacterial periodontal pathogens. *Front. Cell Infect. Microbiol.* 11. doi: 10.3389/fcimb.2021.765942

Souza, J. G. S., Bertolini, M., Thompson, A., Mansfield, J. M., and Dongari-Bagtzoglou, A. (2020). Role of glucosyltransferase r in biofilm interactions between *Streptococcus oralis* and. *Candida albicans*. *ISME J.* 14, 1–16. doi: 10.1038/s41396-020-0608-4

Sridhar, S., Suprabha, B. S., Shenoy, R., Suman, E., and Rao, A. (2020). Association of *Streptococcus mutans*, *Candida albicans* and oral health practices with activity status of caries lesions among 5-Year-Old children with early childhood caries. *Oral. Health Prev. Dent.* 18, 911–919. doi: 10.3290/j.ohpd.a45411

Tao, L., Wang, M., Guan, G., Zhang, Y., Hao, T., Li, C., et al. (2022). *Streptococcus mutans* suppresses filamentous growth of *Candida albicans* through secreting mutanocyclin, an unacylated tetramic acid. *Virulence* 13, 542–557. doi: 10.1080/21505594.2022.2046952

Tinanoff, N., Baez, R. J., Diaz Guillory, C., Donly, K. J., Feldens, C. A., Mcgrath, C., et al. (2019). Early childhood caries epidemiology, aetiology, risk assessment, societal burden, management, education, and policy: global perspective. *Int. J. Paediatr. Dent.* 29, 238–248. doi: 10.1111/ipd.12484

Vadeboncoeur, C., and Pelletier, M. (1997). The phosphoenolpyruvate:sugar phosphotransferase system of oral *streptococci* and its role in the control of sugar metabolism. *FEMS Microbiol. Rev.* 19, 187–207. doi: 10.1111/j.1574-6976.1997.tb00297.x

Vieira-Andrade, R. G., Gomes, G. B., De Almeida Pinto-Sarmento, T. C., Firmino, R. T., Pordeus, I. A., Ramos-Jorge, M. L., et al. (2016). Oral conditions and trouble sleeping among preschool children. *J. Public Health-UK* 24, 395–400. doi: 10.1007/s10389-016-0734-7

Vilchez, R., Lemme, A., Ballhausen, B., Thiel, V., Schulz, S., Jansen, R., et al. (2010). *Streptococcus mutans* inhibits *Candida albicans* hyphal formation by the fatty acid signaling molecule trans-2-decenoic acid (SDSF). *Chembiochem* 11, 1552–1562. doi: 10.1002/cbic.201000086

Wan, S. X., Tian, J., Liu, Y., Dhall, A., Koo, H., and Hwang, G. (2021). Cross-kingdom cell-to-Cell interactions in cariogenic biofilm initiation. *J. Dent. Res.* 100, 74–81. doi: 10.1177/0022034520950286

Wang, X., He, H., Liu, J., Xie, S., and Han, J. (2020). Inhibiting roles of farnesol and HOG in morphological switching of *Candida albicans*. *Am. J. Transl. Res.* 12, 6988–7001.

Witherden, E. A., Shoaie, S., Hall, R. A., and Moyes, D. L. (2017). The human mucosal mycobiome and fungal community interactions. *JoF* 3, 56. doi: 10.3390/jof3040056

Wu, R., Tao, Y., Cao, Y., Zhou, Y., and Lin, H. (2020). *Streptococcus mutans* membrane vesicles harboring glucosyltransferases augment *Candida albicans* biofilm development. *Front. Microbiol.* 11. doi: 10.3389/fmicb.2020.581184

Xiao, J., Grier, A., Faustoferri, R. C., Alzoubi, S., Gill, A. L., Feng, C., et al. (2018a). Association between oral *Candida* and bacteriome in children with severe ECC. *J. Dent. Res.* 97, 1468–1476. doi: 10.1177/0022034518790941

Xiao, J., Hara, T., Anderson,, Kim, D., Zero, T., Domenick,, et al. (2017). Biofilm three-dimensional architecture influences *in situ* pH distribution pattern on the human enamel surface. *Int. J. Oral. Sci.* 9, 74–79. doi: 10.1038/ijos.2017.8

Xiao, J., Huang, X., Alkhers, N., Alzamil, H., Alzoubi, S., Wu, T. T., et al. (2018b). *Candida albicans* and early childhood caries: a systematic review and meta-analysis. *Caries Res.* 52, 102–112. doi: 10.1159/000481833

Xiao, J., Klein, M. I., Falsetta, M. L., Lu, B., Delahunty, C. M., Yates, J. R., et al. (2012). The exopolysaccharide matrix modulates the interaction between 3D architecture and virulence of a mixed-species oral biofilm. *PloS Pathog.* 8, e1002623. doi: 10.1371/journal.ppat.1002623

Xiao, J., Zeng, Y., Rustchenko, E., Huang, X., Wu, T. T., and Falsetta, M. L. (2022). Dual transcriptome of *Streptococcus mutans* and *Candida albicans* interplay in biofilms. *J. Oral. Microbiol.* 15, 2144047. doi: 10.1080/20002297.2022.2144047

Yang, C., Scoffield, J., Wu, R., Deivanayagam, C., Zou, J., and Wu, H. (2018). Antigen I/II mediates interactions between *Streptococcus mutans* and *Candida albicans*. *Mol. Oral. Microbiol.* 33, 283–291. doi: 10.1111/omi.12223

Zeng, L., and Burne, R. A. (2013). Comprehensive mutational analysis of sucrose-metabolizing pathways in *Streptococcus mutans* reveals novel roles for the sucrose phosphotransferase system permease. *J. Bacteriol.* 195, 833–843. doi: 10.1128/JB.02042-12

Antibacterial mechanism of areca nut essential oils against *Streptococcus mutans* by targeting the biofilm and the cell membrane

Shuwei Liu[1,2*†], Tiantian Zhang[1,2†], Zhijin Li[1,3], Yan Wang[2*],
Lei Liu[1,4] and Zhenbo Song[1,4]

[1]National Engineering Laboratory for Druggable Gene and Protein Screening, School of Life Sciences,
Northeast Normal University, Changchun, China, [2]College of Ecology and Environment, Hainan
Tropical Ocean University, Sanya, China, [3]Xiamen Key Laboratory of Natural Medicine Research and
Development, Xiamen Health and Medical Big Data Center (Xiamen Medicine Research Institute),
Xiamen, China, [4]NMPA Key Laboratory for Quality Control of Cell and Gene Therapy Medicine
Products, Northeast Normal University, Changchun, China

Introduction: Dental caries is one of the most common and costly biofilm-dependent oral diseases in the world. *Streptococcus mutans* is the major cariogenic pathogen of dental caries. *S. mutans* synthesizes extracellular polysaccharides by autologous glucosyltransferases, which then promotes bacterial adhesion and cariogenic biofilm formation. The *S. mutans* biofilm is the principal target for caries treatment. This study was designed to explore the antibacterial activity and mechanisms of areca nut essential oil (ANEO) against *S. mutans*.

Methods: The ANEOs were separated by negative pressure hydro-distillation. The Kirby-Bauer method and broth microdilution method were carried out to evaluate the antibacterial activity of different ANEOs. The antibacterial mechanism was revealed by crystal violet staining, XTT reduction, microbial adhesion to hydrocarbon test, extracellular polysaccharide production assay, glucosyltransferase activity assay, lactate dehydrogenase leaking, propidium iodide staining and scanning electron microscopy (SEM). The cytotoxicity of ANEOs was determine by MTT assay.

Results: The ANEOs separated at different temperatures exhibited different levels of antibacterial activity against *S. mutans*, and the ANEO separated at 70°C showed the most prominent bacteriostatic activity. Anti-biofilm experiments showed that the ANEOs attenuated the adhesion ability of *S. mutans* by decreasing the surface hydrophobicity of the bacteria, prevented *S. mutans* biofilm formation by inhibiting glucosyltransferase activity, reducing extracellular polysaccharide synthesis, and reducing the total biofilm biomass and activity. SEM further demonstrated the destructive effects of the ANEOs on the *S. mutans*

biofilm. Cell membrane-related experiments indicated that the ANEOs destroyed the integrity of the cell membrane, resulting in the leakage of lactic dehydrogenase and nucleic acids. SEM imaging of *S. mutans* cell showed the disruption of the cellular morphology by the ANEOs. The cytotoxicity assay suggested that ANEO was non-toxic towards normal oral epithelial cells.

Discussion: This study displayed that ANEOs exerted antibacterial activity against *S. mutans* primarily by affecting the biofilm and disrupting the integrity of the cell membrane. ANEOs has the potential to be developed as an antibacterial agent for preventing dental caries. Additionally, a new method for the separation of essential oil components is presented.

KEYWORDS

Streptococcus mutans, antibacterial activity, antibiofilm mechanism, essential oil, areca nut

1 Introduction

Dental caries is a sugar-driven, biofilm-mediated, multifactorial, and dynamic disease driven by an ecological imbalance in the physiological equilibrium between tooth minerals and oral microbial biofilms, and can result in the phasic demineralization (Pitts et al., 2017). The occurrence of dental caries involves various cariogenic and commensal microbes in biofilms on tooth surfaces (Koo et al., 2013; Zhang et al., 2021), and *Streptococcus mutans* is considered as one of the main etiological bacteria (Lemos et al., 2019). *S. mutans* possesses several virulence properties, including adherence to solid surfaces, biofilm formation, production of acid and extracellular polysaccharide (EPS) (Krzyściak et al., 2014; Sun et al., 2023). The EPS is the critical component of the extracellular matrix for cariogenic biofilm formation, which mainly includes water-insoluble polysaccharide (WIP) and water-soluble polysaccharide (WSP) and is synthesized by glucosyltransferases (Gtfs) secreted by *S. mutans* (Bowen and Koo, 2011; Cugini et al., 2019). Therefore, selectively targeting *S. mutans* in dental biofilms has been proposed as an important direction for the prevention and treatment of dental caries (Bowen, 2016).

Despite the use of anticaries agents has made significant progress in the prevention and treatment of dental caries, such as the application of fluoride and chlorhexidine (CHX), there are still serious challenges in controlling of dental biofilms (Wang et al., 2023). Common antimicrobial agents, such as CHX, effectively kill bacterial pathogens in the planktonic state, but have limited antimicrobial efficacy for bacteria in plaque biofilms (Gao et al., 2016). Continuous excessive use of antimicrobial agents would lead to unwanted side effects, for examples xerostomia, hypogeusia, tongue discoloration, exfoliation of the oral mucosa, parotid swelling, abnormal oral sensation, and even serious anaphylaxis (Tartaglia et al., 2019). Hence, novel oral bactericide inhibiting the

formation of dental caries biofilms is needed (He et al., 2019). Natural products are potential source of novel antibacterial agents, have broad availability and chemical diversity, and have been used to treat oral infections and diseases (Palombo, 2011). Essential oils are important natural products, showed strong antibacterial activity, and have aroused extensive attention (Freires et al., 2015; Wang et al., 2021). However, the chemical components of essential oils are complex, and it is difficult to separate and enrich the active constituents. Currently, few reports about separation and enrichment methods for active constituents of essential oils exist.

Areca catechu L. is a tropical characteristic plant widely distributed in Malaysia, China, India and other Asia countries as well as in the South Pacific islands. The fruit of *Areca catechu*, areca nut, is an important traditional Chinese medicinal material, which has been listed in the Pharmacopoeia of the People's Republic of China, and is also used as herbal medicines in other countries (Peng et al., 2015). The areca nut is commonly used to treat malaria, ascariasis, food retention, diarrhea, beriberi, arthritis, dental caries and strengthen the teeth (National Administration of Traditional Chinese Medicine Chinese Materia Medica Editorial Committee, 2004; Chen et al., 2021; Ansari et al., 2021). Areca nut contains a variety of bioactive substances including flavonoids, phenolics, tannins, alkaloids and others (Peng et al., 2015), and exhibits many biological activities in modern pharmacology research, such as effect on nervous system (Bhandare et al., 2015), anti-inflammatory effects (Bhandare et al., 2010), and antibacterial and antifungal effects (Machová et al., 2021). Despite areca nut is a well-known traditional herbal medicine in China, but there are not enough reports about the essential oils.

Accordingly, in the present study, we achieved enrichment of areca nut essential oil (ANEO) active components in the laboratory using a tailor-made negative pressure device, investigated the antibacterial activity of ANEOs against *S. mutans*, and analyzed

the mechanisms of action of ANEO from the perspectives of biofilm and cell membrane to explore the potential application of ANEO as an oral bactericide.

2 Materials and methods

2.1 Plant material and bacterial strains

Areca nuts were collected from an areca nut plantation in Sanya, Hainan Province, China. Fresh immature green areca nuts with uniform size were selected and dried to constant weight at 50°C for further use. *S. mutans* (ATCC 25175) was purchased from the Guangdong Microbial Culture Collection Center and cultured in brain heart infusion medium (BHI) supplied by HKM (Guangdong, China).

2.2 Preparation of ANEOs

Based on the positive correlation between liquid boiling temperature and air pressure, the ANEOs were extracted in sequence by hydro-distillation under different negative pressures using a tailor-made extraction device (Figure S1 in the Supplementary Material). The dried areca nuts were crushed, passed through a 24-mesh sieve and placed in an extraction flask. The pressure in the essential oil extraction device was adjusted so the extraction solvent boiled at (60 ± 1) °C for 5 h. The areca nut essential oil so obtained was designated as EO-60. The pressure in the device was then adjusted so the extraction solvent boiled at (70 ± 1) °C for 5 h and the essential oil obtained was designated as EO-70. Samples of EO-80, EO-90 and EO-100 were extracted sequentially using this method. The areca nut essential oil extracted by traditional hydro-distillation was designated as EO-Tr. The composition of the ANEOs was analyzed by gas chromatography-mass spectrometry.

2.3 Inhibition zone diameter (DIZ) determination

The DIZ was detected by the Kirby–Bauer (K-B) method (CLSI, 2012). *S. mutans* was cultured overnight, and 100 µL of bacterial suspension (1×10^7 CFU/mL) was spread on a BHI agar plate. Sterile filter paper discs (diameter 6 mm) containing 10 µL (or 10 mg, dissolved in Tween 80) of ANEOs were placed on the surface of the agar plate. A paper disc containing 10 µL of 0.6 mg/mL CHX was used as the positive control (James et al., 2017). Tween 80 was the negative control. The inhibition zone diameter was measured after incubating at 37°C for 24 h.

2.4 Minimum inhibitory concentration (MIC) determination

The MIC was determined using a broth microdilution method (Chen et al., 2016). The ANEO samples were prepared by a double

dilution method using BHI liquid medium in a microplate with final concentrations from 0.015 to 8.0 µL/mL. An equal volume of bacterial suspension (1×10^7 CFU/mL) was added to each well. Tween 80 was used as a cosolvent and the final concentration was 2%. The positive control was CHX and the negative control included 2% Tween 80 but no ANEOs. Twenty microliters of the sterile solution of sodium resazurin (1 mg/mL) were added per well. Finally, the 96-well polystyrene microplates were incubated at 37°C for 24 h. The lowest concentration of ANEOs that prevented the solution from changing from dark blue to pink or light yellow was taken as the MIC value. The above assay was repeated and analyzed at five concentration levels which included the minimum MIC values of the six ANEOs and other four concentration levels.

2.5 Minimum bactericidal concentration (MBC) determination

To determine the MBC of each ANEO, 50 µL of suspensions in the above wells at concentrations equal to or higher than the MIC were spread on BHI agar plates and incubated at 37°C for 24 h. The MBC value was the lowest concentration at which no visible colony was observed on the plate.

2.6 Construction and treatment of microplate biofilms

According to the literature (Aiassa et al., 2016) with slight modifications, the tested bacterial suspension in the logarithmic phase was adjusted to 1×10^7 CFU/mL using BHI supplemented with 0.25% sucrose (BHIS). Aliquots of 200 µL of the prepared suspension were added to each well and the plates were incubated at 37°C for 24 h to form biofilms. After incubation, the supernatant was removed and each well was washed three times with sterile PBS. Next, 200 µL of fresh BHI broth with 1/8, 1/4, 1/2 and 1 MIC of each ANEO were added to the wells and the plates were incubated for another 24 h at 37°C. The biofilms were obtained by washing three times with sterile PBS.

2.7 Crystal violet assay

Crystal violet was used as an indicator of the total biofilm biomass (Leite et al., 2013). An aliquot of 200 µL methanol was added to the above constructed microplate biofilms to fix the biofilm, and discarded after 15 min. After drying at room temperature, each well was filled with 200 µL of a 1% crystal violet solution and allowed to stand for 5 min. Finally, each well was washed three times with distilled water and a mixture of ethanol and acetone (3:7) was added. The absorbance of each well was measured at 595 nm.

2.8 XTT assay

The metabolic activity of the cells in biofilms was evaluated using the XTT [2,3-bis (2-methloxy 4-nitro-5-sulfophenyl)-2H-

tetra zolium-5-carbox-anilide] reduction assay (Huang et al., 2012). PBS (100 µL) and 12 µL of an XTT-menadione solution were added into each well prepared according to section 2.6. The XTT-menadione solution was prepared by mixing 25 µL XTT solution (1 mg/mL in PBS) and 2 µL of menadione solution (1 mmol/L in acetone). The absorbance (A_1) was measured at 492 nm after incubating for 3 h in the dark at 37°C. The absorbance of the negative control group was A_0. The biofilm activity was calculated as follows:

$$\text{Biofilm activity} = \frac{A_1}{A_0} \times 100$$

2.9 Determination of bacterial surface hydrophobicity

Bacterial surface hydrophobicity was evaluated by the microbial adherence test with a hydrocarbon (MATH) (Hernández-Alcántara et al., 2018). The biofilms were prepared according to section 2.6 using six-well cell-culture plates. The bacteria were resuspended and collected after two washes with PBS (pH = 7.2). The bacterial suspension was adjusted to an appropriate concentration ($OD_{560\ nm}$ = 0.6/0.7, A_0), then mixed with an equal volume of n-hexadecane and stirred for 1 min. The absorbance (A_1) of the water phase was measured at 560 nm after standing for 1 h at 37°C. The hydrophobicity was calculated using the following equation.

$$\text{Hydrophobicity}(\%) = \frac{A_0 - A_1}{A_0} \times 100$$

2.10 Extracellular polysaccharide (EPS) quantification

The EPS determination was based on the method of Packiavathy et al. (2012) with a slight refinement. An aliquot of 1.0 mL of bacterial suspension in the log phase and 10 mL of BHIS broth with the ANEOs at a final concentration of MIC were mixed and incubated for 16 h at 37°C. The cultures were centrifuged at 12,000 × g for 30 min at 4°C to collect the supernatant. The sediment was resuspended in sterile water, and centrifuged again. The supernatant collected from both centrifugations was the WSP. The pellet was resuspended in 0.1 mol/L NaOH. The supernatant was collected and filtered through 0.22-µm nitrocellulose membrane filters. The filtered supernatant was precipitated by mixing with three volumes of chilled 95% ethanol and incubating overnight at 4°C to collect the WIP. Negative and positive control groups (CHX) were tested simultaneously.

The EPS were quantified using the phenol/H_2SO_4 according to Dubois and co-workers (DuBois et al., 1956). One volume of ice-cold 5% phenol and five volumes of concentrated sulfuric acid were added to one volume of EPS solution. The mixture was incubated at room temperature for 10 min until a red color appeared. The absorbance of the mixture was detected at 490 nm. The inhibition of EPS production was calculated by the following equation.

$$\text{Inhibition of EPS}(\%)$$
$$= \frac{\text{control } OD_{490} - \text{treated } OD_{490}}{\text{control } OD_{490}} \times 100$$

2.11 Gtf activity assay

A crude Gtf extract was prepared by a method previously reported by Koo et al. (2013) with a few modifications. Aliquots of 20 mL of bacterial solutions in log phase were incubated with 200 mL BHI broth containing 1% sucrose at 37 °C for 24 h. The culture was centrifuged at 12000 × g for 30 min at 4°C to collect the supernatant. Ammonium sulfate was added to the supernatant at a final concentration of 60% and the preparation was allowed to stand overnight at 4°C. The precipitate was collected and dialyzed in PBS (pH 6.8) with 1 mM phenylmethyl sulfonyl fluoride (PMSF) as a protease inhibitor for 48 h. The dialyzed solution was the crude extracellular Gtf and was stored at -20°C until use.

The inhibition of Gtf activity by ANEOs was determined by the ability of the Gtf to catalyze the formation of WIP. The method of Ooshima et al. (2000), slightly modified, was used. The reaction mixtures were composed of 1 mL of sterile PBS containing 0.1 M sucrose and 200 µL of prepared crude Gtf. The ANEO samples were added to the reaction mixtures to a final concentration of the MIC and incubated at 37°C for 18 h. Negative and positive control groups (CHX) were run at the same time. The quantity of WIP was determined using the phenol/H_2SO_4 method (DuBois et al., 1956). The inhibition of Gtf activity was calculated by the following equation.

$$\text{Inhibition of Gtf activity}(\%)$$
$$= \frac{\text{control } OD_{490} - \text{treated } OD_{490}}{\text{control } OD_{490}} \times 100$$

2.12 Lactate dehydrogenase (LDH) assay

Measurement of LDH leakage was carried out according to Hsu et al. (2021) with slight modifications. A log phase bacterial suspension was adjusted to a concentration of 1×10^7 CFU/mL and cultured overnight at 37°C. The culture medium was discarded and fresh medium with ANEOs was added to a final concentration of the MIC, then the bacterial cells were incubated for a further 24 h at 37°C. The activity of LDH was measured every 4 h during incubation using a Cytotoxicity LDH Assay Kit-WST (Dojindo, Kumamoto-ken, JPN).

Aliquots of 100 µL of bacterial suspension and 100 µL of an LDH working solution were mixed and incubated in the dark at room temperature for 30 min. Subsequently, 50 µL of stop solution was added to the mixture. The OD_{490} of the bacterial suspension was measured with a multifunctional microplate reader (SpectraMax i3x, Molecular Devices, California, USA). The negative control group was defined as 0% LDH release, and the group treated with 9% Triton X-100 for 24 h was defined as 100% LDH release (Wijesundara et al., 2021).

2.13 Nucleic acid leakage assay

Nucleic acid leakage of *S. mutans* treated with ANEOs was detected according to Shen et al. (2015) with minor modifications. A bacterial suspension was centrifuged at $600 \times g$ for 15 min, washed three times with PBS and diluted to 1×10^7 CFU/mL. The diluted suspension was incubated for 24 h at 37°C with ANEOs at a final concentration of the MIC. Then, 2–3 mL of suspension was removed every 4 h, filtered through 0.22 μm filter membranes, and the absorption was measured at 260 nm.

2.14 Propidium iodide (PI) assay

The PI assay was carried out using the method of Souza et al. (2022). The *S. mutans* suspension was diluted to a concentration of 1×10^7 CFU/mL. Aliquots of 200 μL of bacterial suspension were added to a 96 well plate and incubated at 37°C for 24 h. The supernatant was removed and the wells were washed twice with PBS. A volume of 200 μL fresh BHI was added to the well and the plate was incubated for another 24 h. The biofilms in the well were washed twice with PBS, then covered with 100 μL PBS containing ANEOs at a concentration of MIC and cultured for 12 h at 37°C. After incubation, the biofilms were washed twice with PBS. Finally, the biofilms were covered with 50 μL PI (1 μg/mL), maintained in the dark for 15 min and observed under a fluorescence microscope (RVL-100-G, ECHO, California, USA).

2.15 Construction of polystyrene biofilms and scanning electron microscopy (SEM) observation

The experiment was carried out according to Ribeiro-Vidal et al. (2020) with minor modifications. The bottom of a sterile polystyrene Petri dish was trimmed to 3×3 mm slices, which were placed in a 24-well cell culture plate. A volume of 100 μL of bacterial culture (1×10^7 CFU/mL) and 900 μL of BHI broth containing ANEOs were added to the wells. The final concentration of ANEOs was 1/4 MIC. The plate was incubated for 168 h and the culture solution was replaced every 24 h. Then the culture solution was discarded and the polystyrene slices were gently washed with saline. The treated slices were fixed in a 2.5% glutaraldehyde solution for 1 h at 4°C and washed twice with PBS. Next, the slices were dehydrated sequentially in 50%, 70%, 90%, 100% ethanol (dehydrated twice), equal volume mixtures of anhydrous ethanol and tert-butanol, and tert-butanol, each for 15 min. Finally, the slice surfaces were coated with gold after freeze-drying for 4 h and observed using a SEM (JSM-7610F PLUS, JEOL, Tokyo, JPN).

2.16 SEM observation

The SEM was used to observe the morphology and structure of *S. mutans* (Bajpai et al., 2013). A log phase bacterial suspension was centrifuged ($600 \times g$, 15 min) and resuspended in PBS for three times. Then the suspension was mixed with ANEOs at the MIC and cultured at 37°C for 12 h. The bacterial cells were obtained by centrifugation and fixed in a 2.5% glutaraldehyde solution overnight at 4°C. Next, the bacterial cells were dehydrated successively using 30%, 50%, 70%, 90% and 100% ethanol and replaced by tertiary butyl alcohol. The dehydrated samples were freeze-dried for 4 h, then sputtered with gold and observed.

2.17 Cytotoxicity assay

Cell viability was tested using the MTT method (Patel et al., 2004). Briefly, the human oral epithelial cells were seeded at a density of 1.0×10^4 cells per well in Dulbecco's modified Eagle's medium supplemented with 10% FBS and incubated for 24 h in a humidified atmosphere containing 5% CO_2 at 37°C. The cells were then incubated with the ANEOs (0.005, 0.05, 0.5 and 5 mg/mL) for 48 h. Next, 20 μL of MTT solution were added to each well and incubated for 4 h. After incubation, the culture medium was removed and an equal volume of DMSO was added to each well. The absorbance was measured at 570 nm. The inhibition rate of cell viability was calculated using the following equation.

$$\text{Inhibition rate } (\%) = \frac{\text{control } OD_{570} - \text{treated } OD_{570}}{\text{control } OD_{570}} \times 100$$

2.18 Statistical analysis

Nine replicates were done for each treatment. The results were expressed as the mean ± standard error. A one-way ANOVA was carried out using the SPSS software version 19.0 (IBM Corp., Armonk, NY, USA). The difference between groups was considered significant when $P < 0.05$. Then, $P < 0.01$ indicated an extremely significant difference and $P > 0.05$ indicated no statistical significance.

3 Results

3.1 Chemical compositions analysis of different ANEOs

The ANEOs extracted under different temperatures are shown in Figure 1A. EO-70, EO-80, and EO-90 are liquid, and the color is golden yellow. EO-60, EO-100, and EO-Tr are solid, and appear yellow or dark yellow. In addition, the density of EO-70 is higher than that of distilled water, belonging to heavy oil, while, the density of the other ANEOs is lower, light oil. Total ion chromatograms from ANEOs are seen in Figure 1B. The retention times and the abundance of chromatographic peaks indicate that the components of the ANEOs extracted at different temperatures were remarkably different. The similarity of the ANEOs was analyzed with the "Similarity Evaluation System for Chromatographic Fingerprint of Traditional Chinese Medicine
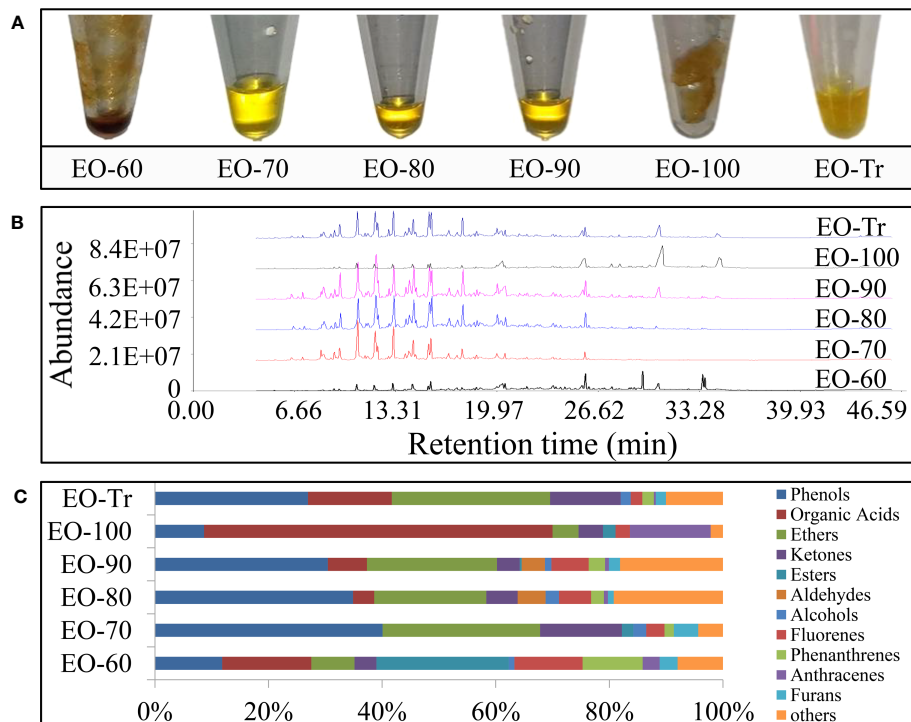
FIGURE 1
Physical property and chemical composition of separated ANEOs. **(A)** ANEOs. **(B)** GC-MS total ion chromatograms of ANEOs. **(C)** Chemical composition of ANEOs.

2004A" software (Qian et al., 2020). The similarity between EO-80 and EO-90 is 0.927, and other ANEOs were less than 0.5 (Table S1 in the Supplementary Material).

A total of 75 compounds were identified from the ANEOs by GC–MS analysis, 36 more compounds than that found in EO-Tr (Table S2 in the Supplementary Material). The types of compounds in ANEOs are showed in Figure 1C, the proportion of phenolics of EO-70 is the highest (40.09%). Overall, the ANEOs were preliminarily separated through negative pressure hydro-distillation and the phenolics were enriched in EO-70.

3.2 Antibacterial activity assessments

The inhibitory activity of the ANEOs on *S. mutans* was assessed by measuring the DIZ, MIC and MBC values (Figure 2). All of the ANEOs showed inhibitory effects on *S. mutans*. EO-70 had the largest DIZ value (16.5 ± 0.18 mm), which was greater than that of CHX (15.61 ± 0.68 mm), and clearly inhibited the growth of *S. mutans*. The DIZ of EO-100 was the smallest, and the DIZs of the separated ANEOs except for EO-100 were all significantly larger than that of EO-Tr ($P < 0.05$) (Figure 2A). The MIC values of EO-70, EO-80 and EO-90 were 0.50 mg/mL, and those of EO-60, EO-100
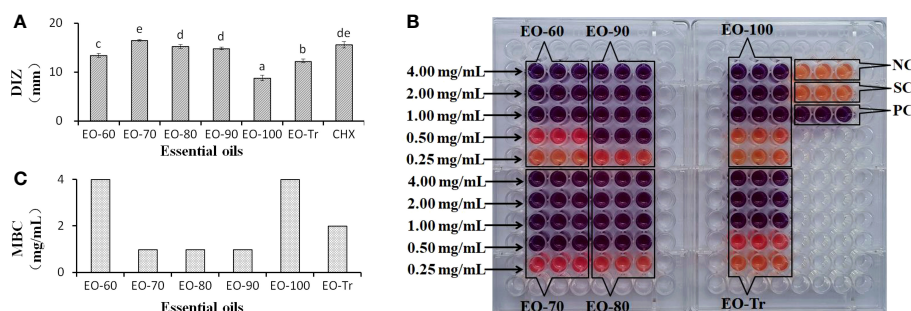

FIGURE 2
DIZ, MIC and MBC of different ANEOs against *S. mutans*. **(A)** DIZs. **(B)** MICs. **(C)** MBCs. Negative control (NC): BHI + *S. mutans*; Solvent control (SC): BHI + *S. mutans* + Tween 80; Positive control (PC): BHI + *S. mutans* + Tween 80 + CHX; Different lowercase letters indicate significant differences ($P < 0.05$).

and EO-Tr were all 1.0 mg/mL (Figure 2B). The MBC values of the ANEOs were shown to be 2 or 4 times of their corresponding MIC values (Figure 2C). These results indicate that there are certain differences in the inhibitory effect of different ANEOs against *S. mutans*, and EO-70 exhibits the best antibacterial activity and contains more active substances.

3.3 Antibiofilm activity

3.3.1 Effect of ANEO on total biofilm biomass

S. mutans develops virulence by the biofilm formation on tooth surfaces. Therefore, we firstly examined the effects of different ANEOs on the biofilm biomass. As shown in Figure 3A, the total biofilm biomass decreases significantly after treatment with the ANEOs at the MIC concentration compared with NC ($P < 0.01$). Of all the ANEOs at MIC concentration, the total biofilm biomass of EO-70 group is the least, which is significantly different from the other groups ($P < 0.05$). Furthermore, the effect of the ANEOs on the total biofilm biomass is positively correlated with the concentration of ANEOs, and the total biomass of all ANEO groups was the least at the MIC. The change of sample concentrations in the EO-100 and EO-Tr groups has little effect on the total biofilm biomass of *S. mutans*.

3.3.2 Effect of ANEO on biofilm activity

The biofilm activity is represented by the percentage of absorbance value of XTT metabolites in this study. As shown in Figure 3B, the biofilm activity of *S. mutans* decreases after culturing with the ANEOs, and the magnitude is positive correlated with the concentration of the ANEOs. At the MIC concentration, the biofilm activity of each ANEO group is extremely significantly less than NC ($P < 0.01$). Furthermore, EO-70 and EO-90 had greater impacts on the biofilm activity than CHX, and still significantly inhibited the bacterial activity at 1/8 MIC. The EO-80, EO-Tr and EO-60 had a moderate inhibitory effect on the biofilm activity, and EO-100

group had the least effect. It can be seen that ANEOs showed a certain inhibitory effect on the biofilm of *S. mutans*.

3.3.3 Effect of ANEO on formation and morphology of biofilm

The effect of different ANEOs on the compactness of the cell arrangement in the biofilm was shown in SEM photography. Figure 4 shows that the compactness of the bacteria was destroyed, the biofilm become thinner, and the bacterial arrangement was not neat but loose. Figures 4B–D, H show that the bacterial cell arrangement after treatment with EO-70, EO-80, EO-90, and CHX became sparse with more pores (red arrow), and the biofilms were thin in some places, even with cells in a monolayer (blue arrow). Figures 4A, E, F show fewer pores, and the cellular arrangement is relatively dense in the biofilms cultured with EO-60, EO-100 and EO-Tr. The biofilm cells in the NC group show an orderly and compact arrangement with few small pores (Figure 4G). This assay demonstrated that the ANEOs could interfere with biofilm formation, affect the cellular arrangement, cause the biofilm to be incomplete, and reduce the biofilm quality, thus reducing the resistance of biofilm to external interference. Simultaneously, the formation of a stable microenvironment becomes difficult, which could reduce the cariogenic capacity of *S. mutans*.

3.4 Antibiofilm mechanism

3.4.1 Effect on cell surface hydrophobicity

Bacterial cell surface hydrophobicity is closely linked to the bacterial adhesion and biofilm formation, and the higher hydrophobicity rates, the easier of the biofilm formation (Abdulla et al., 2014; Vaca et al., 2020). Therefore, the cell surface hydrophobicity can be used to evaluate whether the ANEOs inhibited the biofilm formation. As shown in Figure 5A, the surface hydrophobicity of *S. mutans* decreases with an increase of
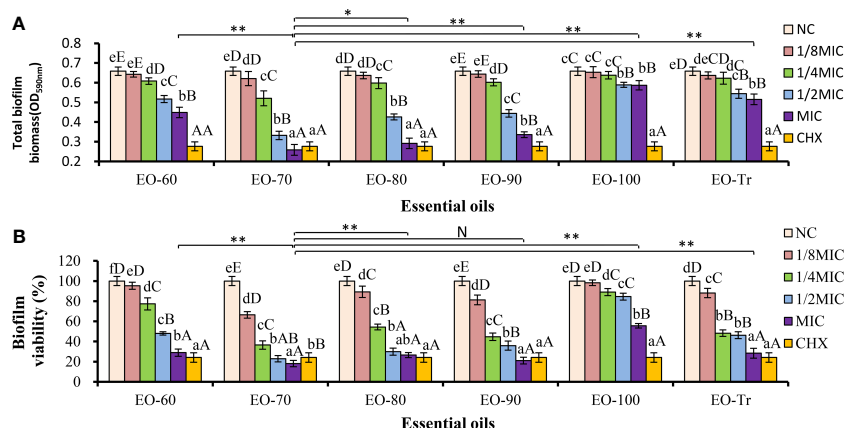

FIGURE 3
Antibiofilm activity of ANEOs on *S. mutans*. **(A)** Effect of ANEOs on the total biofilm biomass of *S. mutans*. **(B)** Effect of ANEOs on bacterial viability in *S. mutans* biofilms. The NC (or CHX) in the six histograms is the same. Different lowercase letters represent statistically significant differences among the groups of the same ANEO ($P < 0.05$), Different uppercase letters represent statistically extremely significant difference among the groups of the same ANEO ($P < 0.01$). *$P < 0.05$, **$P < 0.01$, N represent no statistically significant difference between the groups.
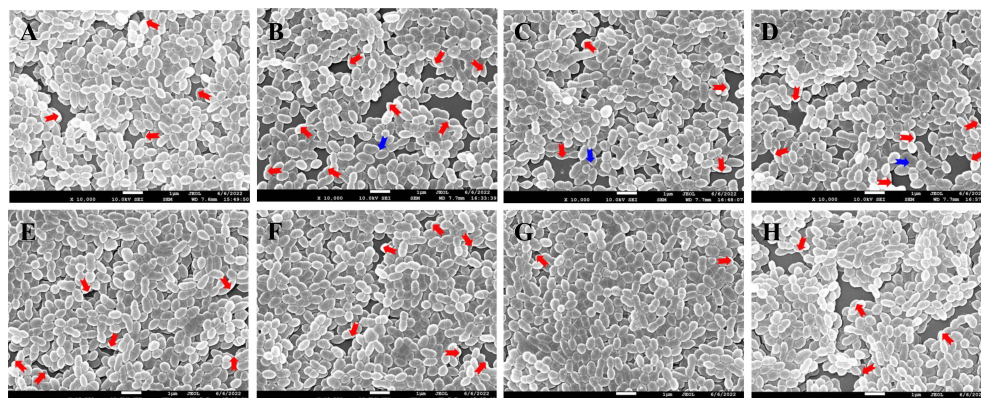
FIGURE 4
SEM photography of *S. mutans* biofilms treated with different ANEOs (1/4 MIC). **(A)** EO-60, **(B)** EO-70, **(C)** EO-80, **(D)** EO-90, **(E)** EO-100, **(F)** EO-Tr, **(G)** NC, **(H)** CHX. Red arrows point to pores, and blue arrows point to monolayers of cells.

the ANEOs concentration in the range of 1/8MIC to MIC. The hydrophobicity rate of *S. mutans* treated with EO-70 was the lowest (39.03 ± 3.38%), obviously less than that of the other ANEOs. The result indicated that ANEOs could prevent bacteria from adhering to form biofilms by reducing the surface hydrophobicity of *S. mutans*.

3.4.2 Effects of ANEOs on EPS production

EPS is considered as a virulence factor of cariogenic biofilms (Lin et al., 2021), and included WSP and WIP. The results of the EPS assay showed that the production of WIP and WSP were both inhibited by ANEOs (Figures 5B, C). EO-70, EO-80 and EO-90 had good inhibitory effects on the production of WIP, and the inhibition

rates were all extremely significantly higher than CHX (*P*< 0.01) (Figure 5B). Figure 5C shows that the inhibitory effect of EO-70 and EO-90 on the production of WSP is greater than that of CHX, and the difference between EO-70 and CHX is extremely significant (*P*< 0.01). These results indicated that EO-70 and EO-90 had a good inhibitory effect on both WIP and WSP.

3.4.3 Effects of ANEOs on Gtf activity

Gtf is considered to be the key enzyme for the assembly of cariogenic biofilms. Gtf activity can affect the cariogenic potential of *S. mutans* (Ma et al., 2021). Figure 5D indicates that all ANEOs exhibit certain inhibition effects on Gtf activity. EO-70 had the greatest inhibitory effects, significantly different than the other five
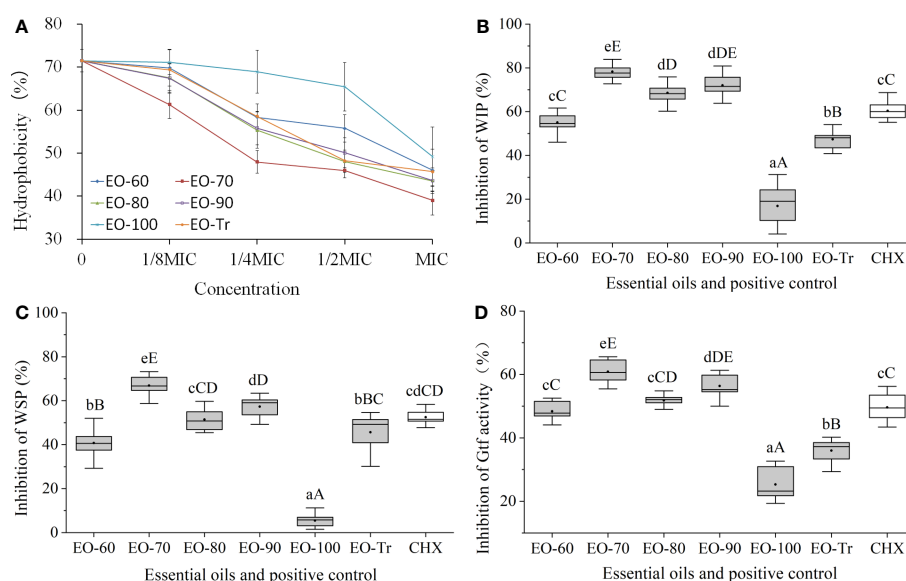

FIGURE 5
Antibiofilm mechanism of ANEOs. **(A)** Effect of ANEOs on cell surface hydrophobicity. **(B)** Inhibitory effect on the production of WIP. **(C)** Inhibitory effect on the production of WSP. **(D)** Inhibitory effect on Gtf activity. Different lowercase letters represent statistically significant differences among the groups (*P* < 0.05). Different uppercase letters represent statistically extremely significant differences among the groups (*P* < 0.01).

ANEOs and CHX ($P < 0.05$). EO-90 significantly decreased the Gtf activity compared with the other ANEOs (except for EO-70) and CHX ($P < 0.05$). The inhibitory effect of EO-80 was greater than that of CHX but not significantly ($P > 0.05$), and the inhibitory effects of EO-60, EO-100 and EO-Tr was weaker than that of CHX. This illustrated that ANEOs could inhibit Gtf (i.e., EPS synthetase) activity, and the results are consistent with that of the EPS quantification.

3.5 Membrane damage studies

3.5.1 Leakage of LDH

LDH is an important intrinsic enzyme in *S. mutans*, which can catalyze the synthesis of lactic acid from pyruvate. LDH plays a crucial role in bacterial resistance to host innate immunity and biofilm formation. LDH does not leak from normal cells, but is released into the culture medium if the cell membrane is damaged (Yin et al., 2020). Figure 6 shows that, compared with NC, the quantity of released LDH in all the experiment groups is significantly greater ($P < 0.01$) after 4 h, indicating that all ANEOs can damage the cell membrane. The percentage of LDH in the medium of the EO-70 group increased rapidly to $86.59 \pm 3.76\%$ within 16 h, and did not increase after 16 h ($P < 0.05$) (Figure 6B). Figures 6A, C–E, F respectively indicate that the percentage of LDH in the EO-60, EO-80, EO-90, EO-100 and EO-Tr groups show a rapid increase during

the first 12 h, to $67.91 \pm 4.82\%$, $77.24 \pm 4.98\%$, $75.41 \pm 4.89\%$, $51.40 \pm 5.88\%$ and $62.95 \pm 5.95\%$, and 12 h later the LDH content reached a steady state ($P < 0.05$). These results suggested that ANEOs could destroy the cell membrane of *S. mutans*, resulting in the release of LDH from the cells (Richardson et al., 2008).

3.5.2 Nucleic acid leakage of *S. mutans*

Cell membrane is a kind of selectively permeable membrane. When the cell membrane is damaged, macromolecules such as nucleic acids leak out of the cell (Frallicciardi et al., 2022). The amount of nucleic acid leakage can be used for the determination and analysis of cell membrane integrity (Sun et al., 2018). As shown in Figure 7B, the OD_{260} of the EO-70 group rapidly increases to 0.628 ± 0.024 from 0 h to 16 h, and then stabilizes after 16 h ($P < 0.05$). From 0 to 12 h, the OD_{260} of other groups increased rapidly, and after 12 h the OD_{260} almost stopped increasing ($P < 0.05$) (Figures 7A, C–F). Compared with NC, the OD_{260} of all the ANEO groups was significantly higher 4 h later ($P < 0.01$). The OD_{260} of the EO-70, EO-80 and EO-90 groups was significantly higher than that of CHX after 4 h, 8 h, and 8 h respectively ($P < 0.05$) (Figures 7B–D). These results combined with the LDH leakage results indicated that all of the ANEOs can destroy the integrity of the cell membrane.

3.5.3 Effects of ANEOs on cell membrane integrity

PI is a membrane impermeable and highly sensitive nucleic acid stain which releases a red fluorescence after the insertion of
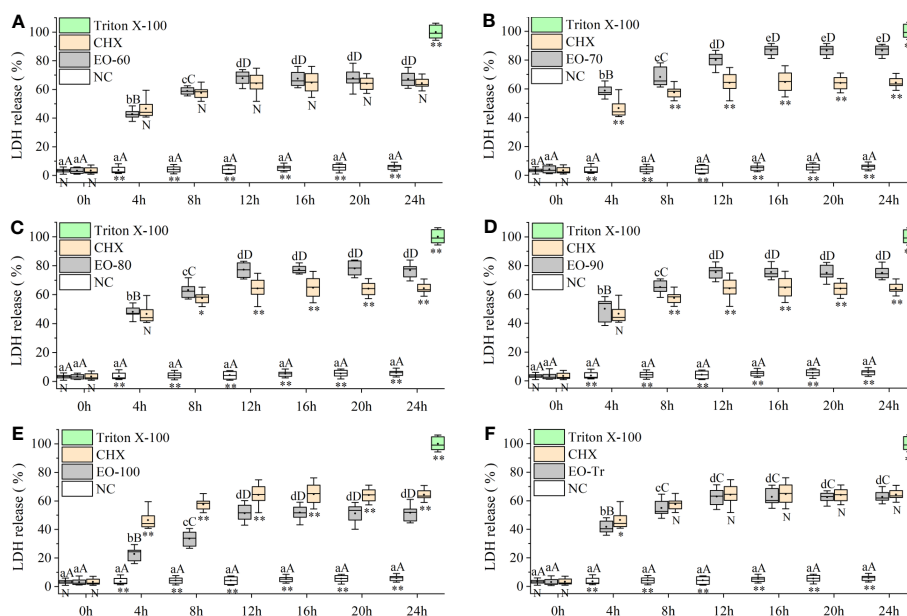

FIGURE 6
Effect of ANEOs on LDH leakage from *S. mutans*. The concentration of each ANEO is the MIC. **(A)** EO-60, **(B)** EO-70, **(C)** EO-80, **(D)** EO-90, **(E)** EO-100, **(F)** EO-Tr. Different lowercase letters represent statistically significant differences among the experimental time points in the same ANEO group (or NC) ($P < 0.05$) and different uppercase letters represent statistically extremely significant differences ($P < 0.01$). * represents statistically significant differences between the NC (or CHX) and the ANEO groups at the same time point ($P < 0.05$), ** represents statistically extremely significant differences ($P < 0.01$), and N represents no significant difference ($P > 0.05$).
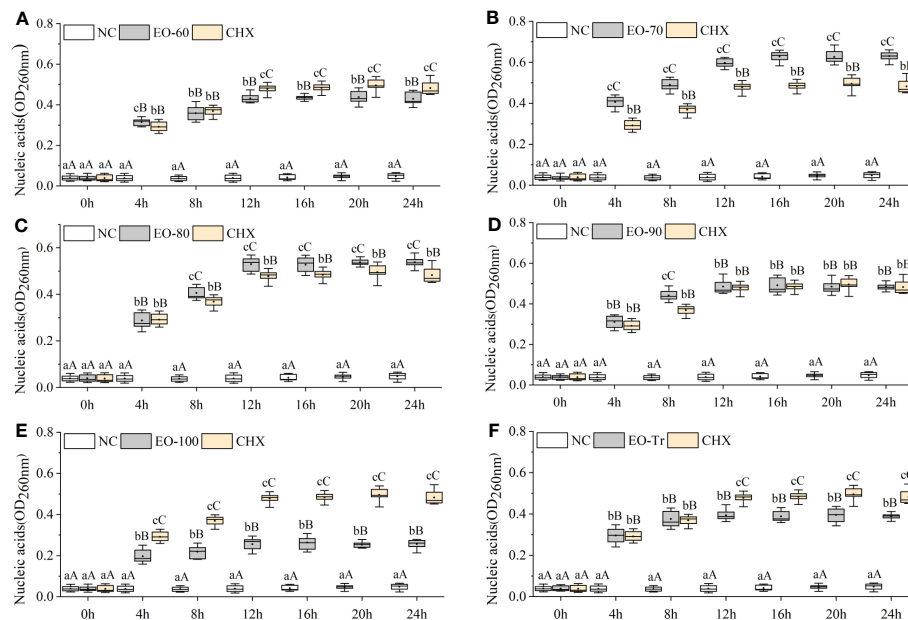
FIGURE 7

Effect of different ANEOs on nucleic acid leakage from *S. mutans*. The concentration of each ANEO is the MIC. **(A)** EO-60, **(B)** EO-70, **(C)** EO-80, **(D)** EO-90, **(E)** EO-100, **(F)** EO-Tr. Different lowercase letters represent statistically significant differences among the experimental time points in the same ANEO group (or NC) (*P* < 0.05), and different uppercase letters represent statistically extremely significant differences (*P* < 0.01). * represents statistically significant differences between the NC (or CHX) and the ANEO groups at the same time point (*P* < 0.05), ** represents statistically extremely significant differences (*P* < 0.01), and N represents no significant differences (*P* > 0.05).

double-stranded DNA when cell membrane is damaged, and PI is usually used to evaluate the integrity of the cell membrane (Rosenberg et al., 2019). As shown in Figure 8, the red fluorescence intensity in the biofilms treated with ANEOs enhances compared with NC (Figure 8G). The fluorescence intensity in the EO-70 group were strongest (Figure 8B), followed by the EO-80 group and the EO-90 group (Figures 8C, D), while weaker fluorescence intensity appeared in the EO-60 and EO-TR groups (Figures 8A, F), and the EO-100 group showed the weakest (Figure 8E). Moreover, Figures 8G, H show that most cells in PBS are living cells, and PI is blocked outside the cell membrane of living cells, and displays weak fluorescence. Thus, the difference in the fluorescence intensity indicated not only that ANEOs could disrupt the structure of the bacterial cell membrane but also the strength of this ability was diverse for different ANEOs.
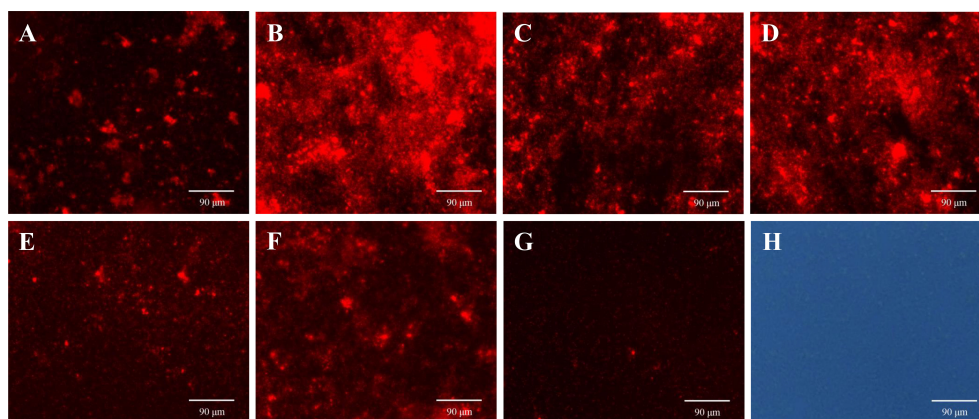

FIGURE 8

Effects of ANEOs on PI crossing the cell membrane of *S. mutans*. **(A)** EO-60, **(B)** EO-70, **(C)** EO-80, **(D)** EO-90, **(E)** EO-100, **(F)** EO-Tr, **(G)** Control (observed with a fluorescence microscope), **(H)** Control (observed with an optical microscope). Images were taken at ×40 objective magnification.

3.6 Effect of ANEOs on the morphology of *S. mutans*

SEM was used to analyze the damage of the *S. mutans* cell structure caused by ANEOs extracted at different temperatures. Figure 9 shows that the structure of *S. mutans* is affected to varying degrees by the ANEOs, compared with NC. Figure 9G shows that the cells have a regular shape, smooth surface, an obvious transverse groove and are chain-like. After treatment with ANEOs and CHX, the bacteria cell surface was rough and even collapse, rupture (Figures 9A–D, F, H). The cells showed granules or granular accumulation (Figures 9A, C, H), and the cell chain was shortened or absent (Figures 9B, D, E). In addition, although no obvious division transverse groove was apparent, atrophy of the cells was evident, which suggests that cell division was blocked (Figures 9A–E, H). These results indicated that the cell morphology of *S. mutans* were damaged, and even the membrane system, which lead to the leakage of the cell contents. It is also apparent that ANEOs could interfere with normal cell division and affect the progress of the normal cell life cycle.

3.7 Cytotoxicity of ANEO in oral cells

To determine the safety of ANEOs, their cytotoxicity on HOECs was evaluated. The IC_{10} values of samples usually indicate non-cytotoxic concentrations (Attoff et al., 2017). As shown in Table 1, the IC_{10} values of six ANEOs to HOECs are higher than their MIC values, and the IC_{10} values of EO-70, EO-80 and EO-90 samples were even higher than their MBC values. The above data showed that the six ANEOs could inhibit the biofilm formation and damage the bacteria cell membrane of oral pathogenic bacteria, but had no cytotoxic effects on oral cells.

4 Discussion

Many infectious diseases in humans are caused or aggravated by biofilms, and dental caries is a typical biofilm-dependent disease (Koo et al., 2013; Horev et al., 2015). One important step in the

TABLE 1 IC_{10} values of ANEOs in HOECs.

Essential oil	IC_{10} values (mg/mL)
EO-60	1.10 ± 0.10
EO-70	3.16 ± 0.09
EO-80	2.19 ± 0.55
EO-90	3.39 ± 0.14
EO-100	2.81 ± 0.07
EO-Tr	1.94 ± 0.69

caries occurrence is that pathogenic bacteria gather on the tooth surface and form a biofilm. Biofilms are highly organized bacterial colonies that are firmly attached to surfaces or interfaces and encased in a 3D extracellular polymeric matrix, such as EPS (Koo et al., 2013; Gao et al., 2016). *S. mutans* is the main contributor to dental caries biofilms, plays a significant role in the induction of dental caries because of its acidogenic, acid-tolerant and biofilm-forming characteristics (Yoo and Jwa, 2018), and is widely used as a target for dental caries research.

As shown in this study, the ANEOs displayed preferable antibacterial and antibiofilm activity against *S. mutans*. At MIC concentrations, all ANEOs could reduce the total biofilm biomass, and the total biofilm biomass of the EO-70 group was less than that of CHX. However, the total biofilm biomass could not entirely reflect the pathogenicity of the biofilm, and the inanimate bacteria in the biofilm may have lost pathogenicity. Thus, we analyzed the vitality of bacteria in the biofilm. The results showed that the metabolic activity of the biofilms treated by ANEOs was decreased, and a large number of bacteria were dead in the biofilm, further showing that the biofilm was less resistant to the ANEOs. In order to intuitively observe the damage of biofilm, we used an optimized biofilm model to observe its integrity. Frequently, to simulate the progression of dental caries, materials such as hydroxyapatite disks, bovine dentin disks or bovine teeth are used by researchers to construct dental caries biofilms (Ribeiro-

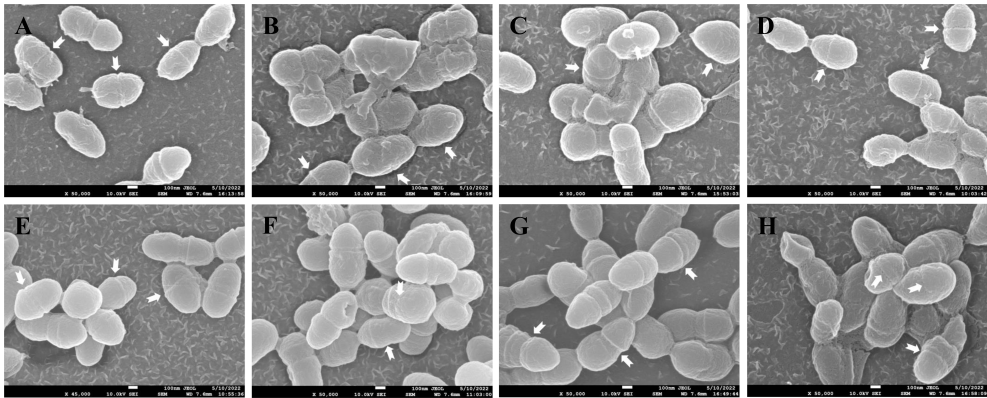

FIGURE 9
Effect of different ANEOs on the morphology of *S. mutans*. **(A)** EO-60, **(B)** EO-70, **(C)** EO-80, **(D)** EO-90, **(E)** EO-100, **(F)** EO-Tr, **(G)** NC (control), **(H)** CHX. Arrows point to division of the transverse groove.

Vidal et al., 2020; Neves et al., 2019; Vertuan et al., 2021). The biofilms formed in these models are relatively loose due to the hydrophobicity of material (Cui et al., 2018), and would not be suitable for analyzing the effects of ANEOs on cell arrangement in the biofilm. In this study, a polystyrene material more conducive to bacterial attachment was used to prepare biofilms. SEM images showed that ANEOs destroyed the dense structure of the biofilm, the layer becomes thinner, and the cell arrangement is irregular or loose (Xi et al., 2019). These data indicated that ANEOs decreased the total biomass and the metabolic activity, disrupted the integrity of the biofilm, reduced the cariogenic potential (Aiassa et al., 2016) and resistance to adverse conditions (i.e., antibiotics, high temperatures) of *S. mutans* biofilms (Muras et al., 2018).

In order to further explore the antibiofilm mechanism of the ANEOs, we analyzed their role in preventing biofilm formation. The dental biofilm life cycle generally includes the adhesion and colonization of bacteria, the assembly and maturation of 3D biofilms, biofilm degradation and re-colonization (Koo et al., 2013; Kumar et al., 2017). The adhesion and colonization of bacteria is the key factor determining whether the biofilm can be formed, and is the first step of biofilm formation. Surface hydrophobicity of bacteria directly affect their adhesion and colonization (Abdulla et al., 2014; Kozmos et al., 2021). ANEOs could reduce the surface hydrophobicity of *S. mutans*, weakening the adhesion and colonization of the bacteria, thus hindering the biofilm formation. EPS is a key component of dental biofilm formation and is also a virulence factor of cariogenic biofilms. (Lin et al., 2021). EPS provides a 3D scaffold for biofilm development, promotes local accumulation of bacteria on the teeth, and protects embedded bacteria (Bowen and Koo, 2011; Klein et al., 2015). The results of the EPS assay showed that every ANEO inhibited the production of WSP and WIP to varying degrees. In order to further explore the inhibition mechanism of ANEOs on EPS production, we analyzed the effect of ANEOs on the activity of the EPS synthetase, Gtf. The results of Gtf activity assay suggested that ANEOs inhibited Gtf activity. Therefore, we speculate that ANEOs prevented the synthesis of EPS by inhibiting the activity of Gtfs, and blocked 3D biofilm assembly, affected the maturity of biofilm and weakened the cariogenic potential of *S. mutans* (Kumar et al., 2017). In addition, EPS is the main material source of bacterial surface hydrophobicity (Devasia et al., 1993), the inhibition of EPS formation also reduced bacterial cell surface hydrophobicity, weakening the adhesion of the bacteria to surfaces.

The cell membrane is a type of selectively permeable membrane that prevents nucleic acids and other macromolecules from freely passing through it when it is in its normal state (Frallicciardi et al., 2022). If the cell membrane is damaged, the intracellular contents will leak; small molecules will flow out first, followed by RNA, DNA, proteins and other macromolecules. Thus, the leakage of intracellular substances such as RNA, DNA, and LDH is an important indicator to evaluate the integrity of the cell membrane (Sun et al., 2018). The results of LDH and nucleic acid leakage showed that ANEOs disrupted the integrity of the *S. mutans* cell membrane. In addition, the results of PI staining showed strong red fluorescence appearing in the ANEO groups, which indicated that PI had been inserted into the double-stranded DNA, and the cell membrane of *S. mutans* had been disrupted by the ANEOs. SEM images of *S. mutans* cells showed that ANEOs disrupted the cellular structure, leading to the disruption of the membrane system.

Based on results above, our study demonstrates that ANEOs have powerful antibacterial effect against dental caries pathogen *S. mutans*. Similarly, previous reports have shown that the extract of areca nut has antibacterial activity against bacterial and fungal strains, such as *Streptococcus, Staphylococcus aureus, Escherichia coli* and others (Peng et al., 2015). The volatile constituents extracted by Machová et al. exhibited best antibacterial effect against *Streptococcus* among 9 bacteria and yeast (Machová et al., 2021).

Some studies believe that chewing of areca nut can induce oral cancer and the arecoline is the main carcinogen (Oliveira et al., 2021). However, in 2020, the International Agency for Research on Cancer (IARC) reassessed the carcinogenicity of arecoline, and found that the evidence regarding cancer in humans for arecoline was "inadequate", and no data were available (Marques et al., 2021). GC-MS data showed that there was no carcinogenic component arecoline in ANEOs. The MTT assay also showed that ANEOs had no cytotoxicity to normal oral cells. Therefore, the ANEO is safe as an oral antibacterial agent. GC-MS data also showed that the content of phenolic compounds in EO-70 was the highest, and the antibacterial activity of EO-70 was also the strongest. We speculate that phenolic compounds were the active antibacterial components of the ANEOs, which is consistent with reports that phenols generally have strong antibacterial activity (Fan et al., 2022), and the antibacterial components of areca nut are mainly polyphenol (Jam et al., 2021; Raju et al., 2021). Overall, the active components of ANEO were preliminarily separated and enriched through negative pressure hydro-distillation compared to the traditional hydro-distillation extraction. In addition, 36 more compounds were identified than traditional hydro-distillation extraction, and the low extraction temperature also can prevent the thermal degradation of essential oil components. Thus, this study sheds new light on the separation and enrichment of essential oil components. It is expected that the active components of essential oils can be precisely enriched and separated by improving the pressure regulation and temperature control elements to finely adjust the separation temperatures in future research.

5 Conclusion

This study successfully achieved preliminary separation of ANEO components by negative pressure hydro-distillation, providing some ideas for the separation of essential oil components of other plant. The obtained ANEOs showed good anti-bacterial and anti-biofilm activities against the main

pathogenic bacteria of dental caries, *S. mutans*, by affecting the biofilm and disrupting the integrity of the cell membrane. These findings indicate that ANEOs might be a potential antibacterial agent for the prevention of dental caries.

Data availability statement

The original contributions presented in the study are included in the article/Supplementary Material. Further inquiries can be directed to the corresponding authors.

Ethics statement

Ethical approval was not required for the studies on humans in accordance with the local legislation and institutional requirements because only commercially available established cell lines were used.

Author contributions

SL made substantial contributions to the design, the acquisition, analysis, and interpretation of data for the work. TZ made contributions to design of methodology, formal analysis, review, and editing. YW revised and edited it critically for important intellectual content and editing. ZL made contributions to design of methodology and formal analysis. LL revised it critically for important intellectual content. ZS made substantial contributions to the conception. All authors contributed to the article and approved the submitted version.

Funding

Conflict of interest

The authors declare that the research was conducted in the absence of any commercial or financial relationships that could be construed as a potential conflict of interest.

Publisher's note

All claims expressed in this article are solely those of the authors and do not necessarily represent those of their affiliated organizations, or those of the publisher, the editors and the reviewers. Any product that may be evaluated in this article, or claim that may be made by its manufacturer, is not guaranteed or endorsed by the publisher.

Supplementary material

The Supplementary Material for this article can be found online at: https://www.frontiersin.org/articles/10.3389/fcimb.2023.1140689/full#supplementary-material

References

Abdulla, A. A., Abed, T. A., and Saeed, A. M. (2014). Adhesion, autoaggregation and hydrophobicity of six Lactobacillus strains. *Br. Microbiol. Res. J.* 4 (4), 381–391. doi: 10.9734/BMRJ/2014/6462

Aiassa, V., Zoppi, A., Becerra, M. C., Albesa, I., and Longhi, M. R. (2016). Enhanced inhibition of bacterial biofilm formation and reduced leukocyte toxicity by chloramphenicol:β-cyclodextrin:N-acetylcysteine complex. *Carbohydr Polym.* 152, 672–678. doi: 10.1016/j.carbpol.2016.07.013

Ansari, A., Mahmood, T., Bagga, P., Ahsan, F., Shamim, A., Ahmad, S., et al. (2021). Areca catechu: A phytopharmacological legwork. *Food Front.* 2 (2), 163–183. doi: 10.1002/fft2.70

Attoff, K., Gliga, A., Lundqvist, J., Norinder, U., and Forsby, A. (2017). Whole genome microarray analysis of neural progenitor C17. 2 cells during differentiation and validation of 30 neural mRNA biomarkers for estimation of developmental neurotoxicity. *PloS One* 12 (12), e0190066. doi: 10.1371/journal.pone.0190066

Bajpai, V. K., Sharma, A., and Baek, K. H. (2013). Antibacterial mode of action of *Cudrania tricuspidata* fruit essential oil, affecting membrane permeability and surface characteristics of food-borne pathogens. *Food control* 32 (2), 582–590. doi: 10.1016/j.foodcont.2013.01.032

Bhandare, A. M., Kshirsagar, A. D., Vyawahare, N. S., Hadambar, A. A., and Thorve, V. S. (2010). Potential analgesic, anti-inflammatory and antioxidant activities of hydroalcoholic extract of *Areca catechu* L. nut. *Food Chem. Toxicol.* 48 (12), 3412–3417. doi: 10.1016/j.fct.2010.09.013

Bhandare, A. M., Vyawahare, N. S., and Kshirsagar, A. D. (2015). Anti-migraine effect of *Areca Catechu* L. nut extract in bradykinin-induced plasma protein extravasation and vocalization in rats. *J. Ethnopharmacol.* 171, 121–124. doi: 10.1016/j.jep.2015.05.052

Bowen, W. H. (2016). Dental caries–not just holes in teeth! A perspective. *Mol. Oral. Microbiol.* 31, 228–233. doi: 10.1111/omi.12132

Bowen, W. H., and Koo, H. (2011). Biology of Streptococcus mutans-derived glucosyltransferases: role in extracellular matrix formation of cariogenic biofilms. *Caries Res.* 45 (1), 69–86. doi: 10.1159/000324598

Chen, X., He, Y., and Deng, Y. (2021). Chemical composition, pharmacological, and toxicological effects of betel nut. *Evidence-Based Complementary Altern. Med.* 2021 1808081. doi: 10.1155/2021/1808081

Chen, Z. F., He, B., Zhou, J., He, D. H., Deng, J. D., and Zeng, R. H. (2016). Chemical compositions and antibacterial activities of essential oils extracted from Alpinia guilinensis against selected foodborne pathogens. *Ind. Crop Prod.* 83, 607–613. doi: 10.1016/j.indcrop.2015.12.063

CLSI (2012). *Performance Standards for Antimicrobial Disk Susceptibility Tests; Approved Standard. 11th ed* (Wayne, PA, USA: Clinical & Laboratory Standards Institute).

Cugini, C., Shanmugam, M., Landge, N., and Ramasubbu, N. (2019). The role of exopolysaccharides in oral biofilms. *J. Dental Res.* 98 (7), 739–745. doi: 10.1177/0022034519845001

Cui, H., Miao, S., Esworthy, T., Zhou, X., Lee, S. J., Liu, C., et al. (2018). 3D bioprinting for cardiovascular regeneration and pharmacology. *Adv. Drug Deliv. Rev.* 132, 252–269. doi: 10.1016/j.addr.2018.07.014

Devasia, P., Natarajan, K. A., Sathyanarayana, D. N., and Rao, G. R. (1993). Surface chemistry of Thiobacillus ferrooxidans relevant to adhesion on mineral surfaces. *Appl. Environ. Microbiol.* 59 (12), 4051–4055. doi: 10.1128/aem.59.12.4051-4055.1993

DuBois, M., Gilles, K. A., Hamilton, J. K., Rebers, P. A., and Smith, F. (1956). Colorimetric method for determination of sugars and related substances. *Anal. Chem.* 28 (3), 350–356. doi: 10.1021/ac60111a017

Fan, X., Jiang, C., Dai, W., Jing, H., Du, X., Peng, M., et al. (2022). Effects of different extraction on the antibacterial and antioxidant activities of phenolic compounds of areca nut (husks and seeds). *J. Food Measurement Characterization* 16 (2), 1502–1515. doi: 10.1007/s11694-021-01244-7

Frallicciardi, J., Melcr, J., Siginou, P., Marrink, S. J., and Poolman, B. (2022). Membrane thickness, lipid phase and sterol type are determining factors in the permeability of membranes to small solutes. *Nat. Commun.* 13 (1), 1–12. doi: 10.1038/s41467-022-29272-x

Freires, I. A., Denny, C., Benso, B., de Alencar, S. M., and Rosalen, P. L. (2015). Antibacterial activity of essential oils and their isolated constituents against cariogenic bacteria: A systematic review. *Molecules.* 20 (4), 7329–7358. doi: 10.3390/molecules20047329

Gao, L., Liu, Y., Kim, D., Li, Y., Hwang, G., Naha, P. C., et al. (2016). Nanocatalysts promote *Streptococcus mutans* biofilm matrix degradation and enhance bacterial killing to suppress dental caries in *vivo*. *Biomaterials* 101, 272–284. doi: 10.1016/j.biomaterials.2016.05.051

He, Z., Huang, Z., Jiang, W., and Zhou, W. (2019). Antimicrobial activity of cinnamaldehyde on *Streptococcus mutans* biofilms. *Front. Microbiol.* 10. doi: 10.3389/fmicb.2019.02241

Hernández-Alcántara, A. M., Wacher, C., Llamas, M. G., López, P., and Pérez-Chabela, M. L. (2018). Probiotic properties and stress response of thermotolerant lactic acid bacteria isolated from cooked meat products. *LWT- Food Sci. Technol.* 91, 249–257. doi: 10.1016/j.lwt.2017.12.063

Horev, B., Klein, M. I., Hwang, G., Li, Y., Kim, D., Koo, H., et al. (2015). pH-activated nanoparticles for controlled topical delivery of farnesol to disrupt oral biofilm virulence. *ACS nano* 9 (3), 2390–2404. doi: 10.1021/nn507170s

Hsu, I. L., Yeh, F. H., Chin, Y. C., Cheung, C. I., Chia, Z. C., Yang, L. X., et al. (2021). Multiplex antibacterial processes and risk in resistant phenotype by high oxidation-state nanoparticles: new killing process and mechanism investigations. *Chem. Eng. J.* 409, 128266. doi: 10.1016/j.cej.2020.128266

Huang, R., Li, M., and Gregory, R. L. (2012). Effect of nicotine on growth and metabolism of *Streptococcus mutans*. *Eur. J. Oral. Sci.* 120, 319–325. doi: 10.1111/j.1600-0722.2012.00971.x

Jam, N., Hajimohammadi, R., Gharbani, P., and Mehrizad, A. (2021). Evaluation of antibacterial activity of aqueous, ethanolic and methanolic extracts of areca nut fruit on selected bacteria. *BioMed. Res. Int.* 2021, 6663399. doi: 10.1155/2021/6663399

James, P., Worthington, H. V., Parnell, C., Harding, M., Lamont, T., Cheung, A., et al. (2017). Chlorhexidine mouthrinse as an adjunctive treatment for gingival health. *Cochrane Database Syst. Rev.* 3, CD008676. doi: 10.1002/14651858.CD008676.pub2

Klein, M. I., Hwang, G., Santos, P. H., Campanella, O. H., and Koo, H. (2015). Streptococcus mutans-derived extracellular matrix in cariogenic oral biofilms. *Front. Cell. Infect. Microbiol.* 5. doi: 10.3389/fcimb.2015.00010

Koo, H., Falsetta, M. L., and Klein, M. I. (2013). The exopolysaccharide matrix: a virulence determinant of cariogenic biofilm. *J. Dental Res.* 92 (12), 1065–1073. doi: 10.1177/0022034513504218

Korshed, P., Li, L., Liu, Z., Mironov, A., and Wang, T. (2018). Antibacterial mechanisms of a novel type picosecond laser-generated silver-titanium nanoparticles and their toxicity to human cells. *Int. J. Nanomed.* 13, 89. doi: 10.2147/ijn.s140222

Kozmos, M., VIrant, P., Rojko, F., Abram, A., Rudolf, R., Raspor, P., et al. (2021). Bacterial adhesion of *Streptococcus mutans* to dental material surfaces. *Molecules* 26 (4), 1152. doi: 10.3390/molecules26041152

Krzyściak, W., Jurczak, A., Kościelniak, D., Bystrowska, B., and Skalniak, A. (2014). The virulence of Streptococcus mutans and the ability to form biofilms. *Eur. J. Clin. Microbiol. Infect. Dis.* 33 (4), 499–515. doi: 10.1007/s10096-013-1993-7

Kumar, A., Alam, A., Rani, M., Ehtesham, N. Z., and Hasnain, S. E. (2017). Biofilms: Survival and defense strategy for pathogens. *Int. J. Med. Microbiol.* 307 (8), 481–489. doi: 10.1016/j.ijmm.2017.09.016

Leite, B., Gomes, F., Teixeira, P., Souza, C., Pizzolitto, E., and Oliveira, R. (2013). Combined effect of linezolid and N-acetylcysteine against Staphylococcus epidermidis biofilms. *Enfermedades Infecciosasy Microbiología Clínica* 31 (10), 655–659. doi: 10.1016/j.eimc.2012.11.011

Lemos, J. A., Palmer, S. R., Zeng, L., Wen, Z. T., Kajfasz, J. K., Freires, I. A., et al. (2019). The biology of *Streptococcus mutans*. *Microbiol. Spectr.* 7 (1), 7–1. doi: 10.1128/microbiolspec.GPP3-0051-2018

Lin, Y., Chen, J., Zhou, X., and Li, Y. (2021). Inhibition of *Streptococcus mutans* biofilm formation by strategies targeting the metabolism of exopolysaccharides. *Crit. Rev. Microbiol.* 47 (5), 667–677. doi: 10.1080/1040841x.2021.1915959

Ma, Q., Pan, Y., Chen, Y., Yu, S., Huang, J., Liu, Y., et al. (2021). Acetylation of glucosyltransferases regulates *Streptococcus mutans* biofilm formation and virulence. *PloS Pathog.* 17 (12), e1010134. doi: 10.1371/journal.ppat.1010134

Machová, M., Bajer, T., Šilha, D., Ventura, K., and Bajerová, P. (2021). Volatiles composition and antimicrobial activities of areca nut extracts obtained by simultaneous distillation-extraction and headspace solid-phase microextraction. *Molecules (Basel Switzerland)* 26 (24), 7422. doi: 10.3390/molecules26247422

Marques, M. M., Beland, F. A., Lachenmeier, D. W., Phillips, D. H., Chung, F. L., Dorman, D. C., et al. (2021). Carcinogenicity of acrolein, crotonaldehyde, and arecoline. *Lancet Oncol.* 22 (1), 19–20. doi: 10.1016/s1470-2045(20)30727-0

Muras, A., Mayer, C., Romero, M., Camino, T., Ferrer, M. D., Mira, A., et al. (2018). Inhibition of *Steptococcus mutans* biofilm formation by extracts of Tenacibaculum sp. 20J, a bacterium with wide-spectrum quorum quenching activity. *J. Oral. Microbiol.* 10 (1), 1429788. doi: 10.1080/20002297.2018.1429788

National Administration of Traditional Chinese Medicine Chinese Materia Medica Editorial Committee (2004). Chinese Materia Medica, Mongolian medicine volume. *Shanghai Sci. Tech. publishers Shanghai*, 396–397.

Neves, A. B., Bergstrom, T. G., Fonseca-Gonçalves, A., Dos Santos, T. M. P., Lopes, R. T., and de Almeida Neves, A. (2019). Mineral density changes in bovine carious dentin after treatment with bioactive dental cements: a comparative micro-CT study. *Clin. Oral. Investig.* 23 (4), 1865–1870. doi: 10.1007/s00784-018-2644-2

Oliveira, N. G., Ramos, D. L., and Dinis-Oliveira, R. J. (2021). Genetic toxicology and toxicokinetics of arecoline and related areca nut compounds: an updated review. *Arch. Toxicol.* 95 (2), 375–393. doi: 10.1007/s00204-020-02926-9

Ooshima, T., Osaka, Y., Sasaki, H., Osawa, K., Yasuda, H., Matsumura, M., et al. (2000). Caries inhibitory activity of cacao bean husk extract in *in-vitro* and animal experiments. *Arch. Oral. Biol.* 45 (8), 639–645. doi: 10.1016/s0003-9969(00)00042-x

Packiavathy, I. A. S. V., Agilandeswari, P., Musthafa, K. S., Pandian, S. K., and Ravi, A. V. (2012). Antibiofilm and quorum sensing inhibitory potential of Cuminum cyminum and its secondary metabolite methyl eugenol against Gram negative bacterial pathogens. *Food Res. Int.* 45 (1), 85–92. doi: 10.1016/j.foodres.2011.10.022

Palombo, E. A. (2011). Traditional medicinal plant extracts and natural products with activity against oral bacteria: potential application in the prevention and treatment of oral diseases. *Evid.-Based Complement. Altern. Med.* 2011, 680354. doi: 10.1093/ecam/nep067

Patel, M., Agarwal, R., and Ardalan, B. (2004). Effects of oxaliplatin and CPT-11 on cytotoxicity and nucleic acid incorporation of the fluoropyrimidines. *J. Cancer Res. Clin. Oncol.* 130 (8), 453–459. doi: 10.1007/s00432-004-0575-6

Peng, W., Liu, Y. J., Wu, N., Sun, T., He, X. Y., Gao, Y. X., et al. (2015). *Areca catechu* L. (Arecaceae): A review of its traditional uses, botany, phytochemistry, pharmacology and toxicology. *J. Ethnopharmacol.* 164, 340–356. doi: 10.1016/j.jep.2015.02.010

Pitts, N. B., Zero, D. T., Marsh, P. D., Ekstrand, K., Weintraub, J. A., Ramos-Gomez, F., et al. (2017). Dental caries. *Nat. Rev. Dis. Primers* 3 (1), 1–16. doi: 10.1038/nrdp.2017.31

Qian, Z., Yiyang, C., Lixia, M., Yue, J., Jun, C., Jie, D., et al. (2020). Study on the fingerprints and quality evaluation of angelica sinensis radix by HPLC coupled with chemometrics based on traditional decoction process of ACPTCM. *Dose-Response* 18 (3), 1559325820951730. doi: 10.1177/1559325820951730

Raju, A., De, S. S., Ray, M. K., and Degani, M. S. (2021). Antituberculosis activity of polyphenols of Areca catechu. *Int. J. Mycobacteriol.* 10 (1), 13–18. doi: 10.4103/ijmy.ijmy_199_20

Ribeiro-Vidal, H., Sánchez, M. C., Alonso-Español, A., Figuero, E., Ciudad, M. J., Collado, L., et al. (2020). Antimicrobial activity of EPA and DHA against oral pathogenic bacteria using an in *vitro* multi-species subgingival biofilm model. *Nutrients* 12 (9), 2812. doi: 10.3390/nu12092812

Richardson, A. R., Libby, S. J., and Fang, F. C. (2008). A nitric oxide–inducible lactate dehydrogenase enables Staphylococcus aureus to resist innate immunity. *Science* 319 (5870), 1672–1676. doi: 10.1126/science.1155207

Rosenberg, M., Azevedo, N. F., and Ivask, A. (2019). Propidium iodide staining underestimates viability of adherent bacterial cells. *Sci. Rep.* 9, 6483. doi: 10.1038/s41598-019-42906-3

Shen, S., Zhang, T., Yuan, Y., Lin, S., Xu, J., and Ye, H. (2015). Effects of cinnamaldehyde on *Escherichia coli* and Staphylococcus aureus membrane. *Food control* 47, 196–202. doi: 10.1016/j.foodcont.2014.07.003

Souza, S. O., Raposo, B. L., Sarmento-Neto, J. F., Rebouças, J. S., Macêdo, D. P., Figueiredo, R. C., et al. (2022). Photoinactivation of yeast and biofilm communities of *candida albicans* mediated by znTnHex-2-pyp^{4+} Porphyrin. *J. Fungi* 8 (6), 556. doi: 10.3390/jof8060556

Sun, Y., Chen, H., Xu, M., He, L., Mao, H., Yang, S., et al. (2023). Exopolysaccharides metabolism and cariogenesis of Streptococcus mutans biofilm regulated by antisense vicK RNA. *J. Oral. Microbiol.* 15 (1), 2204250. doi: 10.1080/20002297.2023.2204250

Sun, X. H., Zhou, T. T., Wei, C. H., Lan, W. Q., Zhao, Y., Pan, Y. J., et al. (2018). Antibacterial effect and mechanism of anthocyanin rich Chinese wild blueberry extract on various foodborne pathogens. *Food Control* 94, 155–161. doi: 10.1016/j.foodcont.2018.07.012

Tartaglia, G. M., Tadakamadla, S. K., Connelly, S. T., Sforza, C., and Martín, C. (2019). Adverse events associated with home use of mouthrinses: a systematic review. *Ther. Adv. Drug Saf.* 10, 2042098619854881. doi: 10.1177/2042098619854881

Vaca, D. J., Thibau, A., Schütz, M., Kraiczy, P., Happonen, L., Malmström, J., et al. (2020). Interaction with the host: the role of fibronectin and extracellular matrix proteins in the adhesion of Gram-negative bacteria. *Med. Microbiol. Immunol.* 209 (3), 277–299. doi: 10.1007/s00430-019-00644-3

Vertuan, M., MaChado, P. F., de Souza, B. M., Braga, A. S., and Magalhães, A. C. (2021). Effect of TiF4/NaF and chitosan solutions on the development of enamel caries under a microcosm biofilm model. *J. Dentistry* 111, 103732. doi: 10.1016/j.jdent.2021.103732

Wang, X., Li, J., Zhang, S., Zhou, W., Zhang, L., and Huang, X. (2023). pH-activated antibiofilm strategies for controlling dental caries. *Front. Cell Infect. Microbiol.* 13. doi: 10.3389/fcimb.2023.1130506

Wang, B., Yan, S., Gao, W., Kang, X., Yu, B., Liu, P., et al. (2021). Antibacterial activity, optical, and functional properties of corn starch-based films impregnated with bamboo leaf volatile oil. *Food Chem.* 357, 129743. doi: 10.1016/j.foodchem.2021.129743

Wijesundara, N. M., Lee, S. F., Cheng, Z., Davidson, R., and Rupasinghe, H. P. (2021). Carvacrol exhibits rapid bactericidal activity against *Streptococcus pyogenes* through cell membrane damage. *Sci. Rep.* 11 (1), 1–14. doi: 10.1038/s41598-020-79713-0

Xi, Y., Wang, Y., Gao, J., Xiao, Y., and Du, J. (2019). Dual corona vesicles with intrinsic antibacterial and enhanced antibiotic delivery capabilities for effective treatment of biofilm-induced periodontitis. *ACS nano* 13 (12), 13645–13657. doi: 10.1021/acsnano.9b03237

Yin, L., Chen, J., Wang, K., Geng, Y., Lai, W., Huang, X., et al. (2020). Study the antibacterial mechanism of cinnamaldehyde against drug-resistant *Aeromonas hydrophila in vitro. Microb. Pathog.* 145, 104208. doi: 10.1016/j.micpath.2020.104208

Yoo, H. J., and Jwa, S. K. (2018). Inhibitory effects of β-caryophyllene on *Streptococcus mutans* biofilm. *Arch. Oral. Biol.* 88, 42–46. doi: 10.1016/j.archoralbio.2018.01.009

Zhang, Q., Ma, Q., Wang, Y., Wu, H., and Zou, J. (2021). Molecular mechanisms of inhibiting glucosyltransferases for biofilm formation in *Streptococcus mutans. Int. J. Oral. Sci.* 13 (1), 1–8. doi: 10.1038/s41368-021-00137-1

Frontiers in
Cellular and Infection Microbiology

Investigates how microorganisms interact with their hosts

Explores bacteria, fungi, parasites, viruses, endosymbionts, prions and all microbial pathogens as well as the microbiota and its effect on health and disease in various hosts.

Discover the latest Research Topics

See more →

frontiers | Research Topics